

Water quality monitoring in
Massachusetts and Cape Cod Bays:
August and September 1993

Massachusetts Water Resources Authority

Environmental Quality Department
Technical Report Series No. 94-12



FINAL

**WATER QUALITY MONITORING
IN
MASSACHUSETTS AND CAPE COD BAYS:
AUGUST AND SEPTEMBER 1993**

by

**John R. Kelly
Carl S. Albro
John T. Hennessy
P. Scott Libby
Battelle Ocean Sciences**

**Jeff Turner
David Borkman
University of Massachusetts — Dartmouth**

**Peter Doering
University of Rhode Island**

prepared for:

**Massachusetts Water Resources Authority
Charlestown Navy Yard
100 First Avenue
Boston, MA 02129
(617) 242-6000**

Environmental Quality Department Technical Report Series 94- 12

Citation:

Kelly, J.R., C.S. Albro, J.T. Hennessy, P.S Libby, J. Turner, D. Borkman, and P. Doering. 1994. **Water quality monitoring in Massachusetts and Cape Cod Bays: August and September 1993.** MWRA Enviro. Quality Dept. Tech. Rpt. Series No. 94-12. Massachusetts Water Resources Authority, Boston, MA. 172 pp.

EXECUTIVE SUMMARY

This report is the fourth of five periodic water column reports for water quality monitoring conducted in 1993 by Battelle Ocean Sciences for the Massachusetts Water Resources Authority (MWRA) Harbor and Outfall Monitoring Program. The report includes results from two surveys conducted during August and two surveys conducted during September of 1993. Each of these surveys included sampling at 21 stations in the nearfield area surrounding the proposed MWRA outfall diffuser about 15 km offshore in western Massachusetts Bay. The late August survey was a combined farfield/nearfield survey that included sampling at an additional 25 stations throughout Massachusetts Bay and Cape Cod Bay. Data on physical, chemical, and biological measurements at the stations are presented in this report; included also is a preliminary discussion of the interrelationships among variables and interpretation of monitoring results.

August-September 1993 was a period of gradual change from a strongly stratified to a weakly stratified water column, a phenomenon induced by the seasonal cooling of surface waters. Weakening of the thermocline was initiated in shallow waters and gradually began to progress seaward.

Within the nearfield, chlorophyll variability over time and over space provided the prime indicator of ecological change and water quality during the period. Concurrent with the gradual water-column destratification from August through September, there was an increase in the average surface-water chlorophyll concentration; a peak value $> 20 \mu\text{g L}^{-1}$ was the highest noted to date during 1992-1993 MWRA monitoring. This progression culminating as a major diatom bloom was the central defining feature of late summer/early fall 1993. The bloom was estimated to encompass a 5-10 m thick surface layer with a minimum chlorophyll concentration $> 10 \mu\text{g L}^{-1}$ and covered roughly 60 km^2 . The bloom in the nearfield occurred prior to complete mixing of surface and bottom water. Moreover, the observations on biology, chemistry, and physical properties suggest that the bloom originated inshore and was largely maintained by seasonally-enhanced export of dissolved nutrients from Boston Harbor.

Chlorophyll also was a principal parameter displaying a regional-scale difference in water quality during the farfield/nearfield survey. For example, surface-water chlorophyll concentrations in western Massachusetts Bay ranged from ~ 1 to $> 10 \mu\text{g L}^{-1}$, compared to values uniformly $< 1 \mu\text{g L}^{-1}$ in Cape Cod Bay. There was little evidence of enrichment of dissolved nutrients (N, P, or Si) near Boston Harbor, but a gradient in chlorophyll was observed, with concentrations highest near the edge of the Harbor and decreasing into western Massachusetts Bay. Geographic variation in physical and chemical parameters throughout the survey area was generally slight, but there was a geochemical distinction between western Massachusetts Bay and Cape Cod Bay surface waters that corresponded with the difference in the chlorophyll biomass of the two areas. Cape Cod Bay stations had surface-water silicate concentrations (2-3 μM) which were higher than silicate concentrations in western Massachusetts Bay waters (0.05-1.4 μM) and which were distinctly high in relation to their salinity compared to other samples. Cape Cod Bay stations had, in general, low phytoplankton counts and reduced diatom abundance relative to western Massachusetts Bay stations. Total nitrogen (TN) concentrations measured at Cape Cod Bay stations also were generally low compared to most Massachusetts Bay stations. A lower nitrogen supply, less phytoplankton growth, and a lower

assimilatory demand for dissolved silicate (because of fewer diatoms) could, in part, explain the observations in Cape Cod Bay relative to western Massachusetts Bay.

Several key monitoring parameters — nutrients, dissolved oxygen (DO), chlorophyll, and phytoplankton (at the surface of one station, N10P) — were measured on each of the four surveys. Other key parameters — phytoplankton, zooplankton, and water column metabolism (production, respiration) — were only measured at 10 "BioProductivity" stations during the farfield survey in late August. Specific findings for each of the key parameters during August-September 1993 period are summarized as follows:

- Nutrients — All dissolved nutrients increased sharply below the thermocline/pycnocline. Aside from regional distinctions for silicate, bottom-waters at a given depth most anywhere in the Bay had similar nutrient concentrations. Deep water in Stellwagen Basin in late August had the highest concentrations of dissolved inorganic nitrogen (DIN) and silicate observed during the period of surveys, about 10 and 19 μM respectively.

The range of DIN concentrations in nearfield surface waters increased during September and DIN values $> 8 \mu\text{M}$ were measured. Highest surface-water nutrient concentrations were noted on the shallower western side of the nearfield and some increase was noted in NH_4 . NH_4 was generally low in bottom water, where NO_3 dominated DIN. In contrast, the increase in the western nearfield in September bore the signature that is characteristic of water exported from the Harbor — enhanced dissolved nutrients, including NH_4 , in slightly less saline water. Bottom-water DIN maxima in the nearfield increased from 5-6 μM in August to 8-9 μM in September.

- Dissolved oxygen (DO) — The surface layer (~ 0 -20 m) was 100-140% saturated. Peak supersaturation ($> 120\%$) occurred in late August and again in late September. A mid-water maximum in percent saturation was observed at the deep, offshore stations; at the nearfield and shallow coastal stations, it was common to have highest supersaturation within the surface 5-10 m. Percent DO saturation regularly declined from the pycnocline to the bottom. At the deepest stations in Stellwagen Basin, DO levels were depressed to 83-87% saturation (~ 8.7 - 9.0 mg L^{-1}) in late August. In the nearfield, bottom-water DO levels decreased from August to September and had reached 81-83% saturation (~ 7.7 - 8.0 mg L^{-1}) by late September.
- Chlorophyll — Some of the main trends were highlighted above. Additionally, it was noted that the nearfield area was often a transition point between coastal and offshore water systems. On the inshore western side of the nearfield, vertical profiles of chlorophyll displayed peak concentrations throughout the surface layer, whereas on the offshore eastern side, the surface layer had low chlorophyll and there was a distinct subsurface chlorophyll maximum regularly present within the pycnocline. In the middle of the field, distinct surface and subsurface chlorophyll peaks sometimes occurred simultaneously. There was a strong linear relationship between chlorophyll and total nitrogen (TN) that roughly confirmed previously-reported patterns. Differences in the vertical distribution of chlorophyll, grading from inshore to offshore across the nearfield, appear to reflect fundamental differences in the source of nitrogen

supply during this stratified period, with surface horizontal transport dominating inshore and vertical flux from bottom waters dominating offshore.

- Phytoplankton — Total phytoplankton counts were correlated with chlorophyll concentration. Where chlorophyll was low and cell counts were $< 10^6$ cells L^{-1} , microflagellates dominated. For samples with cell counts $> 10^6$ cells L^{-1} , diatoms characteristically accounted for the majority of the total cells. Dinoflagellates were not numerically significant. The principal diatom species in late August included *Leptocylindrus danicus*, *Rhizosolenia delicatula*, and *Cerataulina pelagica*; these were found Baywide and occurred at both the surface and chlorophyll maximum sampling depths. The succession of dominant taxa at the surface of station N10P from early August to late September included the above diatoms, microflagellates, cryptomonads, and two other diatoms, *Skeletonema costatum* and *Asterionellopsis glacialis*. *A. Glacialis* alone had attained counts of 2×10^6 cells L^{-1} in late September.

Zooplankton and metabolism data were collected only on the farfield survey in late August, and they provided the following specific results:

- Zooplankton — Highest zooplankton counts were found in the nearfield. A gradient in zooplankton abundance, similar to the chlorophyll gradient from Boston Harbor to the nearfield, was lacking. In general, the abundances of zooplankton and phytoplankton did not co-vary in the Bay. Principal dominant zooplankton taxa, in terms of abundance, were the small copepods, *Oithona similis* and *Paracalanus parvus*, a usual finding. The zooplankton community was fairly consistent, in terms of species composition, across the Bay. *Acartia tonsa*, typically an estuarine indicator species, was present at stations in western Massachusetts Bay that are directly influenced by exported water from Boston Harbor. Interestingly, *A. tonsa* was also present in western Cape Cod Bay.
- Metabolism — Calculated production rates ranged from < 1 mg C $m^{-2} d^{-1}$ to > 4 g C $m^{-2} d^{-1}$. Estimates were generally highest when derived from incubation of a sample taken near the surface, rather than from a subsurface chlorophyll maximum layer. Rates derived from Productivity-Irradiance (P-I) incubations favorably compared to rates predicted using a composite variable ($BZ_p I_0$) derived from the average chlorophyll biomass, the depth of the photic zone, and incident irradiance. The result strengthens the conclusion of a previous modeling comparison with February-June 1993 data that showed the simple $BZ_p I_0$ approach to be valid and cost-effective for estimating production rates in many seasons.

Observations were made on interactions among irradiance, chlorophyll distributions, production, mixing, and nutrients. For example, under stratified conditions, the depth below which chlorophyll concentrations and modeled production rates rapidly declined generally received mid-day irradiance comparable to that in P-I incubations which produced rates in the range where P became dependent on I ($150-300 \mu E m^{-2} sec^{-1}$) and therefore below P_{max} . In the few cases where the water column was well mixed, vertical profiles of chlorophyll and production did not appear to be strictly controlled by light extinction in the water column. A comparison of chlorophyll-nutrient-production patterns between June 1993 and August 1993

data suggested that there were differences between the months in the degree of nutrient- and light-limitation; more importantly, the comparison illustrated the subtlety and complexity of interpreting interaction results when there are a number of interacting factors that influence primary production.

Water column respiration was detected more routinely in samples from the surface than those from depth. Statistically significant rates ranged from 0.008 to 0.038 mg O₂ L⁻¹ d⁻¹. Highest rates were found at the edge of the Harbor, but several nearfield locations with high chlorophyll and/or production in the upper 20 m of the water column also had relatively high respiration rates. However, only 40% of the bottle-incubations of sub-pycnocline water exhibited a statistically significant rate, and even then, the rates were low. Notably, survey-to-survey monitoring of DO in nearfield bottom water also revealed a slow decline; interestingly, the decline was fairly regular in spite of high production and marked increases in chlorophyll biomass in surface layers during August-September 1993.

CONTENTS

Executive Summary		iii
List of Tables		ix
List of Figures		x
1.0 INTRODUCTION		1-1
1.1 Background		1-1
1.2 Survey Objectives		1-2
1.3 Survey Schedule for 1993 Baseline Water Quality Monitoring Program		1-4
1.4 Summary of Accomplishments: Early August to Late September 1993		1-4
2.0 METHODS		2-1
2.1 Field Procedures		2-1
2.1.1 Hydrographic and Water Sampling Stations		2-1
2.1.2 Productivity Measurements		2-2
2.1.3 Respiration Measurements		2-3
2.2 Laboratory Procedures		2-3
2.3 Data Analyses		2-4
3.0 RESULTS OF EARLY AUGUST 1993 NEARFIELD SURVEY (W9310)		3-1
3.1 Distribution of Water Properties from Vertical Profiling		3-1
3.2 Distribution of Water Properties from Towing		3-2
3.3 Water Types and Analysis of Small-Scale Variability		3-3
4.0 RESULTS OF LATE AUGUST 1993 COMBINED FARFIELD/NEARFIELD SURVEY (W9311)		4-1
4.1 Farfield Survey		4-1
4.1.1 Horizontal Distribution of Surface Water Properties		4-1
4.1.2 Water Properties Along Selected Vertical Sections		4-2
4.1.3 Analysis of Water Types		4-3
4.1.4 Distribution of Chlorophyll and Phytoplankton		4-5
4.1.5 Distribution of Zooplankton		4-7
4.1.6 Metabolism: ¹⁴ C Production and Oxygen Respiration Measurements		4-8
4.2 Nearfield Survey		4-10
4.2.1 Distribution of Water Properties from Vertical Profiling		4-10
4.2.2 Distribution of Water Properties from Towing		4-11
4.2.3 Water Types and Analysis of Small-Scale Variability		4-12

5.0	RESULTS OF EARLY SEPTEMBER 1993 NEARFIELD SURVEY (W9312)	5-1
5.1	Distribution of Water Properties from Vertical Profiling	5-1
5.2	Distribution of Water Properties from Towing	5-3
5.3	Water Types and Analysis of Small-Scale Variability	5-4
6.0	RESULTS OF LATE SEPTEMBER 1993 NEARFIELD SURVEY (W9313)	6-1
6.1	Distribution of Water Properties from Vertical Profiling	6-1
6.2	Distribution of Water Properties from Towing	6-2
6.3	Water Types and Analysis of Small-Scale Variability	6-3
7.0	DISCUSSION OF THE LATE-SUMMER/ EARLY FALL PERIOD OF SURVEYS	7-1
7.1	Water Properties	7-1
	7.1.1 Variability at the Regional Scale	7-1
	7.1.2 Variability in the Nearfield	7-1
	7.1.3 Coherence of Nearfield and Farfield Station Properties	7-2
	7.1.4 Special Features: Comparison of 1993 with 1992	7-2
7.2	Water Column Nutrient Dynamics	7-3
	7.2.1 Vertical Structure and Initiation of Seasonal Mixing	7-3
	7.2.2 Inshore-Offshore Gradients	7-4
	7.2.3 Special Features: Comparison of 1993 with 1992	7-4
7.3	Biology in Relation to Water Properties and Nutrient Dynamics	7-5
	7.3.1 Phytoplankton-Zooplankton Relationships and Plankton-Water Property Trends	7-5
	7.3.2 Chlorophyll Biomass and Nutrients	7-6
	7.3.3 Metabolism and Environment	7-8
	7.3.4 Special Features: Comparison of 1993 with 1992	7-10
7.4	Summary and Recommendations	7-11
8.0	REFERENCES	8-1
Appendices	A Station Data Tables and Instrument Calibration Data	26 pp
	B Vertical Profile Data from Farfield and Nearfield Stations	120 pp
	C Comparison of Vertical Profile Data: Scatter Plots	9 pp
	D Additional Towing Profile Data from Nearfield Stations	1 pp
	E Metabolism Data and Productivity-Irradiance Modeling	40 pp
	F Phytoplankton Species Data Tables	9 pp
	G Zooplankton Species Data Tables	7 pp

Note to reader: Appendices A-G are bound separately from this technical report. To request the Appendices, contact the MWRA and ask for one of the MWRA Miscellaneous Publications entitled "Appendices to Water Quality Monitoring in Massachusetts and Cape Cod Bays: August and September 1993."

LIST OF TABLES

- 1-1. Schedule of water quality surveys for calendar year 1993
- 2-1. Field samples and measurements [from Albro *et al.*, 1993]
- 2-2. Water samples to be collected from Niskin or GO-FLO bottles [from Albro *et al.*, 1993]
- 2-3. Laboratory analysis and methods [from Albro *et al.*, 1993]
- 4-1a. Top five dominant phytoplankton taxa in near-surface samples collected in August 1993
- 4-1b. Top five dominant phytoplankton taxa collected from the chlorophyll maximum in August 1993
- 4-2a. Abundance of all identified taxa in near-surface screened (20 μm) samples collected on the farfield survey in August 1993
- 4-2b. Abundance of all identified taxa in chlorophyll-maximum screened (20 μm) samples collected on the farfield survey in August 1993
- 4-3. ^{14}C production ($\text{mg C m}^{-2} \text{ d}^{-1}$) estimated for euphotic layer at BioProductivity stations in August 1993
- 7-1. Abundance of the top five dominant phytoplankton taxa in near-surface whole-water samples at station N10P collected in August and September 1993
- 7-2. Abundance of all identified phytoplankton taxa in near-surface screened samples

LIST OF FIGURES

- Figure 1-1. Water quality sampling stations in Massachusetts and Cape Cod Bays.
- Figure 1-2. Nearfield survey tracklines for August 28, 1993.
- Figure 3-1a. Scatter plots of data acquired by *in situ* sensor package during vertical downcasts at all nearfield stations occupied in early August 1993.
- Figure 3-1b. Scatter plots of data acquired by *in situ* sensor package during vertical downcasts at all nearfield stations occupied in early August 1993.
- Figure 3-2a. DIN vs. depth in early August 1993.
- Figure 3-2b. NH₄ and NO₃ vs. depth in early August 1993.
- Figure 3-2c. PO₄ and SiO₄ vs. depth in early August 1993.
- Figure 3-3a. DIN vs. salinity in early August 1993.
- Figure 3-3b. NH₄ and NO₃ vs. salinity in early August 1993.
- Figure 3-3c. PO₄ and SiO₄ vs. salinity in early August 1993.
- Figure 3-4a. Vertical section contours of temperature generated for tow-yo profiling in early August 1993.
- Figure 3-4b. Vertical section contours of temperature generated for tow-yo profiling in early August 1993.
- Figure 3-5a. Vertical section contours of σ_T generated for tow-yo profiling in early August 1993.
- Figure 3-5b. Vertical section contours of σ_T generated for tow-yo profiling in early August 1993.
- Figure 3-6a. Vertical section contours of fluorescence (as $\mu\text{g Chl L}^{-1}$) generated for tow-yo profiling in early August 1993.
- Figure 3-6b. Vertical section contours of fluorescence (as $\mu\text{g Chl L}^{-1}$) generated for tow-yo profiling in early August 1993.
- Figure 4-1. Surface temperature ($^{\circ}\text{C}$) in the study area in late August 1993.
- Figure 4-2. Surface salinity (PSU) in the study area in late August 1993.

- Figure 4-3. Surface beam attenuation (m^{-1}) in the study area in late August 1993.
- Figure 4-4. Surface *in situ* fluorescence (as $\mu g \text{ Chl L}^{-1}$) in the study area in late August 1993.
- Figure 4-5. Surface dissolved inorganic nitrogen (DIN, μM) in the study area in late August 1993.
- Figure 4-6. Surface nitrate (NO_3 , μM) in the study area in late August 1993.
- Figure 4-7. Surface phosphate (PO_4 , μM) in the study area in late August 1993.
- Figure 4-8. Surface silicate (SiO_4 , μM) in the study area in late August 1993.
- Figure 4-9. Map showing position of four standard transects for which vertical contour plots were produced in following Figures 4-10 to 4-14.
- Figure 4-10a. Vertical section contours of temperature in late August 1993 for standard transects (see Figure 4-9).
- Figure 4-10b. Vertical section contours of salinity in late August 1993 for standard transects (see Figure 4-9).
- Figure 4-10c. Vertical section contours of density (σ_T) in late August 1993 for standard transects (see Figure 4-9).
- Figure 4-11. Vertical section contours of fluorescence (as $\mu g \text{ Chl L}^{-1}$) in late August 1993 for standard transects (see Figure 4-9).
- Figure 4-12. Vertical section contours of beam attenuation in late August 1993 for standard transects (see Figure 4-9).
- Figure 4-13. Vertical section contours of dissolved oxygen (% saturation) in late August 1993 for standard transects (see Figure 4-9).
- Figure 4-14a. Vertical section contours of dissolved inorganic nitrogen (DIN, μM) in late August 1993 for standard transects (see Figure 4-9).
- Figure 4-14b. Vertical section contours of silicate (SiO_4 , μM) in late August 1993 for standard transects (see Figure 4-9).
- Figure 4-15a. Scatter plots of data acquired by *in situ* sensor package during vertical casts at all farfield and nearfield stations occupied in late August 1993.
- Figure 4-15b. Scatter plots of data acquired by *in situ* sensor package during vertical casts at all farfield and nearfield stations occupied in late August 1993.

- Figure 4-16. Map to show station groups designated in Figures 4-17 through 4-22.
- Figure 4-17. Scatter plots of nitrogen forms vs. phosphate during late August 1993.
- Figure 4-18. Scatter plots of nitrogen vs. silicate during late August 1993.
- Figure 4-19. Dissolved inorganic nitrogen vs. salinity in late August 1993.
- Figure 4-20. Ammonia and nitrate vs. salinity in late August 1993.
- Figure 4-21. Phosphate and silicate vs. salinity in late August 1993.
- Figure 4-22. Nitrogen forms vs. salinity in late August 1993.
- Figure 4-23. Chlorophyll (extracted samples) at BioProductivity stations and special station F25 as a function of depth in late August 1993.
- Figure 4-24. Total phytoplankton abundance vs. chlorophyll (extracted samples) at BioProductivity stations in late August 1993.
- Figure 4-25a. Total phytoplankton abundance, by taxonomic groups, at the surface of BioProductivity stations in late August 1993.
- Figure 4-25b. Total phytoplankton abundance, by taxonomic groups, at the chlorophyll maximum of BioProductivity stations in late August 1993.
- Figure 4-26. Zooplankton abundance, by groups, at BioProductivity stations in late August 1993.
- Figure 4-27. Estimated ^{14}C production and chlorophyll (integrated for the photic zone) in late August 1993.
- Figure 4-28a. Scatter plots for nearfield stations in late August. Compare to Figure 4-15.
- Figure 4-28b. Scatter plots for nearfield stations in late August. Compare to Figure 4-15.
- Figure 4-29. DIN vs. depth in late August 1993.
- Figure 4-30a. NH_4 and NO_3 vs. depth in late August 1993.
- Figure 4-30b. PO_4 and SiO_4 vs. depth in late August 1993.
- Figure 4-31a. Vertical section contours of temperature generated for tow-yo profiling in late August 1993.

- Figure 4-31b. Vertical section contours of temperature generated for tow-yo profiling in late August 1993.
- Figure 4-32a. Vertical section contours of σ_T generated for tow-yo profiling in late August 1993.
- Figure 4-32b. Vertical section contours of σ_T generated for tow-yo profiling in late August 1993.
- Figure 4-33a. Vertical section contours of fluorescence (as $\mu\text{g Chl L}^{-1}$) generated for tow-yo profiling in late August 1993.
- Figure 4-33b. Vertical section contours of fluorescence (as $\mu\text{g Chl L}^{-1}$) generated for tow-yo profiling in late August 1993.
- Figure 5-1a. Scatter plots of data acquired by *in situ* sensor package during vertical downcasts at all nearfield stations occupied in early September 1993.
- Figure 5-1b. Scatter plots of data acquired by *in situ* sensor package during vertical downcasts at all nearfield stations occupied in early September 1993.
- Figure 5-2a. DIN vs. depth in early September 1993.
- Figure 5-2b. NH_4 and NO_3 vs. depth in early September 1993.
- Figure 5-2c. PO_4 and SiO_4 vs. depth in early September 1993.
- Figure 5-3a. DIN vs. salinity in early September 1993.
- Figure 5-3b. NH_4 and NO_3 vs. salinity in early September 1993.
- Figure 5-3c. PO_4 and SiO_4 vs. salinity in early September 1993.
- Figure 5-4a. Vertical section contours of temperature generated for tow-yo profiling in early September 1993.
- Figure 5-4b. Vertical section contours of temperature generated for tow-yo profiling in early September 1993.
- Figure 5-5a. Vertical section contours of σ_T generated for tow-yo profiling in early September 1993.
- Figure 5-5b. Vertical section contours of σ_T generated for tow-yo profiling in early September 1993.
- Figure 5-6a. Vertical section contours of fluorescence (as $\mu\text{g Chl L}^{-1}$) generated for tow-yo profiling in early September 1993.

- Figure 5-6b. Vertical section contours of fluorescence (as $\mu\text{g Chl L}^{-1}$) generated for tow-yo profiling in early September 1993.
- Figure 6-1a. Scatter plots of data acquired by *in situ* sensor package during vertical downcasts at all nearfield stations occupied in late September 1993.
- Figure 6-1b. Scatter plots of data acquired by *in situ* sensor package during vertical downcasts at all nearfield stations occupied in late September 1993.
- Figure 6-2a. DIN vs. depth in late September 1993.
- Figure 6-2b. NH_4 and NO_3 vs. depth in late September 1993.
- Figure 6-2c. PO_4 and SiO_4 vs. depth in late September 1993.
- Figure 6-3a. DIN vs. salinity in late September 1993.
- Figure 6-3b. NH_4 and NO_3 vs. salinity in late September 1993.
- Figure 6-3c. PO_4 and SiO_4 vs. salinity in late September 1993.
- Figure 6-4a. Vertical section contours of temperature generated for tow-yo profiling in late September 1993.
- Figure 6-4b. Vertical section contours of temperature generated for tow-yo profiling in late September 1993.
- Figure 6-5a. Vertical section contours of σ_T generated for tow-yo profiling in late September 1993.
- Figure 6-5b. Vertical section contours of σ_T generated for tow-yo profiling in late September 1993.
- Figure 6-6a. Vertical section contours of fluorescence (as $\mu\text{g Chl L}^{-1}$) generated for tow-yo profiling in late September 1993.
- Figure 6-6b. Vertical section contours of fluorescence (as $\mu\text{g Chl L}^{-1}$) generated for tow-yo profiling in late September 1993.
- Figure 7-1. Comparison of the nearfield region in 1993 to the annual cycle of 1992: temperature ($^{\circ}\text{C}$).
- Figure 7-2. Comparison of the nearfield region in 1993 to the annual cycle of 1992: dissolved oxygen (mg/L).

- Figure 7-3. Comparison of the nearfield region in 1993 to the annual cycle of 1992: dissolved inorganic nitrogen (μM).
- Figure 7-4. Zooplankton abundance compared to the average chlorophyll concentration ($n=2$) in the water column in late August 1993.
- Figure 7-5. Chlorophyll and total nitrogen in samples from late August 1993.
- Figure 7-6. ^{14}C production compared to the composite parameter BZ_pI_o for late August 1993.
- Figure 7-7. Comparison of the nearfield region in 1993 to the annual cycle of 1992: chlorophyll ($\mu\text{g/L}$).

1.0 INTRODUCTION

This report is the fourth of five periodic water column reports for water quality monitoring conducted in 1993 for the Massachusetts Water Resources Authority (MWRA) Harbor and Outfall Monitoring Program. The report includes results from four surveys conducted during August and September 1993; each of these surveys included sampling at 21 stations in the nearfield. The late August survey was a combined farfield/nearfield survey that covered 25 additional stations throughout Massachusetts Bay and Cape Cod Bay. Data on physical, chemical, and biological measurements at the stations are presented and interrelationships of these measurements are examined.

The structure of this report is as follows:

- Section 1. Background information on the water quality surveys conducted in 1993.
- Section 2. Field, laboratory, and data analysis methods.
- Sections 3-6. Results of surveys, in chronological order (early August nearfield survey, late August farfield/nearfield survey, early September nearfield survey, late September nearfield survey).
- Section 7. Discussion of the late summer/early fall surveys.

All tables and figures are presented at the end of each section. An extensive set of appendices is bound separately. The appendices provide supporting tables and plots that represent the data being stored in the MWRA database.

1.1 Background

The MWRA is implementing a long-term monitoring plan for the future MWRA effluent outfall that will be located in Massachusetts Bay (Figure 1-1). The purpose of monitoring is to verify compliance with the conditions of the NPDES discharge permit and to assess the potential environmental impact of effluent discharge into Massachusetts Bay. A detailed description of the monitoring and its rationale is provided in the Effluent Outfall Monitoring Plan (MWRA, 1991).

To help establish the present conditions with respect to water properties, nutrients, and other important parameters of eutrophication, the MWRA contracted with Battelle Ocean Sciences to conduct baseline water-quality surveys throughout Massachusetts Bay between 1992 and 1994. Results of the 1992 surveys were presented in a series of three periodic reports (Kelly *et al.*, 1992; Kelly *et al.*, 1993a,b), summarized in an annual report (Kelly *et al.*, 1993c), and used to examine nutrient issues related to the offshore outfall (Kelly, 1994). Three earlier periodic water column reports for 1993 covered surveys conducted from February through July (Kelly *et al.*, 1994a,b,c).

Serving the MWRA's need for rapid dissemination of data and information, the periodic report series also provides a preliminary synthesis of monitoring results. The technical approach used in 1993 to implement the water quality portion of this monitoring plan is presented in a combined work/quality assurance project plan (CW/QAPP; Albro *et al.*, 1993) that was developed specifically for water quality monitoring. The CW/QAPP describes the technical activities performed at sea and in the laboratory, as well as the data quality requirements and assessments, project management, and a schedule of activities and deliverables. In addition, individual survey plans were submitted to MWRA for each survey to provide important operational details. The survey reports submitted for the four surveys discussed in this periodic report describe actual survey tracks, samples collected, and other survey details (Dragos, 1993a,b; Bechtold, 1993; West, 1993). The survey reports should be consulted for pertinent details concerning the sampling tracks and samples obtained at each station. Data reports on nutrients, plankton, and pelagic metabolism have been submitted to MWRA for the surveys conducted during August and September 1993; these data form a portion of the appendices to this report.

1.2 Survey Objectives

The objectives of the water quality surveys are discussed in detail in the MWRA Effluent Outfall Monitoring Plan (MWRA, 1991) and are summarized as follows:

Physical Oceanography

- Obtain high-resolution measurements of water properties throughout Massachusetts Bay.
- Use vertical-profile data at selected sites in Massachusetts and Cape Cod Bays for analysis of large-scale spatial (tens of kilometers) and temporal (seasonal) variability in water properties, and to provide supporting data to help interpret biological and chemical data.
- Use high-resolution, near-synoptic, water-property measurements along transects within the nearfield for analysis of smaller-scale spatial (kilometers) and temporal (semi-monthly) variability in water properties, and develop a three-dimensional picture of water properties near the future outfall.

Nutrients

- Obtain nutrient measurements in water that is representative of Massachusetts and Cape Cod Bays.
- Use vertical-profile data at selected sites in Massachusetts and Cape Cod Bays for analysis of large-scale spatial (tens of kilometers) and temporal (seasonal) variability in nutrient concentrations and to provide supporting data to help to interpret biological data.
- Use vertical-profile data along transects of closely-spaced stations within the nearfield for analysis of smaller-scale spatial (kilometers) and temporal (semi-monthly) variability in nutrient concentrations, and develop a three-dimensional understanding of the nutrient field near the future outfall.

Plankton

- Obtain high-quality identification and enumeration of phytoplankton and zooplankton in water that is representative of Massachusetts and Cape Cod Bays.
- Use vertical-profile data at selected sites in Massachusetts and Cape Cod Bays for analysis of large-scale spatial (tens of kilometers) and temporal (seasonal) variability in plankton distribution.

Water Column Respiration and Production

- Using water that is representative of Massachusetts and Cape Cod Bays, obtain a reasonable estimate of the rates of water-column respiration and production as a function of irradiance.

General

- Evaluate the utility of various measurements to detect change or to help explain observed change.
- Provide data to help modify the monitoring program to allow a more efficient means of attaining monitoring objectives.
- Use the data appropriately to describe the water-quality conditions (over space and time) in Massachusetts and Cape Cod Bays.

1.3 Survey Schedule for 1993 Baseline Water Quality Monitoring Program

Throughout 1993 and 1994, Battelle and its subcontractors, the University of Rhode Island (URI) and the University of Massachusetts at Dartmouth (UMD), have been conducting surveys similar to those initiated in 1992. The schedule of surveys conducted in 1993 is given in Table 1-1. The survey schedule was designed to match the 1992 schedule. The surveys discussed in this report were conducted during the weeks planned: August 11-12 (Survey W9310), August 24-28 (Survey W9311), September 8-9 (W9312), and September 28-29 (W9313).

1.4 Summary of Accomplishments: Early August to Late September 1993

For the combined farfield/nearfield survey in late August (W9311), *in situ* measurements were taken and samples were collected at the stations shown in Figure 1-1. Samples for laboratory analyses were collected to obtain the following types of data:

- Dissolved inorganic nutrients: nitrate, nitrite, ammonium, phosphate, and silicate.
- Chlorophyll *a* and phaeopigments in extracts of filtered water.
- *In situ* fluorometric measurements of chlorophyll, optical-beam transmittance (attenuation), light irradiance, salinity, temperature, and dissolved oxygen.
- Total suspended solids and dissolved oxygen in discrete water samples.

- Organic nutrients: dissolved carbon, nitrogen, and phosphorus; particulate carbon and nitrogen.
- Phytoplankton and zooplankton identification and enumeration.
- Rates of water-column production (^{14}C) vs. irradiance from shipboard incubations.
- Rates of water-column dark respiration (dissolved oxygen) from shipboard incubations.

For the nearfield surveys, one day was dedicated to vertical profiling, including collection of the following data:

- Dissolved inorganic nutrients: nitrate, nitrite, ammonium, phosphate, and silicate.
- *In situ* fluorometric measurements of chlorophyll, optical-beam transmittance (attenuation), light irradiance, salinity, temperature, and dissolved oxygen.
- Chlorophyll *a* and phaeopigments in extracts of filtered water, as well as oxygen samples for titration, all to be used to calibrate *in situ* readings.
- Phytoplankton samples for analysis and archival.

A second day of each nearfield survey was dedicated to high-resolution "tow-yo" profiling. With the towfish oscillating from near surface to near bottom as the ship progressed at 4 to 7 kt, the towfish containing the *in situ* sensors (as above, minus irradiance) was used to obtain profiles along the nearfield tracks between the vertical stations. The trackline from survey W9311, for example, is shown in Figure 1-2.

Samples that were collected for analysis have been analyzed, and *in situ* sensor measurements have been calibrated and processed. Both types of data are presented in this report and all are summarized in accompanying Appendices A through G.

Table 1-1. Schedule of water quality surveys for calendar year 1993. This report provides data from the surveys conducted in August and September 1993.

SURVEY	SURVEY DATES
W9301 (Combined Farfield/Nearfield)	Feb 23-27
W9302 (Combined Farfield/Nearfield)	Mar 09-12
W9303 (Nearfield)	Mar 24-25
W9304 (Combined Farfield/Nearfield)	Apr 06-10
W9305 (Nearfield)	Apr 29-May 1
W9306 (Nearfield)	May 20-21
W9307 (Combined Farfield/Nearfield)	Jun 22-26
W9308 (Nearfield)	Jul 07-08
W9309 (Nearfield)	Jul 28-29
W9310 (Nearfield)	Aug 11-12
W9311 (Combined Farfield/Nearfield)	Aug 24-28
W9312 (Nearfield)	Sep 08-09
W9313 (Nearfield)	Sep 28-29
W9314 (Combined Farfield/Nearfield)	
W9315 (Nearfield)	
W9316 (Nearfield)	

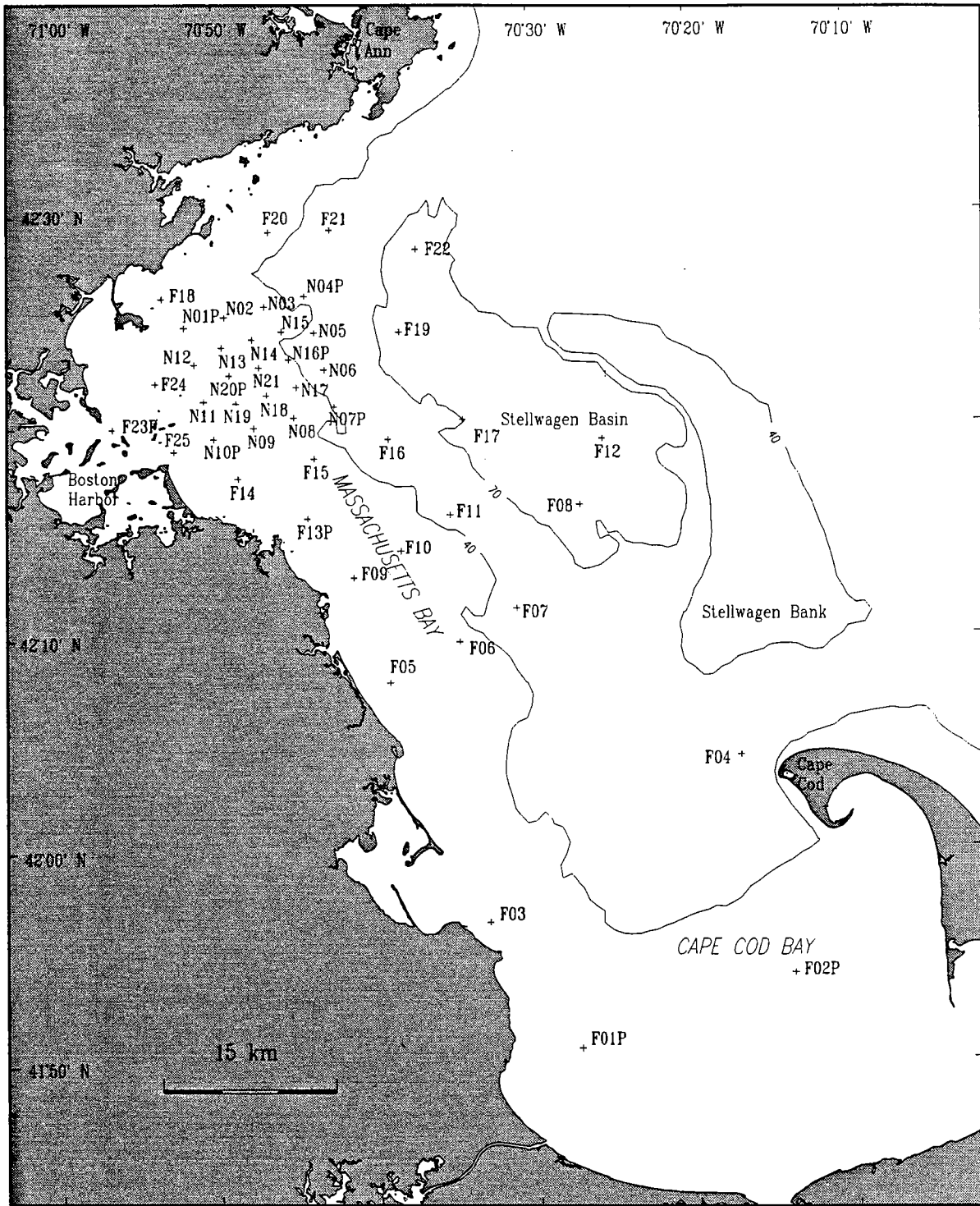


Figure 1-1. Water quality sampling stations in Massachusetts and Cape Cod Bays. Station codes — F: Farfield, N: Nearfield, P: Biology/Productivity. Depth contours are in meters.

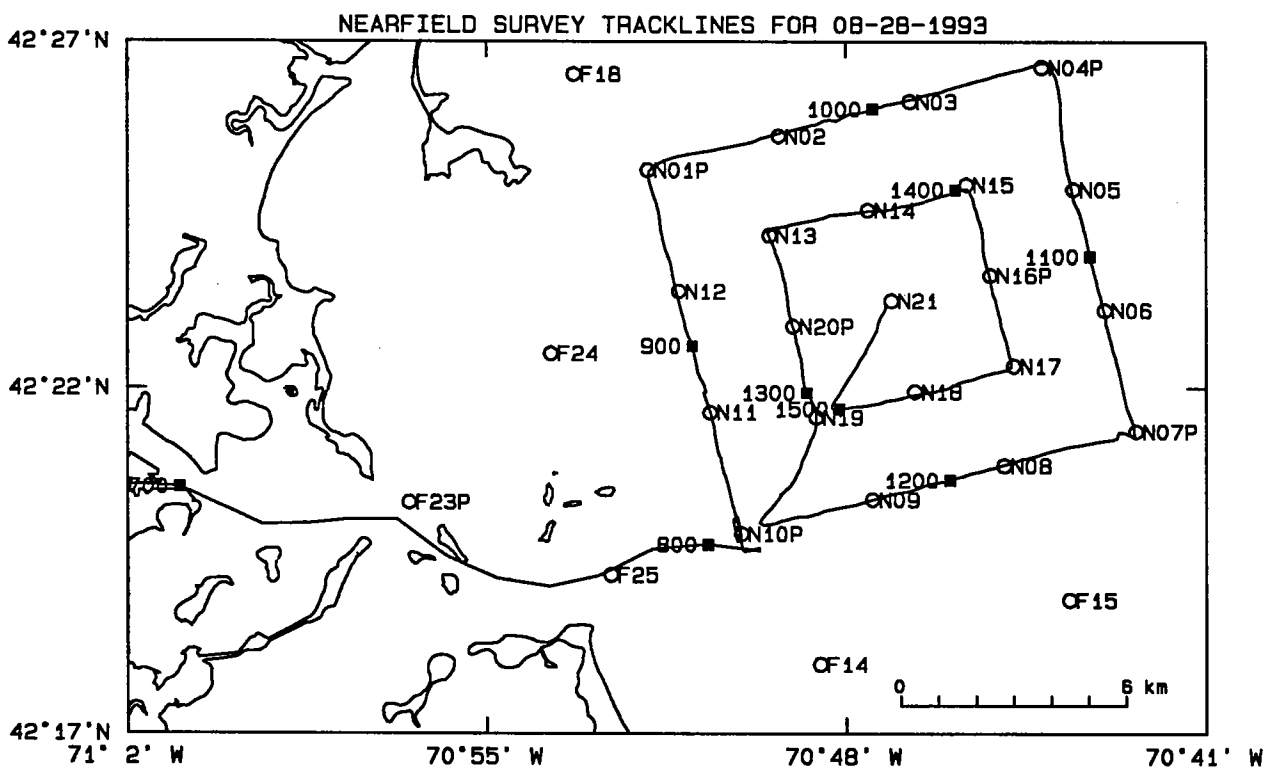


Figure 1-2. Nearfield survey tracklines for August 28, 1993. Tow-yo operations were conducted clockwise from N10P to N10P and from N19 to N19. Tow-yo operations were also conducted along transects between N10P and N19, and between N19 and N21. The hour of the day is indicated along the track. [From Dragos, 1993b]

2.0 METHODS

Field sampling equipment and procedures, sample handling and custody, sample processing and laboratory analysis, and instrument performance specifications and data quality objectives are discussed in the water quality monitoring CW/QAPP (Albro *et al.*, 1993). The plan is detailed and should be consulted for standard survey methods. In general, only deviations from the CW/QAPP are described in this report.

2.1 Field Procedures

2.1.1 Hydrographic and Water Sampling Stations

Tables 2-1 and 2-2 summarize the planned sampling, and indicate the types of measurements and samples taken at nearfield and farfield stations (Albro *et al.*, 1993). For a combined farfield/nearfield survey, additional biology/productivity measurements were made at a subset of 10 stations (4 farfield and 6 nearfield); these stations are termed "BioProductivity" stations and labeled with a "P" (see Figure 1-1). The six "P" stations in the nearfield were repeatedly sampled for a broad suite of parameters as part of the farfield survey, again during hydrographic profiling—dissolved nutrient stations on the vertical sampling day of nearfield survey, and lastly as part of the towing track sampled on a second day of the nearfield survey. Nearly all planned samples were collected. Principal deviations from the CW/QAPP for each survey are given below; most deviations are reported in the appropriate survey report that was prepared after the completion of each survey.

In addition to the methods described in the CW/QAPP, the following procedures were applicable to the early August nearfield survey(W9310):

- Dissolved oxygen samples were collected from five depths at six "P" stations and were used to calibrate the dissolved oxygen sensor (Appendix A).
- One bottle sample for nutrients (station N02) was not collected due to malfunction of the Niskin sampler.

In addition to the methods described in the CW/QAPP, the following procedures were applicable to the combined farfield/nearfield survey in late August (W9311):

- No samples were collected for oxygen incubations to determine production. Production measurements were made using ^{14}C (described below). However, oxygen samples were collected at 21 stations at 3 to 5 depths and were used to calibrate the dissolved oxygen sensors (Appendix A). Also, samples were incubated for determination of dark-bottle respiration. This was the second survey of the year for which respiration was measured.
- Chlorophyll samples were taken at 15 stations (2 or 3 depths) and were used to calibrate the *in situ* fluorescence sensor (Appendix A). In addition to chlorophyll, a sample for total suspended solids was collected at station F25, as well as at the planned stations.

In addition to the methods described in the CW/QAPP, the following procedure was applicable to the nearfield survey in early September (W9312) and late September (W9313):

- Dissolved oxygen samples were collected from five depths at six "P" stations and were used to calibrate the dissolved oxygen sensor (Appendix A).

2.1.2 Productivity Measurements

Productivity measurements differed slightly from those described in the CW/QAPP. First, at the request of MWRA and due to the preference of the Outfall Monitoring Task Force, only the ^{14}C method was used to estimate primary production; the oxygen light-dark method was not used. At two depths of each BioProductivity station, ^{14}C primary production was measured by exposing samples to a

light gradient as described by Albro *et al.* (1993) for the oxygen method. Fifteen 300-mL BOD bottles were inoculated with 2.5 μCi of ^{14}C -sodium bicarbonate. Three bottles were incubated in the dark. The remaining 12 bottles were exposed to irradiance levels ranging from about 20 to 2000 $\mu\text{E m}^{-2} \text{sec}^{-1}$, with several bottles exposed in the range of 200-600 $\mu\text{E m}^{-2} \text{sec}^{-1}$. Samples for dissolved inorganic carbon (DIC) were taken from the same GO-FLO bottle as samples used for productivity incubations. DIC was analyzed as described in the next section and was used to calculate primary production rates (Section 2.3).

2.1.3 Respiration Measurements

Following practices established for the June 1993 (W9307) survey (Kelly *et al.*, 1994c), dark-bottle incubations in 300-mL BOD bottles were conducted for approximately 8 h, rather than for 6 h as stated in the CW/QAPP. Incubations were lengthened to measure the relatively low respiration rates suggested by the 4- to 6-h incubations conducted during the summer 1992 studies. Results of the respiration calculations are included in Appendix E and follow the procedures described in the CW/QAPP.

2.2 Laboratory Procedures

Table 2-3 summarizes laboratory methods for chemistry and biology samples as detailed in the CW/QAPP. The DIC method used by URI is a "purge-and-trap" method (I.O. Corp., 1984) and was not described in the CW/QAPP. Samples are collected in a 40-mL screw-cap VOC vial with a septum. The bottle is filled and overflowed, the sample is then "killed" with mercury chloride, and the bottle is sealed. In the laboratory, the vial is placed in a total carbon analyzer where the vial septum is pierced. A sample is then withdrawn, acidified, bubbled with nitrogen (N_2) and the carbon dioxide (CO_2) in the gas stream is collected on a molecular sieve. The sieve is heated to 200°C, releasing the CO_2 into a

new stream of N₂, the carrier gas that transports the CO₂ to an IR detector where the CO₂ content is measured.

The difference between replicates, estimated from samples taken and reported in the first 1993 periodic report (Kelly *et al.*, 1994a), averaged < 1% ($\bar{x} \pm \sigma = 0.47\% \pm 0.73\%$, range = 0.08-2.68%, $n = 12$). The average difference between sampling replicates was also < 1% ($\bar{x} \pm \sigma = 0.25\% \pm 0.31\%$, range = 0.01-0.81%, $n = 6$).

2.3 Data Analyses

To calculate ¹⁴C production rates, the data for light bottles were first corrected by subtracting uptake measured in dark bottles. Volumetric production rates were then calculated, as described in the CW/QAPP (Albro *et al.*, 1993). The dark-bottle uptake was calculated as the mean of the three dark bottles, excluding samples where a value was an outlier, as determined by statistical testing using the Dixon Criterion (Appendix E).

The Dixon Criterion (Natrella, 1963) evaluates the relative range between values in an ordered set. Thus, if three values (X_1 , X_2 , and X_3) are arranged from lowest to highest, the criterion for the *highest* value being an outlier is

$$X_3 = (X_3 - X_2)/(X_3 - X_1)$$

The criterion for the *lowest* value being an outlier is

$$X_1 = (X_2 - X_1)/(X_3 - X_1)$$

These calculated values may be compared to a tabled value. For example, if X_3 or X_1 exceed 0.941, then there is a 95% chance that the value in question is an outlier.

X_3 and X_1 are calculated for each set of three dark-bottles replicates. When X_3 or X_1 exceeds the tabled value of 0.941 for $n=3$, the outlier is rejected and not used in calculations. Appendix E provides results of testing for data collected on survey W9311.

The P-I curve modeling for ^{14}C differed slightly from that described for oxygen in the CW/QAPP. A sequence of two models was used to fit data from ^{14}C incubations. Dark-corrected values were normalized to chlorophyll determined for the sample depth being measured. Following this, a sequence of two models was used to fit the data.

The first model fit three parameters, including a photoinhibition term, and followed the Platt *et al.* (1980) model to predict net production

$$P_B = P_{SB} (1 - e^{-a}) e^{-b}$$

where

- P_B = production (chlorophyll-normalized)
- P_{SB} = theoretical maximum production (chlorophyll-normalized) without photoinhibition
- a = $\alpha I/P_{SB}$
- b = $\beta I/P_{SB}$
- α = initial slope of the rise in net production with light increasing from zero irradiance [units of $(\mu\text{gC } \mu\text{gChl}^{-1} \text{ h}^{-1})/(\mu\text{E m}^{-2} \text{ sec}^{-1})$], calculated from I (light irradiance level, $\mu\text{E m}^{-2} \text{ sec}^{-1}$) and P_{SB} .

In the CW/QAPP and in the first periodic report for 1993 (Kelly *et al.*, 1994a), the second model used was a hyperbolic tangent function (Platt and Jassby, 1976). Although Platt *et al.* (1980) claim equivalence of the two models in terms of α and P_{\max} , Frenette *et al.* (1993) have shown this not to be the case. For the second model, following the suggestion of Frenette *et al.* (1993), the negative exponential formulation given by Webb *et al.* (1974) was used.

Here $P_B = P_{max} [1 - e (-\alpha I/P_{max})]$
 P_{max} = light-saturated maximal productivity and
 α = the initial slope for the curve where productivity is proportional to light intensity (I)

The two models are equivalent where the photoinhibition term (b) is zero. Note that use of this second model marks a return to that used in initial modeling for 1992, minus only a respiration term (cf. Kelly *et al.*, 1992).

The parameters in each model were fit simultaneously by least squares using the NLIN procedure in SAS (1985) for each incubation series that measured paired P_B and irradiance. Fitting was accomplished where parameters were estimated if, within 50 iterations, the model converged on a suitable simultaneous fit (SAS, 1985). A derivative-free method was used that compares favorably with methods using partial derivatives (Frenette *et al.*, 1993). If the three-parameter model (Platt *et al.*, 1980) fitting did not converge on a fit, the two-parameter model (Webb *et al.*, 1974) was used. Volumetric production rates, chlorophyll-normalized P-I curves, and model coefficients (Appendix E), were used to calculate integrated water column rates of production, which were expressed as a rate per square meter of surface generally following the procedure described by Kelly *et al.* (1993c) which is briefly described in the following text.

Because irradiance varies throughout the day and stations are sampled at different times, the light conditions were standardized. Within a survey, the average incident irradiance (I_0) measured by the deck cell during a mid-day (1000 to 1400 h) period was used to standardize conditions. Then, for each station an extinction coefficient (k) was determined by regressing $\ln(I_z/I_0)$ vs. depth, where I_z is the irradiance at depth Z , and the slope of the resultant line estimates k . The coefficient (k) was then used with the survey I_0 to generate the standardized light profile using the model $I_0 = I_z e^{-kz}$ and to determine $Z_{0.5\% I_0}$. Estimated rates were expressed per square meter of surface and integrated to the depth where photosynthetically active radiation (PAR) equals 0.5% of PAR incident at the surface. A 1% to 0.5% isolume ($Z_{0.5\% I_0}$) is commonly accepted as the level to which net production (in excess of respiration) is achieved by plankton.

Next, for each station and each incubation series ("surface" or "chlorophyll maximum" sample), the fitted P-I model was combined with the standardized light profile to yield chlorophyll-normalized production rates ($\mu\text{gC } \mu\text{gChl}^{-1} \text{ h}^{-1}$) at 0.5-m intervals to coincide with 0.5-m BIN-averaged chlorophyll values generated from a vertical downcast. To calculate depth-integrated rates, the predicted hourly, chlorophyll-normalized rate was then multiplied by the chlorophyll fluorescence at each depth interval from the surface to the $Z_{0.5\% I_0}$. The values were then appropriately summed over depth and units were converted to m^{-2} from a volumetric basis.

The above procedure estimated hourly mid-day rates. Conversion to full day-time rates was made by multiplying by 7, a factor which recognizes that about 55-60% of the production generally occurs during the 4-h period (1000-1400 h) when the irradiance is highest (Vollenweider, 1966). Final modeled rates provide an estimate of day-time primary production as $\text{mgC } \text{m}^{-2} \text{ d}^{-1}$.

The same procedure was applied to both surface and chlorophyll-maximum samples, each of which yielded independent estimates at each station. For the productivity incubations conducted as part of survey W9311, these estimates are listed in a table (Section 4) that summarizes P-I modeling results (provided in detail in Appendix E).

Table 2-1. Field samples and measurements [from Albro et al., 1993].

Parameter	Stations	Sample Volume	Sample Containers	Shipboard Processing/ Preservation
Following samples are subsampled from water collected with Poly Vinyl Chloride Niskin GO-FLO Bottles				
Dissolved Inorganic Nutrients	All	60 mL	100 mL polyethylene bottle	Pass through a filter. Fix with chloroform.
Dissolved Oxygen	10 Biology/ Productivity and 3 Nearfield	300 mL	300 mL glass BOD	Fix per Oudot <i>et al.</i> (1988). Titrate within 24 h.
Dissolved Organic Carbon	10 Biology/ Productivity and F25	50 mL	100 mL amber glass bottle	Pass through a pre-ashed glass fiber filter. Fix with 0.5 mL of phosphoric acid.
Dissolved Organic Nitrogen	10 Biology/ Productivity and F25	20 mL	50 mL glass digestion tube	Pass through a filter. Digest within 8 h.
Dissolved Organic Phosphorus	10 Biology/ Productivity and F25	20 mL	50 mL glass digestion tube	Pass through a filter. Digest within 8 h.
Particulate Organic Carbon	10 Biology/ Productivity and F25	50 mL	Whatman GF/F glass fiber filter	Pass through a pre-ashed glass fiber filter. Freeze (-5 °C).
Particulate Organic Nitrogen	10 Biology/ Productivity and F25	50 mL	Whatman GF/F glass fiber filter	Pass through a pre-ashed glass fiber filter. Freeze (-5 °C).
Total Suspended Solids	10 Biology/ Productivity and 3 Nearfield	200 mL	Petri dish	Pass through a filter. Freeze (-5 °C)
Chlorophyll <i>a</i> / Phaeopigments	10 Biology/ Productivity and 3 Nearfield	2 x 10 mL	Whatman GF/F glass fiber filter	Pass through filter. Fix with 1% MgCO ₃ solution, wrap in foil, store over desiccant, and refrigerate.
Phytoplankton (Whole Water)	10 Biology/ Productivity	800 mL	1000 mL glass bottle	Preserve with Utermohl's solution.
Phytoplankton (Screened Water)	10 Biology/ Productivity	2000 mL	100 mL polyethylene bottle	Strain through a 20- μ m mesh; wash retained organisms into a jar. Fix with Utermohl's solution.
¹⁴ C Production	10 Biology/ Productivity	300 mL	300 mL glass BOD	Inoculate with 2.5 μ Ci of Na ₂ ¹⁴ CO ₃ and incubate.
Following sample is collected with a vertically towed net				
Zooplankton	10 Biology/ Productivity	800 mL	1000 mL glass bottle	Wash into jar. Fix with a 5-10% formalin solution.
The following measurements are collected by the Battelle Ocean Sampling System				Precision
Conductivity	All	---	Floppy disk	0.01 mS/cm
Temperature	All	---	Floppy disk	0.001 °C
Pressure	All	---	Floppy disk	0.01 decibars
Dissolved Oxygen	All	---	Floppy disk	0.05 mg/L
Chlorophyll <i>a</i> Fluorescence	All	---	Floppy disk	0.01 μ g/L
Transmissometry	All	---	Floppy disk	0.01 m ⁻¹
<i>In situ</i> Irradiance	All	---	Floppy disk	1 μ E m ⁻² s ⁻¹
Surface Irradiance	All	---	Floppy disk	1 μ E m ⁻² s ⁻¹
Bottom Depth	All	---	Floppy disk	1 m
Navigational Position	All	---	Floppy disk	0.00017 deg

Table 2-2. Water samples to be collected from Niskin or GO-FLO bottles [from Albro et al., 1993].

Refer to Notes Below for Stations IDs	Nearfield Nutrient/Hydrography Surveys						Biology/Productivity Surveys			Farfield Nutrient/Hydrography Surveys				Totals for all Surveys		
	Note 1	Note 2	Note 3	Note 4	Note 5	Totals per Survey	Totals for 32 Surveys	Note 6	Totals per Survey	Totals for 12 Surveys	Note 7	Note 8	Totals per Survey		Totals for 12 Surveys	
Number of Hydrographic Stations	1	5	3	3	9	21	672	10	10	120	20	1	21	252	1044	
Dissolved Inorganic Nutrients	5	5	5	5	5	105	3360	5	50	600	5	5	105	1260	5220	
Chlorophyll a and Phaeopigments (2 reps)				2		6	192	2	20	240					0	432
Total Suspended Solids (2 reps)				2		6	192	2	20	240					0	432
Dissolved Organic Nitrogen and Phosphorus (2 reps)								2	20	240		2	2	24	264	264
Dissolved Organic Carbon								2	20	240		2	2	24	264	264
Particulate Carbon and Nitrogen (2 reps)								2	20	240		2	2	24	264	264
Phytoplankton (whole water) to analyze	1					1	32	2	20	240						272
Phytoplankton (whole water) to archive			1			5	160	3	30	360						520
Phytoplankton (screened) to analyze	1					1	32	2	20	240						272
Phytoplankton (screened) to archive			1			5	160	3	30	360						520
Initial Dissolved Oxygen (Note 9)				2		6	192	9	90	1080						1272
Respiration (Note 9)								9	90	1080						1080
Pmax by Carbon-14 (Note 10)								12	120	1440						1440
Pmax by Oxygen (Note 11)								6	60	720						720
P(l) by Carbon-14 (Note 12)								20	200	2400						2400
P(l) by Oxygen (Note 12)								20	200	2400						2400
Zooplankton								1	10	120						120

Notes:

- 1 Station N10P
- 2 Stations N01P, N04P, N07P, N16P, and N20P
- 3 Any 3 nearfield stations
- 4 Any 3 nearfield stations (the same or different ones from Note 3)
- 5 Nine Stations not used for oxygen or chlorophyll a calibrations
- 6 Stations F01P, F02P, F13P, F23P, N01P, N04P, N07P, N10P, N16P, and N20P
- 7 All farfield stations except F25
- 8 Station F25
- 9 Collect 3 samples at 3 depths
- 10 Collect 6 samples at 2 depths
- 11 Collect 3 samples at 2 depths
- 12 Collect 10 samples at 2 depths

Table 2-3. Laboratory Analysis and Methods [From Albro et al., 1993]

<i>Parameter</i>	<i>Units</i>	<i>Method</i>	<i>Reference¹</i>	<i>Maximum Holding Time</i>	<i>Preservation</i>
Dissolved Ammonia	μM	Technicon II AutoAnalyzer	Lambert and Oviatt (1986)	3 mo.	Chloroform
Dissolved Nitrate	μM	Technicon II AutoAnalyzer	Lambert and Oviatt (1986)	3 mo.	Chloroform
Dissolved Nitrite	μM	Technicon II AutoAnalyzer	Lambert and Oviatt (1986)	3 mo.	Chloroform
Dissolved Phosphate	μM	Technicon II AutoAnalyzer	Lambert and Oviatt (1986)	3 mo.	Chloroform
Dissolved Silicate	μM	Technicon II AutoAnalyzer	Lambert and Oviatt (1986)	3 mo.	Chloroform
Dissolved Oxygen	mg L^{-1}	Autotitrator	Oudot <i>et al.</i> (1988)	24 h	dark/cool
Dissolved Organic Carbon	μM	O.I. Model 700 TOC Analyzer	Menzel and Vaccaro (1964)	3 mo.	Fix with 0.5 mL of phosphoric acid.
Dissolved Organic Nitrogen	μM	Technicon II AutoAnalyzer	Valderrama (1981)	3 mo.	Add reagents immediately, heat to 100°C within 8 hours.
Dissolved Organic Phosphorus	μM	Technicon II AutoAnalyzer	Valderrama (1981)	3 mo.	Add reagents immediately, heat to 100°C within 8 hours.
Particulate Organic Carbon	μM	Carlo Erba Model 1106 CHN elemental analyzer	Lambert and Oviatt (1986)	3 mo.	Dry over desiccant.
Particulate Organic Nitrogen	μM	Carlo Erba Model 1106 CHN elemental analyzer	Lambert and Oviatt (1986)	3 mo.	Dry over desiccant.
Total Suspended Solids	mg L^{-1}	Cahn Electrobalance	See Section 12.7.7	6 mo.	Dry over desiccant.
Chlorophyll <i>a</i> / Phaeopigments	$\mu\text{g L}^{-1}$	Model 111 Turner Fluorometer	Lorenzen (1966)	2 wk	Fix with 1% MgCO_3 solution, wrap in foil, store over desiccant, and refrigerate.
Phytoplankton (Whole Water)	Cells L^{-1}	Sedgwick-Rafter counting chambers	Turner <i>et al.</i> (1989)	3 y	Preserved with Utermohl's solution, store at room temperature.
Phytoplankton (Screened Water)	Cells L^{-1}	Sedgwick-Rafter counting chambers	Turner <i>et al.</i> (1989)	3 y	Fix with Utermohl's solution, store at room temperature.
¹⁴ C Production	$^{14}\text{C hr}^{-1}$	Liquid Scintillation Counter (Bechman LS-3801)	Strickland and Parsons (1972)	2 wk	Scintillation fluid
Zooplankton	Cells L^{-1}	Dissecting Microscope	Turner <i>et al.</i> (1989)	3 y	Fix with a 5-10% Formalin solution, store at room temperature.

¹See Section 20 of Albro *et al.*, 1993 for literature references.

3.0 RESULTS OF EARLY AUGUST 1993 NEARFIELD SURVEY (W9310)

3.1 Distribution of Water Properties from Vertical Profiling

Vertical profiles were obtained at all 21 nearfield stations (Appendices A and B). Scatter plots using *in situ* sensor data are shown in Figure 3-1. The range in salinity was narrow, slightly <31 to almost 32 PSU (Figure 3-1a); higher salinity was characteristic of bottom water. In contrast, the range in temperature was broad — sometimes >19°C at the surface and <6°C at depth. Vertical profiles, with minor variation, characteristically displayed a distinct surface layer near 5 m depth, a thermocline/pycnocline from about 5 m to 15-20 m, and a bottom layer underlying this (Appendix B). Beam attenuation ranged from about 0.7 to 2 m⁻¹. Higher readings were associated with lower salinity (near 31 PSU; Figure 3-1a). Profiles show that turbidity was highest in the surface layer of most stations along the western edge of the nearfield; a mid-depth peak in turbidity at about 5-10 m (Appendix B) was observed at several stations in the middle of the field (N18, N19, N21, and N20P). The profiles of turbidity and chlorophyll were usually similar, both in terms of vertical profiles and geographic variation; thus a relationship between the two parameters was apparent (Figure 3-1a). Chlorophyll ranged from near zero to about 7 µg L⁻¹, the latter concentrations reached within the surface layer (Figure 3-1b). At many stations, a mid-depth maximum occurred at 15-20 m, where chlorophyll concentrations were about 1 to 3 µg L⁻¹.

Dissolved oxygen (DO) was supersaturated throughout most of the water column, but generally decreased at each station from the pycnocline down. In water from the bottommost Niskin bottle, DO values ranged between ~9.15 to 10.36 mg L⁻¹. Concentrations were generally 93-99% of saturation but saturation values of 100-106% were measured in the deepest bottle samples from several stations near the middle of the nearfield (N18, N19, N20P, N21) (see Appendix A).

Dissolved inorganic nitrogen (DIN) concentrations $>0.5 \mu\text{M}$ (Figure 3-2a) were limited to only a few samples from the surface 10 m. Below 10-15 m, DIN concentrations increased almost linearly with increasing depth, culminating in values $\sim 6-7 \mu\text{M}$ at 40-50 m. Most of the increase over depth was due to nitrate (NO_3), but ammonium (NH_4) also increased (Figure 3-2b).

Both phosphate (PO_4) and silicate (SiO_4) concentrations increased with depth (Figure 3-2c). Surface water concentrations of phosphate were always well above detection and thus the N/P ratio in surface samples was very low. Concentrations of PO_4 at depth approached $0.8 \mu\text{M}$. At many locations, silicate concentrations were low at the surface and there was more scatter in the relationship with depth than for other nutrient forms. Silicate concentrations reached $6-8 \mu\text{M}$ at intermediate depth, but were only $4 \mu\text{M}$ in the deepest waters sampled.

The patterns of nutrient concentrations relative to salinity demonstrated increasing concentration ranges with higher salinity and, on average, higher concentrations at higher salinity (Figure 3-3). These patterns basically reflect the general changes in parameters over depth. However, the generally broader range in nutrient concentrations at salinities >31.25 PSU may arise from some horizontal variability in water quality across the nearfield at mid-depth.

3.2 Distribution of Water Properties from Towing

Thermal and density layering were noted consistently throughout the nearfield; a sharp thermocline/pycnocline was observed between 5 and 20 m (Figures 3-4 and 3-5). Overall, the spatial pattern was uniform and the only notable physical feature was slightly cooler surface water along the outer western track and station N02 (e.g., Figure 3-4a).

Measurements made during towing resulted in several clear trends for chlorophyll concentrations. First, the vertical distribution varied from inshore to offshore. The middle of the nearfield was a transition point. Inshore from there, chlorophyll was highest near the surface or occurring as a thin layer within the top 5-15 m (Figure 3-6a). A deeper subsurface chlorophyll maximum from 15-30 m

was found at offshore locations. At the transition point, near the location of the inner western track (stations N19-N13; Figure 3-6b), both surface and deeper layers were present. Interestingly, the inshore-offshore transition that was obvious for chlorophyll was less obvious as a transition in physical features (Figures 3-4 and 3-5). On further inspection it was evident that inshore chlorophyll layering tracked along a depth having a temperature near 13°C and a density (σ_T) of -22.75 to 23.5. At the transition area, along the inner western track, this surface was slightly deeper than along the outer western track. The broader, less intense, chlorophyll-maximum layer offshore tracked a different surface, with a temperature near 9°C and a σ_T of 23.5 to 24.5. The second main chlorophyll trend was that the western side of the nearfield regularly had highest chlorophyll concentrations, with values $> 8 \mu\text{g L}^{-1}$ (Figure 3-6b). The third general observation was that the chlorophyll distribution suggested horizontally extensive layers and gradual transitions, rather than a high degree of isolated patchiness.

3.3 Water Types and Analysis of Small-Scale Variability

The general features and trends observed were similar for each day of the two-day survey. On each day, the vertical distribution of parameters near stations N19 and N20P differed slightly from the rest of the field, suggesting that this middle nearfield location was a transitional area between an inshore water type and an offshore water type. This distinction, however, could not easily be made based on physical characteristics. There were no perturbations or irregularities of vertical structure that suggested an inshore-offshore front or upwelling. Some variability in nutrient concentrations with salinity and depth corresponded to the subtle inshore-offshore distinction and, perhaps in part, was related to physical mixing and biological activity in the transition area. But the transition was most evident as a shift in the vertical distribution of biology as indicated by chlorophyll. The shift may relate to nutrient sources. Inshore, the Harbor and shallower coastal waters serve as a source of nutrients to the surface layers; offshore, the main source of nutrients is from enriched bottom waters. Because the shift did not appear to follow a density surface, horizontal mixing along a given layer from inshore to offshore may not have been the main mechanism for controlling chlorophyll distribution beyond the middle of the nearfield. At that point, the strength of vertical nutrient flux from bottom

waters may begin to outweigh the horizontal nutrient mixing across density surfaces. Regardless of mechanism, distinct ecosystems — perhaps functioning differently even if they were taxonomically similar — were apparent in spite of uniform physical layering.

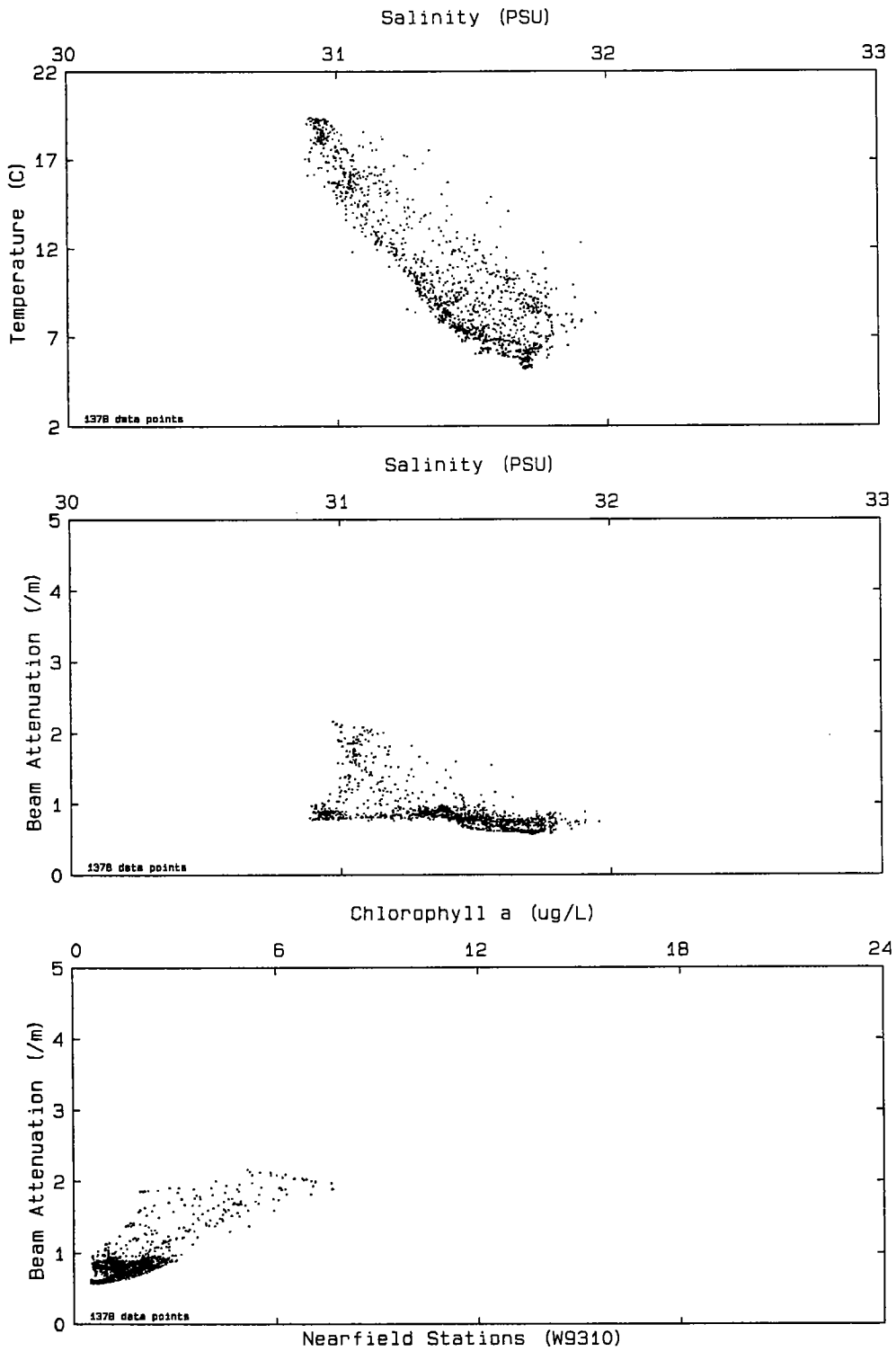


Figure 3-1a. Scatter plots of data acquired by *in situ* sensor package during vertical downcasts at all nearfield stations occupied in early August 1993. Individual station casts that were used to produce this composite are in Appendix B. Chlorophyll is estimated from *in situ* fluorescence.

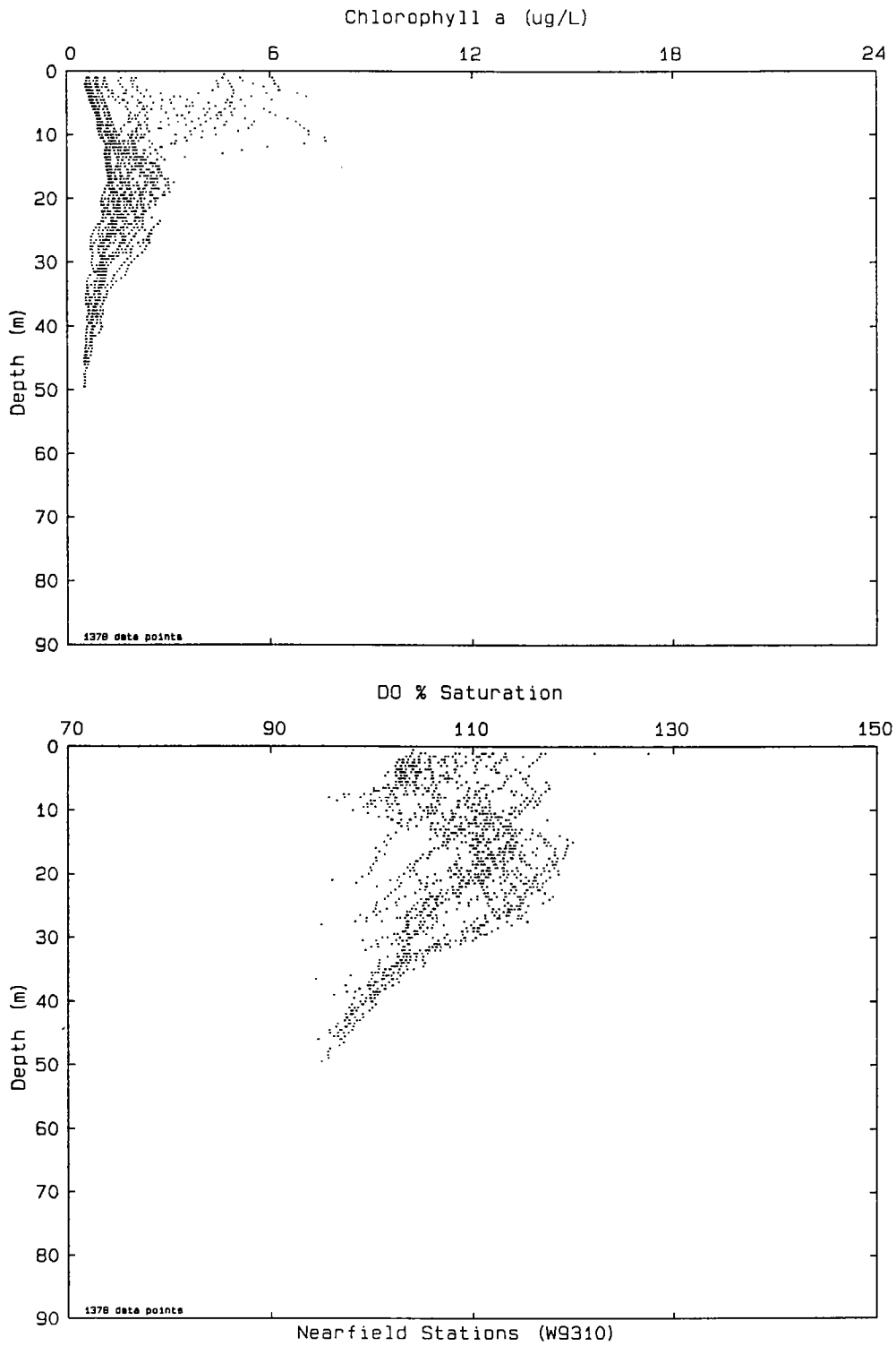


Figure 3-1b. Scatter plots of data acquired by *in situ* sensor package during vertical downcasts at all nearfield stations occupied in early August 1993. Individual station casts that were used to produce this composite are in Appendix B. Chlorophyll is estimated from *in situ* fluorescence.

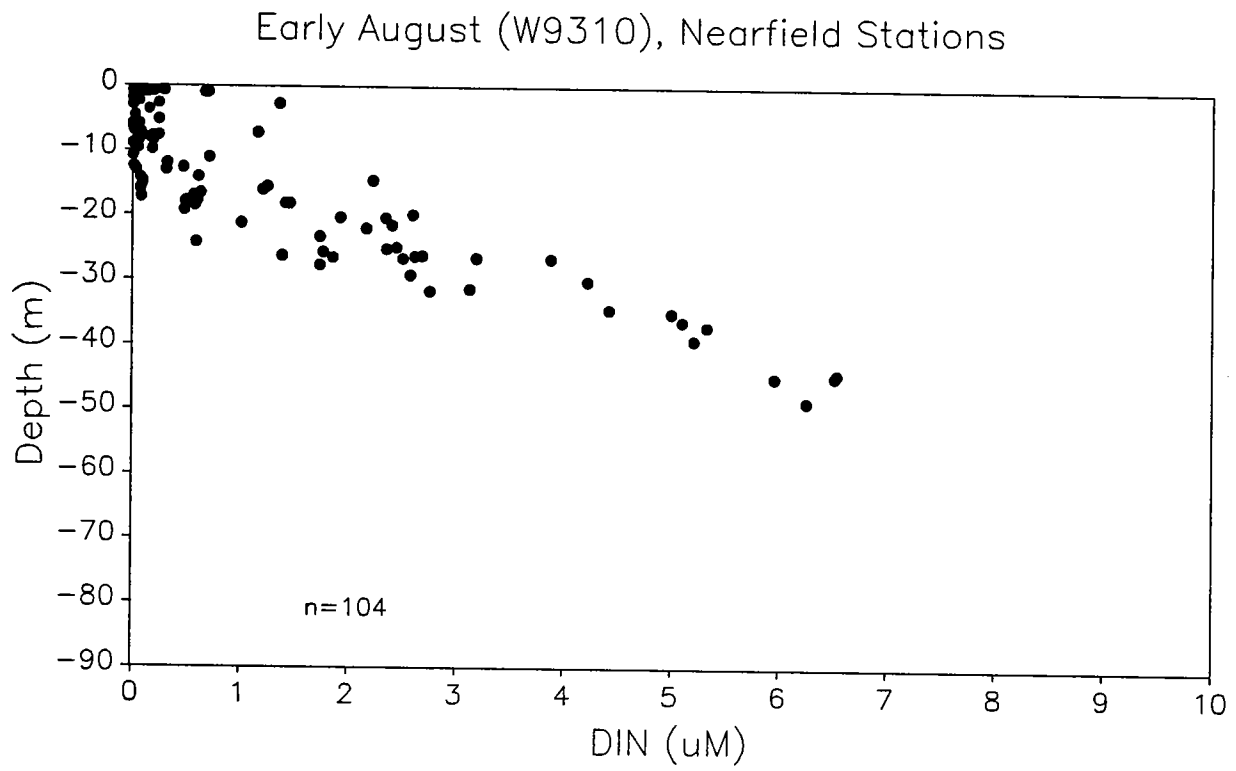
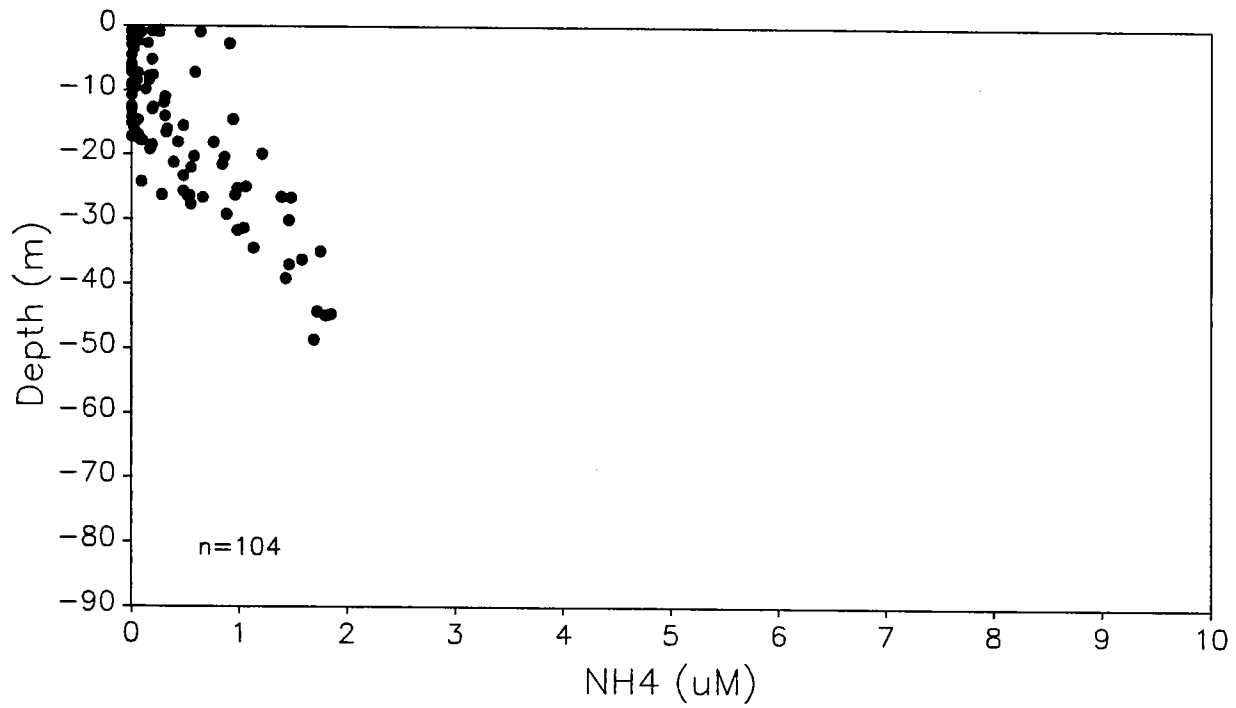


Figure 3-2a. DIN vs. depth in early August 1993.

Early August (W9310), Nearfield Stations



Early August (W9310), Nearfield Stations

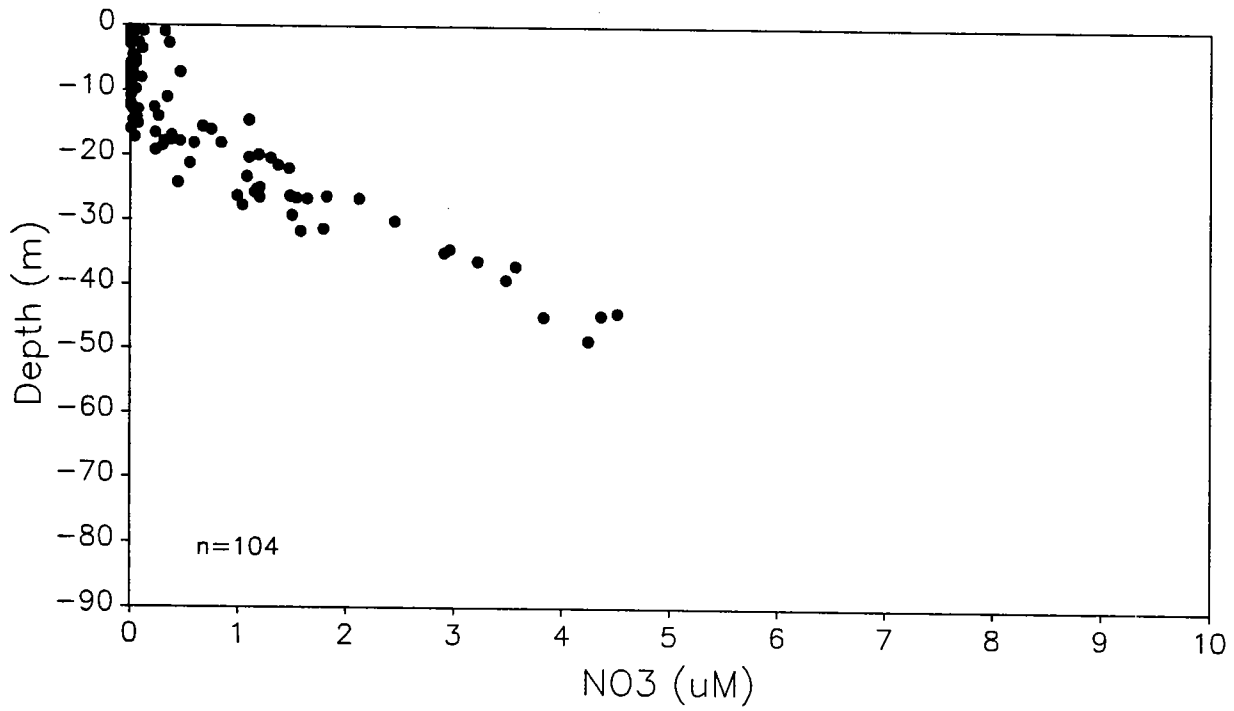
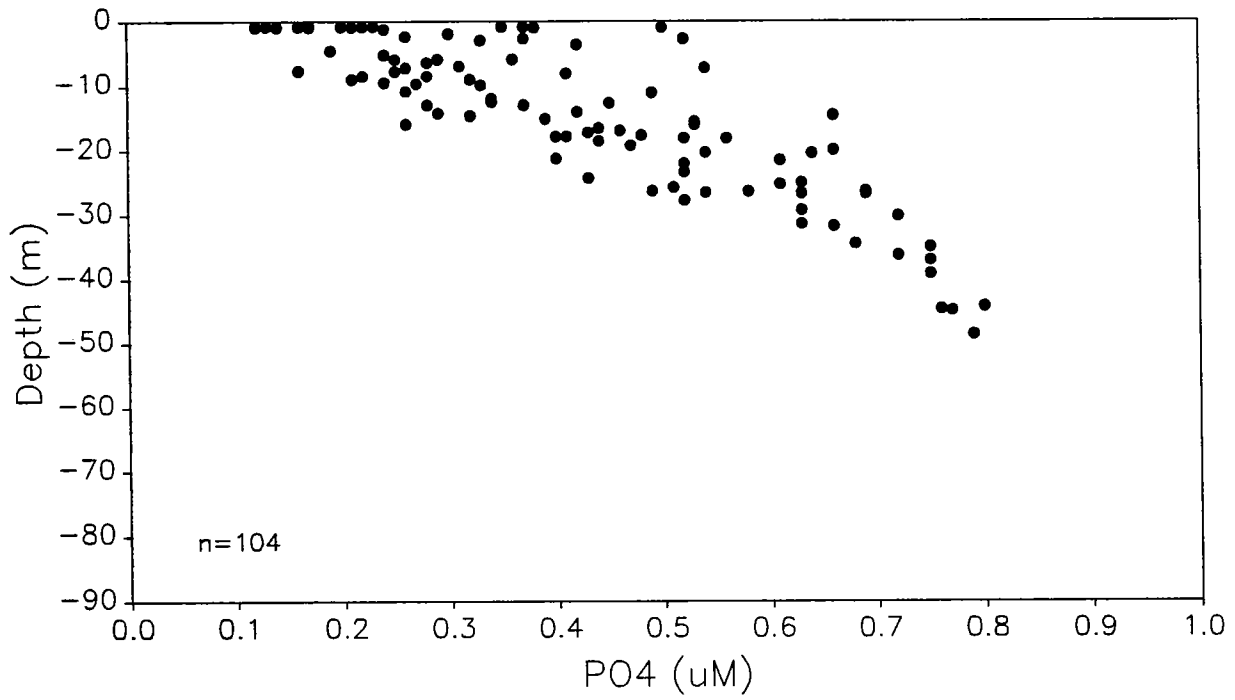


Figure 3-2b. NH_4 and NO_3 vs. depth in early August 1993.

Early August (W9310), Nearfield Stations



Early August (W9310), Nearfield Stations

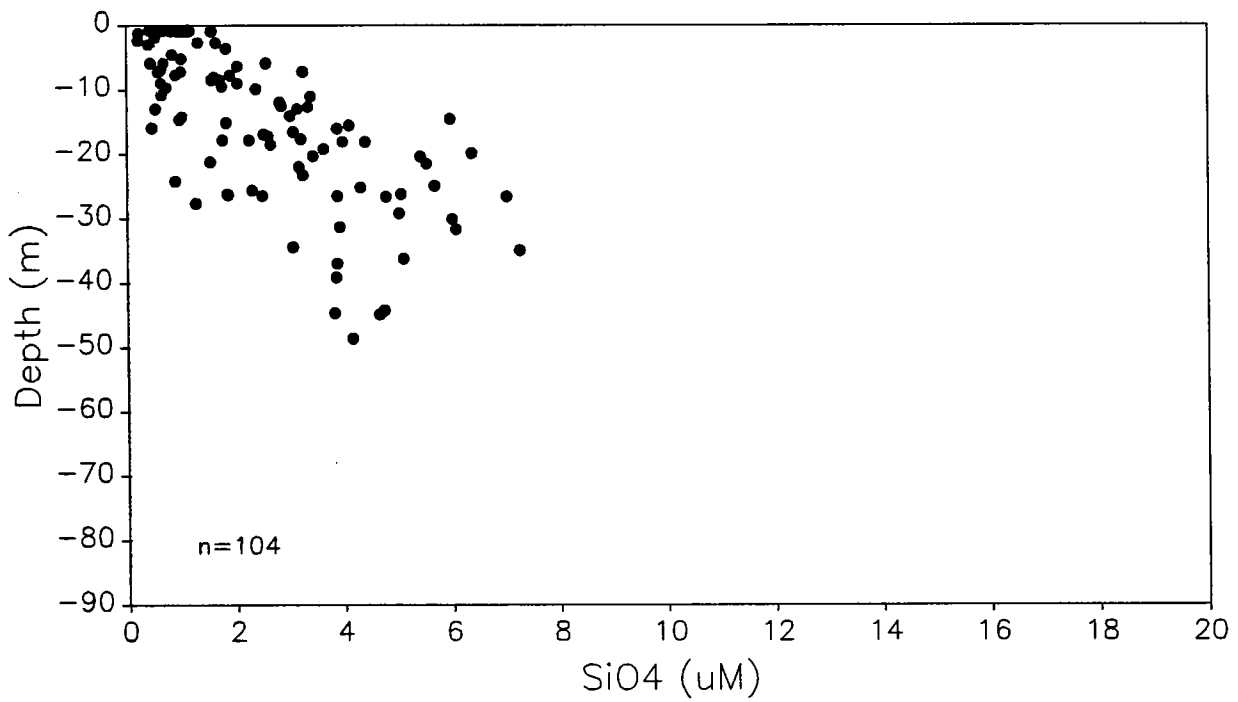


Figure 3-2c. PO₄ and SiO₄ vs. depth in early August 1993.

Early August (W9310), Nearfield Stations

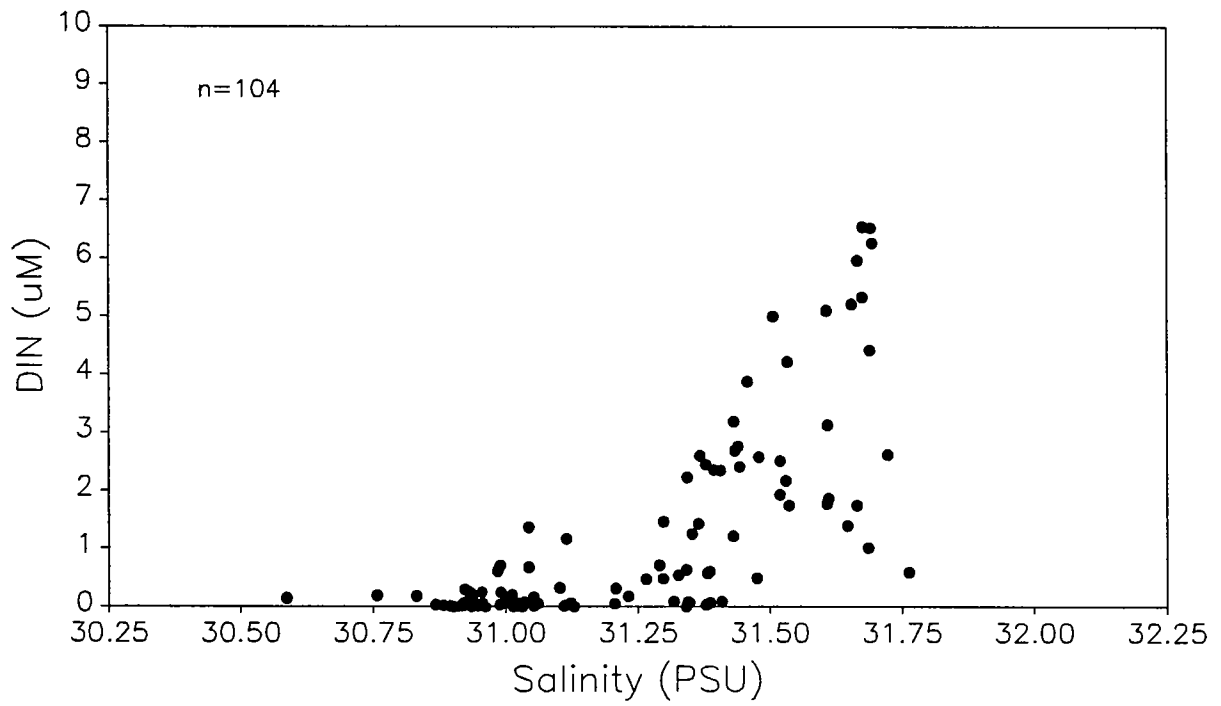
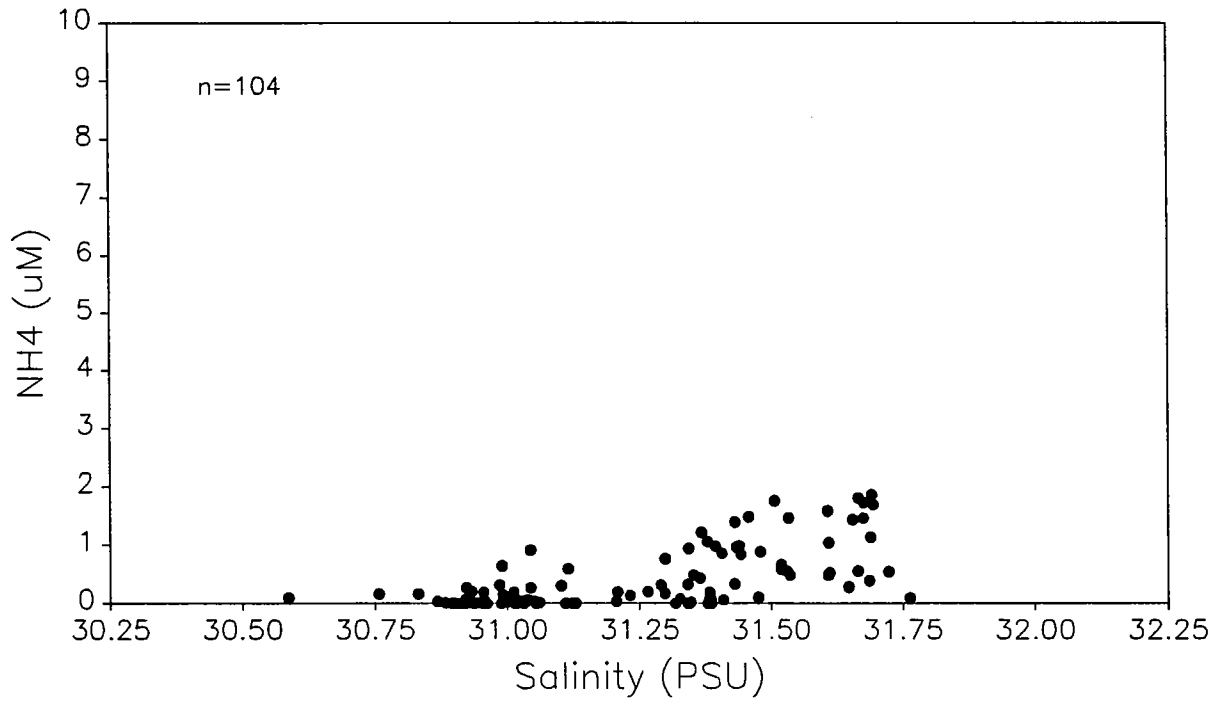


Figure 3-3a. DIN vs. salinity in early August 1993.

Early August (W9310), Nearfield Stations



Early August (W9310), Nearfield Stations

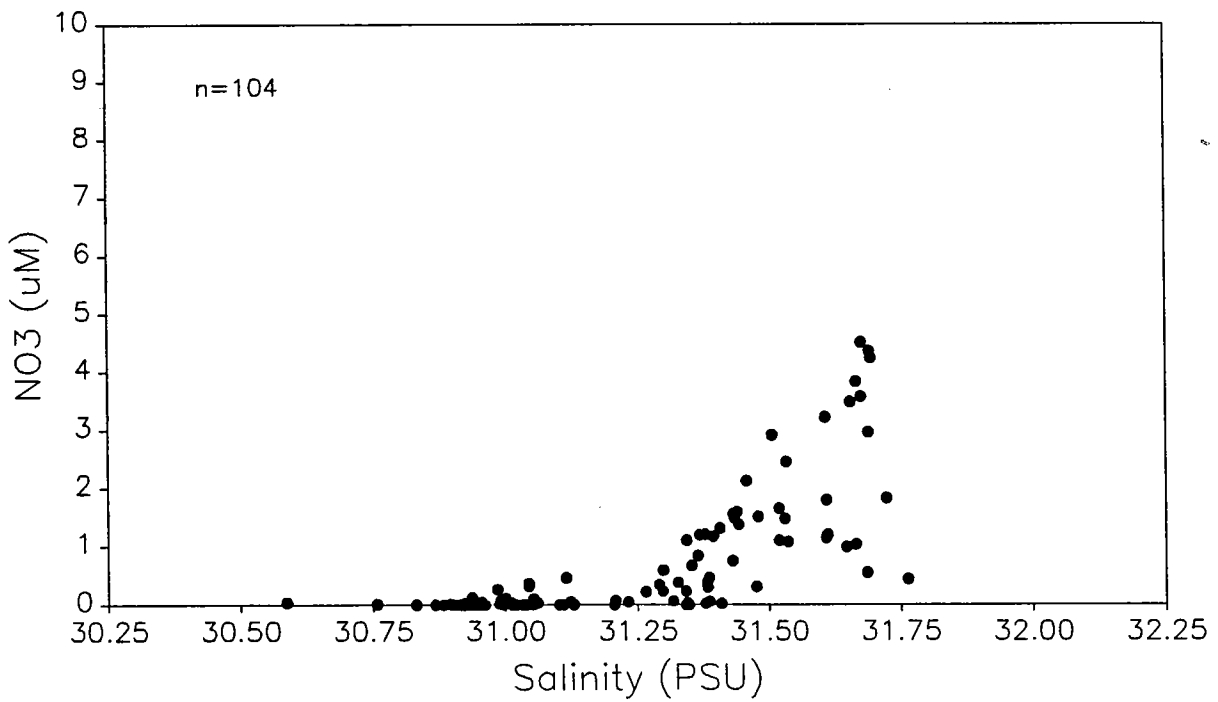
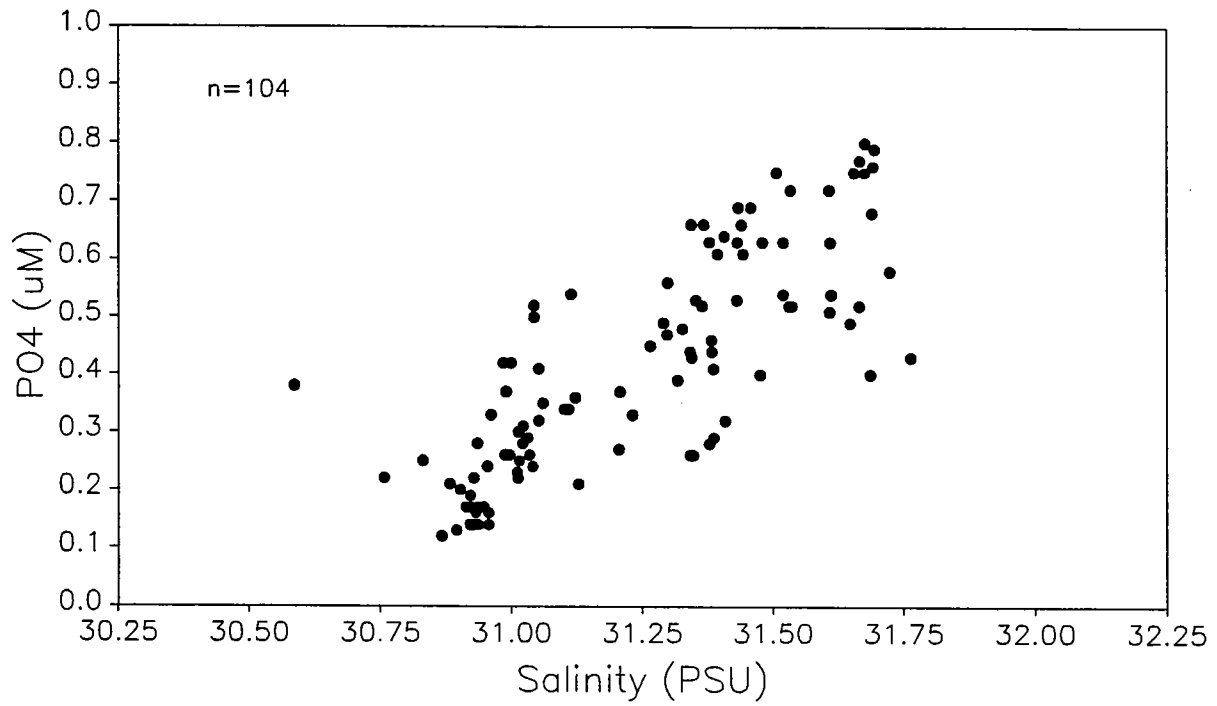


Figure 3-3b. NH_4 and NO_3 vs. salinity in early August 1993.

Early August (W9310), Nearfield Stations



Early August (W9310), Nearfield Stations

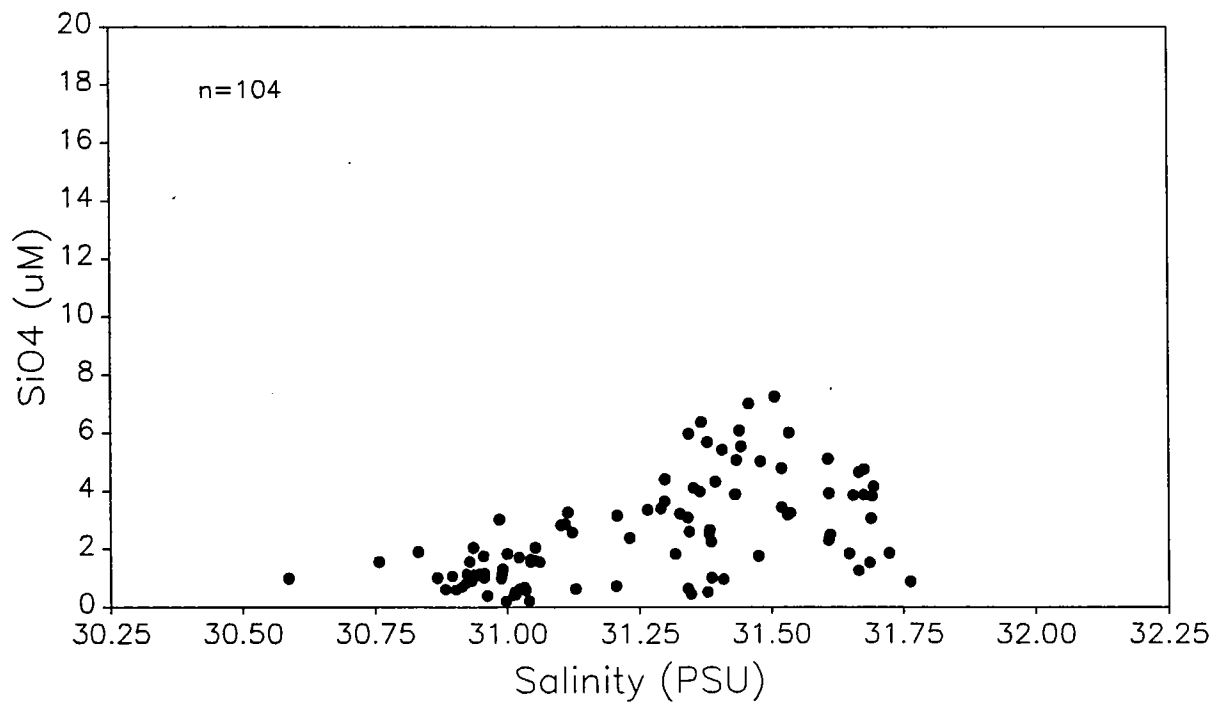


Figure 3-3c. PO₄ and SiO₄ vs. salinity in early August 1993.

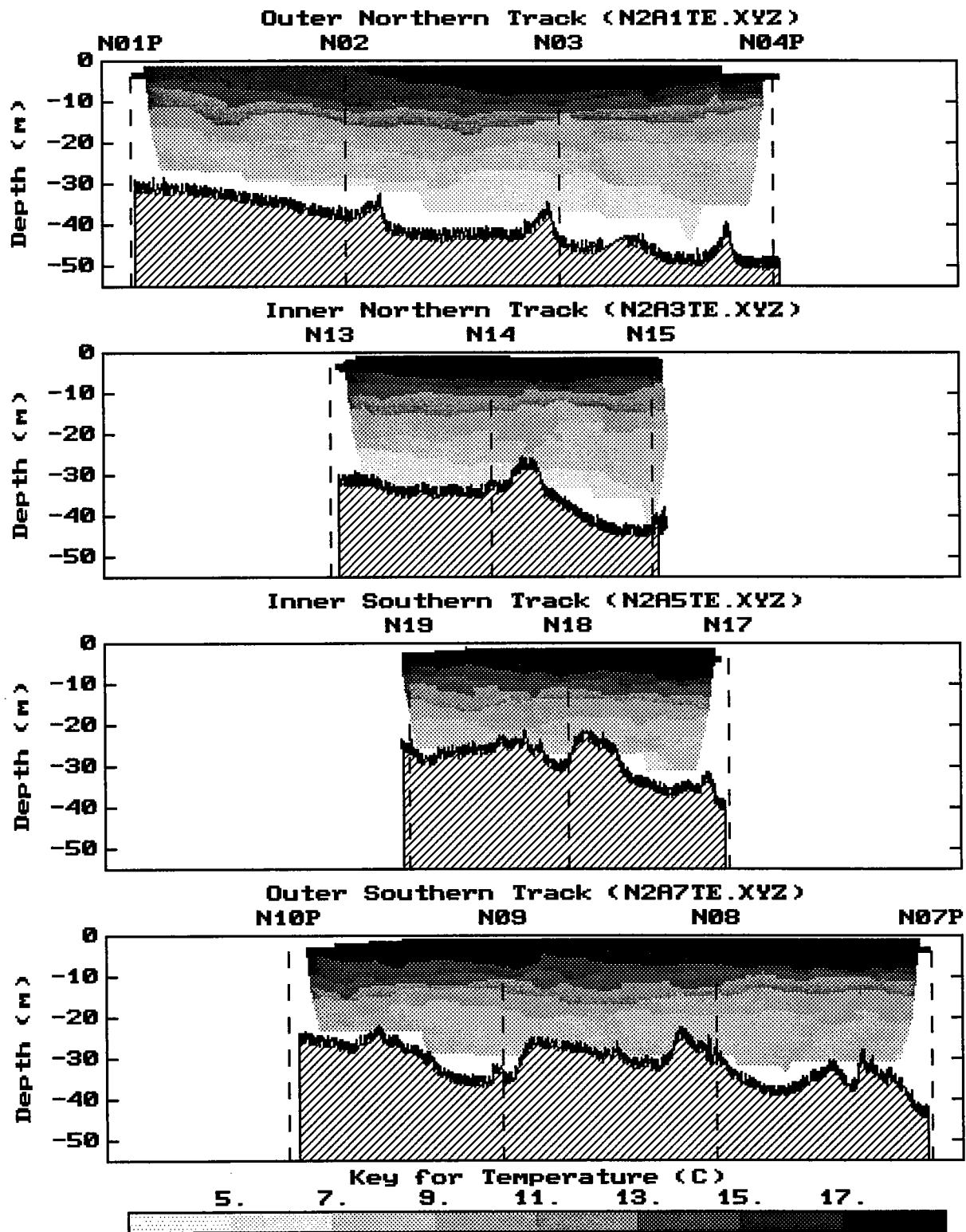


Figure 3-4a. Vertical section contours of temperature generated for tow-yo profiling in early August 1993. The view is towards the North.

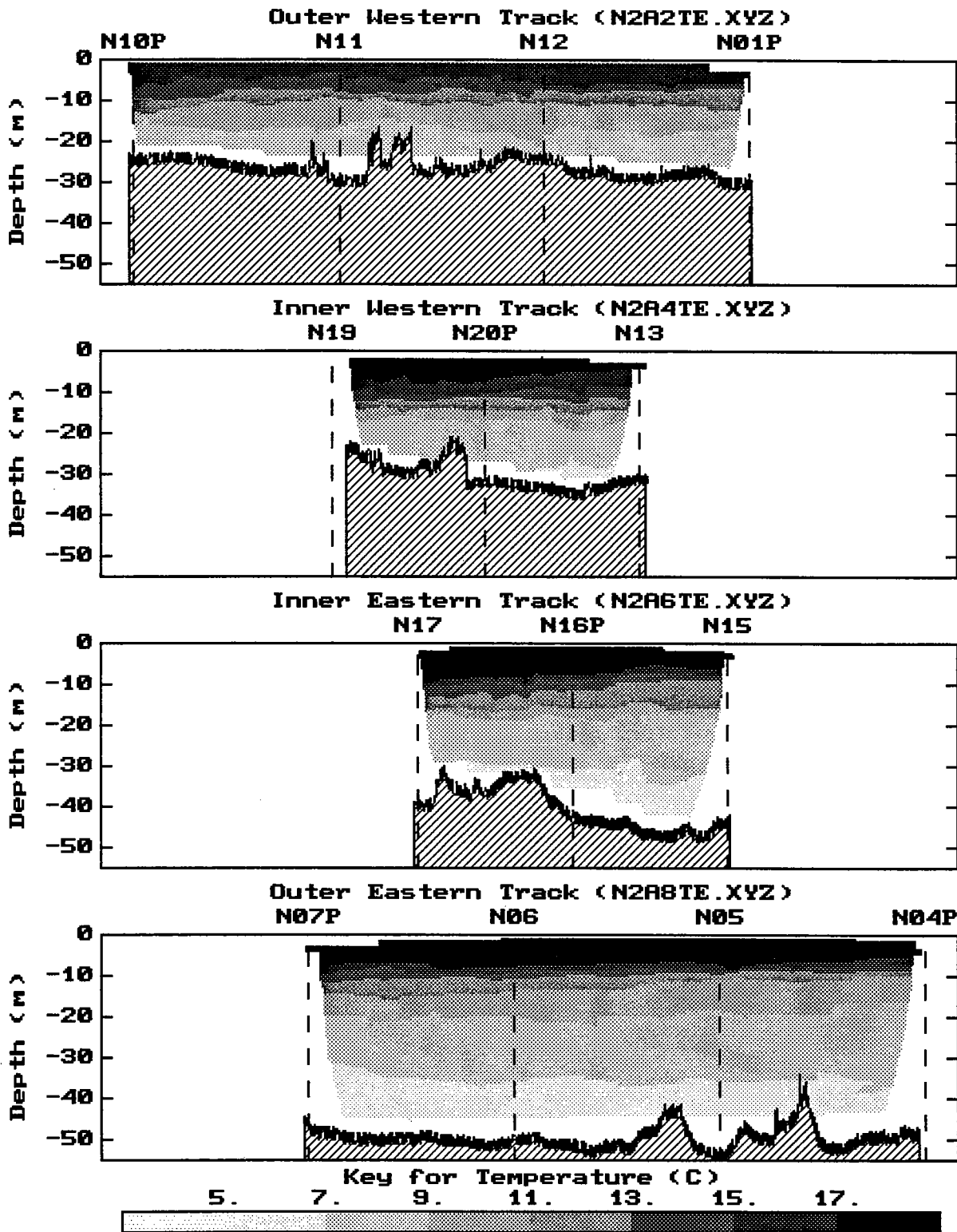


Figure 3-4b. Vertical section contours of temperature generated for tow-yo profiling in early August 1993. The view is towards Boston Harbor.

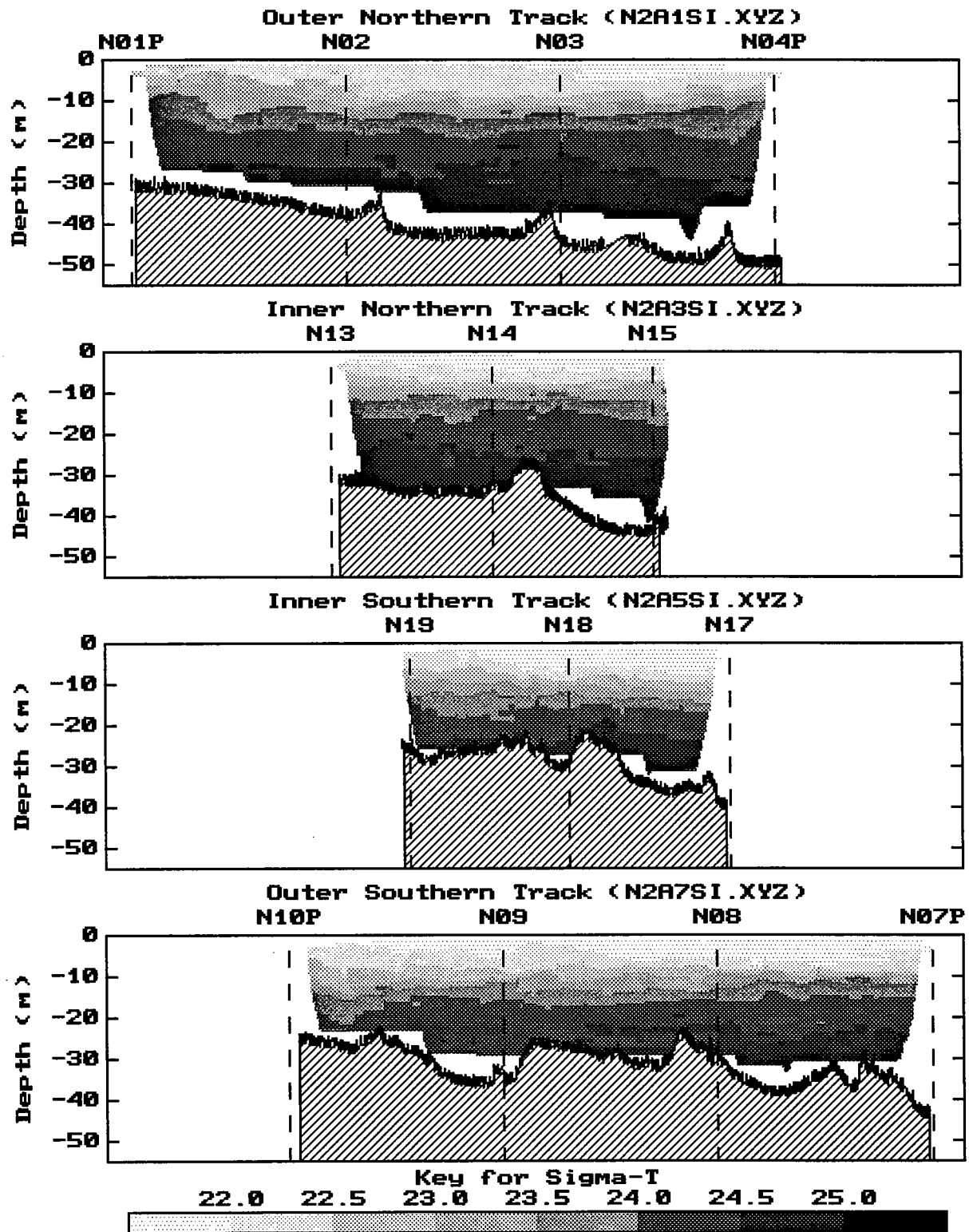


Figure 3-5a. Vertical section contours of σ_T generated for tow-yo profiling in early August 1993. The view is towards the North.

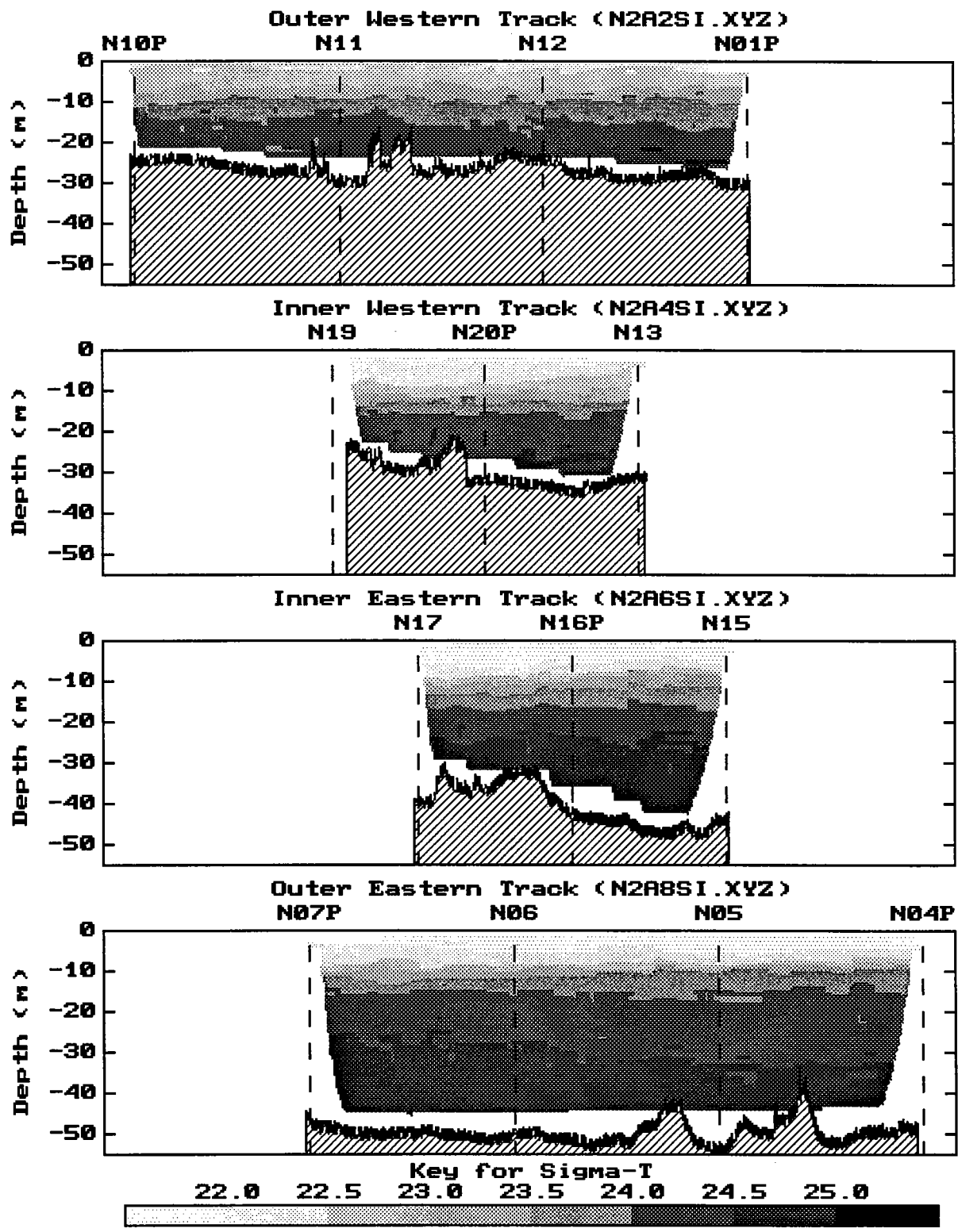


Figure 3-5b. Vertical section contours of σ_T generated for tow-yo profiling in early August 1993. The view is towards Boston Harbor.

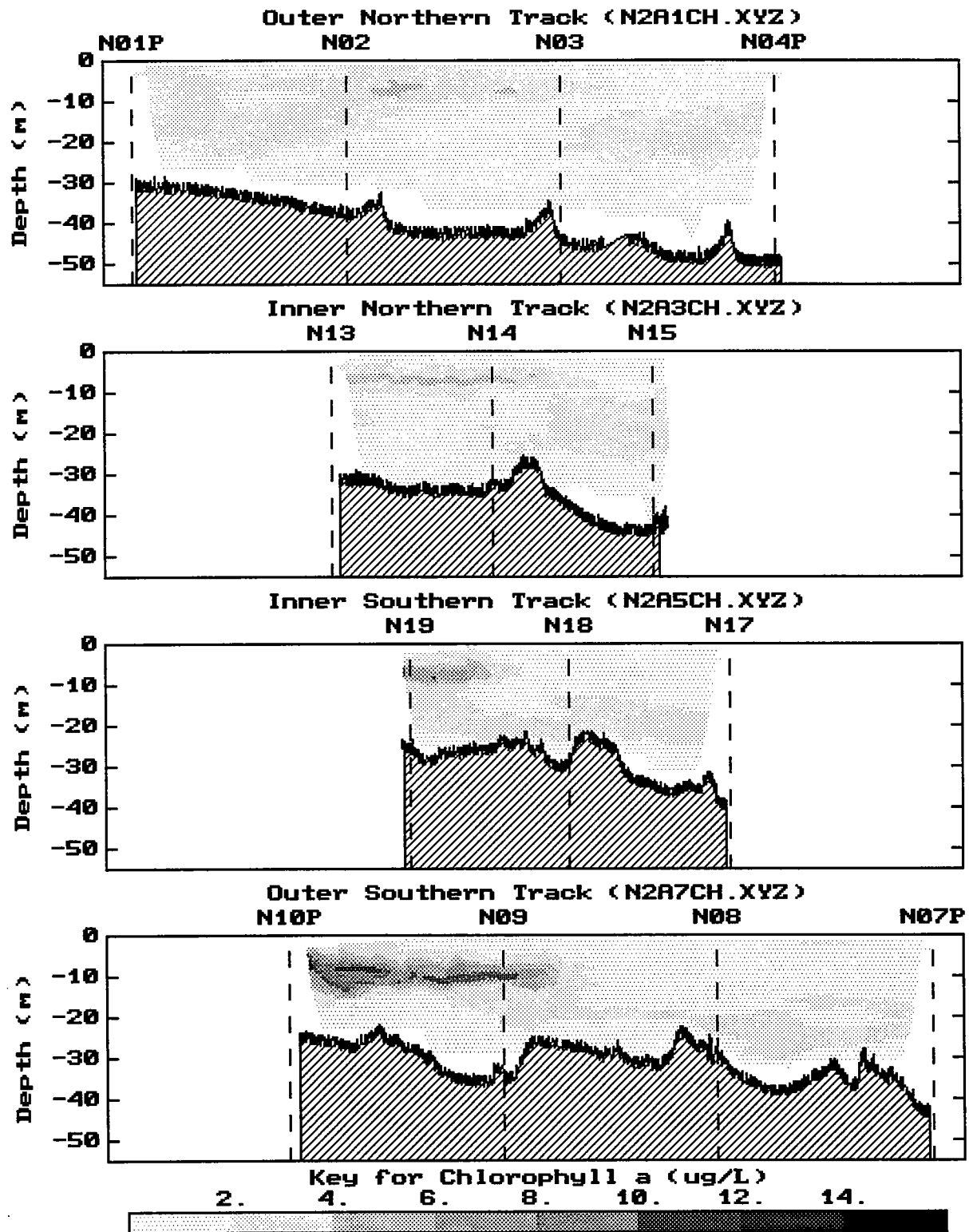


Figure 3-6a. Vertical section contours of fluorescence (as $\mu\text{g Chl L}^{-1}$) generated for tow-yo profiling in early August 1993. The view is towards the North.

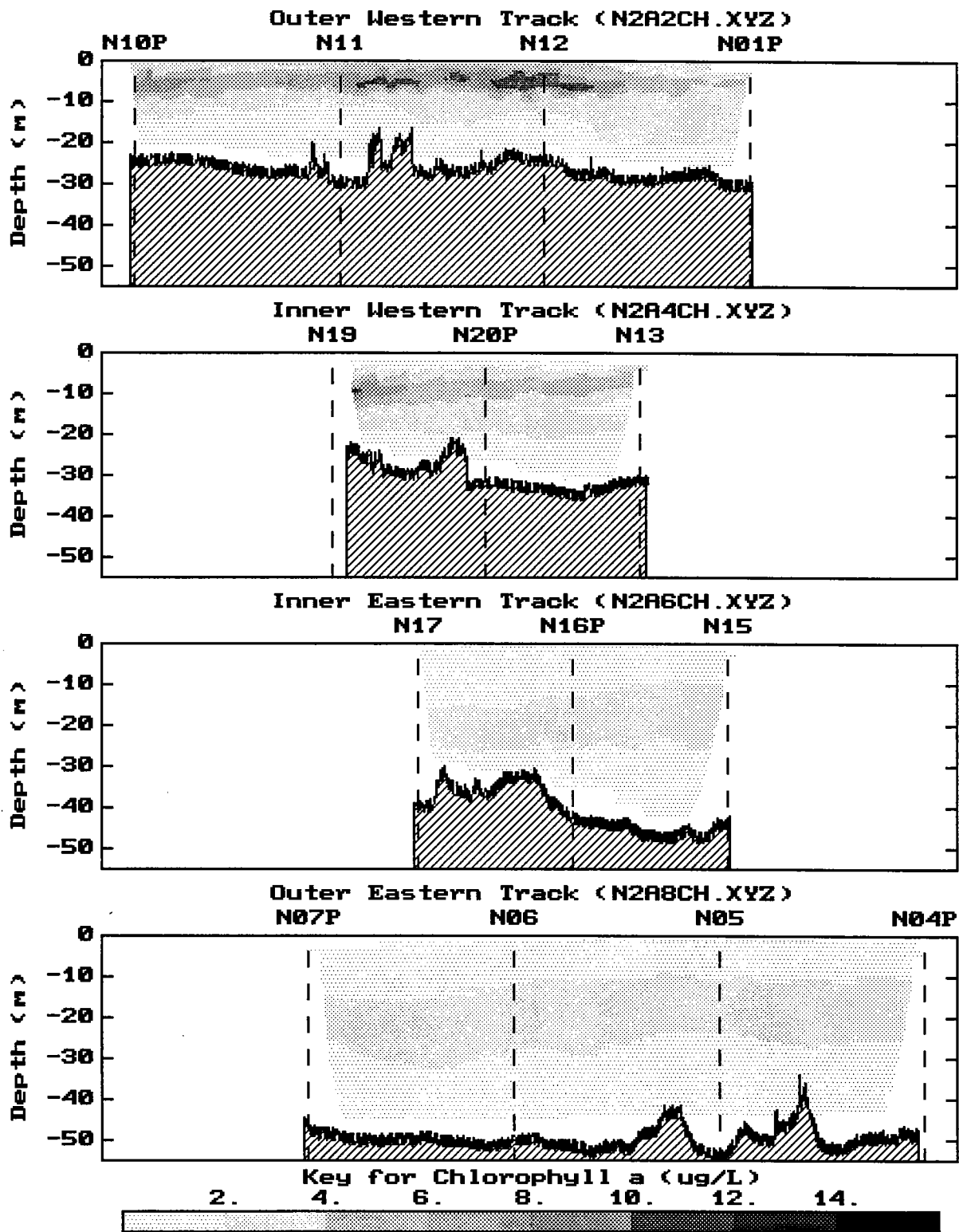


Figure 3-6b. Vertical section contours of fluorescence (as $\mu\text{g Chl L}^{-1}$) generated for tow-yo profiling in early August 1993. The view is towards Boston Harbor.

4.0 RESULTS OF LATE AUGUST 1993 COMBINED FARFIELD/NEARFIELD SURVEY (W9311)

4.1 Farfield Survey

4.1.1 Horizontal Distribution of Surface Water Properties

In late August, surface waters along the shoreline from Boston Harbor south were often cooler than offshore (Figure 4-1). In general, the near-coastal waters were $< 17.6^{\circ}\text{C}$. Coolest surface waters ($15.6\text{-}16.4^{\circ}\text{C}$) were found near Marshfield and off Plymouth Bay. The water temperature at most offshore Massachusetts Bay locations and in Cape Cod Bay ranged between 18 and 19.5°C .

Surface water salinity ranged narrowly between 30.89 and 31.26 PSU (Figure 4-2). Overall, salinities were higher in Cape Cod Bay than in Massachusetts Bay, an apparent latitudinal trend. The salinity gradient out from Boston Harbor, often observed on MWRA surveys, was scarcely detectable. Salinity nearest Boston Harbor was, at most, 0.1 PSU lower than in the nearfield and offshore Massachusetts Bay.

As shown in Figures 4-3 and 4-4, similar regional patterns were noted for beam attenuation and chlorophyll (as fluorescence). Values for both parameters were high off Boston Harbor and in western Massachusetts Bay, but were low in Cape Cod Bay and offshore Massachusetts Bay. Chlorophyll concentrations were more enhanced just outside the Harbor (e.g., stations F24, N01P, and N10P) than at the Harbor edge. The nearshore-to-offshore decreasing gradient was sharper for chlorophyll than for beam attenuation.

Concentrations of dissolved forms of inorganic nitrogen were low to undetectable in surface waters (Figures 4-5 and 4-6). At station N20P, a slightly enriched concentration of DIN ($\sim 1\mu\text{M}$) was coincident with low beam attenuation and low chlorophyll concentration. No regional trends were

noted for DIN concentrations. Although the concentrations were generally very low, the near-Harbor area and Cape Cod Bay stations were slightly enriched in phosphate relative to the offshore area (Figure 4-7). A striking regional gradient was noted for silicate, with higher surface concentrations (2-3 μM) in Cape Cod Bay and low values ($< 1 \mu\text{M}$) in much of northern Massachusetts Bay (Figure 4-8). To a large degree, silicate and chlorophyll showed inverse patterns from north to south along the Bay axis.

4.1.2 Water Properties Along Selected Vertical Sections

The standard four transect sections were produced from vertical profiles at stations (see Figure 4-9). Temperature sections shown in Figure 4-10a reveal a warm, thin surface layer throughout Massachusetts Bay, with slightly lower surface temperatures and more vertically mixed conditions outside Boston Harbor (stations F23P-F24) and along the coast near Marshfield (station F05). The thermocline extended to the bottom at stations $< 30\text{-}35$ m. Bottom temperatures at Stellwagen Basin stations (F22, F19, F17, and F12) were near or $< 5^\circ\text{C}$; an interesting trend noted was that the depth of the 5°C isotherm was shallower at the southern end of the Basin (F12), progressively becoming deeper to the north (F22).

Salinity showed vertical layering, but the range of the profiles from top to bottom was small (Figure 4-10b). Layering appeared to be fairly uniform, with similar salinities at similar depths across all sections. The exception, however, was that salinity in the bottom water toward the southern end of Stellwagen Basin was slightly higher than the salinity of bottom water at the northern end. This axial trend paralleled the trend in temperature and is apparent in the density sections (Figure 4-10c). The obvious tilting of a deepwater density surface within the Basin may imply a deepwater current flow towards the north.

Section contours of chlorophyll and beam attenuation, which are presented in Figures 4-11 and 4-12, often show similar features: (1) a mid-water maximum as a 5-10 m layer near 10-20 m depth in the northern and Marshfield transects, and offshore in the other transects, and (2) a more concentrated

near-surface maximum near Boston Harbor and along the coast off Cohasset. Deepwater at most Stellwagen Basin stations had higher beam attenuation, but not higher chlorophyll, at the bottom of the profile; this feature suggests a near-bottom nepheloid layer of suspended or resuspended particulate matter.

DO was apparently supersaturated throughout the surface layer and well into the thermocline/pycnocline. The deepest water at most stations in Stellwagen Basin was about 85% of saturation (see Appendix A).

Dissolved inorganic nitrogen (DIN) was uniformly depleted in the surface layer and increased below the pycnocline (Figure 4-14a). In the nearfield (stations N20P and N16P), lower concentrations were found below the pycnocline than in bottom water at similar overall water depth (30-45 m) at other stations. At Stellwagen Basin stations, bottom waters exceeded $7 \mu\text{M}$ and a maximum of about $10.5 \mu\text{M}$ was observed in deepest water at station F12. Relatively more ammonia was present in bottom water at stations F22 and F19 ($\sim 2 \mu\text{M}$) at the northern end of the Basin, than at stations at the southern end ($\sim 1 \mu\text{M}$) (see Appendix A). Patterns for silicate (Figure 4-14b) were similar to DIN patterns. The only strong geographic difference appeared to be in nearfield bottom waters, in which silicate concentrations were similar to those in deeper waters in other regions.

4.1.3 Analysis of Water Types

Physical parameters varied mostly in vertical dimension at most locations such that regional differences were not dramatically pronounced and most profiles followed a broad temperature-salinity (T-S) trend (Figure 4-15a). Highest beam attenuation was found at lower salinity surface water, but some low beam attenuation was also associated with low salinity water. Some intermediate beam attenuation was found at high salinity, which represents data from within the nepheloid layer suggested above (Figure 4-15a).

Data suggest a very broad relationship between beam attenuation and chlorophyll concentrations. Chlorophyll may be more useful in distinguishing regions than some of the physical variables. At all coastal and nearfield stations, chlorophyll in the upper 10 m was above $3 \mu\text{g L}^{-1}$, often well above $6 \mu\text{g L}^{-1}$ and, in some locations, as high as $\sim 15 \mu\text{g L}^{-1}$ (Figure 4-15b; also see Appendix C). In contrast, with few exceptions (station F15), peak chlorophyll concentrations at other regions were $< 3 \mu\text{g L}^{-1}$ (Appendix C). Nearfield stations that were exceptionally high in chlorophyll also had exceptionally high DO supersaturation ($> 130\%$); in general, the degree of supersaturation was related to the intensity of the chlorophyll bloom.

Thus, in spite of few physical distinctions, chlorophyll concentrations in the nearfield and at most coastal locations differed from those in other regions. To further assess this water quality characteristic, it was necessary to determine whether chemical water quality signatures were due to regional differences in biological and biogeochemical activity.

In all regions, the DIN- PO_4 trend was similar (Figure 4-17). N and P simultaneously increased with increasing depth. Compared to the offshore/northern transect stations, DIN and NO_3 concentrations at some of the nearfield stations were depleted at higher PO_4 concentrations. Overall, however, the N/P coherence was strong and consistent throughout the Bays.

The coherence between DIN and SiO_4 was also strong, although more variability was noted (Figure 4-18). A number of samples from Cape Cod Bay were high in silicate but lower in N than samples from other stations. Few other regional or geographic trends were noted.

The familiar summer pattern of increasing nutrient concentrations at higher salinity (depth) was illustrated in the plots of dissolved nutrients versus salinity. This pattern was easily detected despite the narrow salinity range (Figures 4-19 to 4-21). Whether the trend appears more linear (e.g., PO_4) or more exponential (e.g., DIN or SiO_4) depends, in part, on the degree of surface water depletion (lowest salinity). The nutrient-salinity plots also revealed some regional differences. For example, at intermediate salinities, some nearfield and coastal samples are slightly enriched in NH_4 (Figure 4-20) and PO_4 (Figure 4-21). Relative to its salinity, some samples from Cape Cod Bay were enriched in

silicate (Figure 4-21). It is important to note that all of these regional distinctions are modest and occur at depth. In the surface layer dissolved forms of nutrients were uniformly depleted.

When organic forms of nitrogen are included, a different pattern with salinity was noted for the samples from selected stations within three of the main regional groups (Figure 4-22). One reason for the pattern difference was that the samples were restricted to surface productive layers. Particulate organic nitrogen (PON) makes up virtually all the DIN + PON and there is no clear salinity-related or region-specific trend. When salinity is plotted against total nitrogen (TN), a decrease with salinity is suggested, but variability was high and the salinity range was very narrow. Cape Cod Bay samples had highest salinity readings and were at the low end of the TN concentration range.

In summary, regional differences in chlorophyll concentrations are more pronounced than differences in physical or chemical parameters, although minor regional differences were noted for the latter. Despite some strong differences in nutrient fluxes and process rates (reflected in DO and production, see below), it is possible that nutrients were cycling so quickly in the warm stratified surface waters that measurements of dissolved nutrients did not reflect this activity because the concentrations were essentially depleted. With other forms of nitrogen included, measurements of total nitrogen (TN) should more effectively capture such differences. A range in TN may indeed suggest some regional differences, but with the few samples available, this is difficult to estimate with much confidence.

4.1.4 Distribution of Chlorophyll and Phytoplankton

Figure 4-23 presents concentrations of extracted chlorophyll for samples collected from the surface and chlorophyll maximum at a subset of BioProductivity and special stations. As noted in the full profiles based on fluorescence (Figure 4-15b), the data in Figure 4-23 generally show high concentrations of chlorophyll throughout the surface layer of the nearfield and at the few coastal stations, but lower concentrations at the two Cape Cod Bay stations. A similar geographic pattern was observed for the phytoplankton counts. In about 50% of the samples, total cell counts were $> 10^6$ cells L^{-1} and cell counts correlated well with chlorophyll (Figure 4-24).

In samples with cell counts $\leq 10^6$ cells L^{-1} , diatoms were part of the community but microflagellates characteristically dominated (Figure 4-25a and 4-25b). Diatom and microflagellate counts were both higher in samples where total counts were $> 10^6$ cells L^{-1} ; diatoms, rather than microflagellates, were characteristically more than 50% of the total number of cells in these samples. Numerically, dinoflagellates and other miscellaneous forms were always a small component of the phytoplankton community.

In general, high chlorophyll concentrations throughout western Massachusetts Bay (coastal and nearfield stations) were due to enhanced diatom growth, as well as to some increase in the microflagellate community. By taxa, microflagellates were virtually always dominant (Table 4-1a, 4-1b) and their cell counts generally varied only about two-fold across samples (i.e., ~ 0.5 - 1.0×10^6 cells L^{-1}). Cryptomonads were also regularly dominant, although the numbers of cells were much lower (~ 0.05 - 0.08×10^6 cells L^{-1}). The same assemblage of diatom species was dominant in all samples; principal diatoms species were *Leptocylindrus danicus*, *Rhizosolenia delicatula*, and *Cerataulina pelagica*. These species were a seasonal component of the community during this period in 1992 (Kelly *et al.*, 1993c; 1994a). Overall, the composition was strikingly similar in both the surface and chlorophyll-maximum samples as well as across stations.

As a group, the dinoflagellates were not numerous and there were no dominant individual taxa (Tables 4-2a and 4-2b). About 20 species were detected, none of which were more abundant than 10^2 cells L^{-1} . In contrast to other locations, more species and higher cell counts at the chlorophyll maximum were observed in samples from Cape Cod Bay (stations F01P and F02P). Tintinnids (not dinoflagellates) were high at the Harbor-edge station (F23P). Finally, *Alexandrium tamarense*, a species of concern for its toxicity but not usually prevalent during this season, was not detected.

4.1.5 Distribution of Zooplankton

Across stations, total zooplankton numbers generally varied by a factor of two (Figure 4-26). The geographic distribution did not always follow that of the phytoplankton (cf. Figures 4-25 and 4-26). At station F23P, for example, high phytoplankton counts, but relatively low zooplankton counts were recorded. In all cases, most of the zooplankton were copepods or their nauplii.

Taxonomic results for all zooplankton samples are tabulated in Appendix G. With one exception, the small copepods *Oithona similis* and *Paracalanus parvus* were numerically dominant everywhere, as has generally been found throughout 1992 and 1993. *Pseudocalanus newmani* and *Temora longicornis* were regularly present and often abundant. *Centropages typicus* and *Calanus finmarchicus* were regularly present, but in lower abundance. Overall, the taxonomic results suggest a fairly similar community throughout the Bays.

Station F23P at the edge of the Harbor was the exception noted in the preceding paragraph. At this station, *Oithona* and *Paracalanus* were present and relatively abundant, but absolute numbers were lower than those observed at other locations. The copepod species *Acartia tonsa* was numerically dominant at station F23P. This species has been regularly observed near the Harbor and, because it is more typically estuarine than coastal, is usually found in fresher waters. *Acartia tonsa* was absent in the samples from station F13P south of the nearfield area and station F02P in eastern Cape Cod Bay. Its presence throughout the nearfield, although in lower numbers than at the Harbor edge, has often been noted and is an indicator that some of the water in the nearfield originated in the Harbor.

The presence of *Acartia* in western Cape Cod Bay (station F01P) is interesting. Its absence at station F13P interrupted the distribution between western Massachusetts Bay and southern waters. That, coupled with increasing salinity into Cape Cod Bay (Figure 4-2), perhaps argues the absence of a continuous coastal plume that would allow the water from the north to mix to or "seed" station F01P. A sporadic coastal transport of water could explain the observed *Acartia* distribution, but it is likely that another resident population source exists closer to F01P — perhaps Plymouth-Duxbury Bay or the Cape Cod Canal. Additionally or alternatively, cross-Basin trends in the physical structure of the Cape

Cod Bay water column (usually more well mixed on the western side) may support a small resident population at station F01P, but not at F02P.

The occasional presence of *Acartia* in Cape Cod Bay has been noted throughout the baseline monitoring period (e.g., Kelly *et al.*, 1994a). Patterns in some numerically minor community components may or may not bear much ecological significance, but as species can be very strong water-type indicators, minor taxon anomalies may be interesting: especially when compiled over time even minor features may direct towards data analyses or additional studies that can add significant insight on the functioning and interaction of waters in the Bay.

4.1.6 Metabolism: ^{14}C Production and Oxygen Respiration Measurements

Data from P-I incubations at the 10 BioProductivity stations are presented in Appendix E. Table 4-3 summarizes results of modeling to derive integrated water column production rates. Figure 4-27 presents production rates derived for each incubation at a station (surface or chlorophyll maximum sample) as a function of integrated photic-zone chlorophyll.

Estimates of production were primarily in the range of 1.5-2.5 g C m⁻² d⁻¹. One estimate was < 1 g C m⁻² d⁻¹ and several were ~4 g C m⁻² d⁻¹. At two stations (F02P and F23P), incubation of samples from the surface generated a lower production estimate than the chlorophyll-maximum samples. At all other locations, the surface sample usually provided a higher estimate (Figure 4-27) because P_{max} estimates for surface samples were higher. The correlation between integrated chlorophyll and production was strong for the surface samples ($R^2 = 0.74$, $n = 10$) and weak for chlorophyll-maximum samples ($R^2 = 0.20$, $n = 10$).

Even though maximum rates (P_{max}) from P-I incubations were lower in most chlorophyll-maximum samples, photoinhibition at highest light intensity was rarely indicated. Most curves were best modeled with the Webb *et al.* (1974) model without the inhibition term. Generally P_{max} was approached at a light intensity between ~150 and 300 $\mu\text{E m}^{-2} \text{sec}^{-1}$ (Appendix E). In most cases, the mid-day irradiance

at this intensity range either (1) was located at the depth of a distinct subsurface chlorophyll maximum or (2) generally defined the deepest extent of the high-chlorophyll surface layer. Production rates fell sharply at depths below this intensity range, because of the sharp decrease in chlorophyll as well as in light. Exceptions were noted at stations F23P and N10P, neither of which were distinctly stratified nor had a very deep mixed layer. Vertical mixing probably occurred quickly enough to maintain most of the water column population at higher average intensity, resulting in chlorophyll concentrations distributed to greater depths. These observations suggest that vertical distribution of chlorophyll and production were controlled by water column stratification/mixing. More importantly, these results may define, for this survey, a light limit beyond which biomass and production were sharply curtailed under stratified conditions. For these cases, it is important to note that this mid-day light level ($150-300 \mu\text{E m}^{-2} \text{sec}^{-1}$) was well above the 0.5 or even 1% isolume, and characteristically occurred at about 10-14 m, or about one-half the depth of $Z_{0.5\%I_0}$ (Table 4-3).

The depth profile for production generally followed the depth profile for chlorophyll. Where chlorophyll was higher at mid-depth, but well within the photic zone, volumetric production rates peaked near this depth (e.g., station N20P). The surface sample incubations most likely provide a better integrated rate estimate than the chlorophyll maximum sample.

Dark-bottle incubations (~8 h) were performed on samples from three depths at each of the ten BioProductivity stations; incubation temperatures approximated the *in situ* temperatures. Surface water samples were incubated at near-ambient surface temperatures and chlorophyll-maximum samples were held at ~12-15°C, except for the station F23P sample, which was mixed and incubated at the surface incubation temperature of 21°C. Bottom-layer samples were incubated at ~8-9°C. The proportion of incubations that showed a significant decrease in DO, decreased with increasing depth of the sample. For example, for surface-water incubations, initial and final DO concentrations were significantly different at the 95% significance level for 7 of 10 incubations and at the 90% significance level for 9 of 10 incubations (Appendix E). For chlorophyll-maximum samples (usually 8-18 m depth), only 4 of 10 and 6 of 10 were significant at the 95% and 90% levels, respectively. Four of the ten bottom-layer incubations (samples from ~22-47 m depth) were significant at the 90 and 95% levels.

For those changes that were significant, apparent respiration rates ranged from an uptake of 0.008 to 0.038 mg DO L⁻¹ h⁻¹ (Appendix E). Respiration rates were highest (0.035 to 0.038 mg L⁻¹ h⁻¹) for all three samples from station F23P. Rates were also fairly high (0.027 to 0.034 mg L⁻¹ h⁻¹) at selected locations throughout the nearfield: station N04P (surface and chlorophyll-maximum samples) and the surface samples from stations N07P and N10P. Elsewhere, including station F13P along the south shore and the two Cape Cod Bay stations, rates were lower or not significant, ranging between 0.01 and 0.02 mg L⁻¹ h⁻¹. In general, higher rates occurred near the surface where temperatures were high, but also where chlorophyll concentrations (and thus production rates) were high (cf. Figure 4-4 and Appendix A).

4.2 Nearfield Survey

4.2.1 Distribution of Water Properties from Vertical Profiling

Figure 4-28 provides scatter plots for parameters measured *in situ* in the nearfield; these plots may be compared to plots for all stations shown in Figure 4-15. The T-S pattern was tight and relatively few data points fell off the trend. Surface water was fresh and warm (about 31 PSU, 18-19°C) and the deepest bottom water was 31.63 PSU and about 6.3°C (Figure 4-28a). Review of vertical profiles for physical data in Appendix B supports an observation that, with only a few subtle exceptions, the temperature, salinity, and density layering was very similar across the nearfield.

Higher beam attenuation was suggested at lower salinities (Figure 4-28a), indicating that turbidity was generally highest near the surface. A significant amount of scatter was noted between turbidity and chlorophyll; at many locations where beam attenuation was high (> 2 m⁻¹), chlorophyll concentrations were not particularly high. Chlorophyll concentrations were high in the surface layer to about 20 m, and a mid-depth maximum near 10 m was routinely noted. As previously noted, high concentrations of chlorophyll in the surface layer resulted in high DO supersaturation (Figure 4-28b).

A strong relationship between nutrient concentrations and depth was noted at nearly all stations, perhaps related to the consistency in vertical structure (Figures 4-29 through 4-30). As a reference, nearfield station data are shown with data from farfield stations. DIN concentrations in the nearfield increased almost linearly with depth and reached $\sim 7 \mu\text{M}$, which was much lower than that observed in deeper water offshore or at station F22 on the northern transect. In the nearfield, the same linear trend with depth was observed for nitrate, but NH_4 increased sharply at the pycnocline and then remained at $\sim 2 \mu\text{M}$ between the pycnocline and the bottom (Figure 4-30a). Phosphate concentrations increased with depth where they were comparable to concentrations in deeper offshore bottom waters (Figure 4-30b). In contrast to DIN, PO_4 was not depleted in surface waters. The silicate pattern resembled the pattern for DIN in that nearfield bottom waters were less enriched than offshore water (and Cape Cod Bay bottom water); the nearfield surface layer was nearly depleted in silicate (Figure 4-30b).

4.2.2 Distribution of Water Properties from Towing

Across the field, high-resolution tow-yo profiling confirmed the physical uniformity of the vertical layering (Figure 4-31). The pycnocline began slightly deeper in the water column at offshore stations in the southern portion of the nearfield. For example, at stations N07P, N06, N05, N17, and N16P, the top of the pycnocline was characteristically found near 10 m, compared with 5 m inshore (Figure 4-32). Interestingly, stations along the outer northern track, even to the northeast corner (station N04P) maintained a thinner surface layer similar to that observed at the inshore stations. The chlorophyll distribution vividly illustrated these subtle physical-gradient features (Figure 4-33). At both the western and northern tracks, a thin near-surface layer very high in chlorophyll was observed as a continuous mass rather than in patches. In contrast, high concentrations of chlorophyll in the surface layer offshore were not observed but a subsurface maximum within the upper pycnocline was characteristically found.

4.2.3 Water Types and Analysis of Small-Scale Variability

The data from this survey indicated that there was distinct variability in chlorophyll. In contrast, a field-wide similarity was noted in the relationship between dissolved nutrient concentrations and water depth. Additionally, physical variations across the nearfield were small; stratification was uniformly strong and only gradual horizontal gradients in the depth of the surface layer were observed. The geographic variability in biological activity, as assessed by chlorophyll, seemed to parallel the minor physical variability. In summary, the parallel suggests questions that cannot be easily addressed with these data alone, but which relate to water mass classification and the interaction of waters across depth regions in the Bays. Does chlorophyll signal an amplified biological response to small and horizontally-smooth physical gradients? Is chlorophyll simply higher near the surface wherever a significant portion of the water mass of this layer is of inshore origin, carrying a distinct shallow-water biology as a seed and perhaps also higher total, if not dissolved, nutrients?

The variability between beam attenuation and chlorophyll is of interest because turbidity and chlorophyll are often strongly co-variant. This relationship may be useful in characterizing water mass mixing and the lack of coherence between the turbidity and chlorophyll may be an interesting diagnostic tool (e.g., Kelly and Albro, 1994). Vertical profiles of beam attenuation and chlorophyll were reviewed (Appendix B). On the nearfield survey day (August 27), beam attenuation was very high ($> 3 \text{ m}^{-1}$) near the surface of a number of northwest corner stations. Beam attenuation at most of the other stations was high ($> 2 \text{ m}^{-1}$) but, at several stations along the eastern track (N04P, N05, N06), values were $< 1.5 \text{ m}^{-1}$. The highest beam attenuation values were clearly associated with very high chlorophyll concentrations. But, for a number of stations with near-surface beam attenuation $> 2 \text{ m}^{-1}$, there was no similarity in the shapes of the depth versus turbidity and chlorophyll profiles. Specifically, high beam attenuation throughout a surface layer was often measured, even when chlorophyll was not particularly high or rose only to a *subsurface* peak at 5-10 m (e.g., stations N14, N15, N16P, N17, N18, N19, N20P, and N21). Many, if not all, of the stations having this pattern were in the center of the nearfield. Although no unusual activity was reported in the area (Dragos, 1993b) and there were no indications that the instruments were not operating properly, the data, nevertheless, suggested some surface turbidity that could not be attributed to chlorophyll. This type of

signature (high turbidity without concomitantly high chlorophyll) may be characteristic of Harbor water when compared with water in the Harbor-Bay mixing zone (cf. Kelly and Albro, 1994). It could also arise if particles, or light-absorbing dissolved matter, were released at the surface within the field itself.

Table 4-1a. Top five dominant phytoplankton taxa in near-surface samples collected in August 1993.

	COASTAL STATIONS		NEARFIELD STATIONS								CAPE COD BAY STATIONS	
	F23P	F13P	N01P	N04P	N07P	N10P	N16P	N20P	F01P	F02P		
CERATAULINA PELAGICA	.129 (5)	.196 (2)	.413 (2)	.911 (1)	.12 (2)	.387 (3)	.317 (3)	.383 (2)				
CERATIUM FUSUS										.022 (3)		
CRYPTOMONADS	.153 (4)	.051 (4)	.051 (5)	.039 (5)	.067 (3)	.074 (5)	.079 (5)	.057 (3)	.052 (2)			
CYLINDROTHECA CLOSTERIUM									.012 (4)	.022 (3)		
GYMNODINIUM SPP.								.037 (4)				
LEPTOCYLINDRUS DANICUS	.658 (2)	.031 (5)	.236 (3)	.18 (3)	.02 (5)	.128 (4)	.241 (4)	.032 (5)	.021 (3)	.039 (2)		
MICROFLAGELLATES	.974 (1)	.641 (1)	1.027 (1)	.834 (2)	.495 (1)	.766 (1)	.72 (1)	.401 (1)	.504 (1)	.493 (1)		
RHIZOLENIA DELICATULA	.285 (3)	.073 (3)	.173 (4)	.107 (4)	.023 (4)	.642 (2)	.582 (2)			.018 (4)		
STEPHANOPYXIS PALMERIANA									.009 (5)			
THALASSIONEMA NITZSCHOIDES										.015 (5)		

Units are 10^6 cells L^{-1}
 Values in parentheses are give rank order of abundance

Table 4-1b. Top five dominant phytoplankton taxa collected from the chlorophyll maximum in August 1993.

	COASTAL STATIONS					NEARFIELD STATIONS					CAPE COD BAY STATIONS		
	F23P	F13P	N01P	N04P	N07P	N10P	N16P	N20P	F01P	F02P			
CERATAULINA PELAGICA	.078 (4)	.052 (4)	.472 (2)	.236 (2)	.188 (2)	.581 (3)	.407 (2)	.125 (2)	.012 (4)	.011 (4)			
CHAETOCEROS DIDYMUS						.057 (5)							
CRYPTOMONADS		.059 (3)	.074 (5)	.093 (4)	.026 (3)		.079 (5)	.066 (3)	.063 (2)	.062 (2)			
CYLINDROTHECA CLOSTERIUM	.05 (5)					.057 (5)			.01 (5)				
LEPTOCYLINDRUS DANICUS	1.228 (1)	.033 (5)	.107 (4)	.023 (5)	.014 (5)	.062 (4)	.127 (4)			.01 (5)			
LICMOPHORA SPP.									.014 (3)				
MICROFLAGELLATES	1.018 (2)	.774 (1)	.653 (1)	1.004 (1)	.619 (1)	.673 (1)	.509 (1)	.505 (1)	.637 (1)	.524 (1)			
PYRAMIMONAS/TETRAELEMIS SPP.								.029 (5)					
RHIZOLENIA DELICATULA	.05 (5)	.074 (2)	.327 (3)	.105 (3)	.024 (4)	.664 (2)	.132 (3)	.055 (4)					
SKELETONEMA COSTATUM	.105 (3)												
THALASSIONEMA NITZSCHOIDES										.012 (3)			
UNID. CENTRALES				.023 (5)					.014 (3)				

Units are 10⁶ cells L⁻¹
 Values in parentheses are give rank order of abundance

Table 4-2a. Abundance of all identified taxa in near-surface screened (20µm) samples collected on the farfield survey in August 1993.

SPECIES	STATION		F01P	F02P	F13P	F23P	NH1P	N04P	N07P	N10P	N16P	N20P
	SAMPLE ID	DATE										
		AUG 26	AUG 26	AUG 25	AUG 27	AUG 25	AUG 25	AUG 25	AUG 25	AUG 24	AUG 24	AUG 24
ALEXANDRIUM TAMARENSE		0	0	0	0	0	0	0	0	0	0	0
ALORICATE CILIATES		18	5	0	80	0	0	0	0	3	10	3
CERATIUM FUSUS		173	198	363	120	288	676	235	243	70	210	145
CERATIUM LONGIPES		43	40	133	10	13	140	33	70	30	140	140
CERATIUM MACROCEROS		18	5	3	0	0	3	0	0	0	8	0
CERATIUM TRIPOS		8	33	65	20	70	90	45	45	45	40	65
DICTYOCCHA FIBULA		0	0	0	3	0	0	0	0	0	0	0
DICTYOCCHA SPECULUM		0	3	0	48	0	0	0	3	0	0	0
DINOPHYSIS ACUMINATA		0	0	3	5	13	8	35	10	13	13	0
DINOPHYSIS NORVEGICA		3	3	0	0	0	5	0	20	8	8	3
DIPLOPSALIS SPP.		0	0	0	0	0	0	0	0	0	0	0
EBRIA TRIPARTITA		0	0	3	0	0	0	0	0	0	0	0
EUTREPTIA/EUTREPTIELLA SPP.		0	0	0	3	0	0	0	0	0	0	0
GLENODINIUM ROTUNDUM		0	0	0	23	0	0	0	0	0	0	0
GONYAULAX SPINIFERA		0	0	0	0	0	0	0	0	0	0	0
GONYAULAX SPP.		0	0	0	0	0	0	0	0	0	0	0
GYMNODINIUM SPP.		0	0	0	0	0	0	0	0	0	0	0
GYRODINIUM SPIRALE		3	5	0	0	0	0	0	0	0	0	0
GYRODINIUM SPP.		0	0	0	0	0	0	0	0	0	0	0
HETEROCAPSA TRIQUETRA		0	0	0	0	0	0	0	0	0	0	0
MESODINIUM RUBRUM		0	0	0	5	3	0	0	0	0	0	0

Table 4-2a. Abundance of all identified taxa in near-surface screened (20µm) samples collected on the farfield survey in August 1993 (Continued).

SPECIES	STATION	F01P	F02P	F13P	F23P	N01P	N04P	N07P	N10P	N16P	N20P
	SAMPLE ID	W93110425	W93110401	W93110289	W93110523	W93110242	W93110257	W93110273	W93110091	W93110072	W93110056
	DATE	AUG 26	AUG 26	AUG 25	AUG 27	AUG 25	AUG 25	AUG 25	AUG 24	AUG 24	AUG 24
PROCENTRUM MICANS		0	0	0	113	0	0	0	0	0	5
PROCENTRUM MINIMUM		0	0	3	0	0	0	3	0	0	0
PROTOPERIDINIUM BIPES		0	0	0	5	0	0	0	0	0	0
PROTOPERIDINIUM BREVE		0	0	0	0	0	0	0	0	0	0
PROTOPERIDINIUM DEPRESSUM		3	0	5	3	3	10	0	10	0	8
PROTOPERIDINIUM PELLUCIDUM		0	0	0	0	0	0	0	0	0	0
PROTOPERIDINIUM PENTAGONUM		0	0	0	10	0	0	0	0	0	0
PROTOPERIDINIUM SPP.		0	3	0	218	10	5	10	30	13	3
SCRIPPSIELLA TROCHOIDEA		8	0	5	20	5	5	10	70	3	0
TINTINNIDS		0	5	3	1892	40	5	23	38	25	5
UNID. ATHECATE DINOFAGELLATE		0	3	0	48	0	3	3	3	0	5
UNID. THECATE DINOFAGELLATES		5	0	8	15	3	10	10	10	5	0

Values are Cells/L

Table 4-2b. Abundance of all identified taxa in chlorophyll-maximum screened (20 µm) samples collected on the farfield survey in August 1993.

SPECIES	STATION	F01P	F02P	F13P	F23P	N01P	N04P	N07P	N10P	N16P	N20P
	SAMPLE ID	W93110423	W93110399	W93110287	W93110521	W93110241	W93110255	W93110272	W93110088	W93110070	W93110054
	DATE	AUG 26	AUG 26	AUG 25	AUG 27	AUG 25	AUG 25	AUG 25	AUG 24	AUG 24	AUG 24
ALORICATE CILIATES		8	5	10	45	28	3	0	18	18	5
CERATIUM FUSUS		250	38	178	48	395	883	285	203	661	438
CERATIUM LINEATUM		0	0	0	0	3	0	0	0	0	0
CERATIUM LONGIPES		175	373	163	13	98	693	58	108	548	323
CERATIUM MACROCEROS		0	0	0	0	0	3	3	0	3	0
CERATIUM TRIPOS		38	25	53	3	138	150	85	38	105	105
DICTYOCOA SPECULUM		25	45	20	33	5	80	13	5	63	40
DINOPHYSIS ACUMINATA		10	8	3	5	43	3	23	8	0	0
DINOPHYSIS NORVEGICA		55	430	23	10	5	220	13	13	165	13
DINOPHYSIS OVUM		0	0	0	0	0	3	0	0	0	3
EBBIA TRIPARTITA		0	0	0	0	0	3	0	0	0	0
GONYAULAX SPINIFERA		0	0	3	0	0	0	0	0	0	0
GYRODINIUM SPIRALE		3	3	0	0	0	0	0	5	0	0
MERISMOPEDIA SPP.		0	0	0	0	5	0	0	0	0	0
PROROCENTRUM MICANS		0	0	0	5	3	0	0	0	5	0
PROROCENTRUM MINIMUM		0	0	0	3	0	3	3	0	3	0
PROTOPERIDINIUM BIPES		3	0	0	3	0	0	0	0	0	0
PROTOPERIDINIUM BREVE		0	0	0	5	0	0	0	0	0	0
PROTOPERIDINIUM DEPRESSUM		28	15	33	0	3	45	0	20	35	5
PROTOPERIDINIUM PALLIDUM		0	0	0	0	0	5	3	0	0	0

Table 4-2b. Abundance of all identified taxa in chlorophyll-maximum screened (20 μ m) samples collected on the farfield survey in August 1993 (Continued).

SPECIES	STATION	F01P	F02P	F13P	F23P	N01P	N04P	N07P	N10P	N16P	N20P
	SAMPLE ID	W93110423	W93110399	W93110287	W93110521	W93110241	W93110255	W93110272	W93110088	W93110070	W93110054
	DATE	AUG 26	AUG 26	AUG 25	AUG 27	AUG 25	AUG 25	AUG 25	AUG 24	AUG 24	AUG 24
PROTOPERIDINIUM PENTAGONUM		0	0	0	35	0	0	0	0	0	0
PROTOPERIDINIUM SPP.		3	8	0	385	10	0	10	8	0	8
SCRIPSIELLA TROCHOIDEA		0	3	0	23	0	10	5	0	113	0
TINTINNIDS		0	8	0	1522	70	8	3	63	8	10
UNID. ATHECATE DINOFLAGELLATE		0	3	3	8	8	0	0	0	0	5
UNID. THECATE DINOFLAGELLATES		10	0	0	18	15	3	10	0	5	3

Values are Cells/L

Table 4-3. ^{14}C production ($\text{mg C m}^{-2} \text{d}^{-1}$) estimated for euphotic layer at BioProductivity stations in August 1993.

	COASTAL STATIONS				NEARFIELD STATIONS												CAPE COD BAY STATIONS			
	F23P	F13P ⁶		N01P	N04P	N07P	N10P		N16P	N20P	F01P ⁶		F02P							
Water depth (m) ⁷	25	25		30	50	52	25		40	32	27		33							
Z _(0.5%I₀) (m)	11.5	24		23.5	25.5	27.5	16		21.5	24.5	28.5		25							
Samples ¹	S	C	S	C	S	C	S	C	S	C	S	C	S	C						
Rate ($\text{mg C m}^{-2}\text{d}^{-1}$)	2469	3768	1691	1443	2655	1665	2701	2727	3945	2187	2442	1244	680	1978						
Model ²	W	W	W	P	W	W	W	W	W	P	W	W	W	W						
P _{SP} or P _{MAX} ³	5.98	9.57	10.18	8.12	5.57	3.26	6.75	5.58	7.40	3.82	15.58	5.39	5.95	13.31						
α^4	0.046	0.062	0.035	0.069	0.033	0.032	0.037	0.093	0.036	0.043	0.080	0.118	0.031	0.156						
β^5	-	-	-	0.003	-	-	-	-	-	0.001	-	-	-	-						

¹ S: Surface sample and P-I incubations on it.

C: Chlorophyll max sample and P-I incubations on it.

² P: Platt *et al.* (1980).

W: Webb *et al.* (1974).

³ P_{SP}: Production parameter for Platt *et al.* model.

P_{MAX}: Production parameter for Webb *et al.* model.

⁴ Parameter for both models.

⁵ Parameter for Platt *et al.* model.

⁶ Z_(0.5%I₀) was greater than the profile depths at stations F01P (24.5 m) and F13P (23 m).

⁷ Water depth data were not available, depths indicated are from CW/QAPP (Albro *et al.* 1993).

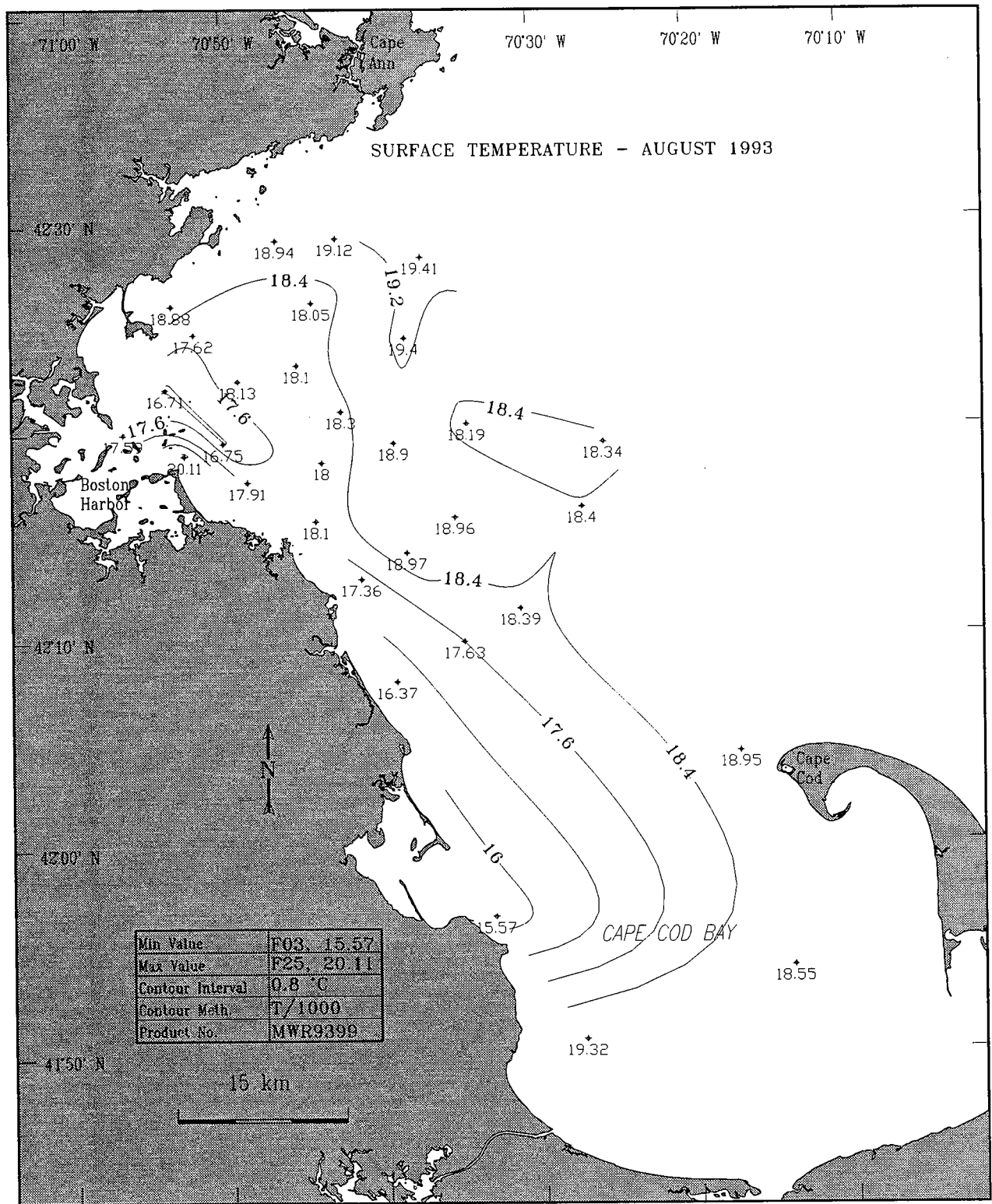


Figure 4-1. Surface temperature (°C) in the study area in late August 1993. Data are from the surfacemost sample at all farfield survey stations, including the BioProductivity stations within the nearfield grid (Appendix A).

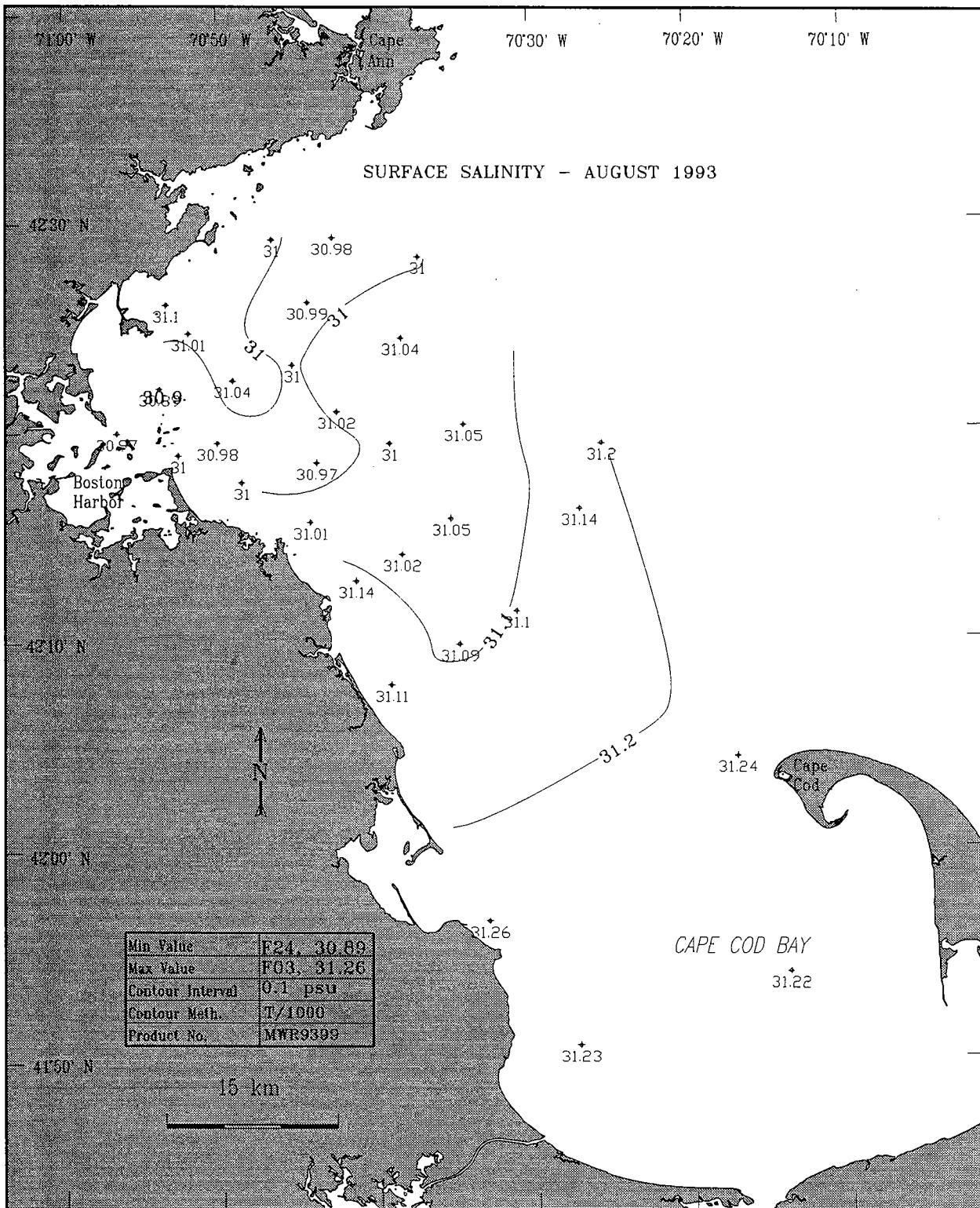


Figure 4-2. Surface salinity (PSU) in the study area in late August 1993. Data are from the surfacemost sample at all farfield survey stations, including the BioProductivity stations within the nearfield grid (Appendix A).

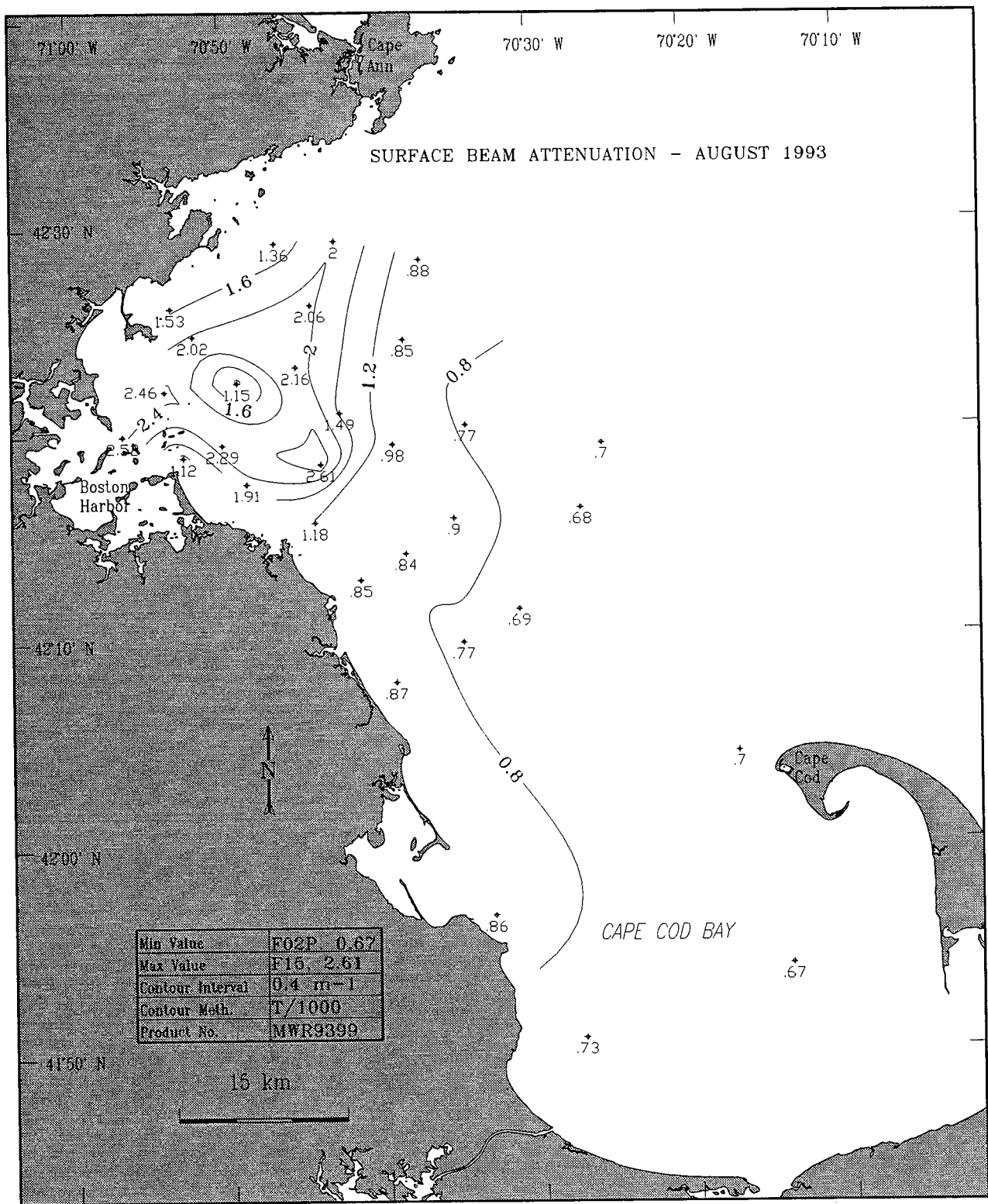


Figure 4-3. Surface beam attenuation (m^{-1}) in the study area in late August 1993. Data are from the surfacemost sample at all farfield survey stations, including the BioProductivity stations within the nearfield grid (Appendix A).

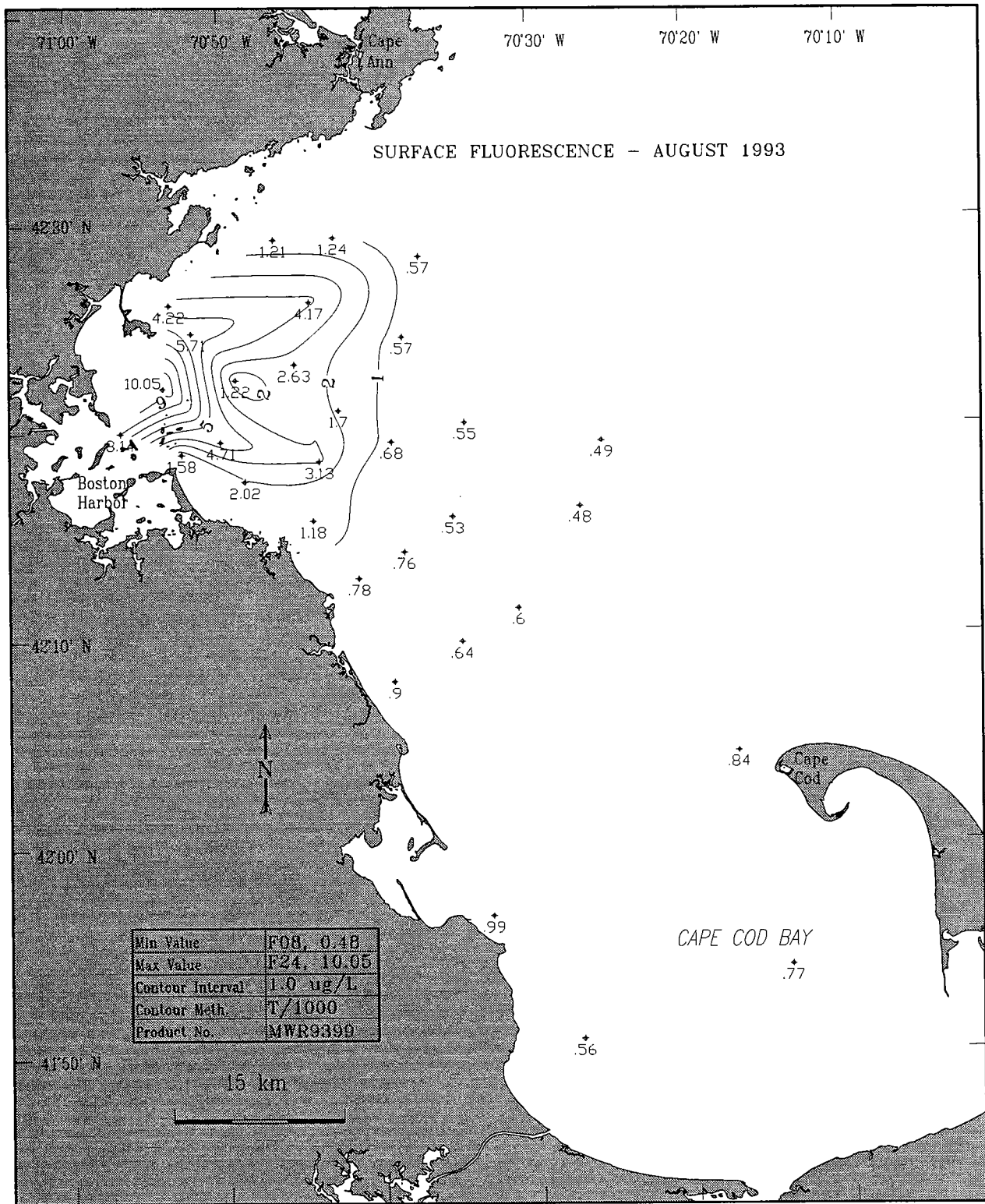


Figure 4-4. Surface *in situ* fluorescence (as $\mu\text{g Chl L}^{-1}$) in the study area in late August 1993. Data are from the surfacemost sample at all farfield survey stations, including the BioProductivity stations within the nearfield grid (Appendix A).

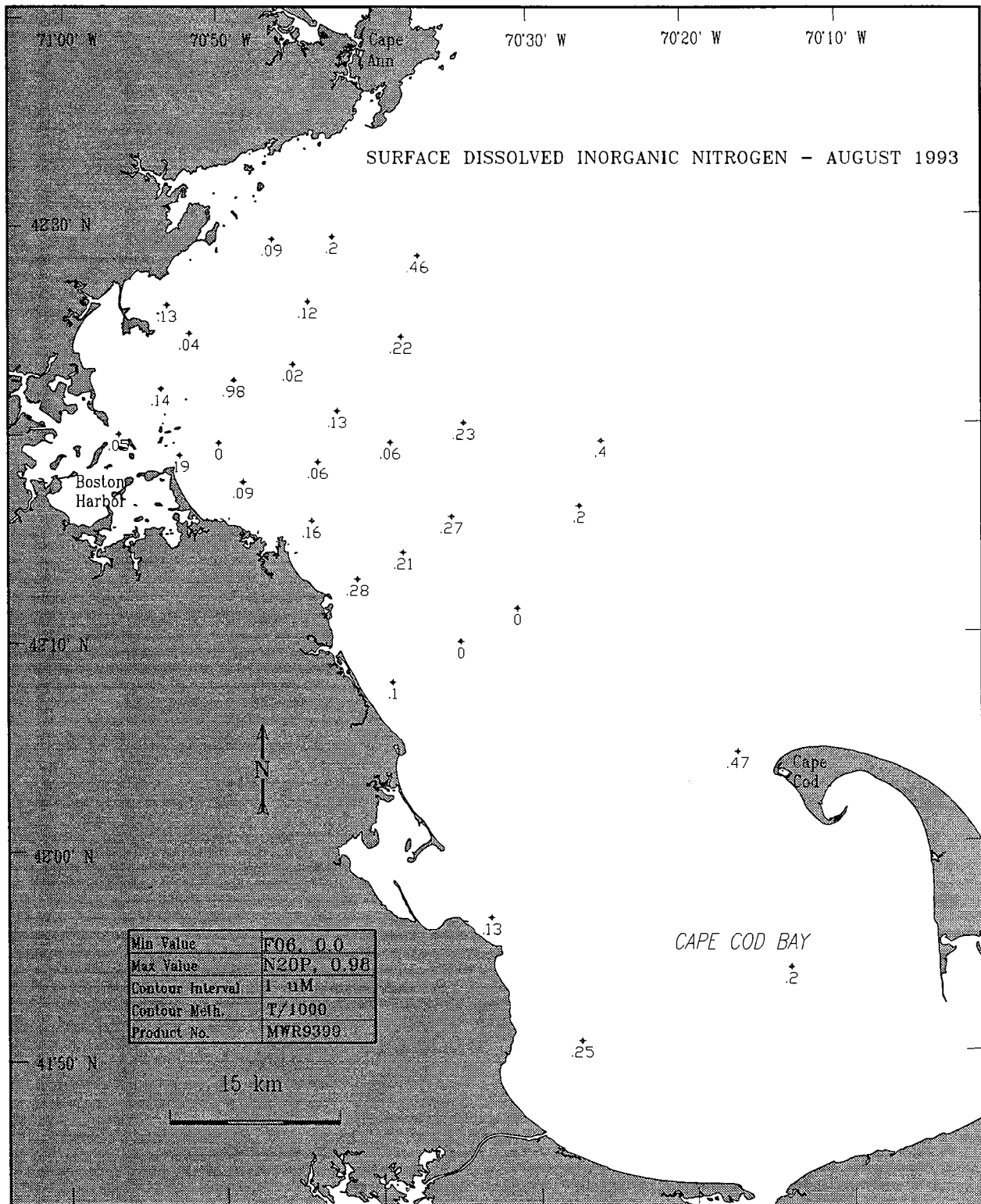


Figure 4-5. Surface dissolved inorganic nitrogen (DIN, μ M) in the study area in late August 1993. Data are from the surfacemost sample at all farfield survey stations, including the BioProductivity stations within the nearfield grid (Appendix A).

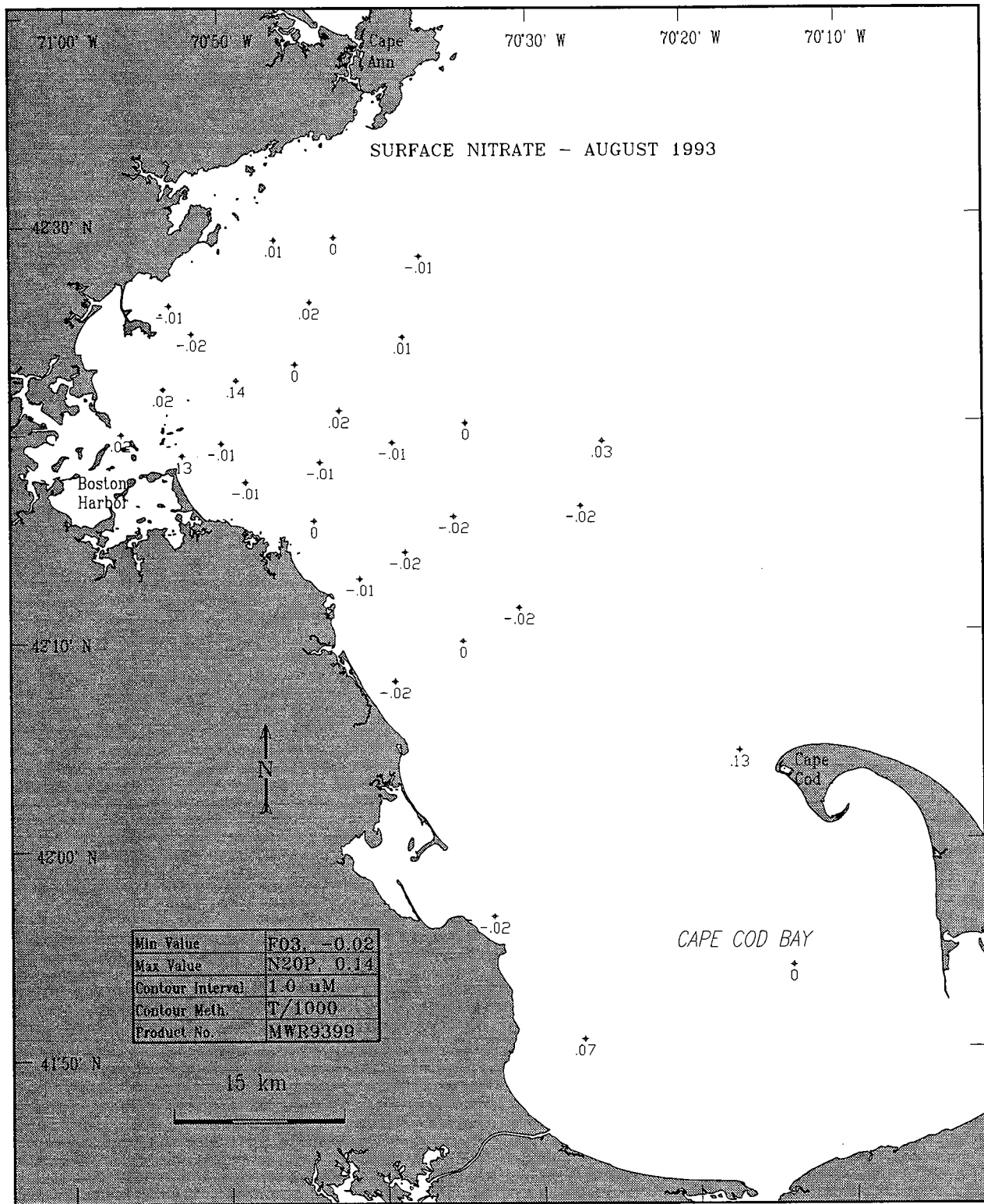


Figure 4-6. Surface nitrate (NO_3 , μM) in the study area in late August 1993. Data are from the surfacemost sample at all farfield survey stations, including the BioProductivity stations within the nearfield grid (Appendix A).

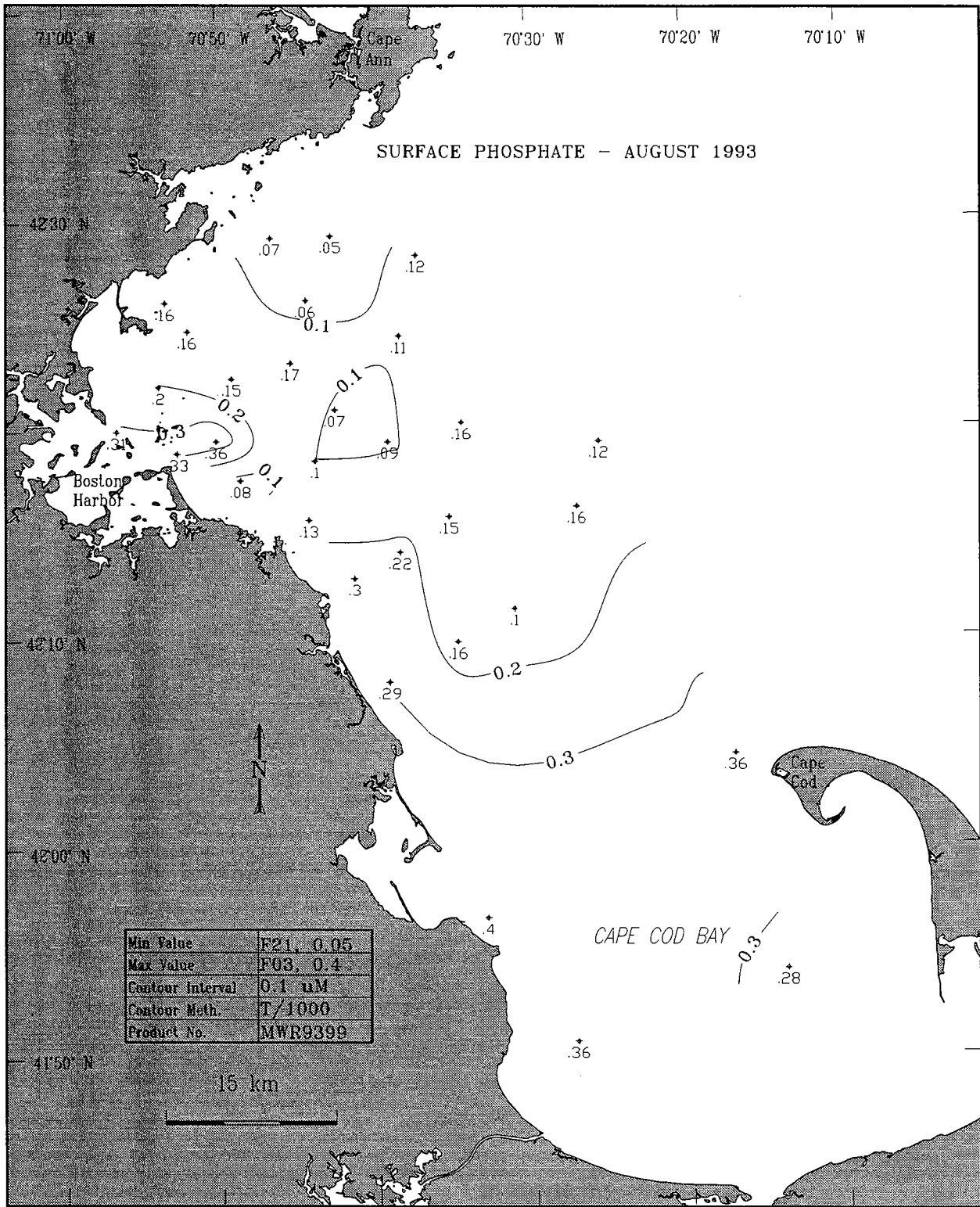


Figure 4-7. Surface phosphate (PO_4 , μM) in the study area in late August 1993. Data are from the surfacemost sample at all farfield survey stations, including the BioProductivity stations within the nearfield grid (Appendix A).

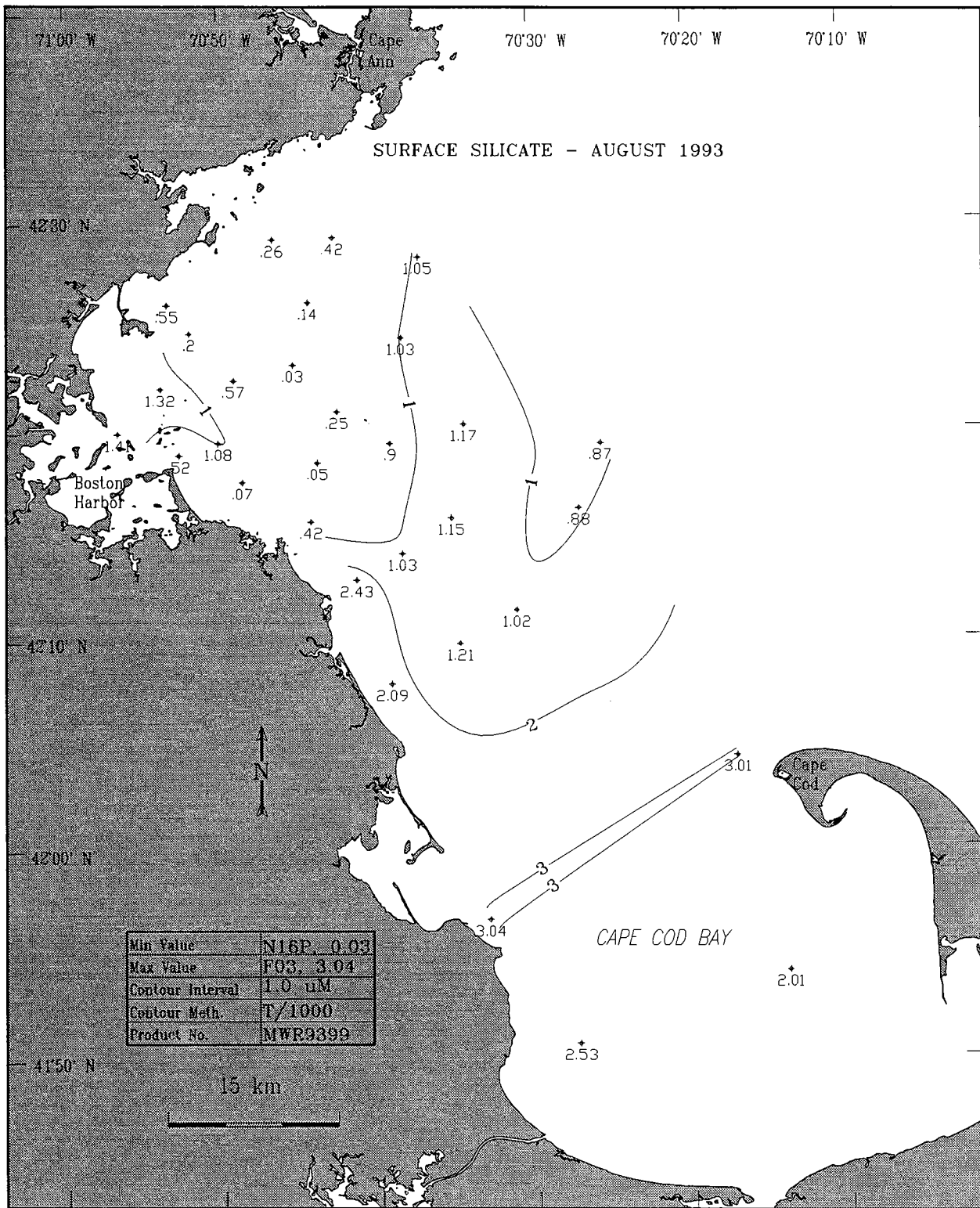


Figure 4-8. Surface silicate (SiO_4 , μM) in the study area in late August 1993. Data are from the surfacemost sample at all farfield survey stations, including the BioProductivity stations within the nearfield grid (Appendix A).

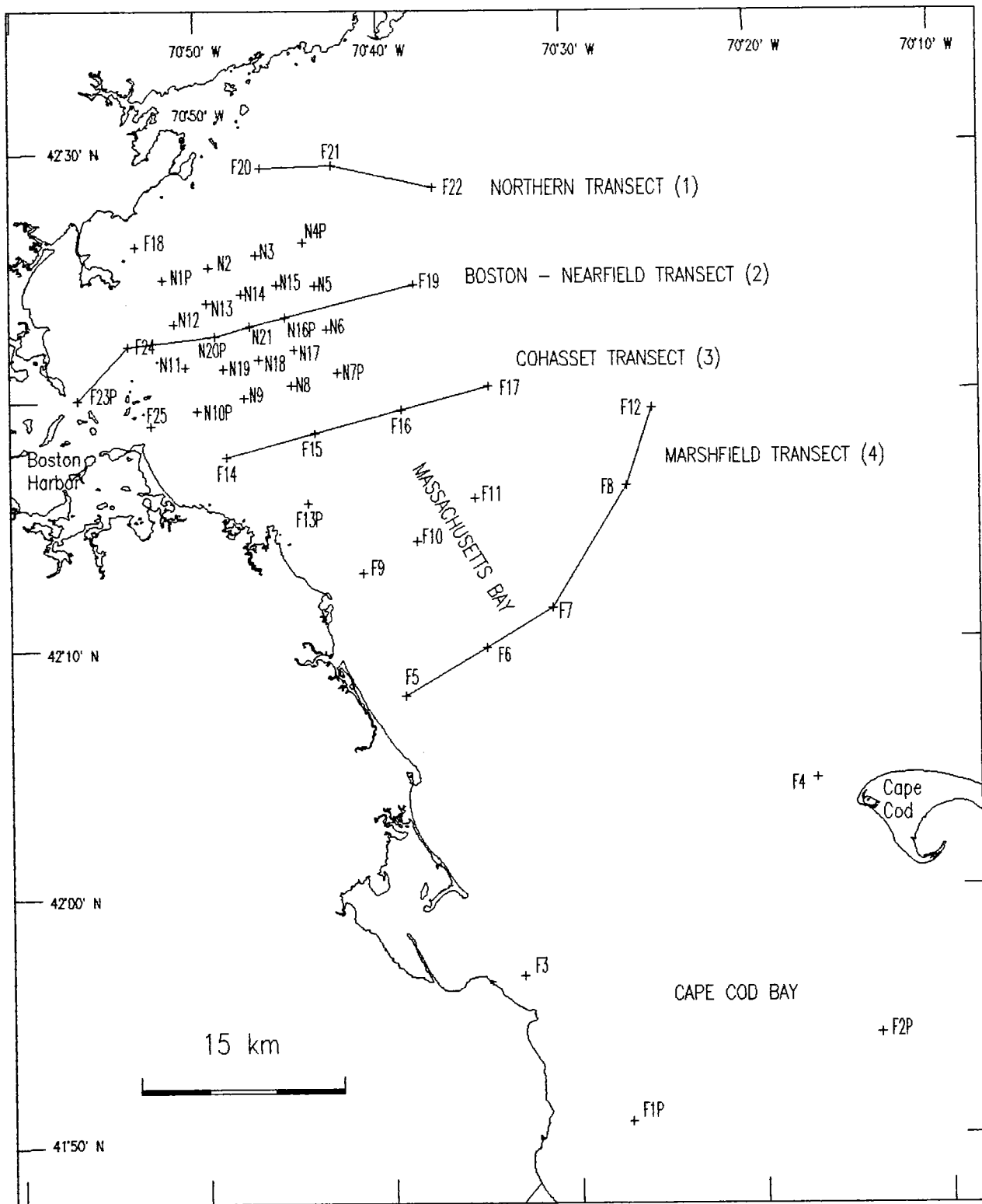


Figure 4-9. Map showing position of four standard transects for which vertical contour plots were produced in following Figures 4-10 to 4-14.

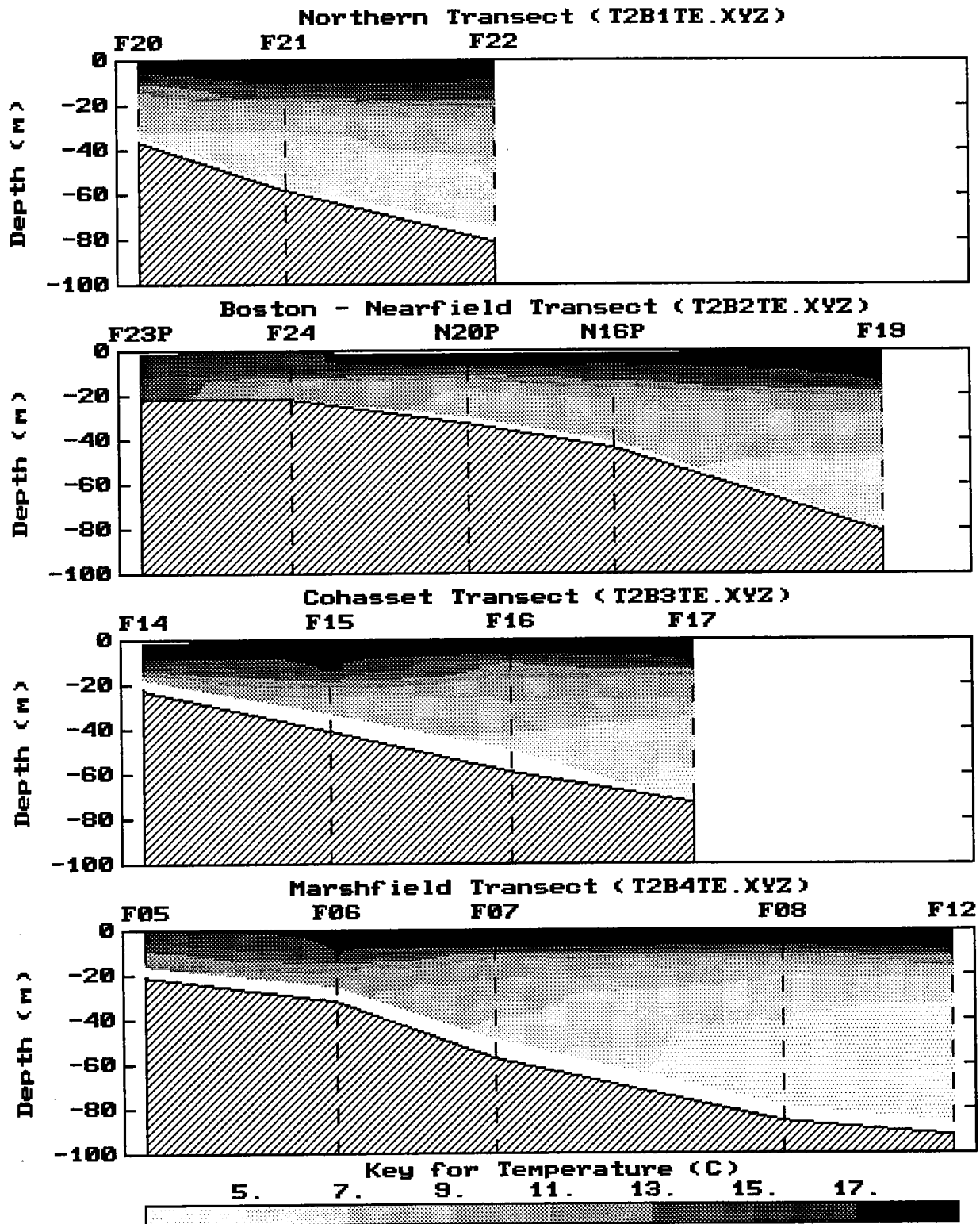


Figure 4-10a. Vertical section contours of temperature in late August 1993 for standard transects (see Figure 4-9). The data used to produce contours are from high-resolution continuous vertical profiles taken from the downcast at each station.

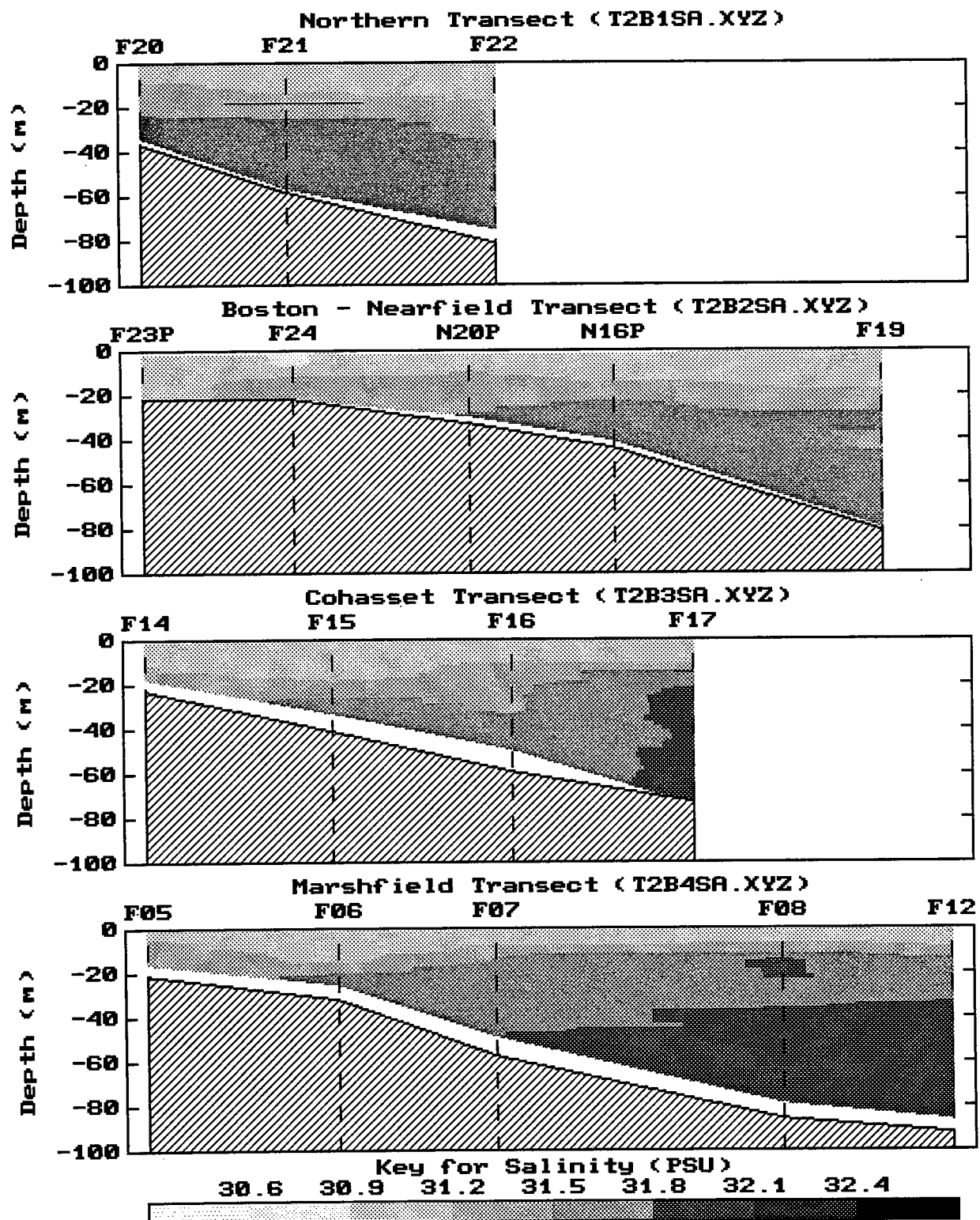


Figure 4-10b. Vertical section contours of salinity in late August 1993 for standard transects (see Figure 4-9). The data used to produce contours are from high-resolution continuous vertical profiles taken from the downcast at each station.

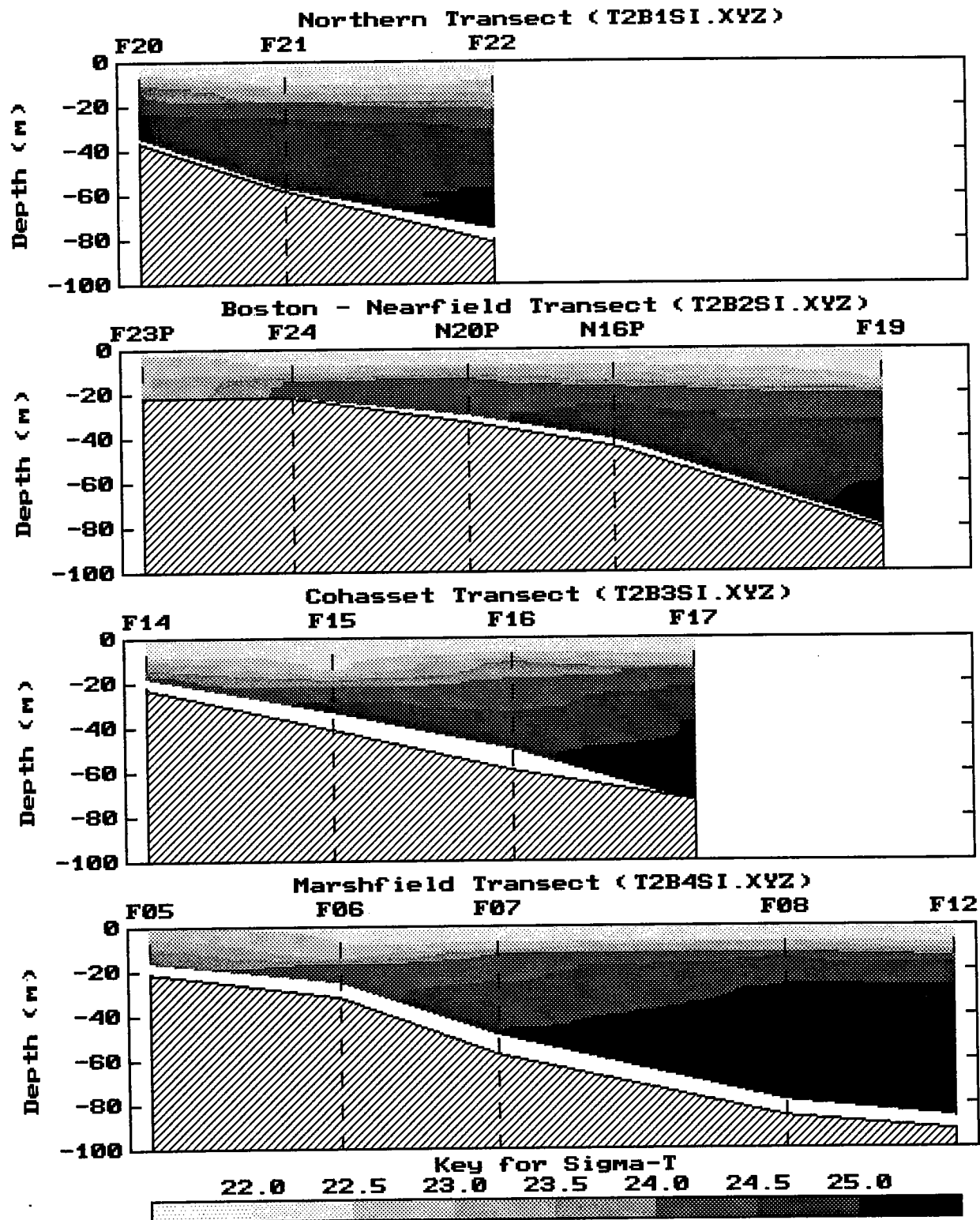


Figure 4-10c. Vertical section contours of density (σ_T) in late August 1993 for standard transects (see Figure 4-9). The data used to produce contours are from high-resolution continuous vertical profiles taken from the downcast at each station.

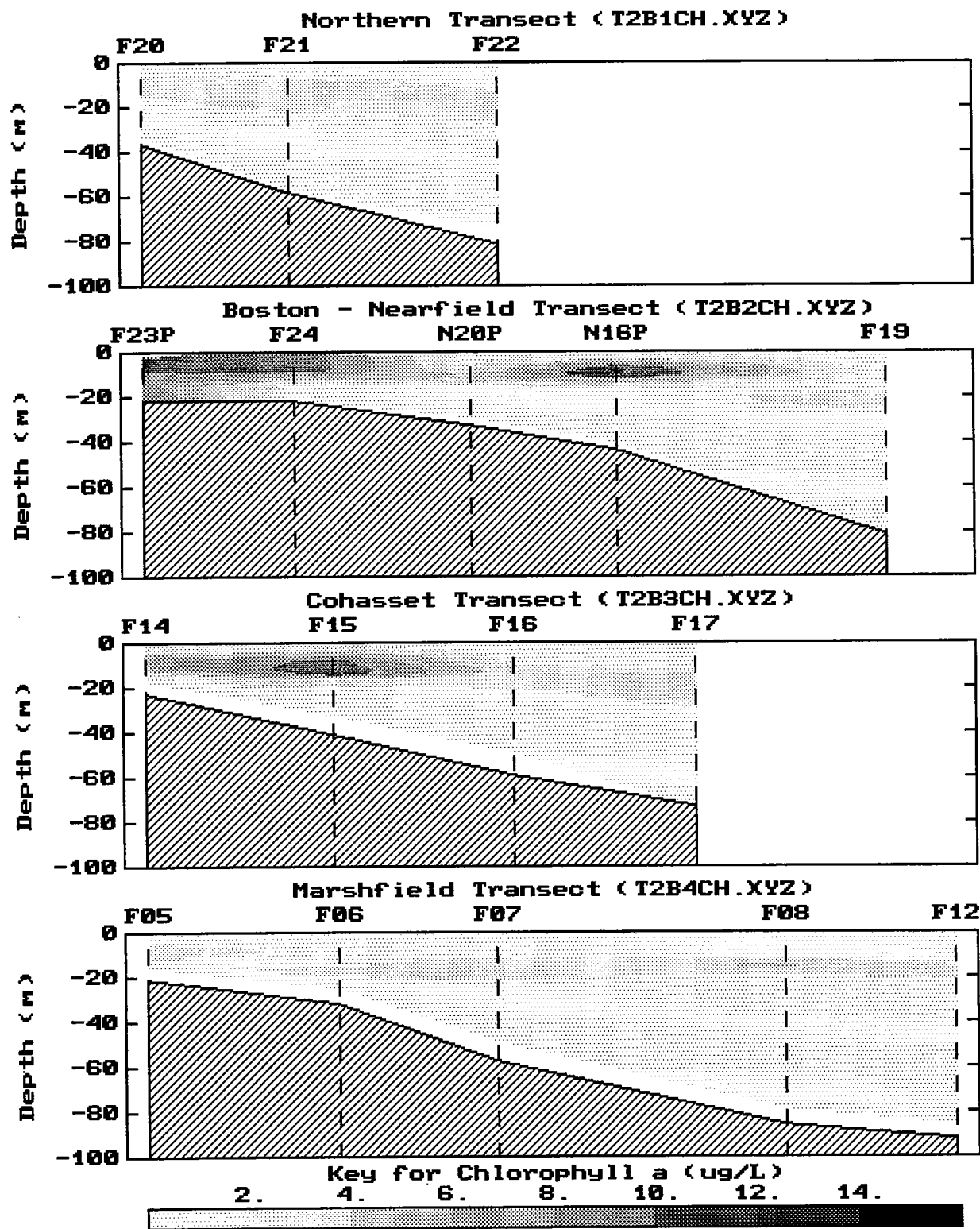


Figure 4-11. Vertical section contours of fluorescence (as $\mu\text{g Chl L}^{-1}$) in late August 1993 for standard transects (see Figure 4-9). The data used to produce contours are from high-resolution continuous vertical profiles taken from the downcast at each station.

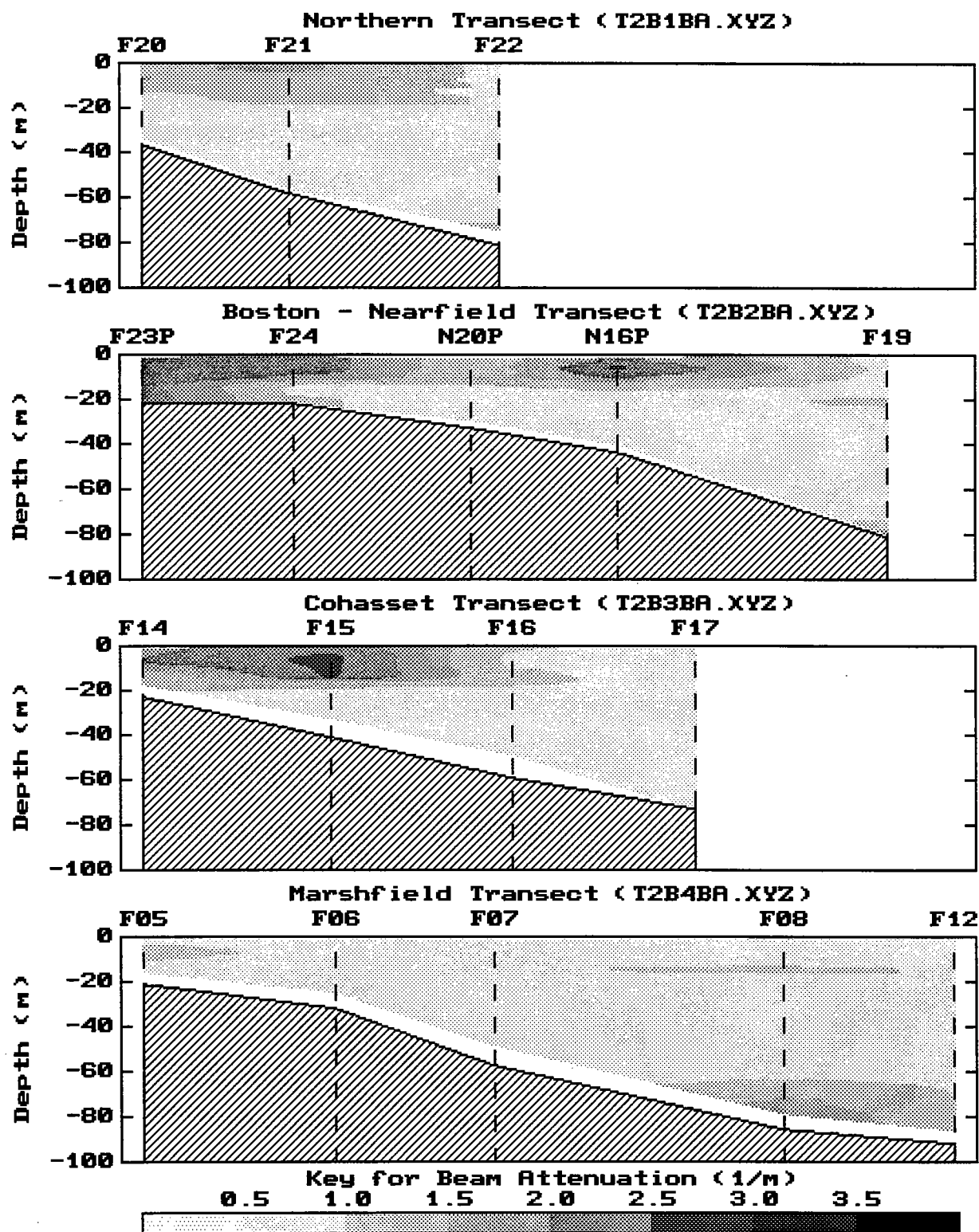


Figure 4-12. Vertical section contours of beam attenuation in late August 1993 for standard transects (see Figure 4-9). The data used to produce contours are from high-resolution continuous vertical profiles taken from the downcast at each station.

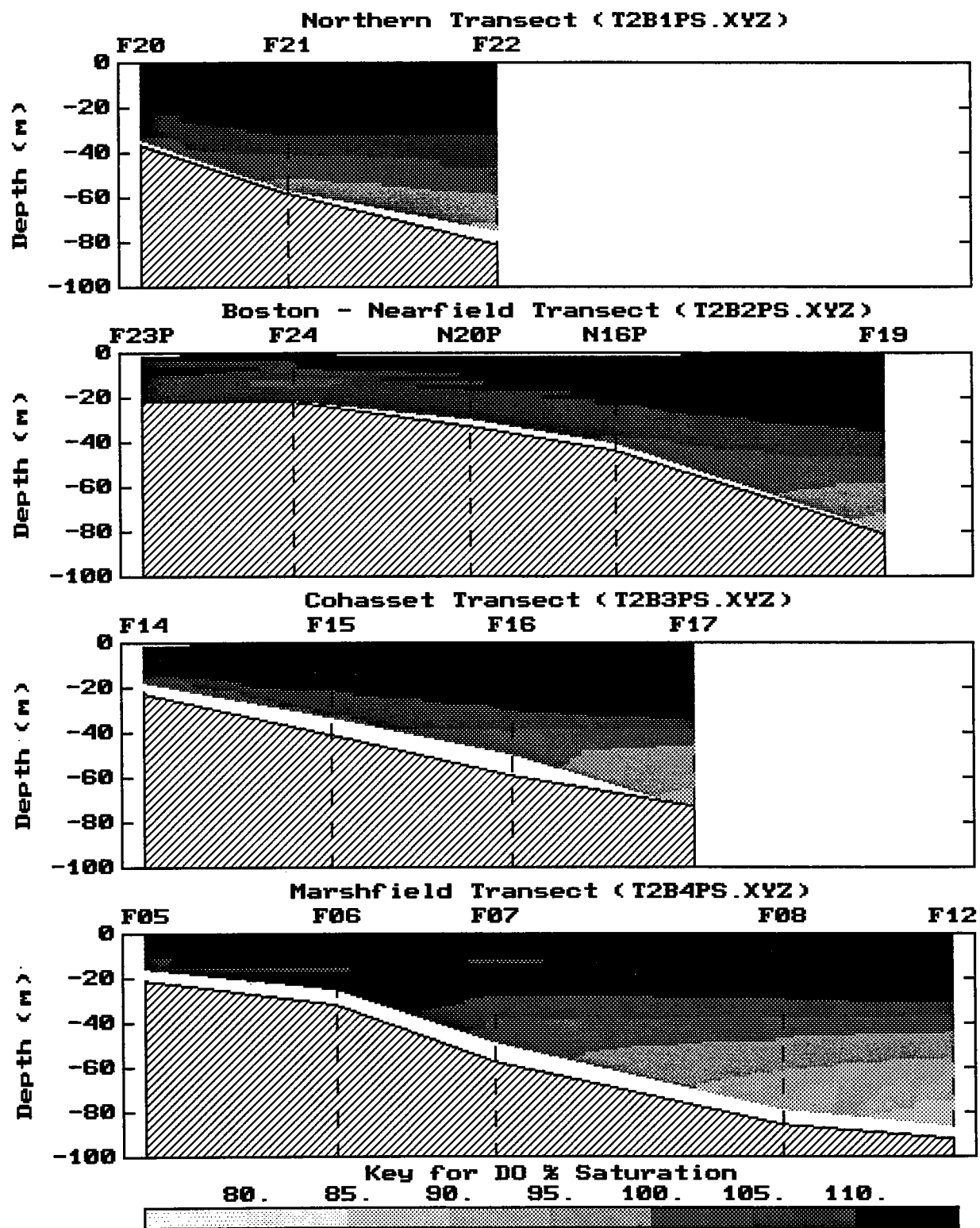


Figure 4-13. Vertical section contours of dissolved oxygen (% saturation) in late August 1993 for standard transects (see Figure 4-9). The data used to produce contours are from high-resolution continuous vertical profiles taken from the downcast at each station.

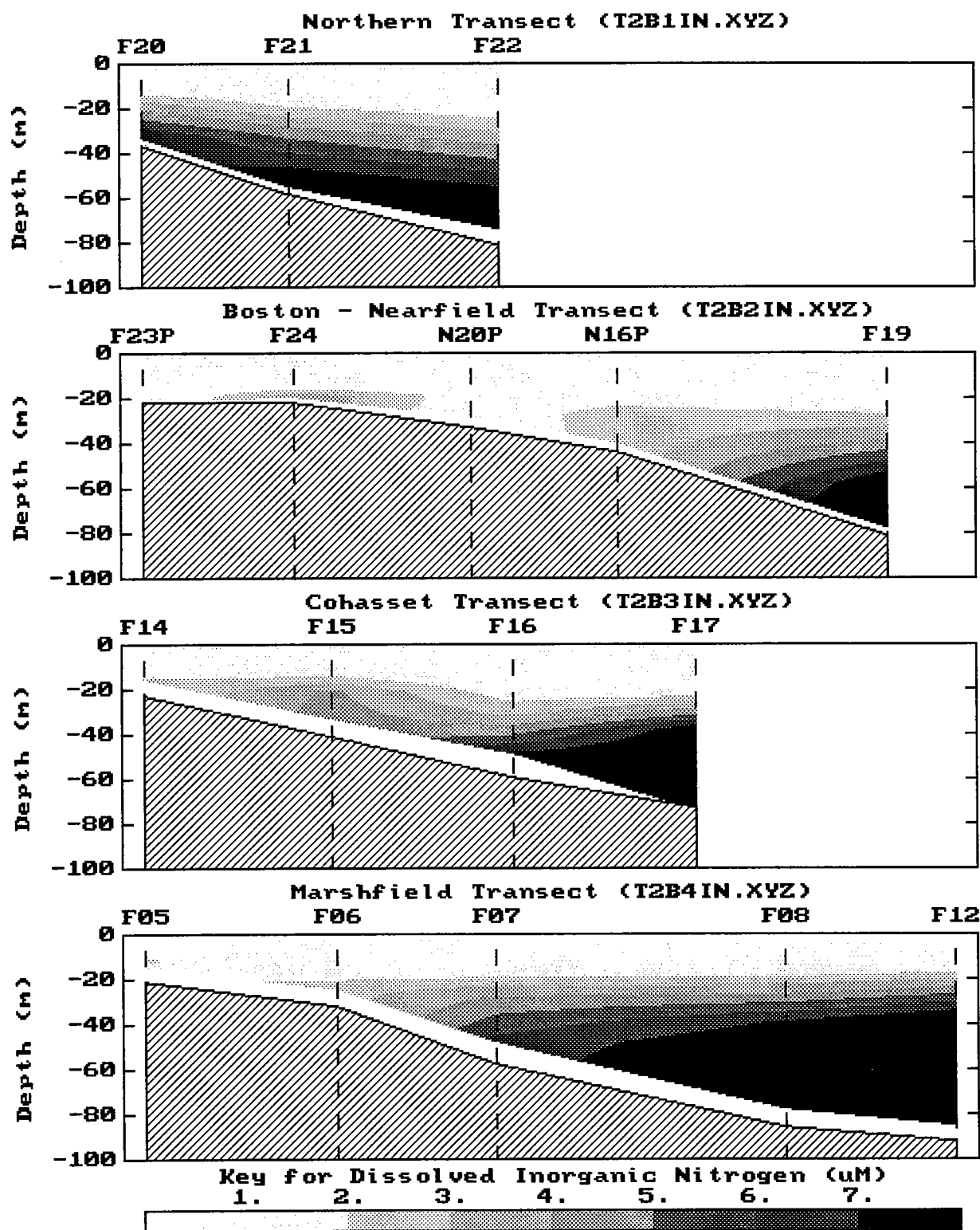


Figure 4-14a. Vertical section contours of dissolved inorganic nitrogen (DIN, μM) in late August 1993 for standard transects (see Figure 4-9). The data used to produce contours are from discrete bottle samples (Appendix A).

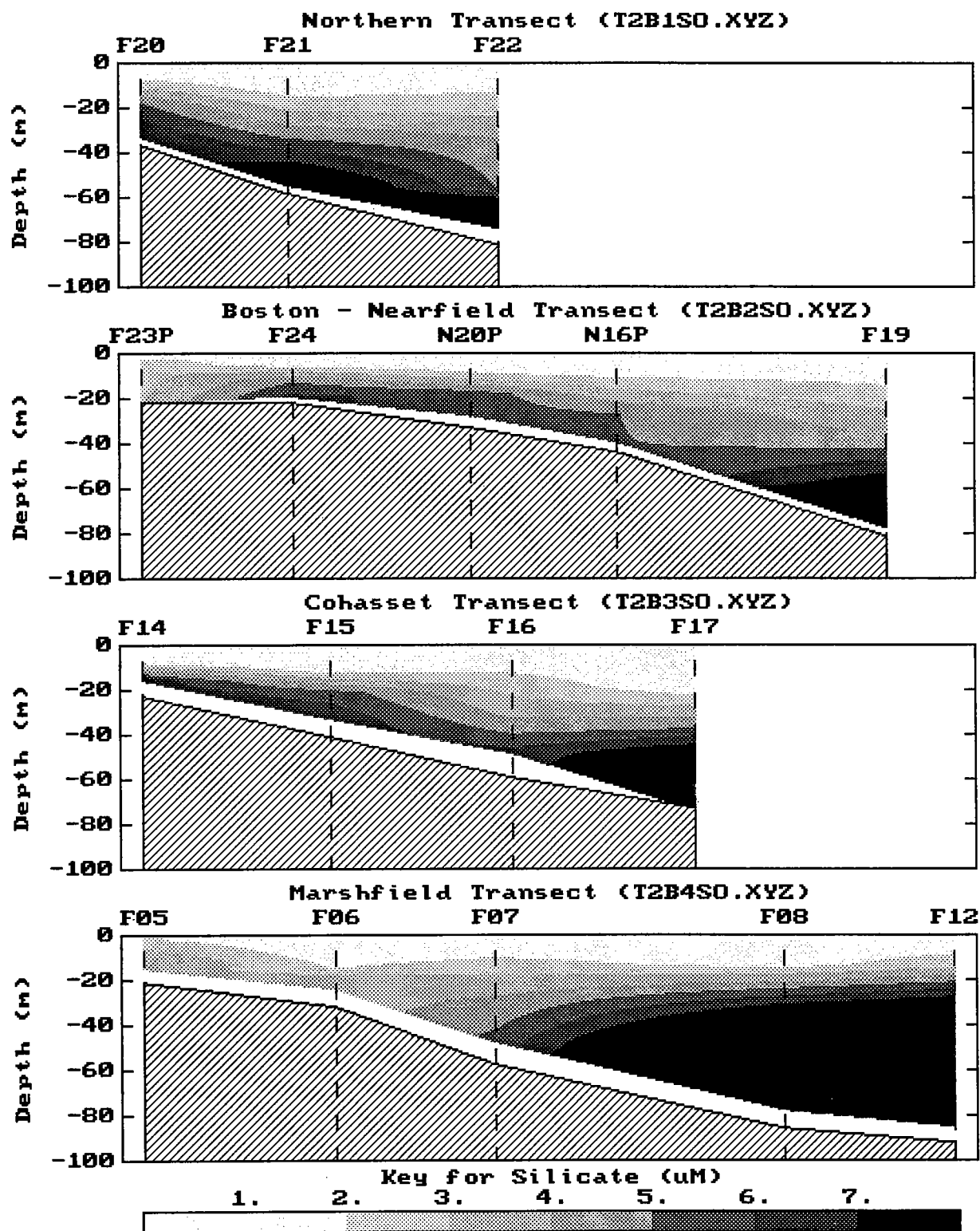


Figure 4-14b. Vertical section contours of silicate (SiO_4 , μM) in late August 1993 for standard transects (see Figure 4-9). The data used to produce contours are from discrete bottle samples (Appendix A).

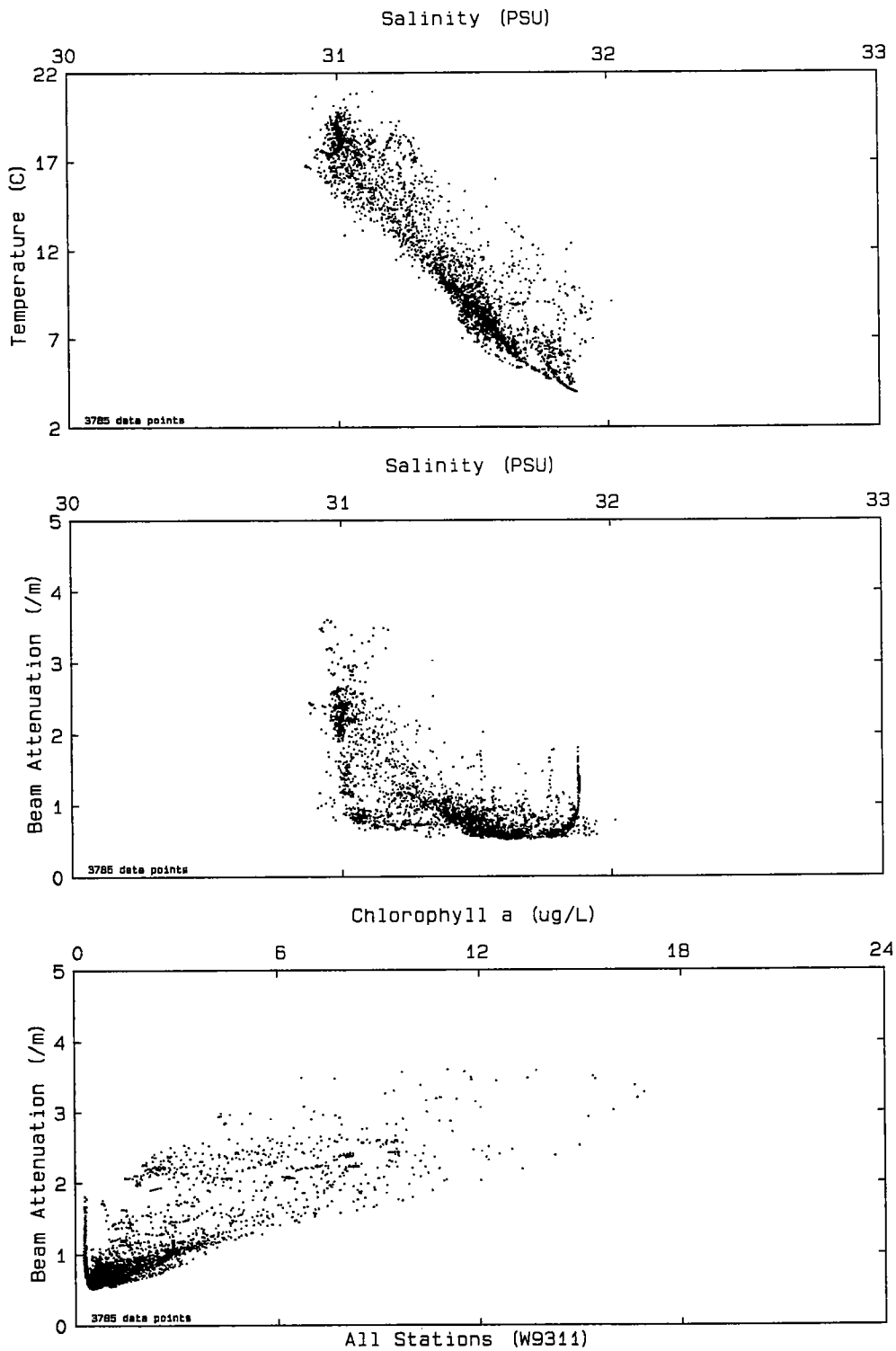


Figure 4-15a. Scatter plots of data acquired by *in situ* sensor package during vertical casts at all farfield and nearfield stations occupied in late August 1993. Regional plots are in Appendix C. Chlorophyll is estimated from *in situ* fluorescence.

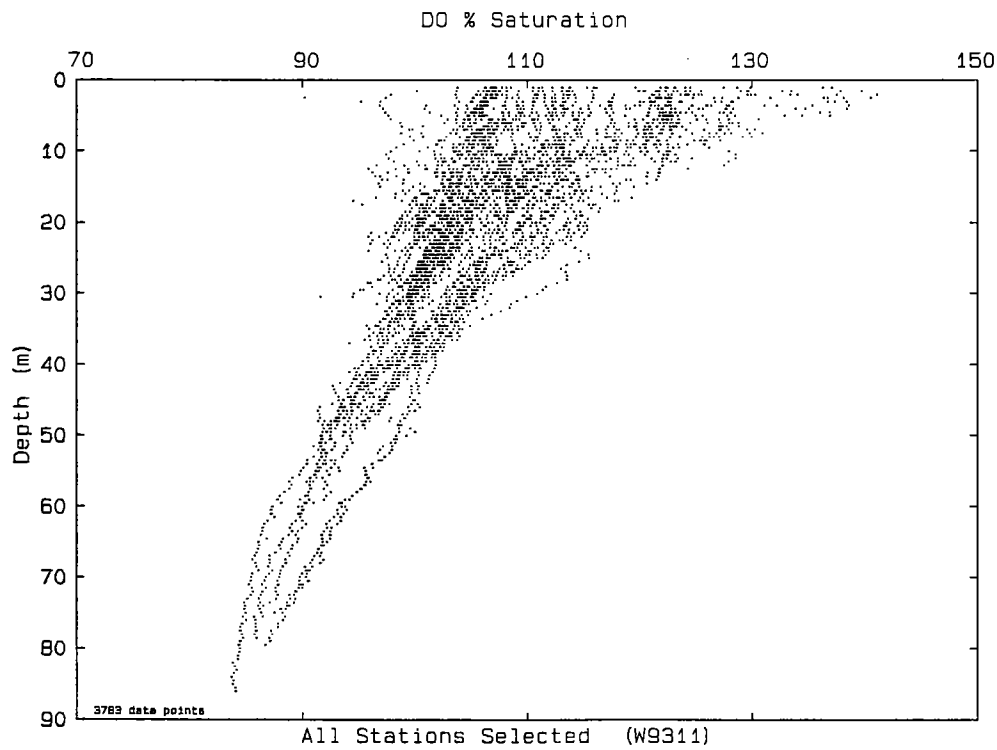
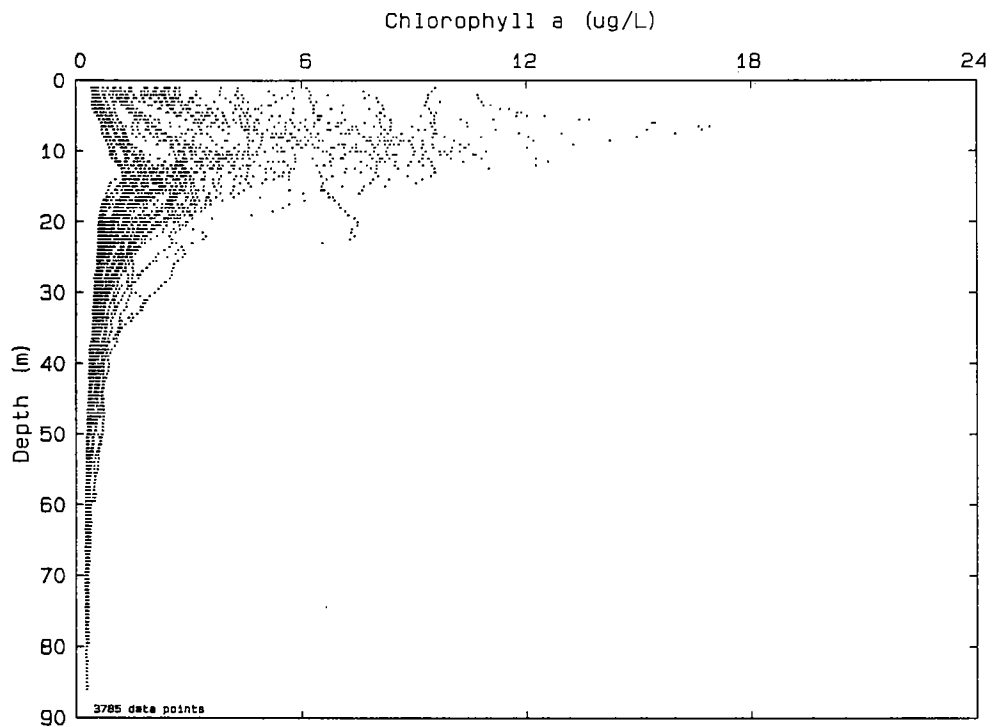


Figure 4-15b. Scatter plots of data acquired by *in situ* sensor package during vertical casts at all farfield and nearfield stations occupied in late August 1993. Regional plots are in Appendix C. Chlorophyll is estimated from *in situ* fluorescence.

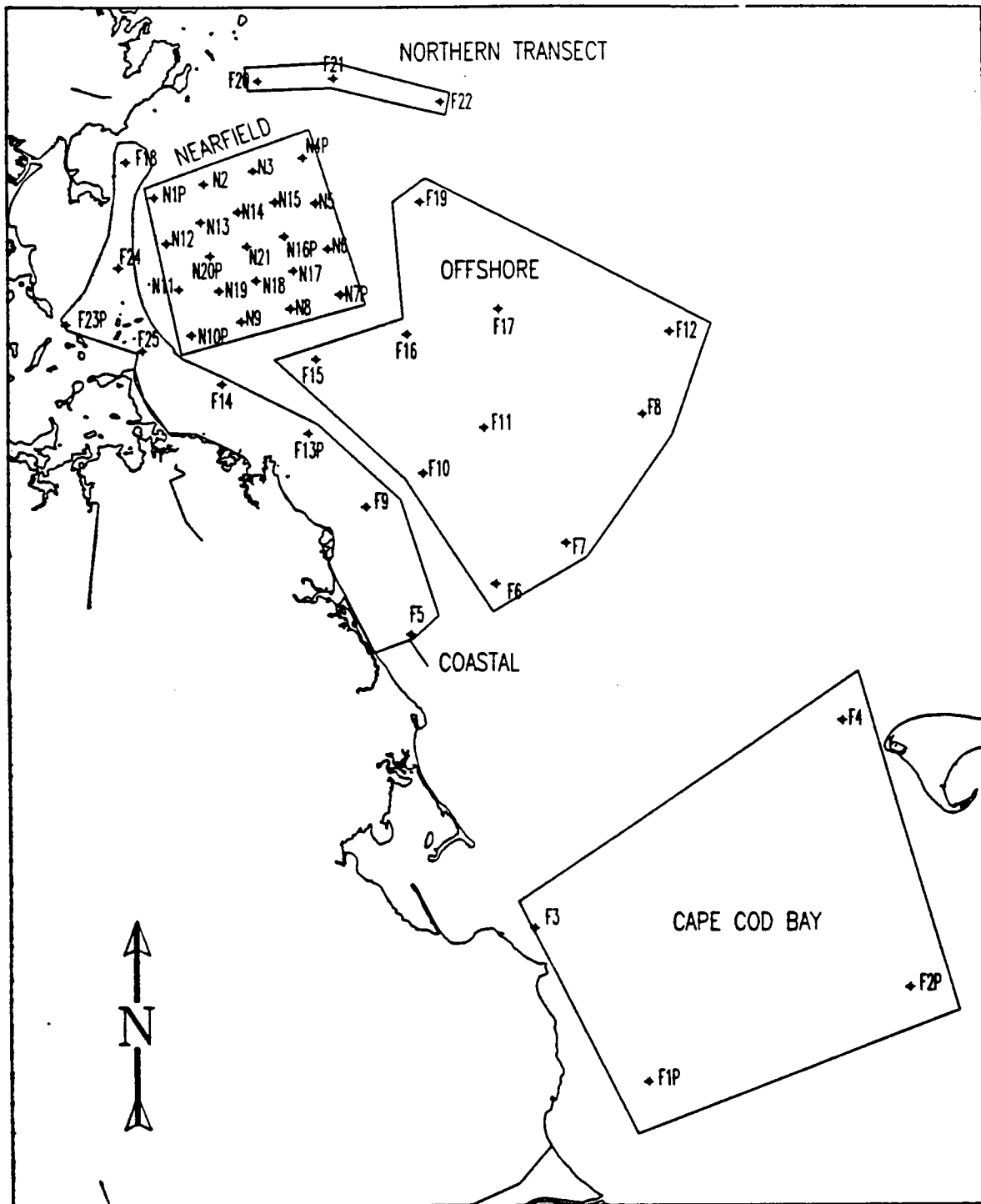
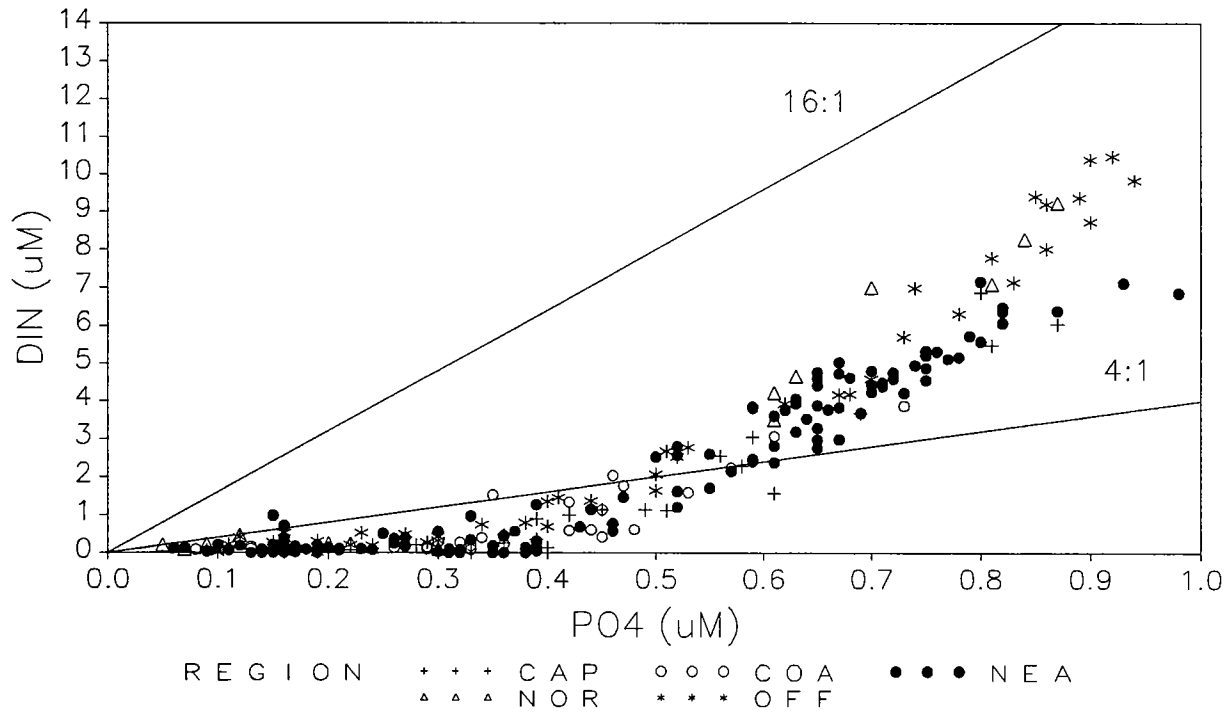


Figure 4-16. Map to show station groups designated in Figures 4-17 through 4-22. Massachusetts Bay stations were separated into four groups based on water depth and geographic position; Cape Cod Bay has four stations.

Late August (W9311)



Late August (W9311)

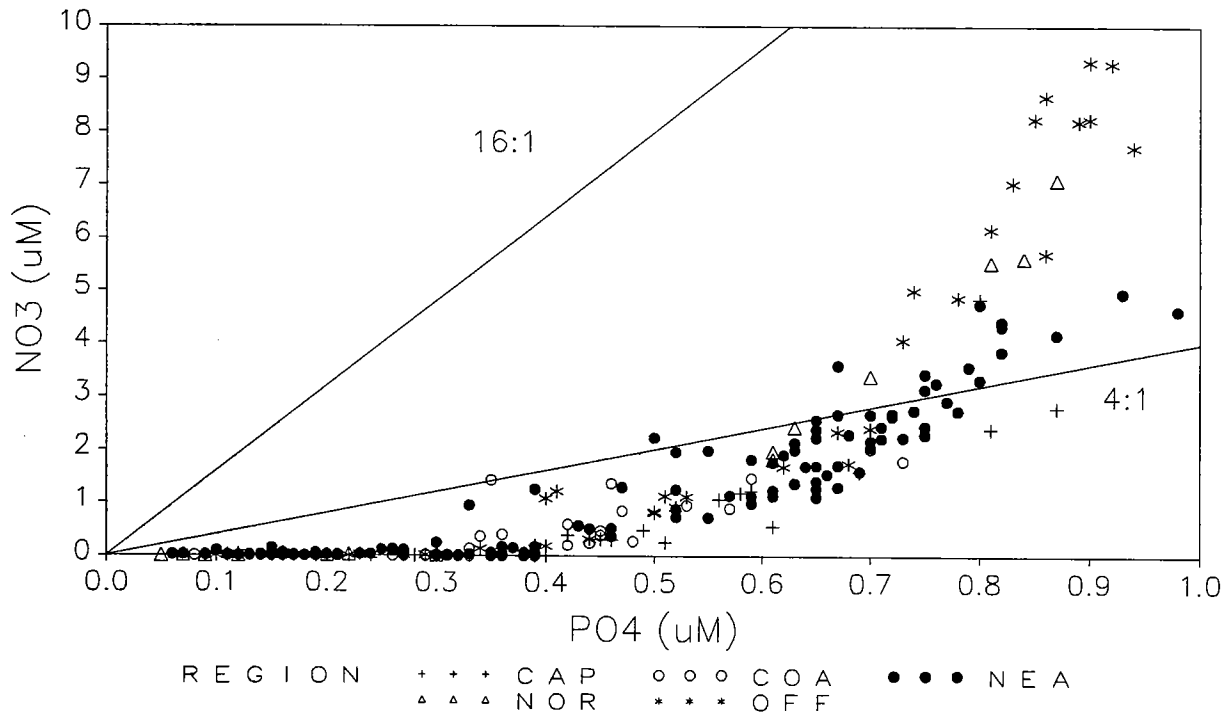


Figure 4-17. Scatter plots of nitrogen forms vs. phosphate during late August 1993. All stations and depths are included. Lines show constant proportions of nitrogen relative to phosphorous. Data are given in Appendix A. The regions correspond to the groups of stations shown in Figure 4-16.

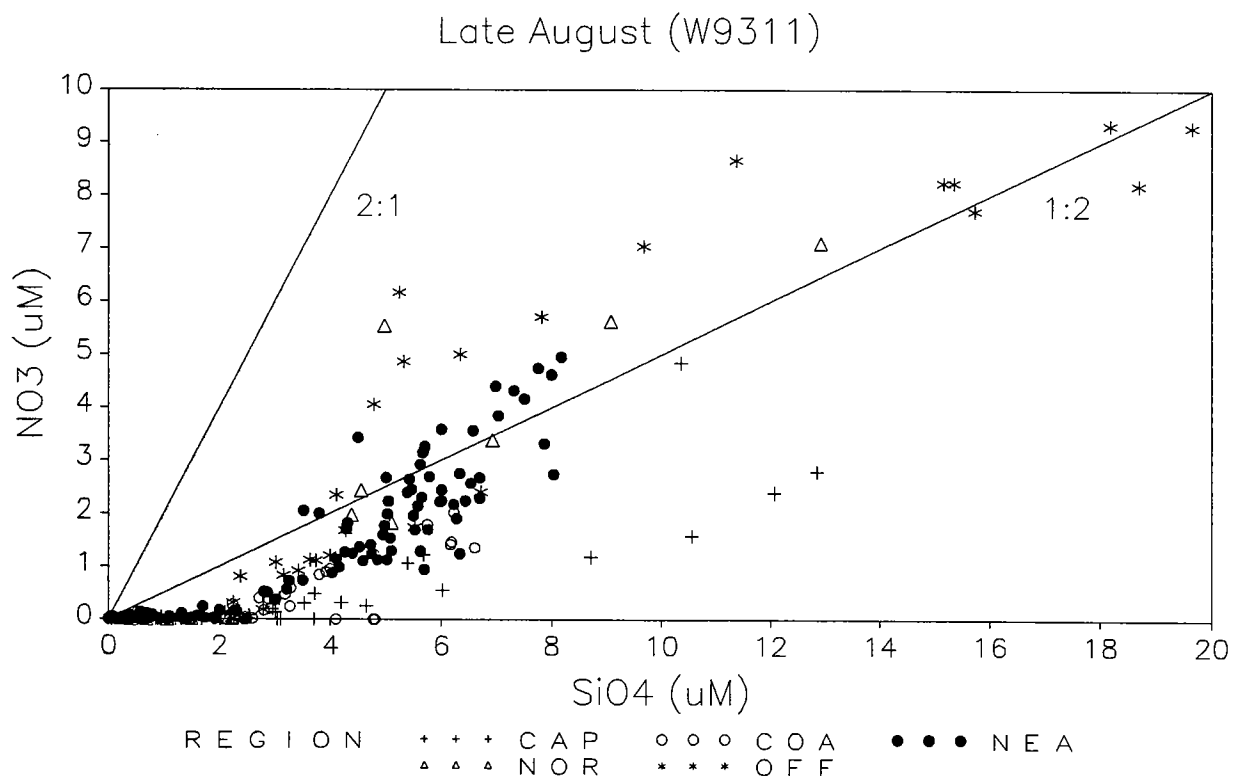
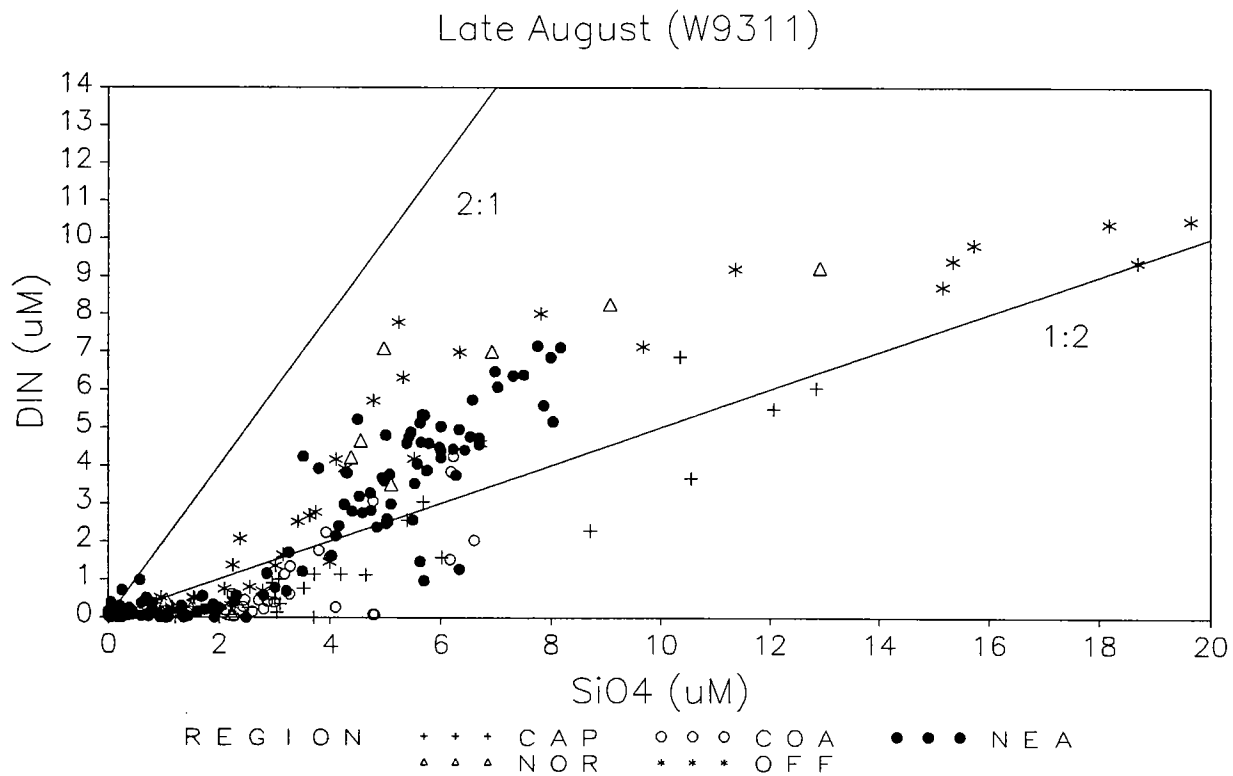


Figure 4-18. Scatter plots of nitrogen vs. silicate during late August 1993. All stations and depths are included. Lines show constant proportions of nitrogen relative to silicate. Data are given in Appendix A. The regions correspond to the groups of stations shown in Figure 4-16.

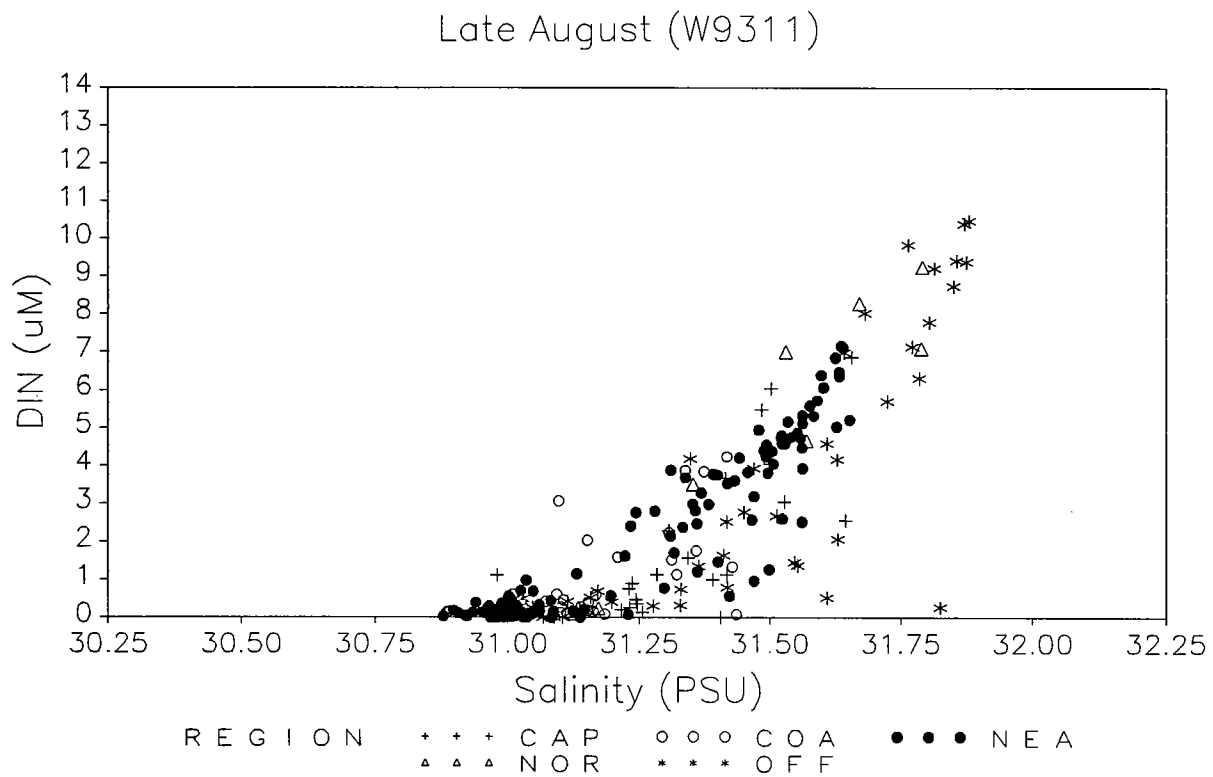
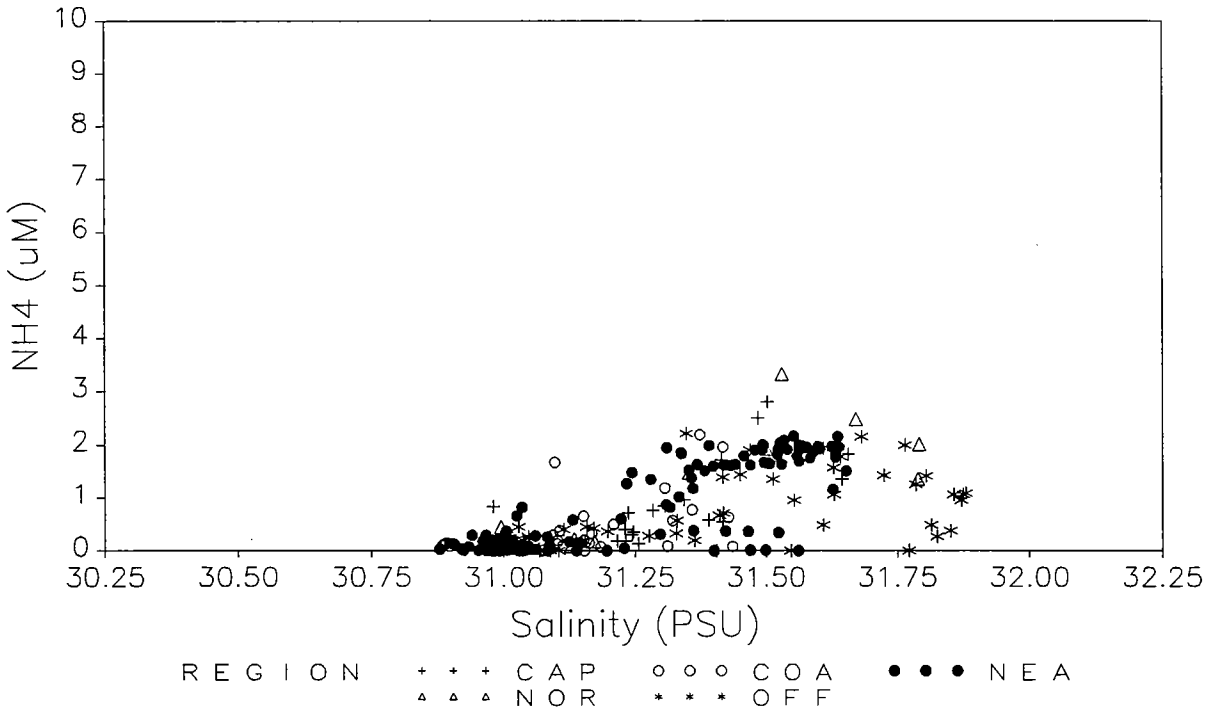


Figure 4-19. Dissolved inorganic nitrogen vs. salinity in late August 1993. All stations and depths are included. Data are given in Appendix A. The regions correspond to the groups of stations shown in Figure 4-16.

Late August (W9311)



Late August (W9311)

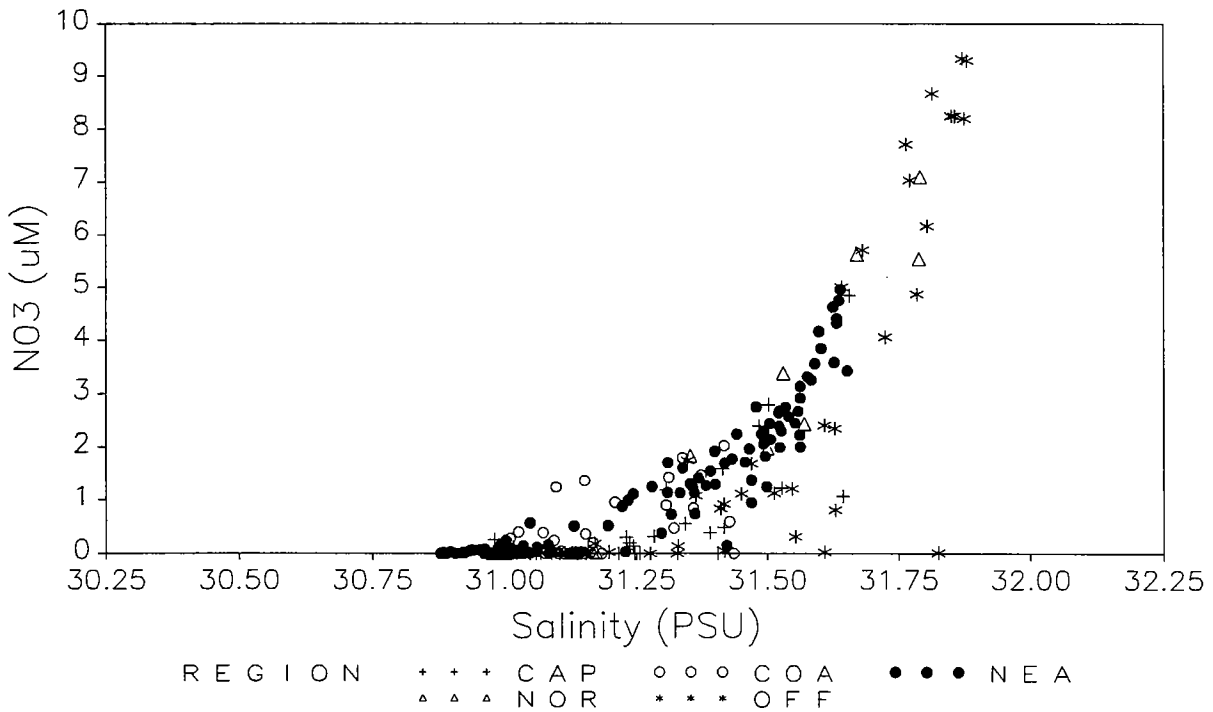


Figure 4-20. Ammonia and nitrate vs. salinity in late August 1993. All stations and depths are included. Data are given in Appendix A. The regions correspond to the groups of stations shown in Figure 4-16.

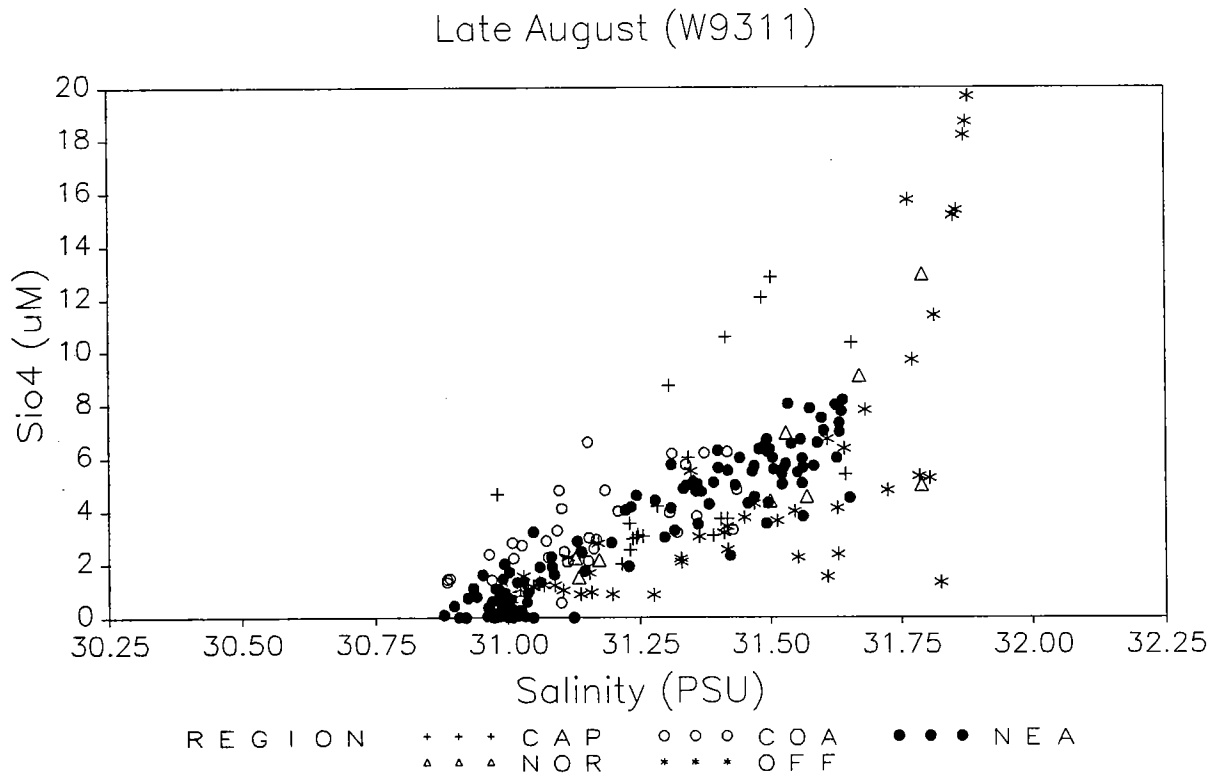
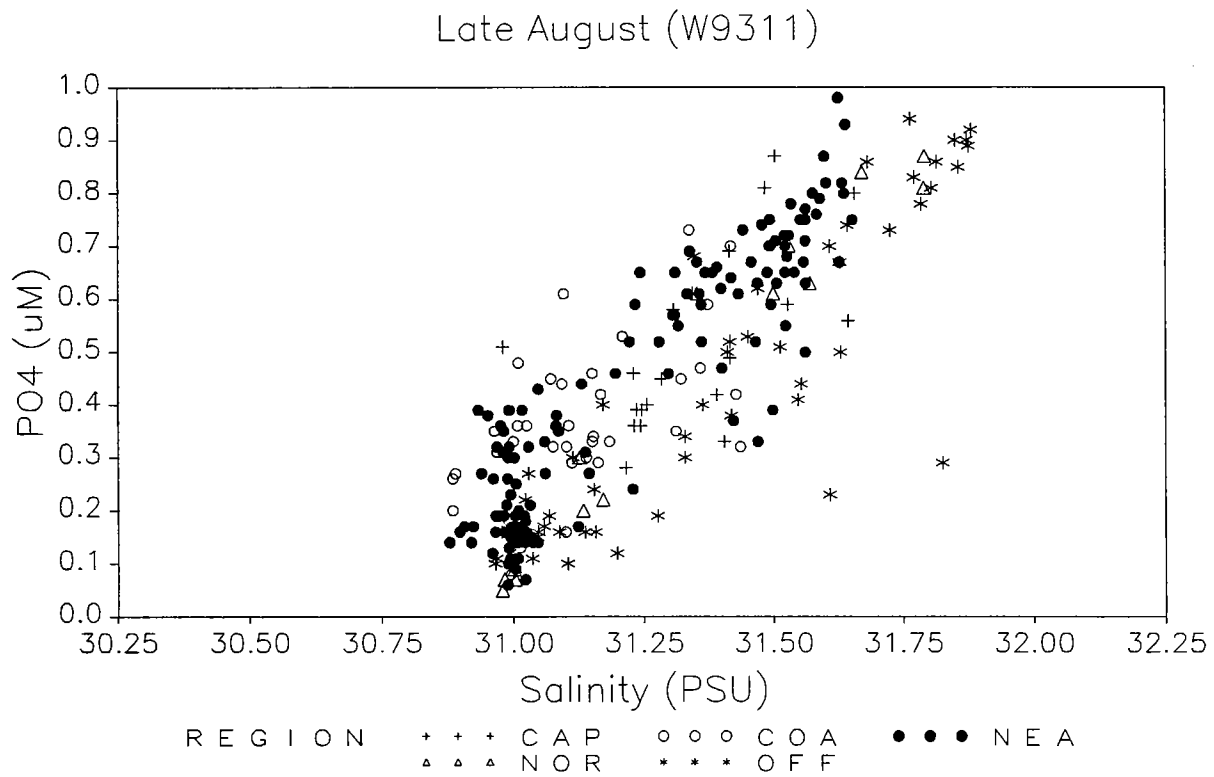


Figure 4-21. Phosphate and silicate vs. salinity in late August 1993. All stations and depths are included. Data are given in Appendix A. The regions correspond to the groups of stations shown in Figure 4-16.

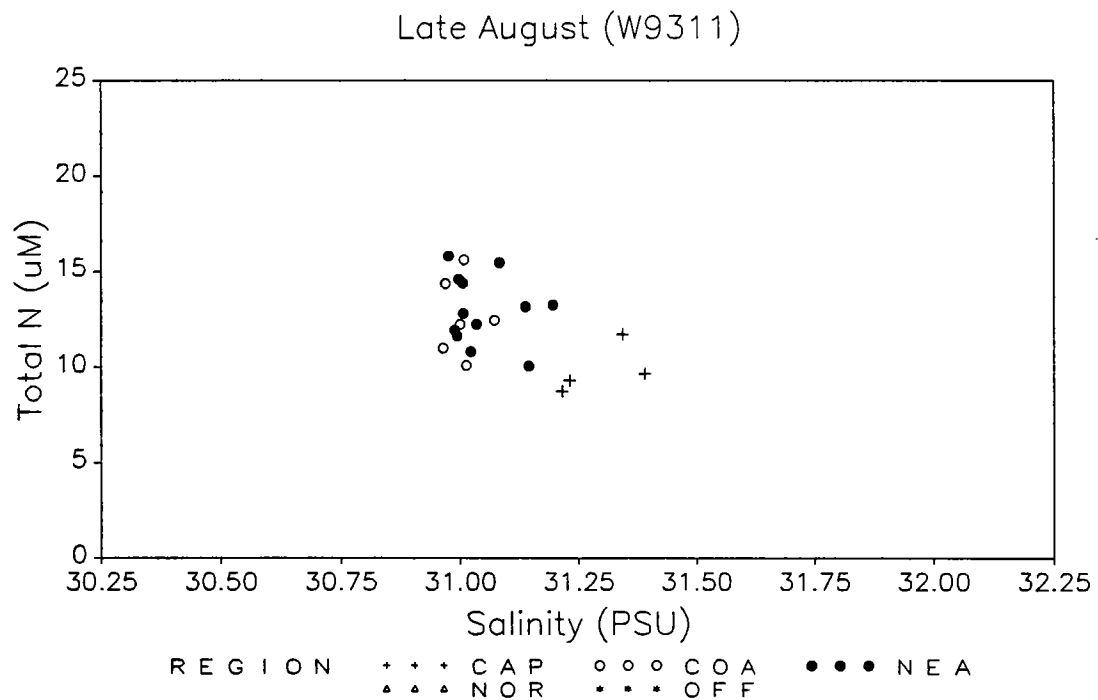
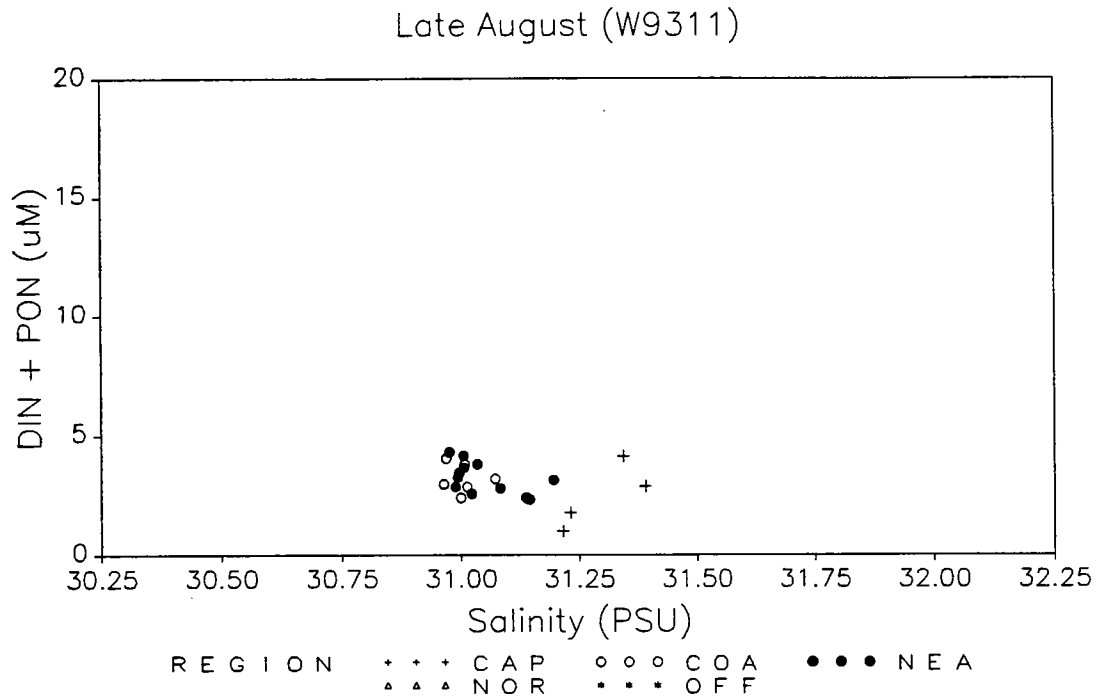


Figure 4-22. Nitrogen forms vs. salinity in late August 1993. Data are from BioProductivity stations and special station F25. The station groups are coded as given in Figure 4-16; there are no BioProductivity stations in the offshore or northern transect groups. Data are given in Appendix A. Dissolved inorganic nitrogen = DIN, Particulate organic nitrogen = PON, Total nitrogen (TN) = Total dissolved nitrogen (TDN) + PON. The regions correspond to the groups of stations shown in Figure 4-16.

Late August (W9311)

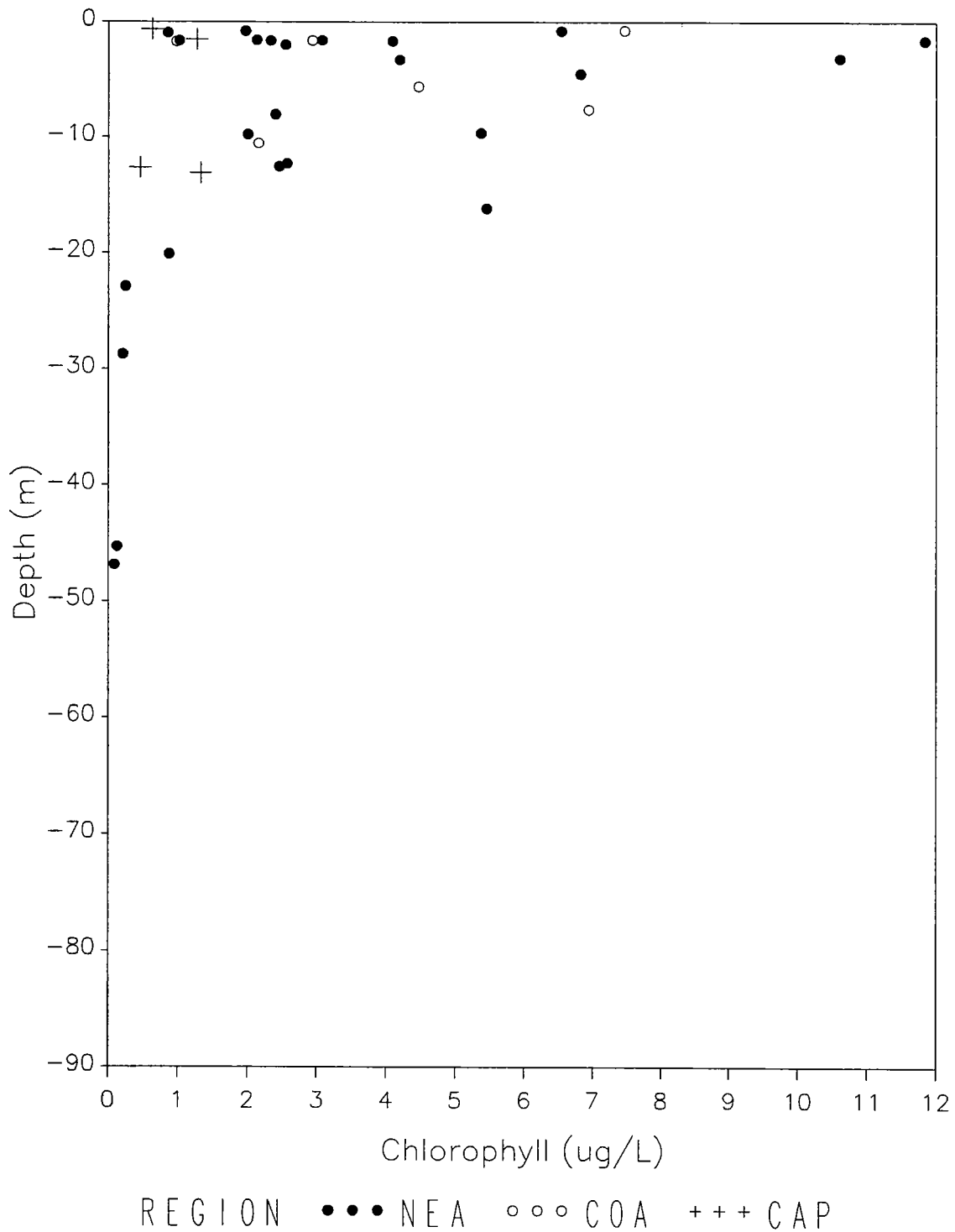


Figure 4-23. Chlorophyll (extracted samples) at BioProductivity stations and special station F25 as a function of depth in late August 1993. Data are from farfield (n=22) and nearfield (n=12) surveys. The regions correspond to the groups of stations shown in Figure 4-16.

Late August (W9311)

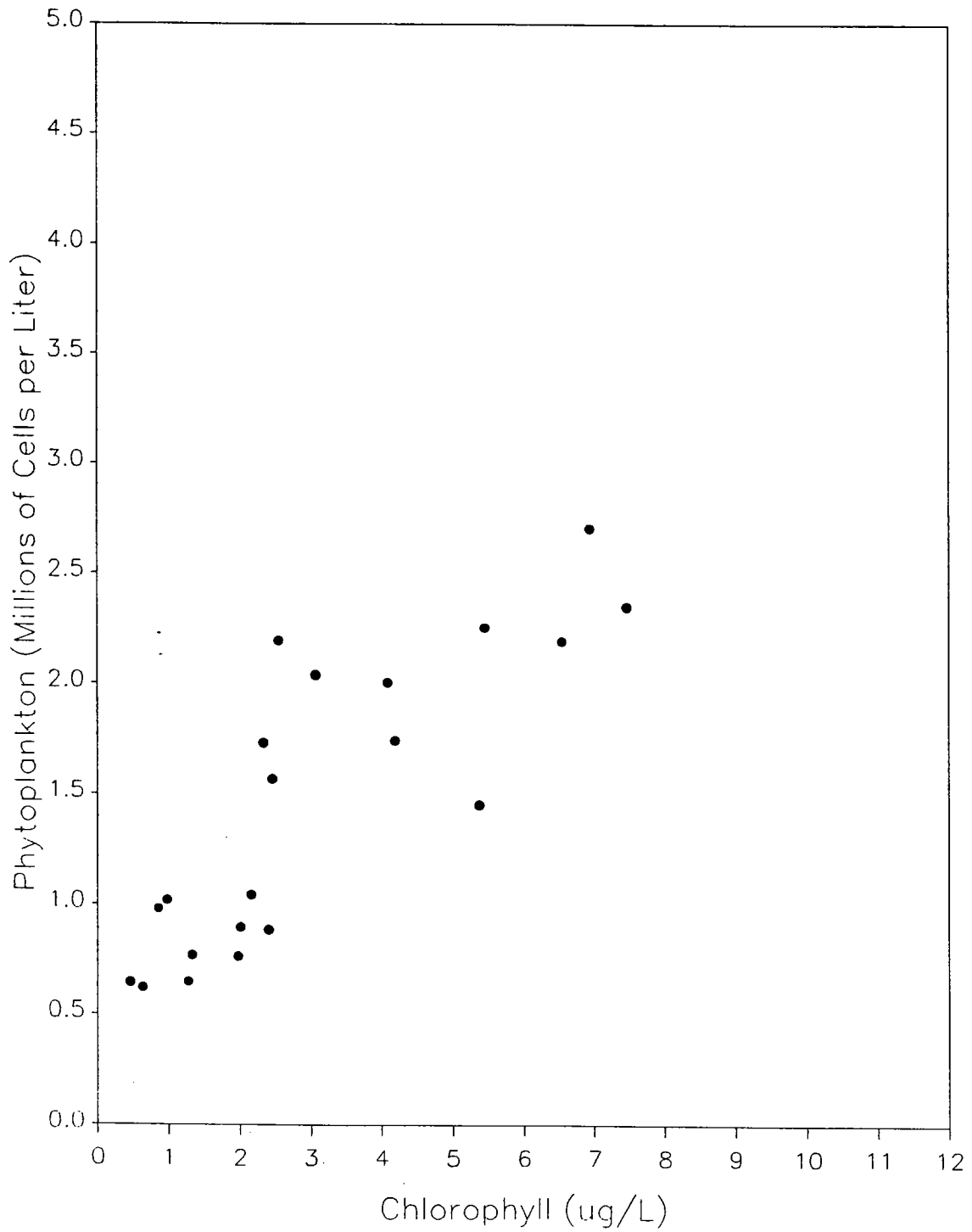


Figure 4-24. Total phytoplankton abundance vs. chlorophyll (extracted samples) at BioProductivity stations in late August 1993. Station N10P surface was analyzed for both farfield and nearfield surveys. Data are given in Appendices A and F.

Phytoplankton – August 1993
(Surface Sample)

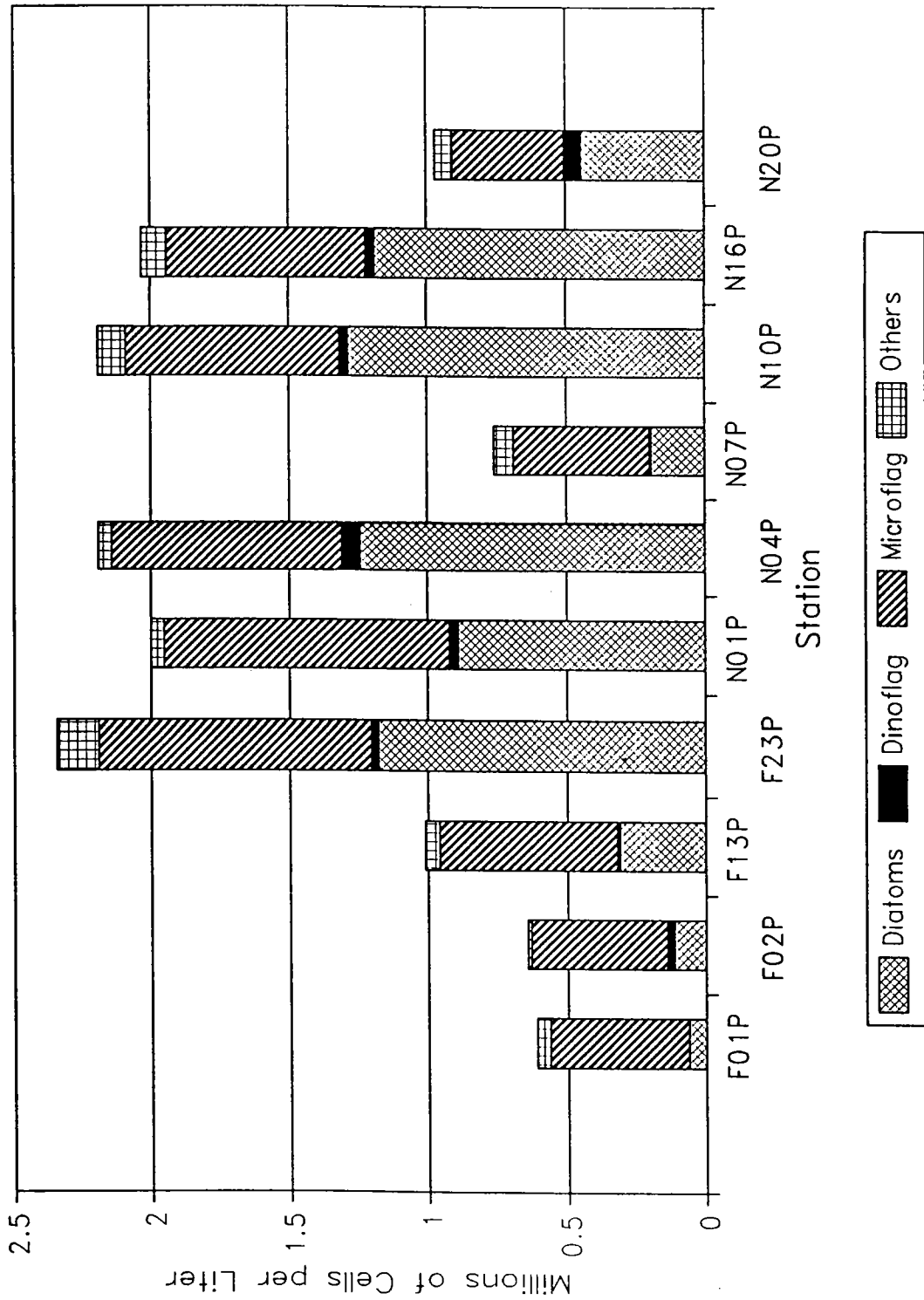


Figure 4-25a. Total phytoplankton abundance, by taxonomic groups, at the surface of BioProductivity stations in late August 1993. Data are given in Appendix F.

Phytoplankton – August 1993
(Chlorophyll Maximum)

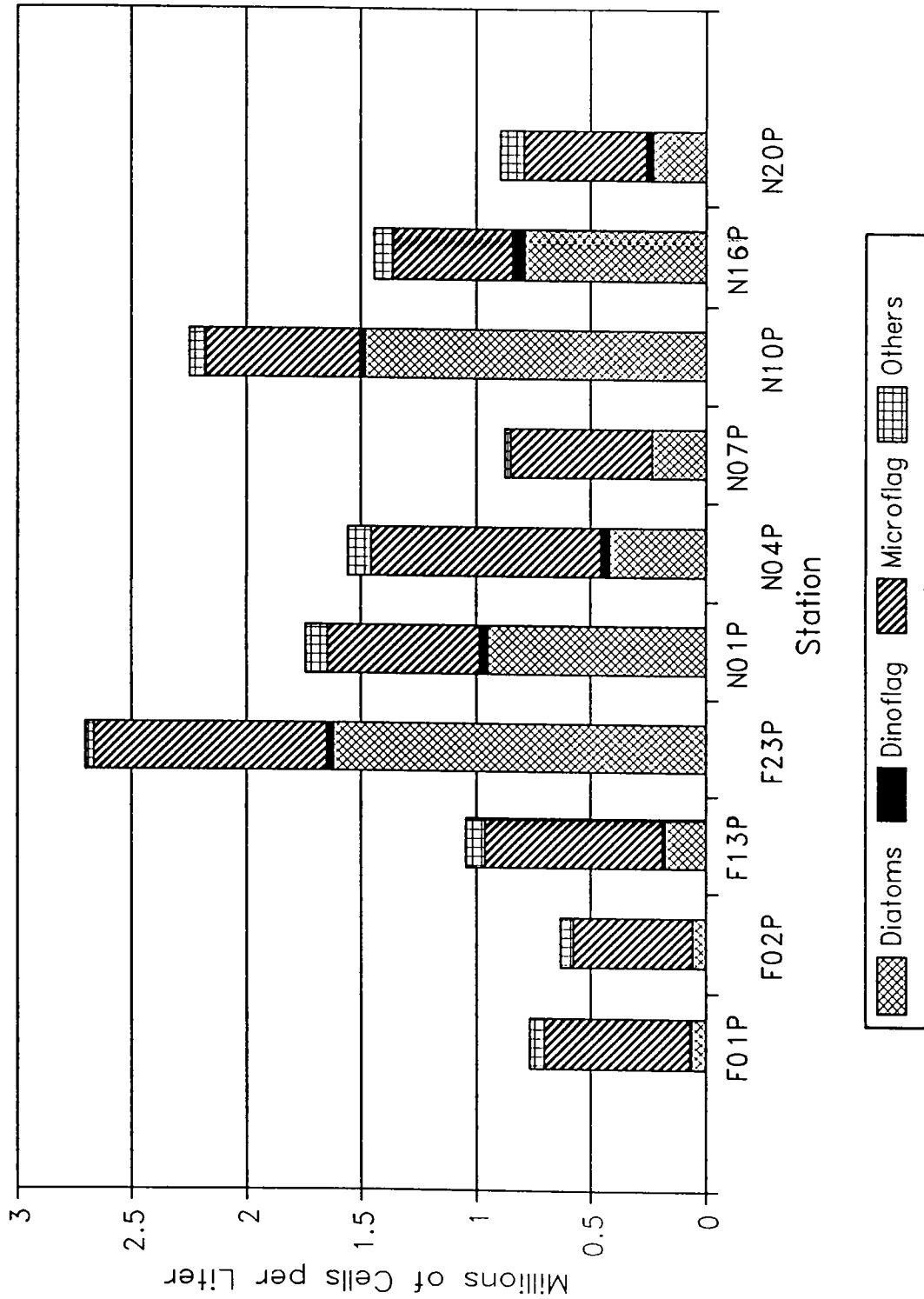


Figure 4-25b. Total phytoplankton abundance, by taxonomic groups, at the chlorophyll maximum of BioProductivity stations in late August 1993. Data are given in Appendix F.

Zooplankton – August 1993

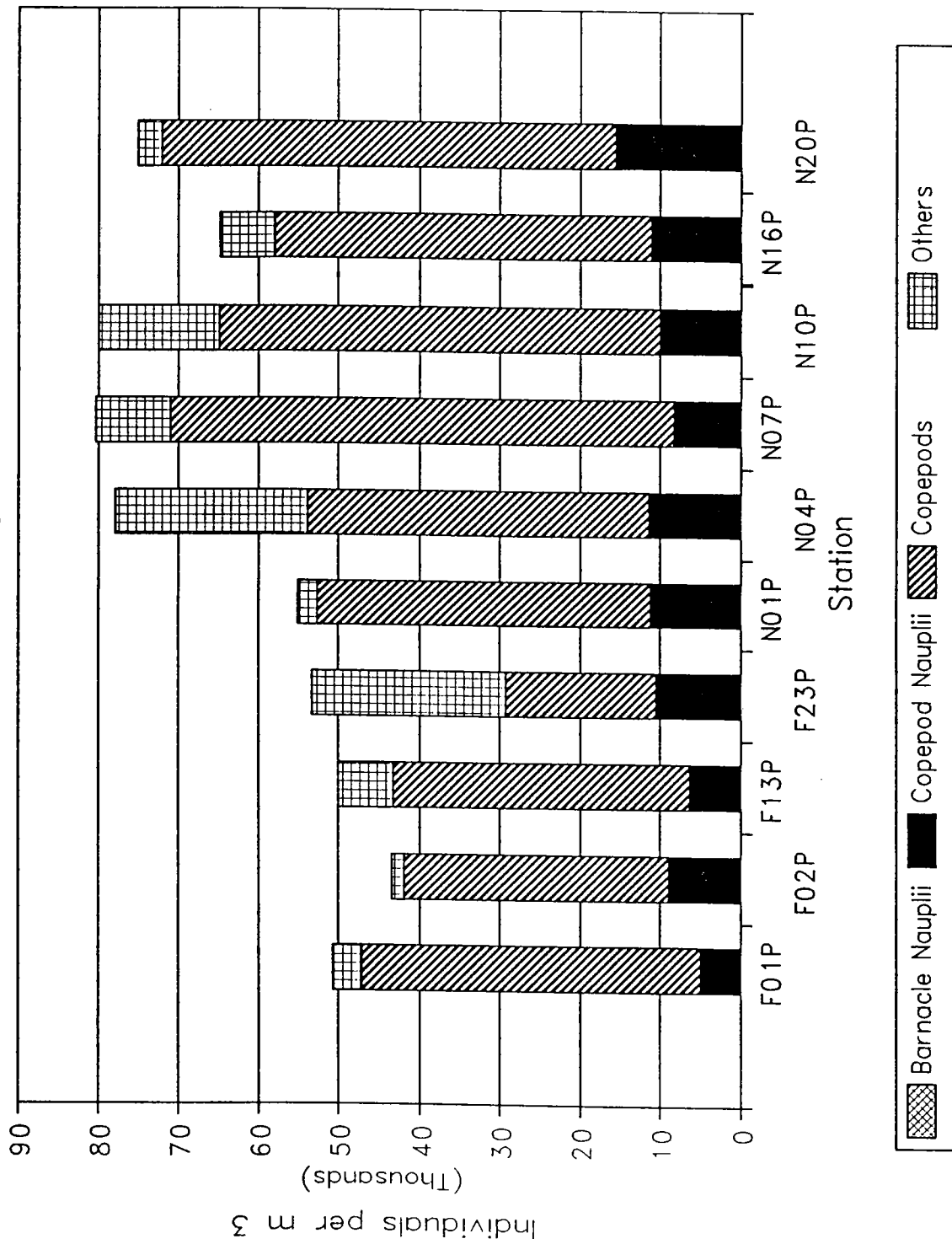


Figure 4-26. Zooplankton abundance, by groups, at BioProductivity stations in late August 1993. Data are given in Appendix G.

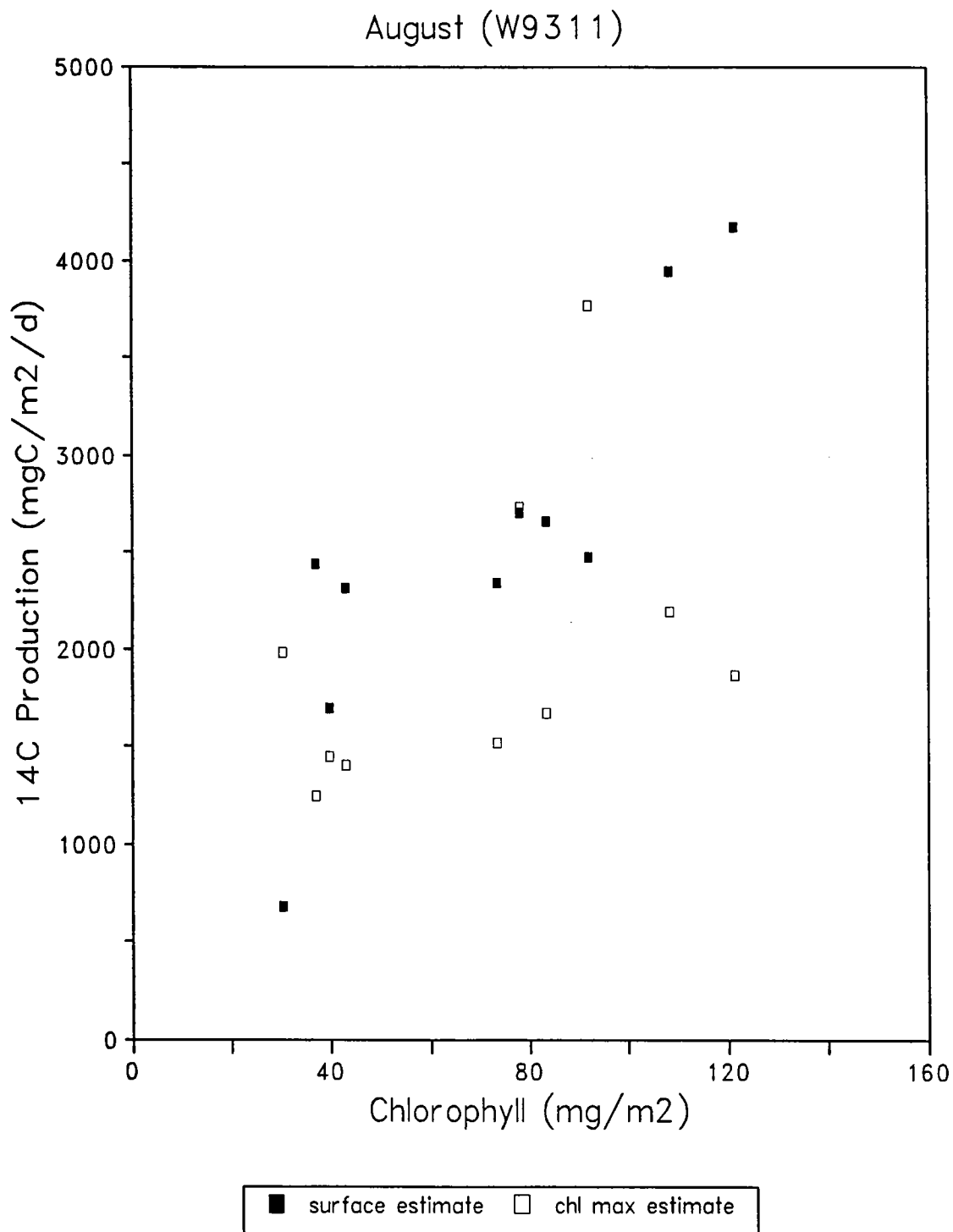


Figure 4-27. Estimated ¹⁴C production and chlorophyll (integrated for the photic zone) in late August 1993. (See also Table 4-3).

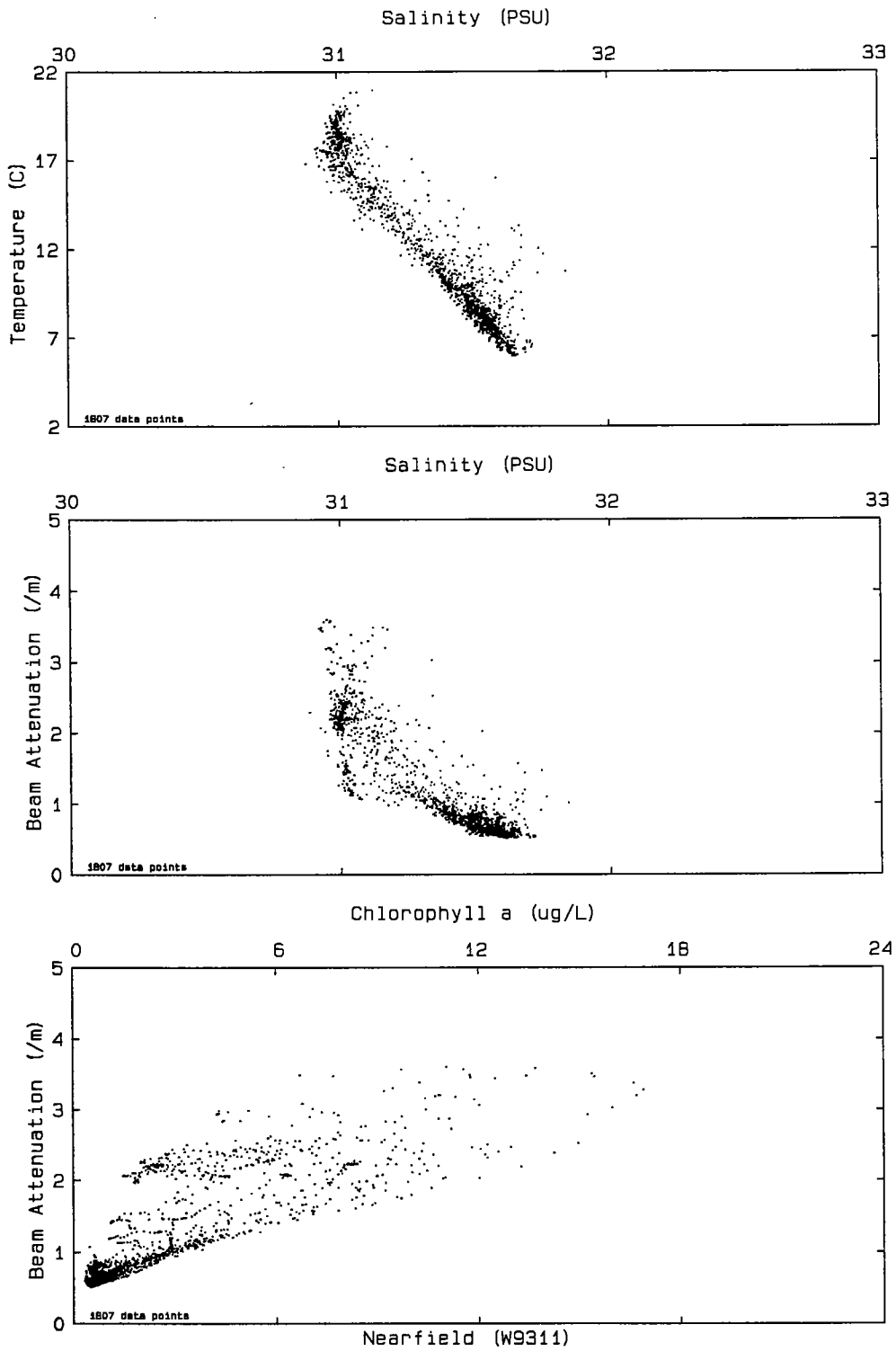


Figure 4-28a. Scatter plots for nearfield stations in late August. Compare to Figure 4-15.

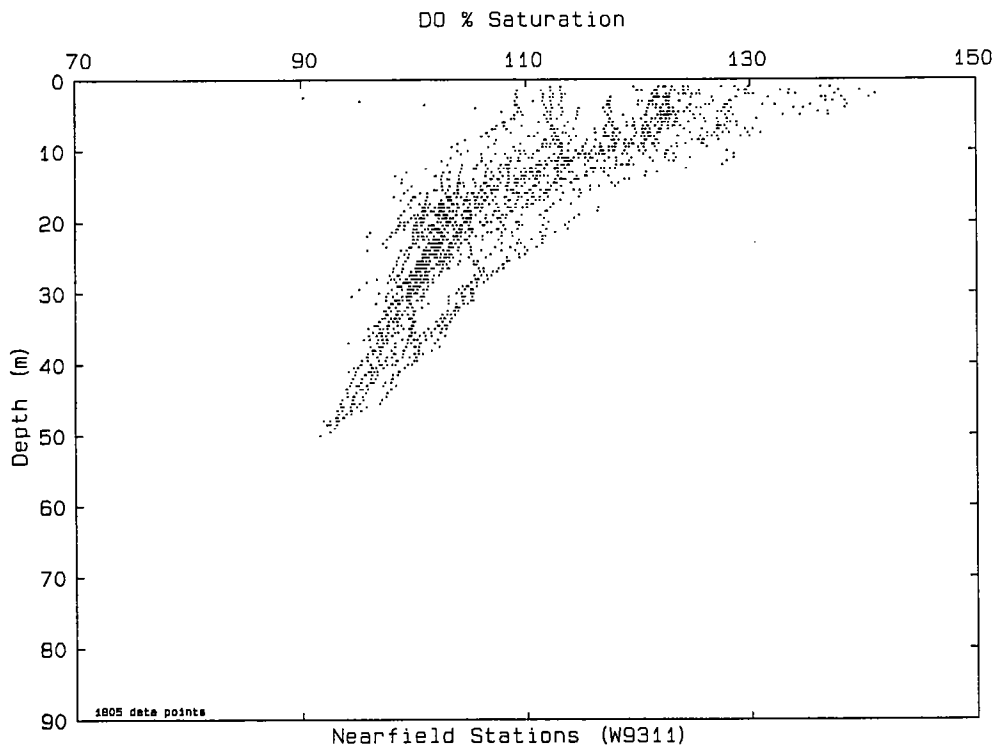
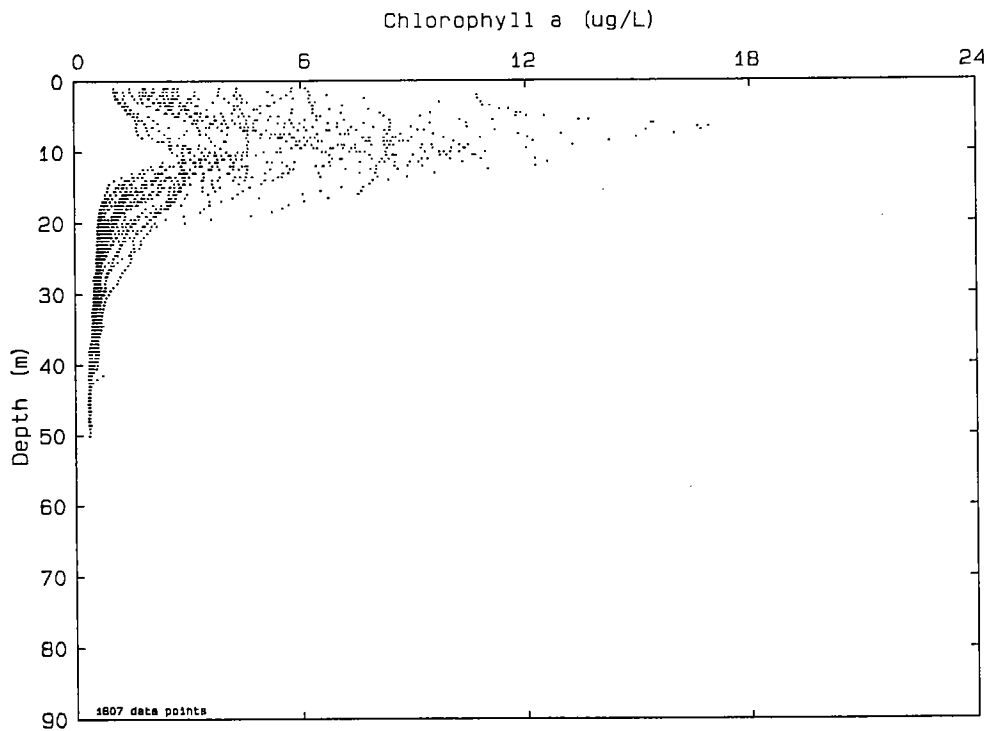


Figure 4-28b. Scatter plots for nearfield stations in late August. Compare to Figure 4-15.

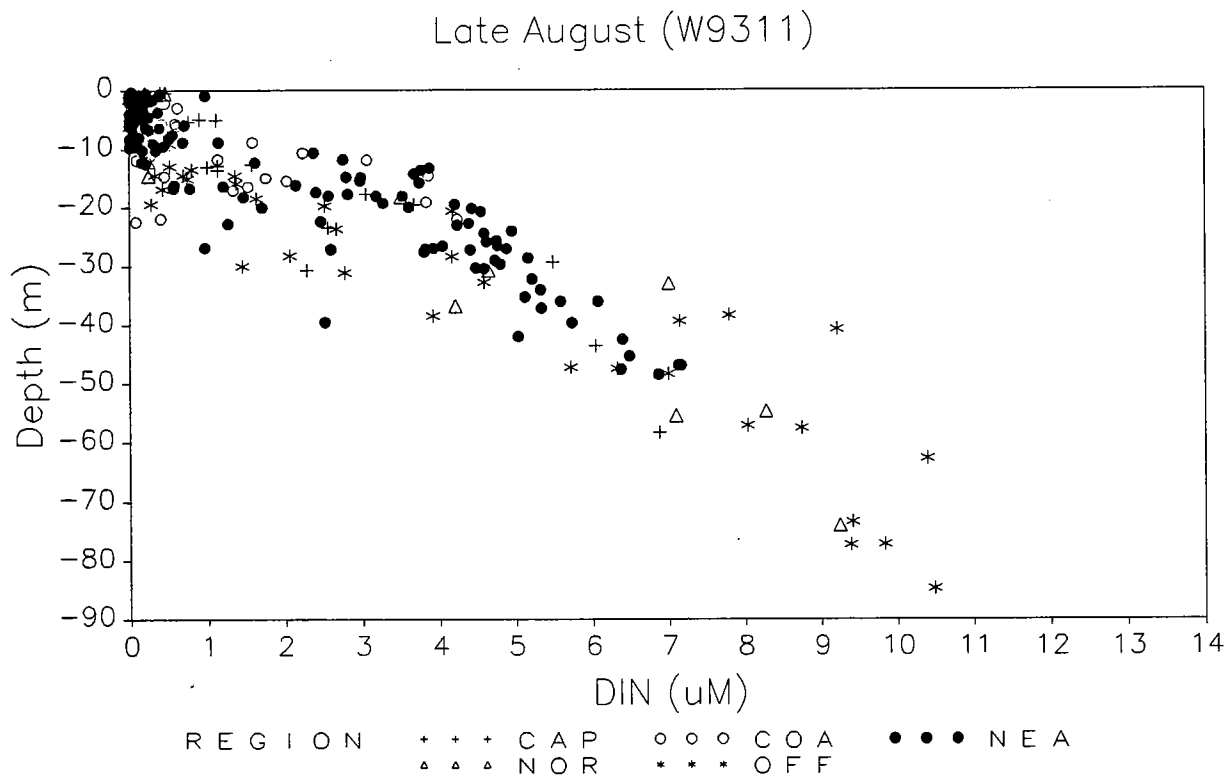
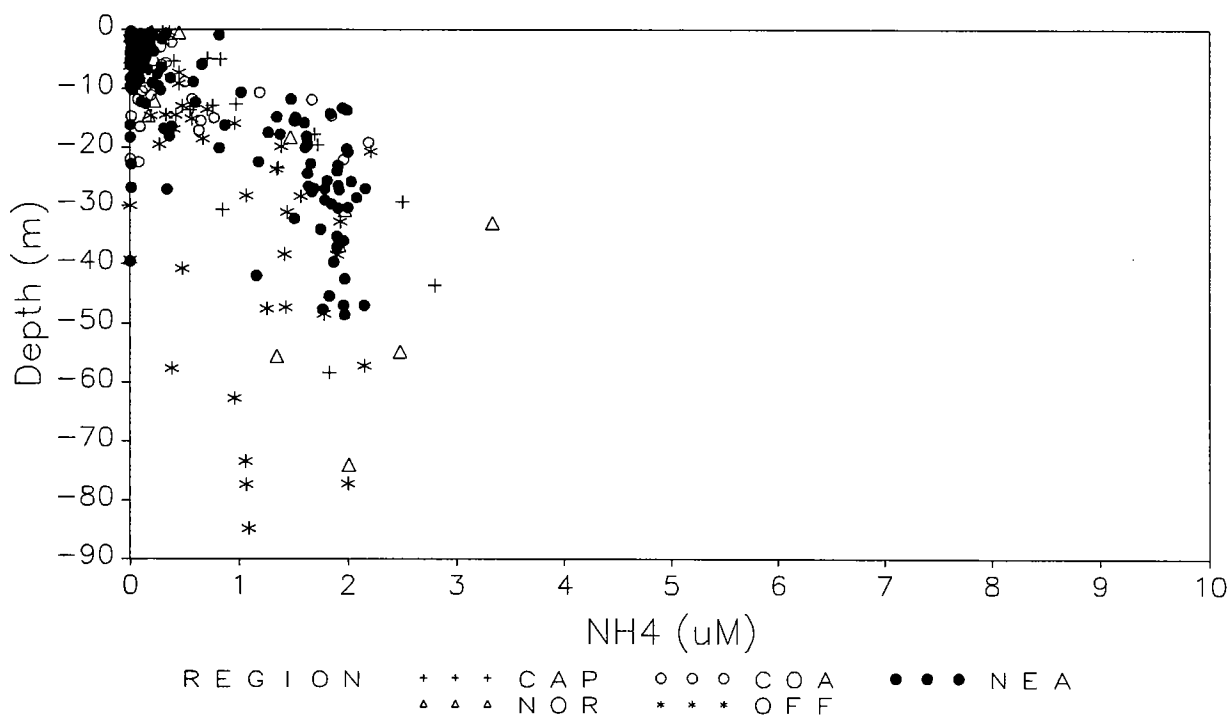


Figure 4-29. DIN vs. depth in late August 1993. The regions correspond to the groups of stations shown in Figure 4-16.

Late August (W9311)



Late August (W9311)

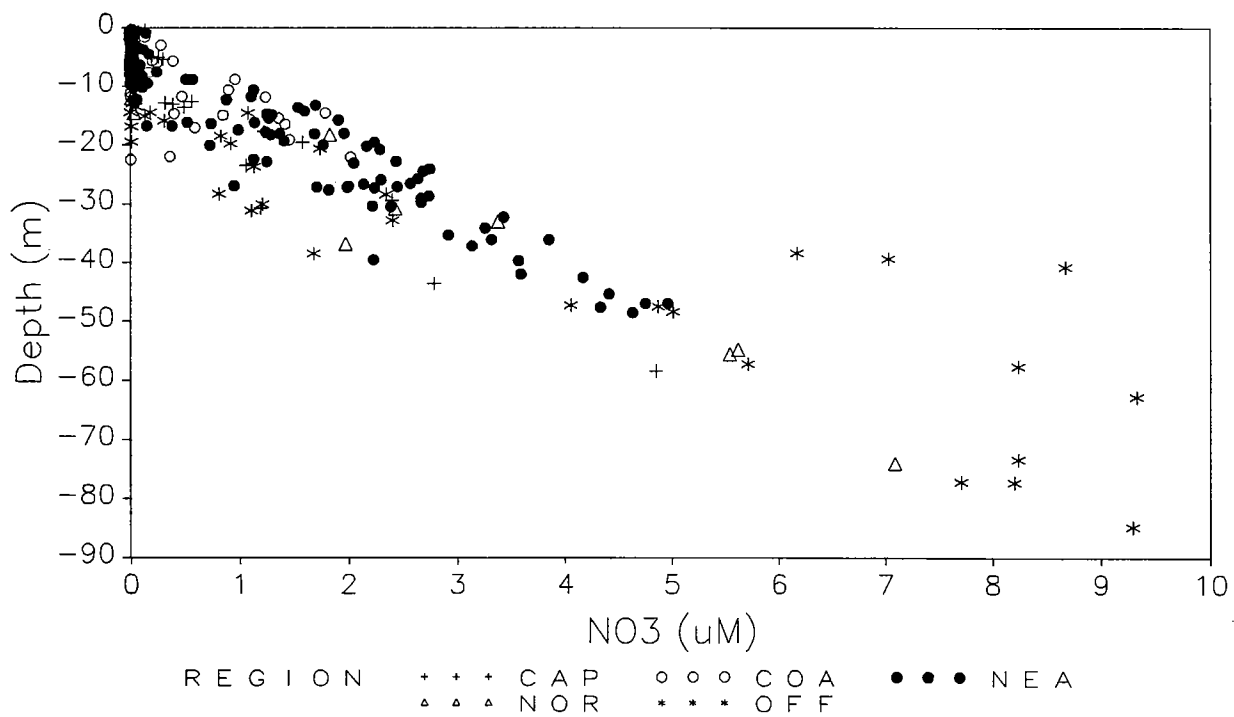


Figure 4-30a. NH_4 and NO_3 vs. depth in late August 1993. The regions correspond to the groups of stations shown in Figure 4-16.

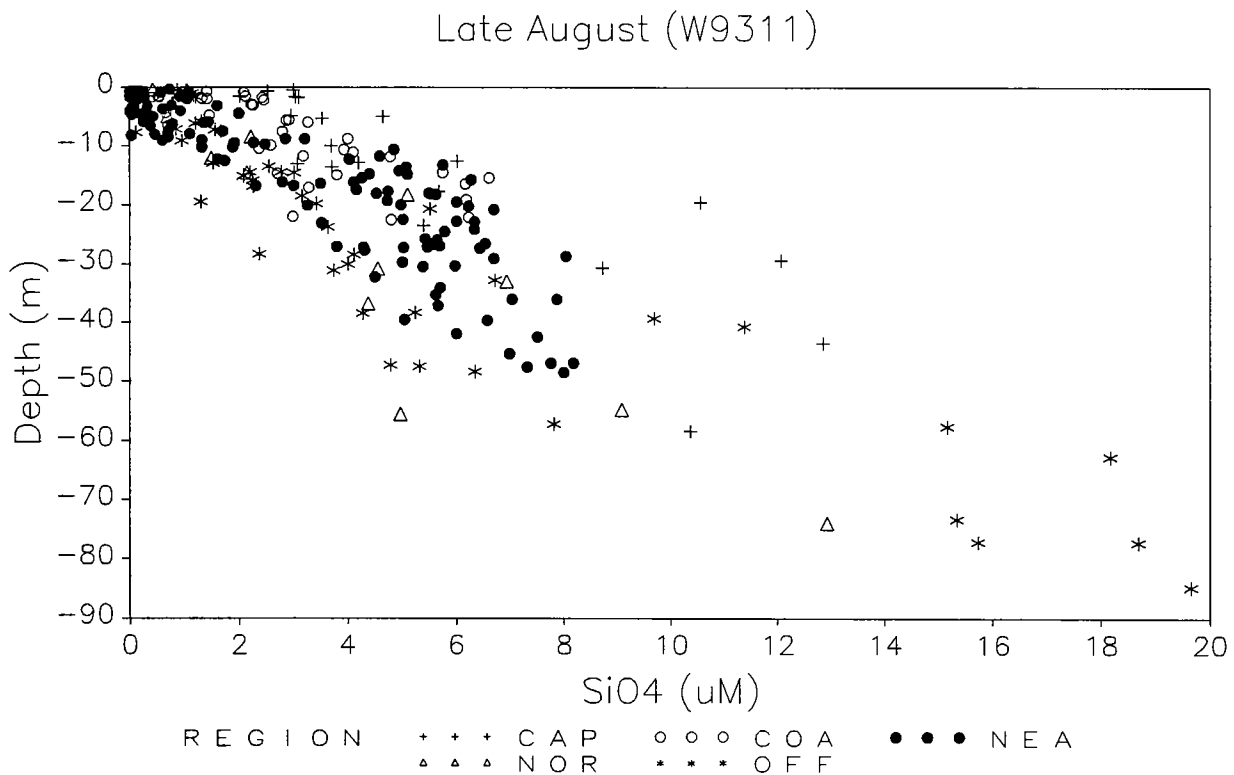
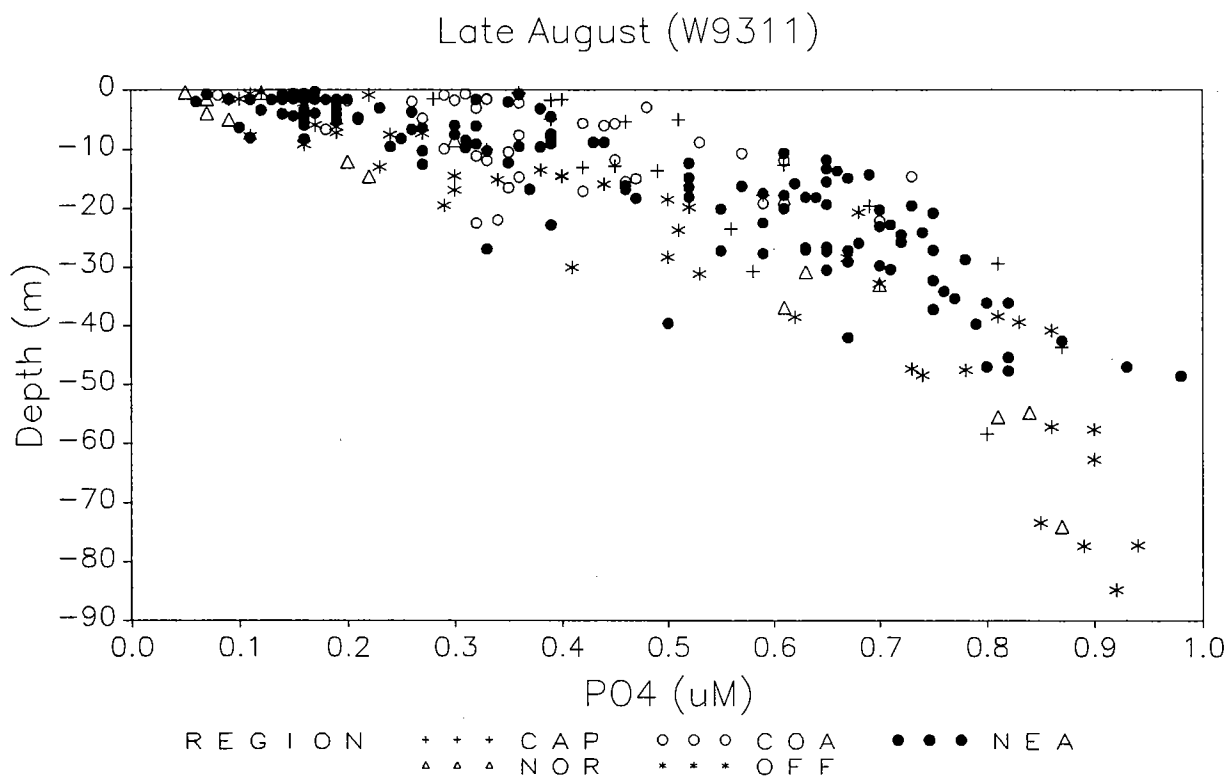


Figure 4-30b. PO_4 and SiO_4 vs. depth in late August 1993. The regions correspond to the groups of stations shown in Figure 4-16.

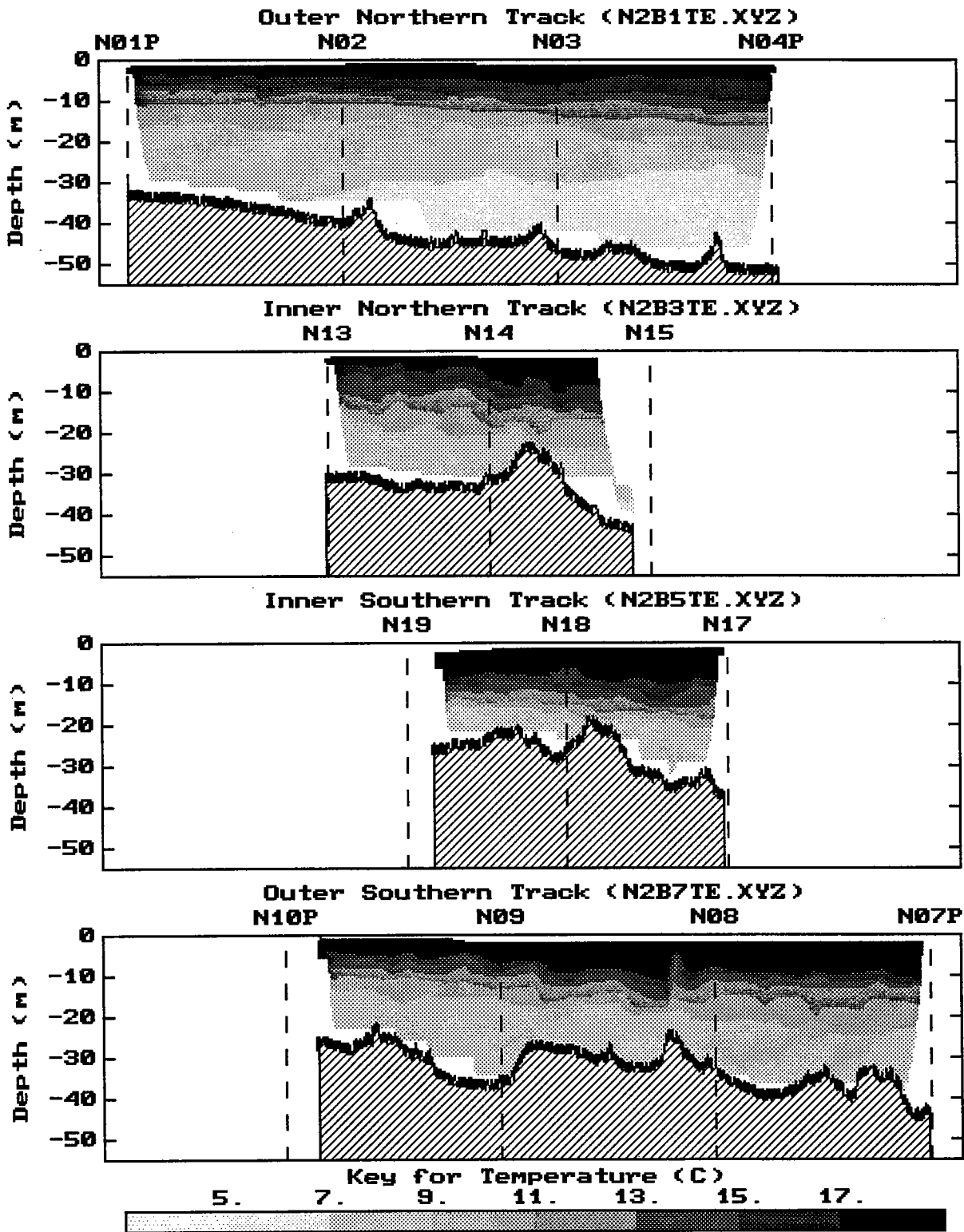


Figure 4-31a. Vertical section contours of temperature generated for tow-yo profiling in late August 1993. The view is towards the North.

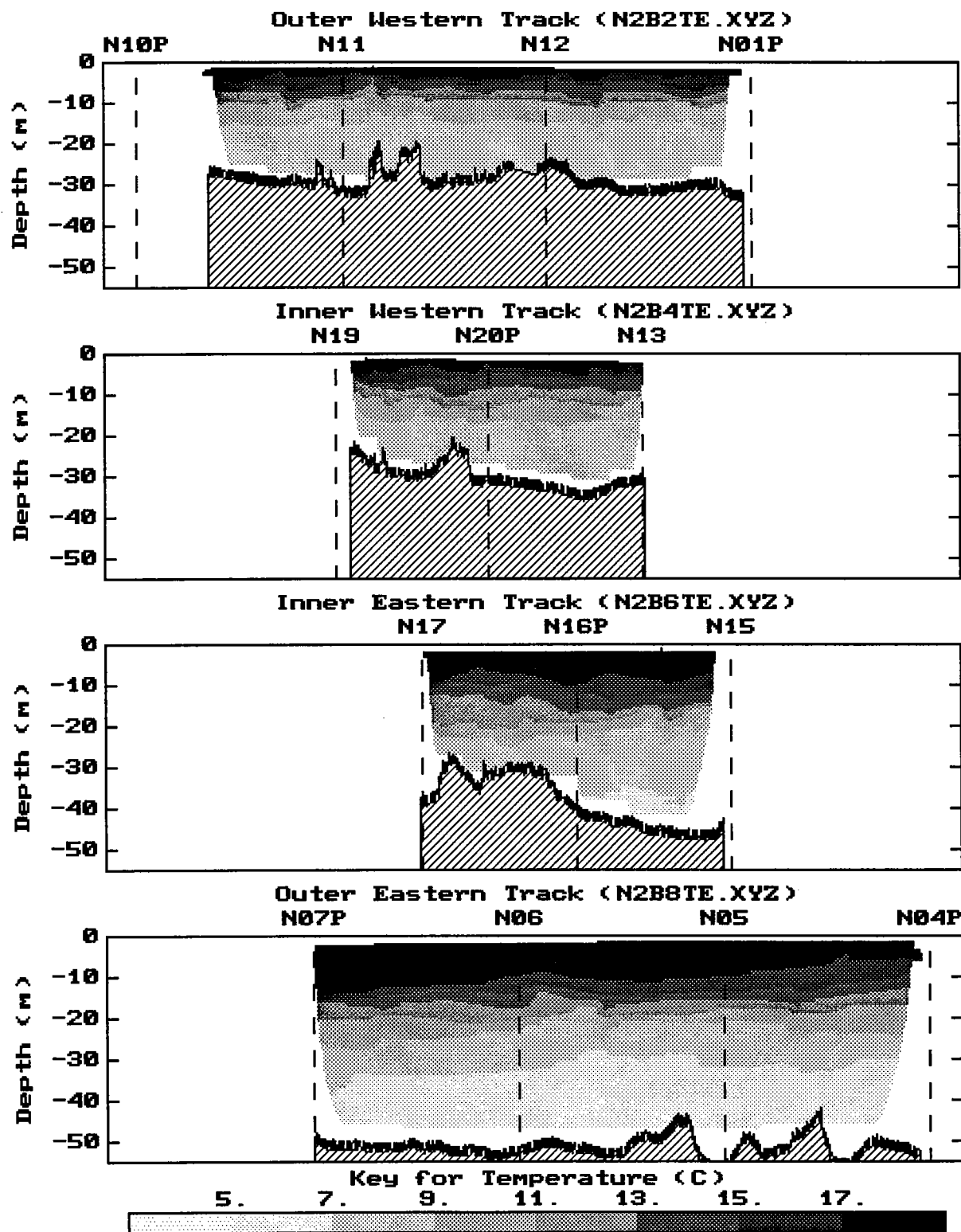


Figure 4-31b. Vertical section contours of temperature generated for tow-yo profiling in late August 1993. The view is towards Boston Harbor.

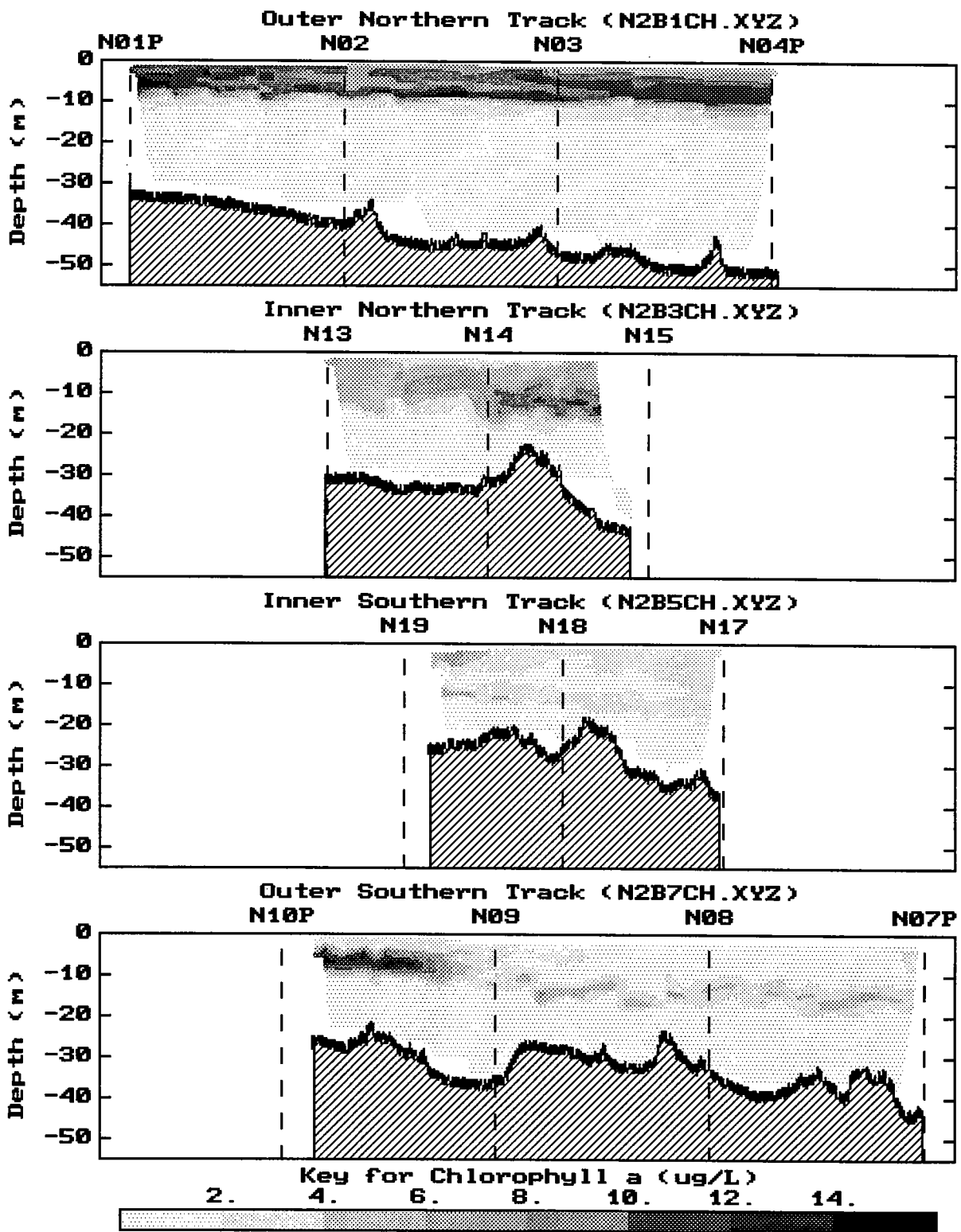


Figure 4-33a. Vertical section contours of fluorescence (as $\mu\text{g Chl L}^{-1}$) generated for tow-yo profiling in late August 1993. The view is towards the North.

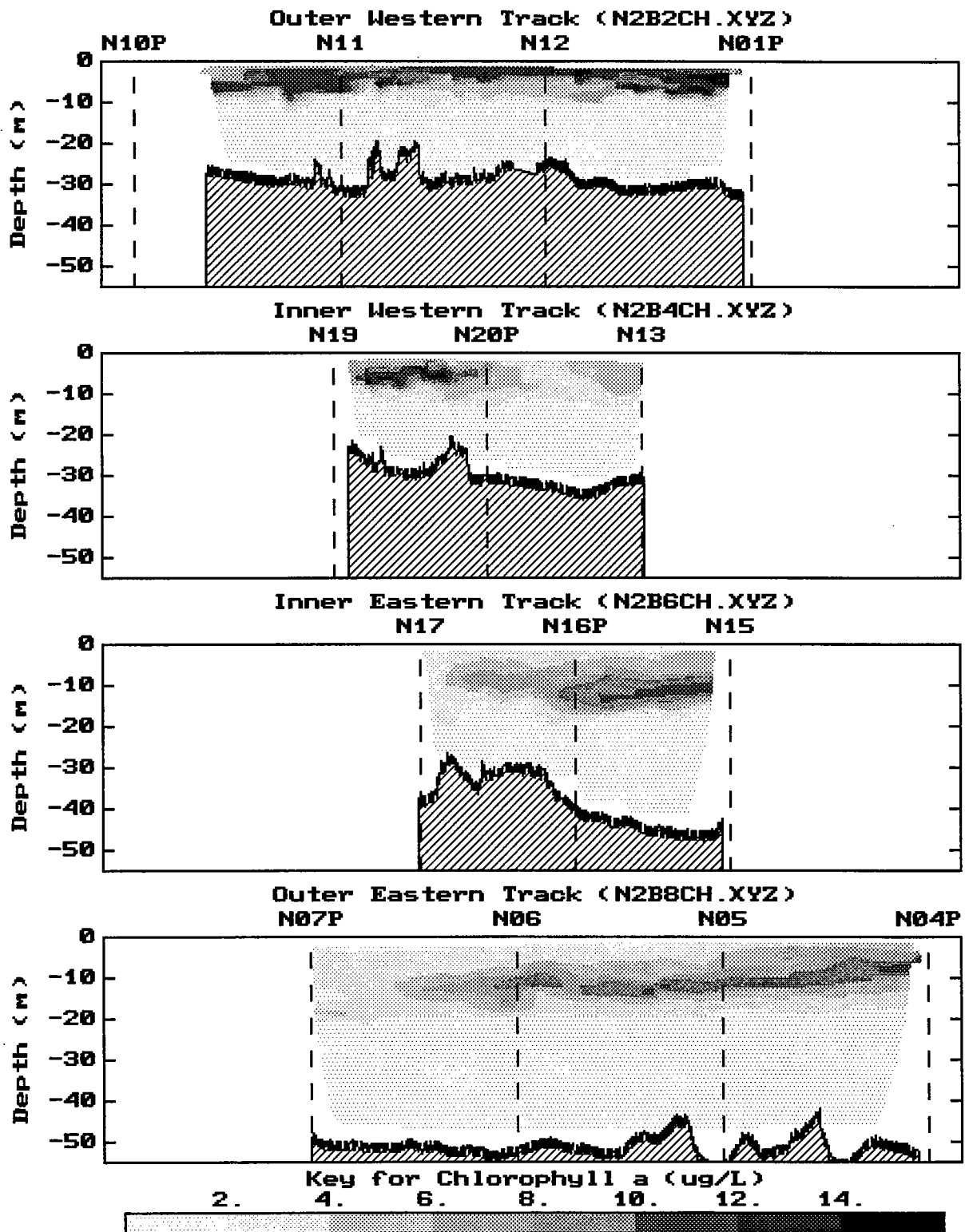


Figure 4-33b. Vertical section contours of fluorescence (as $\mu\text{g Chl L}^{-1}$) generated for tow-yo profiling in late August 1993. The view is towards Boston Harbor.

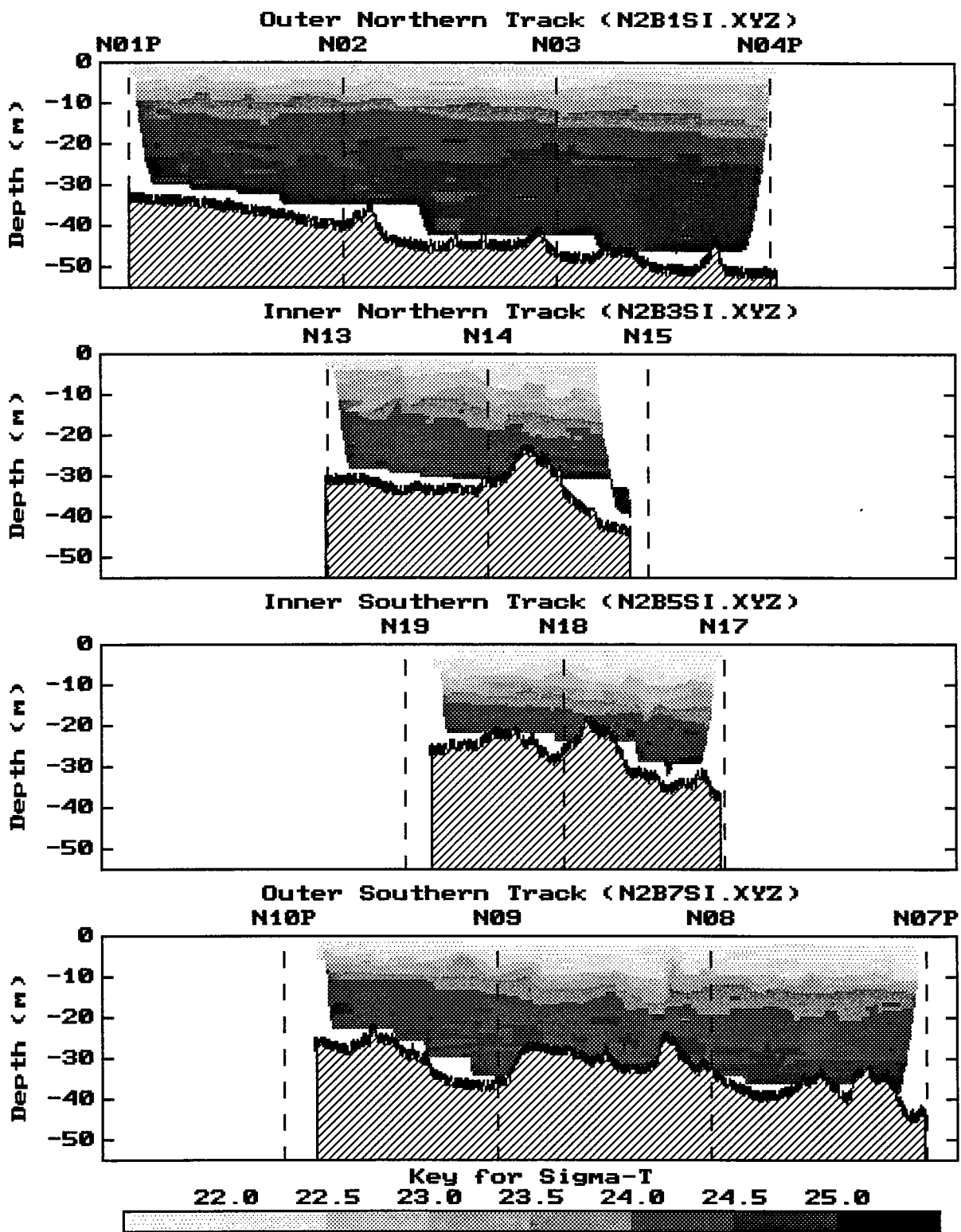


Figure 4-32a. Vertical section contours of σ_T generated for tow-yo profiling in late August 1993. The view is towards the North.

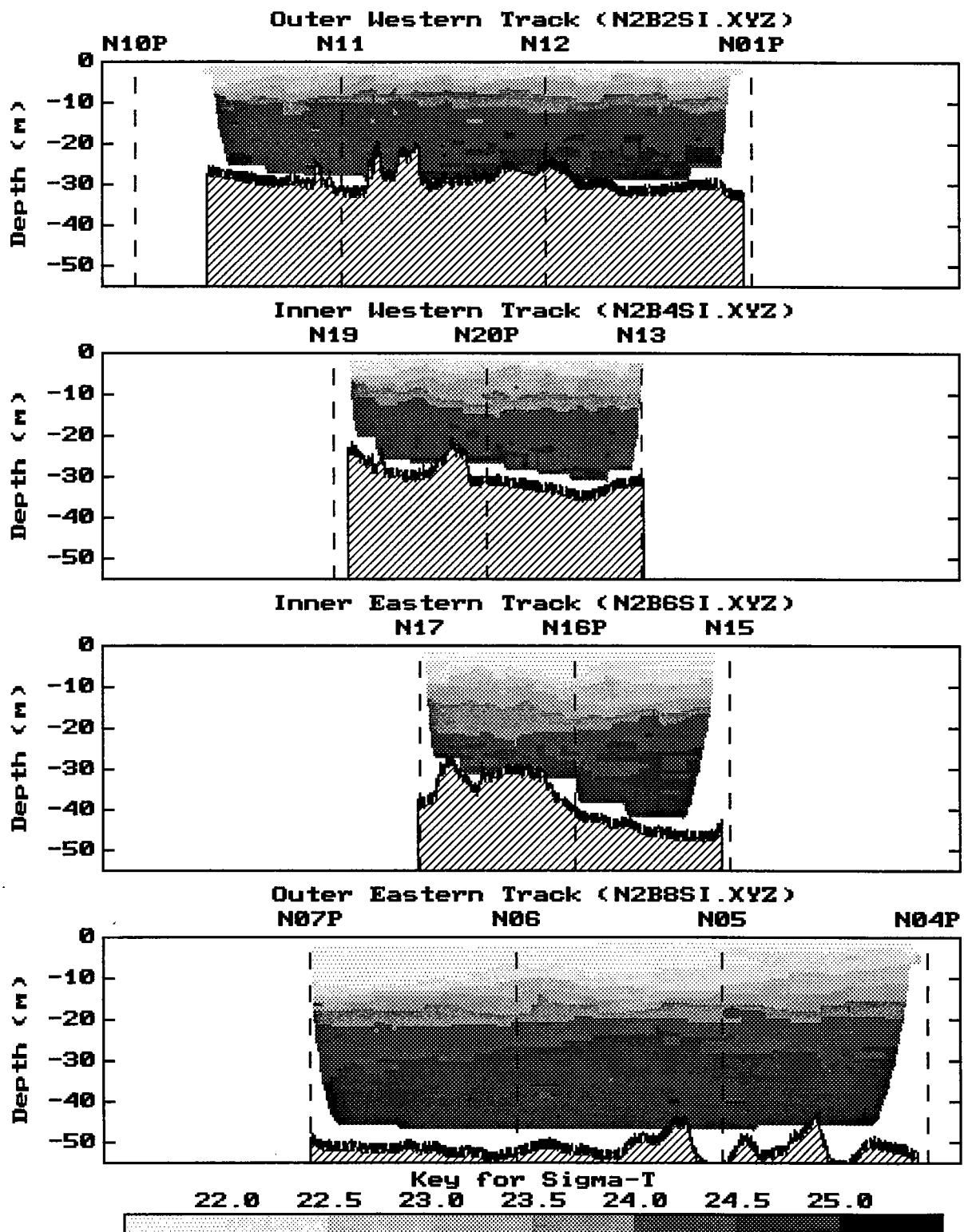


Figure 4-32b. Vertical section contours of σ_T generated for tow-yo profiling in late August 1993. The view is towards Boston Harbor.

5.0 RESULTS OF EARLY SEPTEMBER 1993 NEARFIELD SURVEY (W9312)

5.1 Distribution of Water Properties from Vertical Profiling

The temperature-salinity pattern observed at all stations during the early September survey was less coherent than during late August (Figure 5-1a) and there were minor shifts in the ranges for the parameters. Surface salinity in early September was similar to late August (about 31 PSU), but highest salinities near the bottom increased from ~31.7 to 31.9 PSU. The surface temperatures were generally cooler (maximum at 18°C) and bottom water temperatures increased from 6°C to >7°C.

Vertical stratification was still noted in all station profiles and the start of the thermocline/pycnocline was generally within 5-10 m of the surface (Appendix B). In most cases, the thin surface layer was crisply defined by a sharp pycnocline, but in the area of the southwest corner of the nearfield (especially stations N10P, N09, and N19), the surface layer was less defined. At the latter locations, the vertical gradient was more diffuse and the surface temperatures as much as 2°C cooler than at other locations in the field. Because this area receives surface water directly from southern Boston Harbor, it could easily have been influenced by turbulence from Harbor-Bay water exchanges. Regardless, these observations suggest initiation of the early fall cooling that generally begins in shallow water. Surface salinity in this area of the southwest corner was similar to that at other stations but, at depth, the salinity was lower than at comparable temperatures in deeper offshore water. These features were, in part, responsible for some of the scatter observed in the T-S plot (Figure 5-1a).

In general, beam attenuation decreased slightly as salinity increased. Beam attenuation readings, which ranged narrowly between 0.5 and 1.4 m^{-1} , were much lower than measurements made just two weeks earlier in late August. The range of chlorophyll concentrations was also narrower than the range observed in late August, but the average was still ~3 $\mu\text{g L}^{-1}$ and the high >8 $\mu\text{g L}^{-1}$. As shown in Figure 5-1a, beam attenuation and chlorophyll are broadly related.

Overall, higher chlorophyll concentrations were found in the surface layer; a mid-depth maximum was routinely detected near 10 m, a point from which concentrations declined nearly exponentially with depth (Figure 5-1b). DO, as percent saturation, generally matched this vertical pattern (Figure 5-1b). The surface layer was supersaturated, but not to the extent observed in late August. Minimum DO concentrations at depth were regularly 82-88% of saturation.

DIN concentrations ranged between 0 and 8 μM . Concentrations were depleted at the surface and increased with depth below the pycnocline (Figure 5-2a). As noted during the July and August surveys, NO_3 concentrations drove this pattern. NH_4 was detectable below 10 m, where the concentration ranged from ~1 to 3 μM (Figure 5-2b). PO_4 and silicate concentrations paralleled the DIN pattern, but without a surface depletion of PO_4 (Figure 5-2c). A broad range of concentrations was detected for all the nutrients at intermediate depths. Silicate concentrations, for example, were higher at the 30-m depth than in deeper water (Figure 5-2c).

As shown in Figure 5-3, nutrient concentrations were routinely low at low salinity (~31 PSU). The only exceptions were for three samples from the upper 10 m at station N10P. The salinity of these samples ranged between 31.08 and 31.29 PSU, and concentrations of all forms of nutrients were higher ($\text{NH}_4 = 1.2\text{-}3.4 \mu\text{M}$; $\text{NO}_3 = 0.44\text{-}2.37 \mu\text{M}$; $\text{PO}_4 = 0.45\text{-}0.83 \mu\text{M}$; $\text{SiO}_4 = 0.89\text{-}4.89 \mu\text{M}$). In addition to being relatively cool, the water at station N10P may indicate the beginning of a seasonal increase in dissolved nutrient content in the Harbor and its export to the Bay.

Concentrations of all forms of nutrients were highly variable at depth and did not show a strong relationship to salinity. This could be due, in part, to variations in water stratification (described above), resulting in an influence of biological processes on the nutrient concentrations to different water depths at different stations. The nutrient-salinity distribution illustrated in Figure 5-3 could also indicate the mixing of different water masses each with a distinct nutrient-salinity signature. Compared to late August, the increase in bottom-water salinity noted during the early September survey suggests an advection of bottom water into the nearfield.

5.2 Distribution of Water Properties from Towing

Tow-yo profiling confirmed a persistent thermal and density stratification (Figures 5-4 and 5-5). Some spatial variability was noted for both the depth and sharpness of the thermocline. Notably, the surface at station N10P was cooler than other parts of the field, an observation similar to that noted on the day of vertical profiling. Also, the pycnocline was diffuse at station N10P and isopycnals (similar density surfaces) impinged upon the bottom in the area of stations N09 and N10P, perhaps signaling the initiation of seasonal mixing in the most shallow waters of the Bay. Characteristically, the bottom water along the shallow outer western track, and particularly this southwest region, was relatively high in NH_4 concentration; for the salinity range (-31.5 to 31.6 PSU), the water also was high in silicate. The nutrient signature could reflect interaction of bottom waters with shallower inshore water. The inshore region, extending from north to south along the western edge of the nearfield, is the location of most of the depositional bottom sediments within the nearfield (see Giblin *et al.*, 1994). In these depositional sediments, high metabolism was measured in early fall as bottom water temperatures increased, and the elevated NH_4 and SiO_4 concentrations in bottom waters could relate to high local benthic nutrient remineralization as well as to interaction with inshore water.

In contrast to the southwest corner of the nearfield, a very distinct bottom layer persisted offshore and through the northern half of the nearfield. Bottom water with $\sigma_T \geq 24.5$ was present from about 20 m to the bottom at the entire outer eastern track, the inner eastern track, and the northern side of the inner western track (Figure 5-5b). Along the northern side of the field, this water extended inshore just shy of station N01P, but was not found as far west along the southern tracklines (Figure 5-5a). This distinct bottom water was characteristically high in NO_3 , low in NH_4 , and lower in SiO_4 concentrations than observed in inshore waters of equivalent salinities.

The striking features of the chlorophyll distributions (Figure 5-6) were that they corresponded with the principal physical-geochemical variations across the nearfield. High chlorophyll concentrations were detected in the surface layer at station N10P and at other locations across the southwest corner of the nearfield, stretching in a radius from station N12 along the outer western track (Figure 5-6b) to stations N20P, N18, and then N09-N08 along the southern track (Figure 5-6a). In areas of distinct physical

layering, and a well-defined and uniform bottom water layer, chlorophyll concentrations were lower and confined primarily to the subsurface maximum near the bottom of the pycnocline (about 20 m). This subsurface chlorophyll maximum was found throughout the outer eastern track (Figure 5-6b) and on the outer northern track (Figure 5-6a). Note that from offshore to inshore, and from the north-northeast to south-southwest, the chlorophyll maximum shoaled from a distinct, deep subsurface layer to a broad surface layer with more intense concentrations. These gradients were similar to many observed earlier in the summer of 1993, although for the early September survey, the transition between the two regions was less abrupt than noted earlier in the summer (see Section 3).

5.3 Water Types and Analysis of Small-Scale Variability

The major geographic distinctions have been noted above and are summarized here. Based on physical and chemical properties, inshore water was apparently detected at station N10P. Water at this location was characterized by cooler surface temperatures, higher nutrient and chlorophyll concentrations, and less distinct stratification. Locations along the entire inshore (western track) were characteristically higher in chlorophyll; mixing with water in the inshore regions of Broad Sound (see Kelly and Albro, 1994) seems likely. However, aside from station N10P, surface water along the western edge did not carry the characteristic signature of water from an inshore source. Instead, different pools of bottom water were suggested as sources to the surface water, including (1) inshore water having relatively high nutrient concentrations that may indicate local benthic nutrient recycling and (2) water from an area across much of the northeastern triangle (north of a line from station N01P to station N07P). The latter area was characterized by high salinity bottom water which may have advected into the nearfield from offshore.

The main spatial patterns emerging during the vertical profiling were also apparent during towing. Without examining variability on a station-by-station basis, sub-areas of the nearfield region were distinct and persistent during the early September survey.

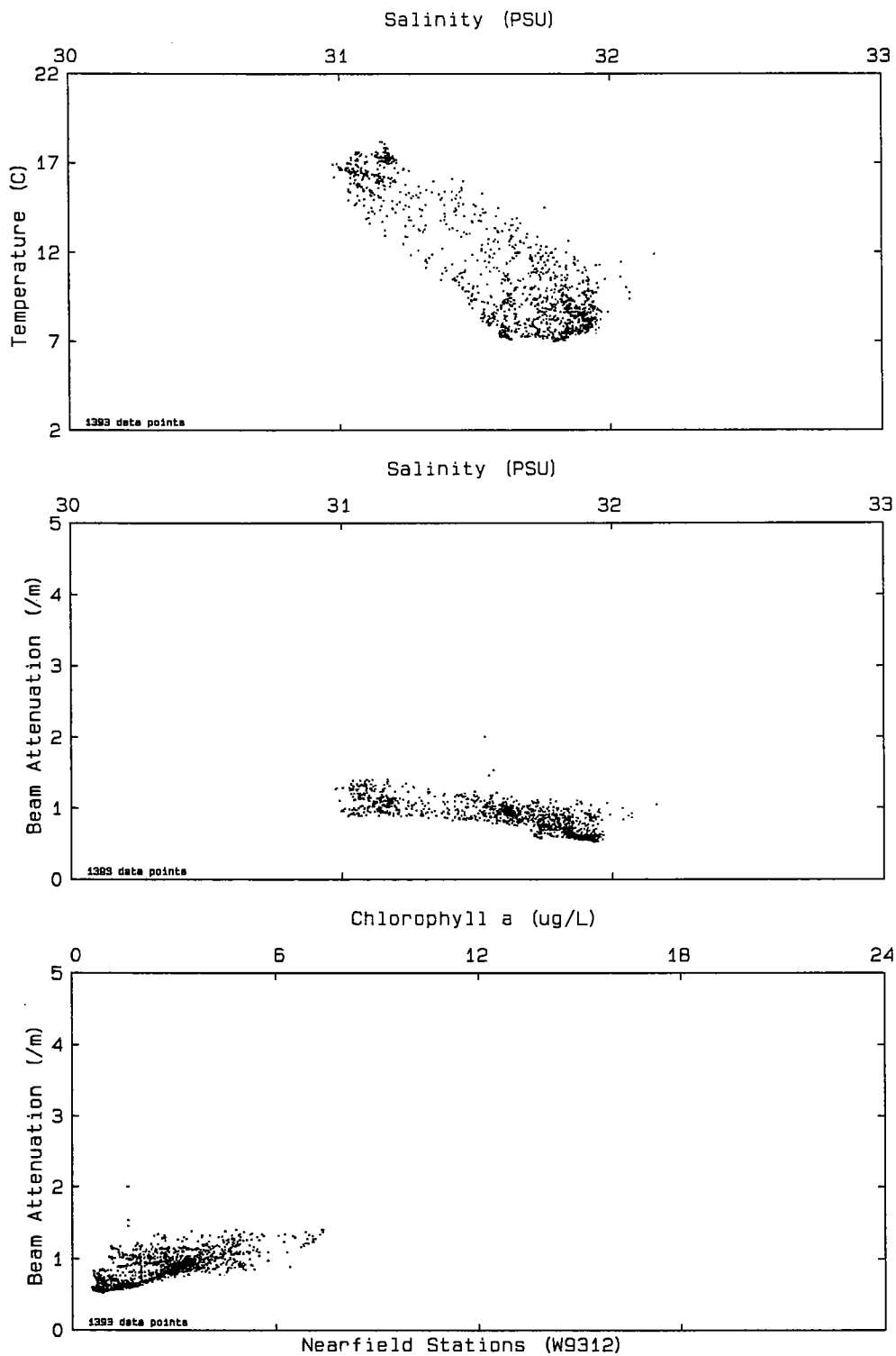


Figure 5-1a. Scatter plots of data acquired by *in situ* sensor package during vertical downcasts at all nearfield stations occupied in early September 1993. Individual station casts that were used to produce this composite are in Appendix B. Chlorophyll is estimated from *in situ* fluorescence.

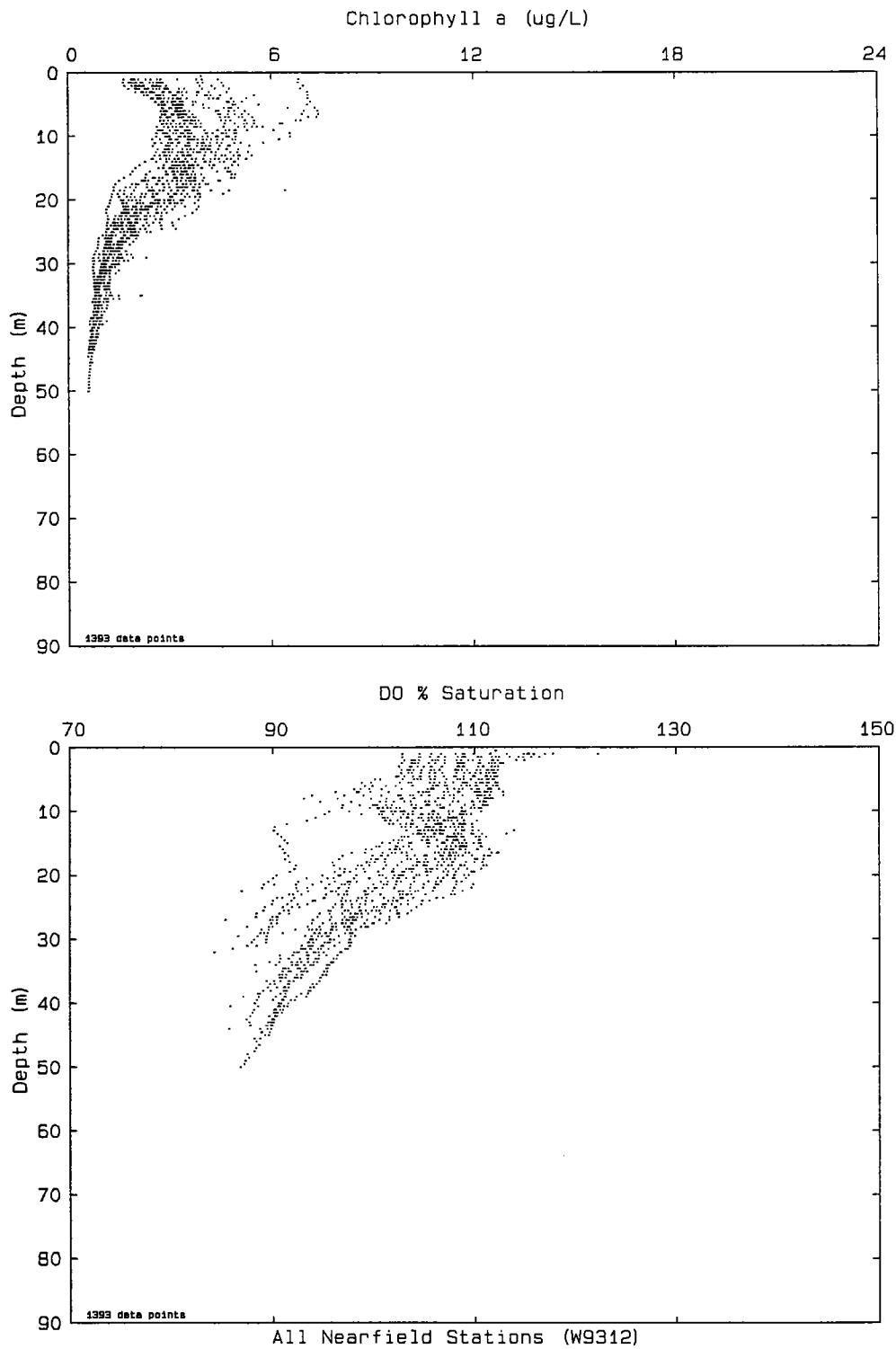


Figure 5-1b. Scatter plots of data acquired by *in situ* sensor package during vertical downcasts at all nearfield stations occupied in early September 1993. Individual station casts that were used to produce this composite are in Appendix B. Chlorophyll is estimated from *in situ* fluorescence.

Early September (W9312), Nearfield Stations

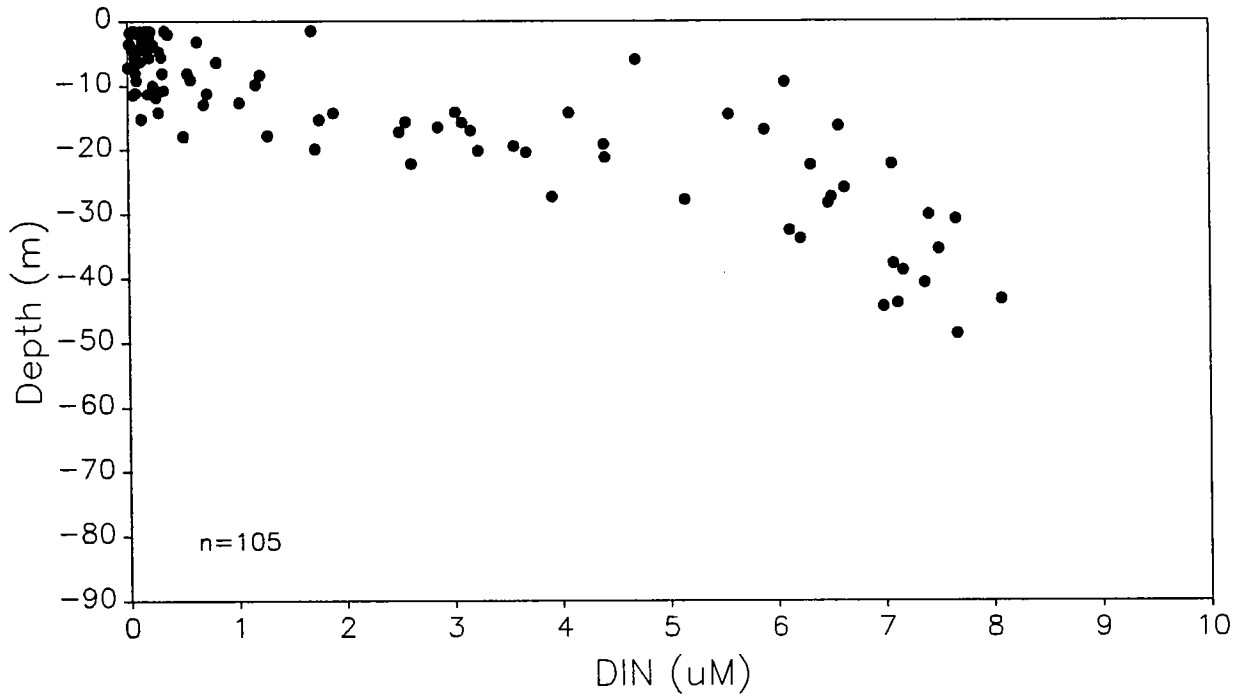
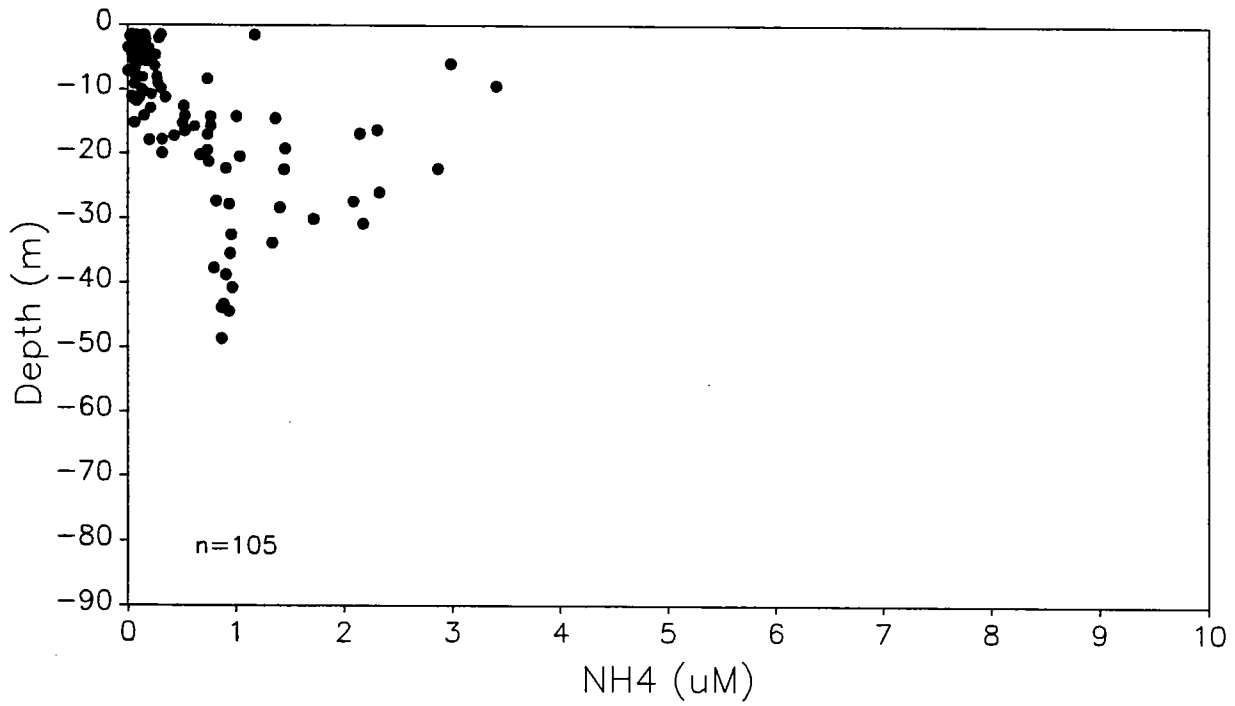


Figure 5-2a. DIN vs. depth in early September 1993.

Early September (W9312), Nearfield Stations



Early September (W9312), Nearfield Stations

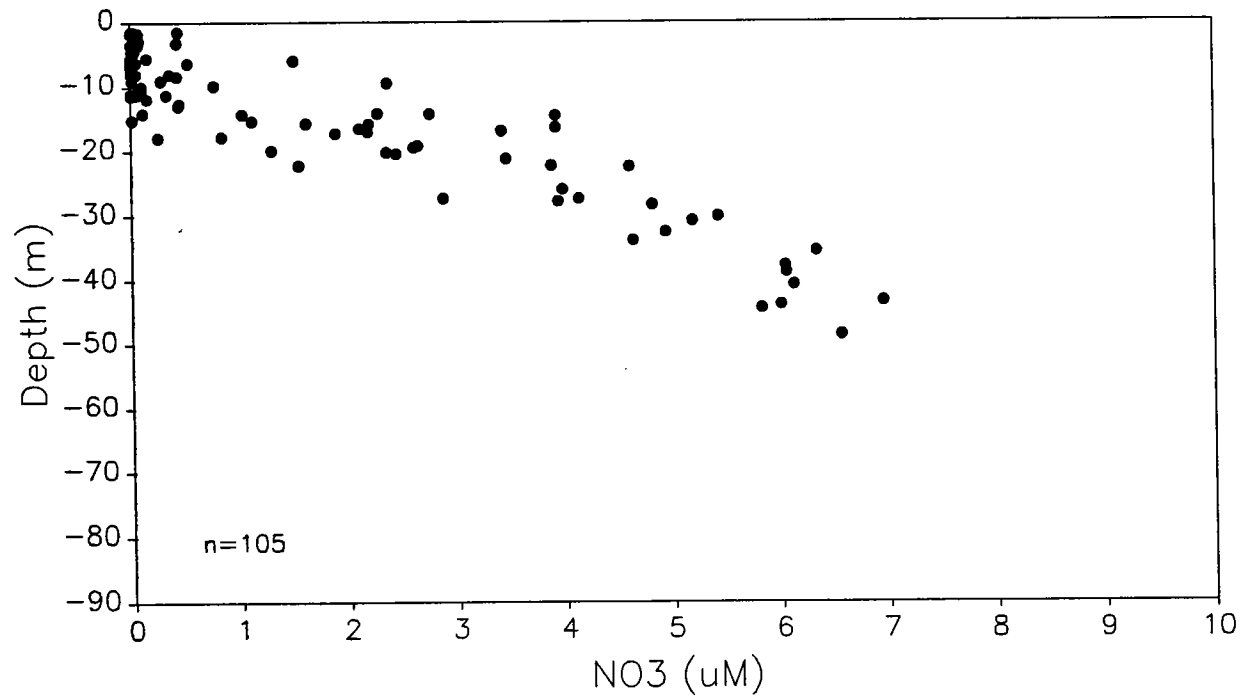
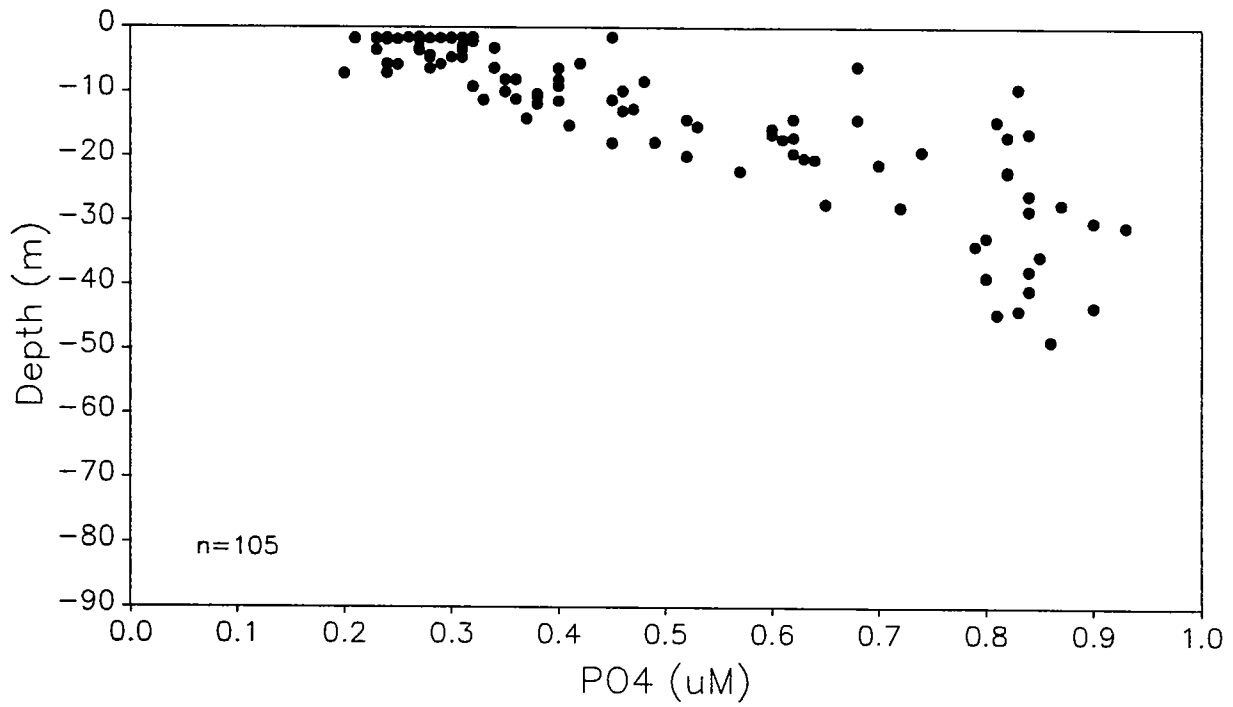


Figure 5-2b. NH_4 and NO_3 vs. depth in early September 1993.

Early September (W9312), Nearfield Stations



Early September (W9312), Nearfield Stations

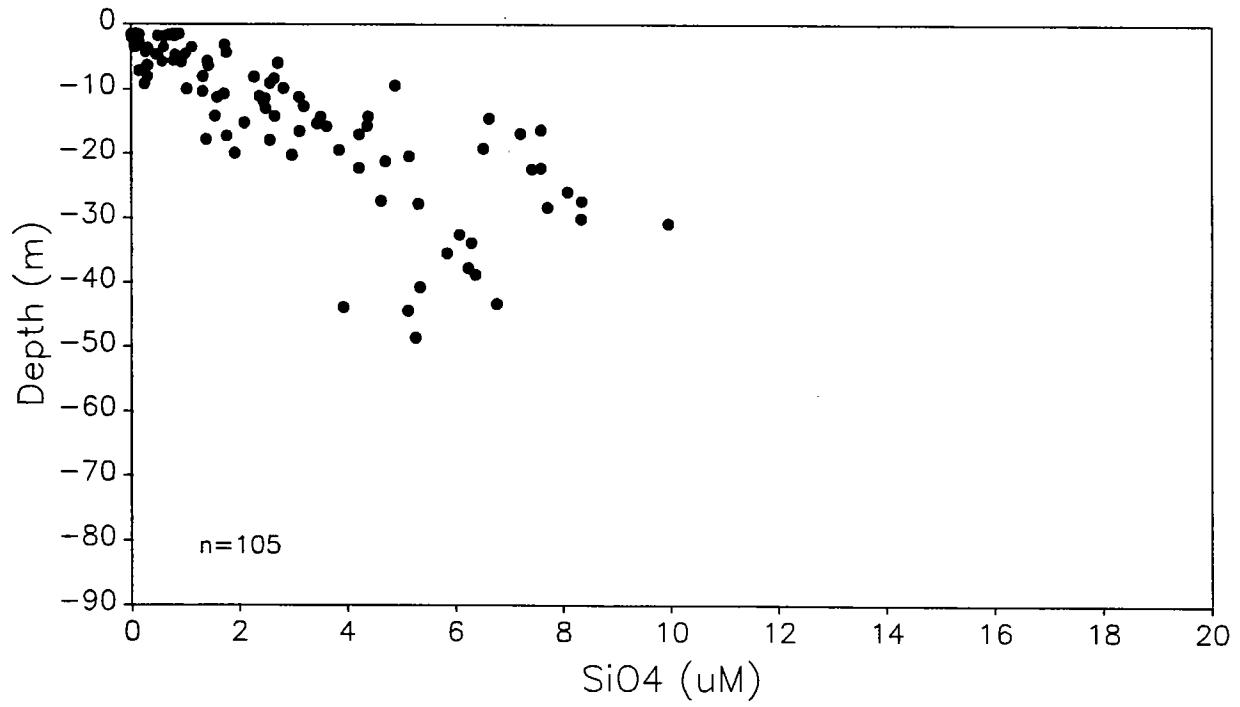


Figure 5-2c. PO_4 and SiO_4 vs. depth in early September 1993.

Early September (W9312), Nearfield Stations

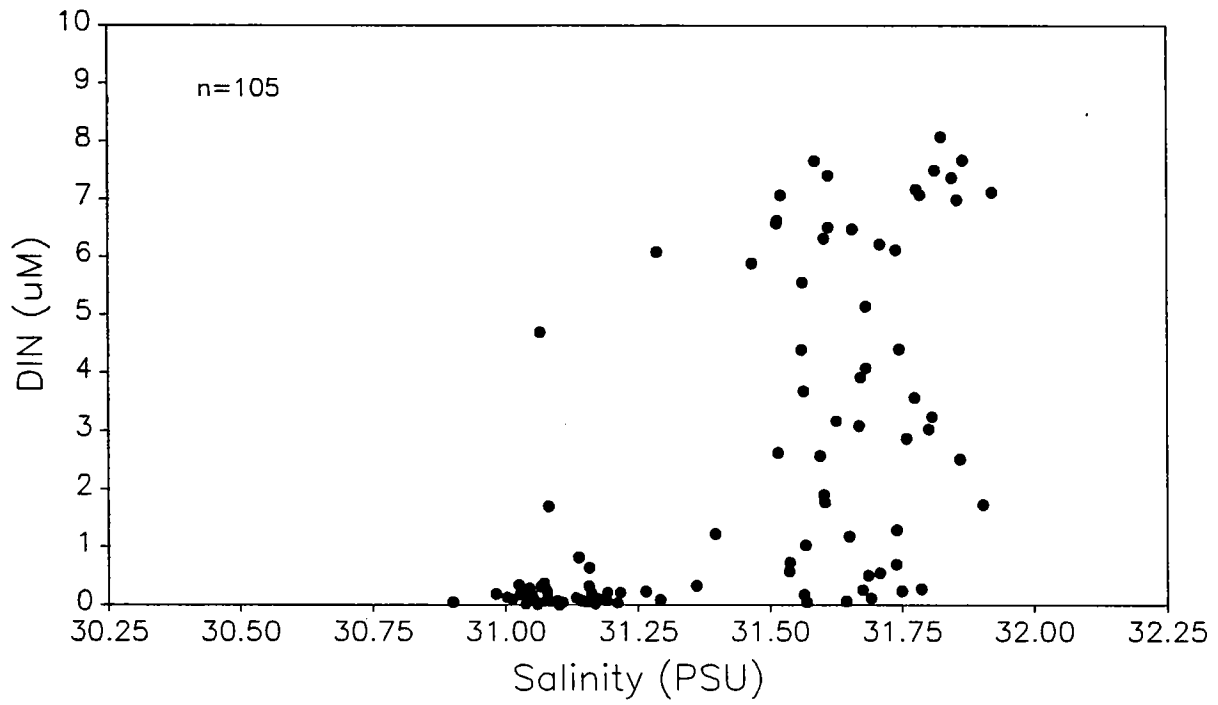
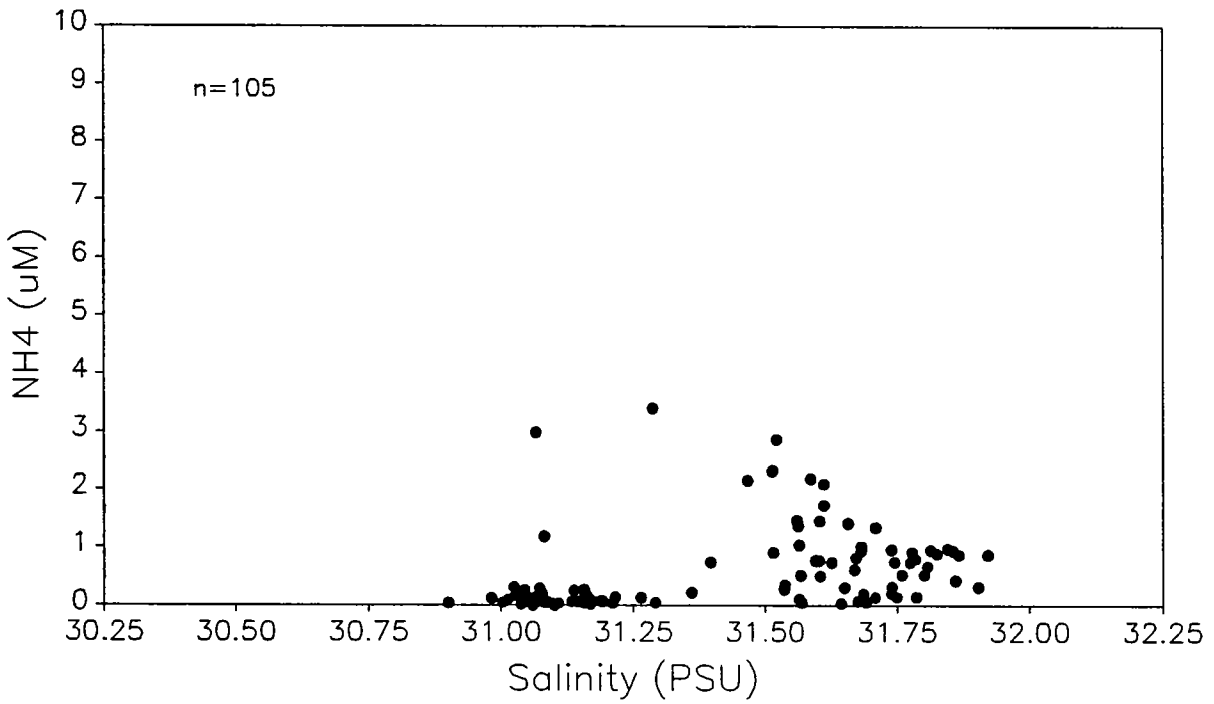


Figure 5-3a. DIN vs. salinity in early September 1993.

Early September (W9312), Nearfield Stations



Early September (W9312), Nearfield Stations

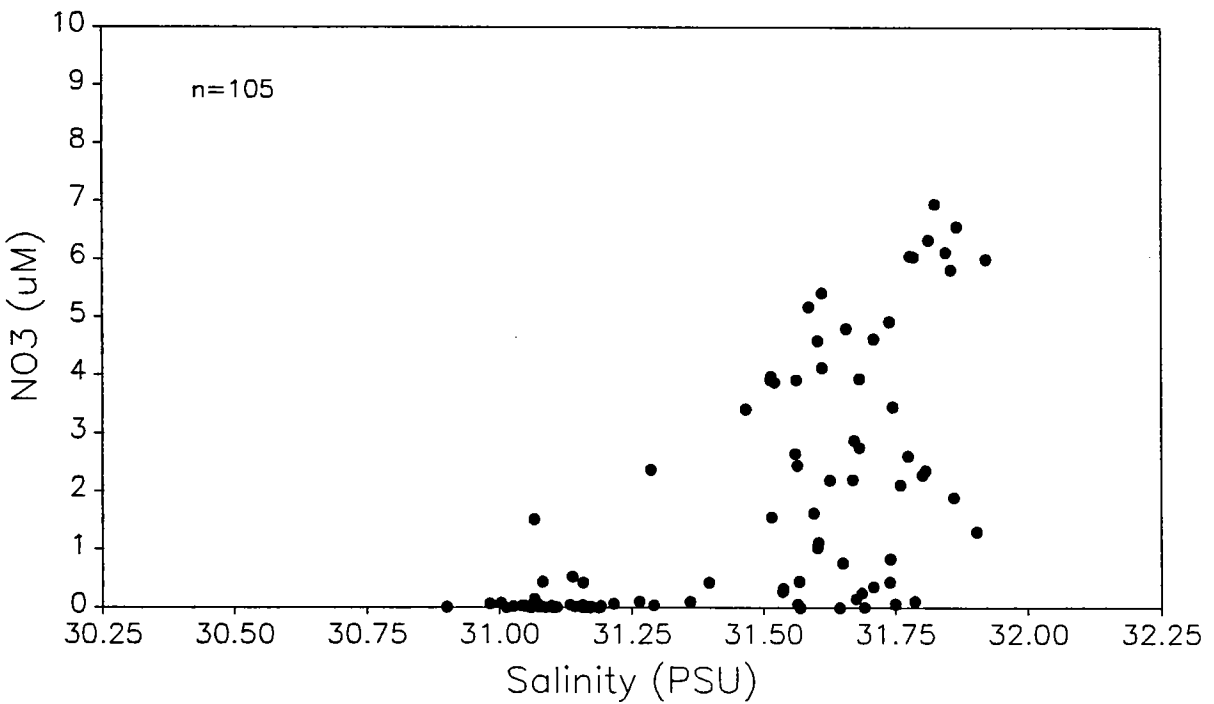
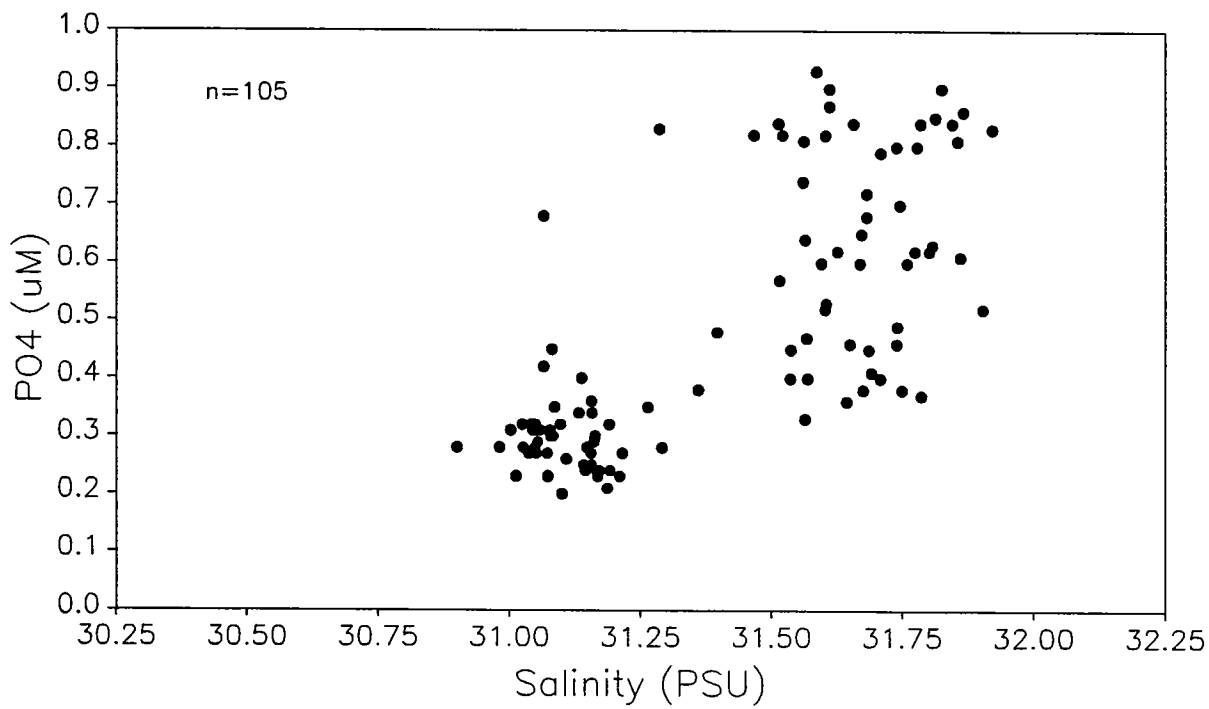


Figure 5-3b. NH₄ and NO₃ vs. salinity in early September 1993.

Early September (W9312), Nearfield Stations



Early September (W9312), Nearfield Stations

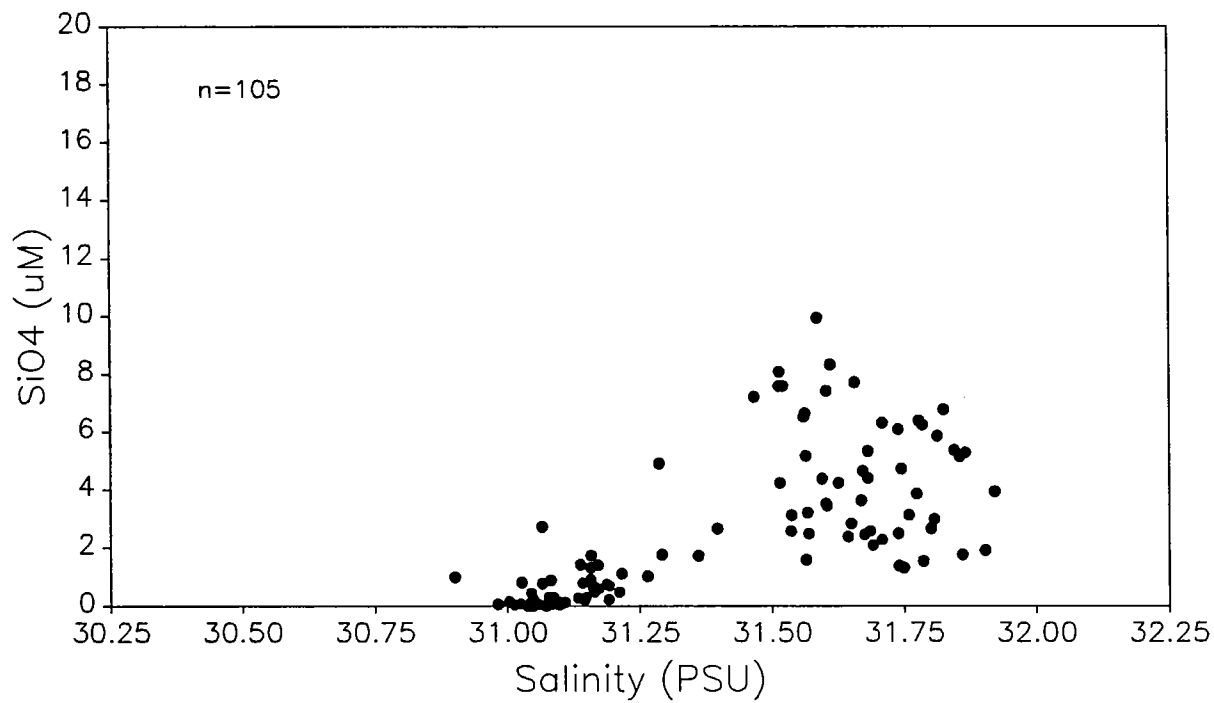


Figure 5-3c. PO₄ and SiO₄ vs. salinity in early September 1993.

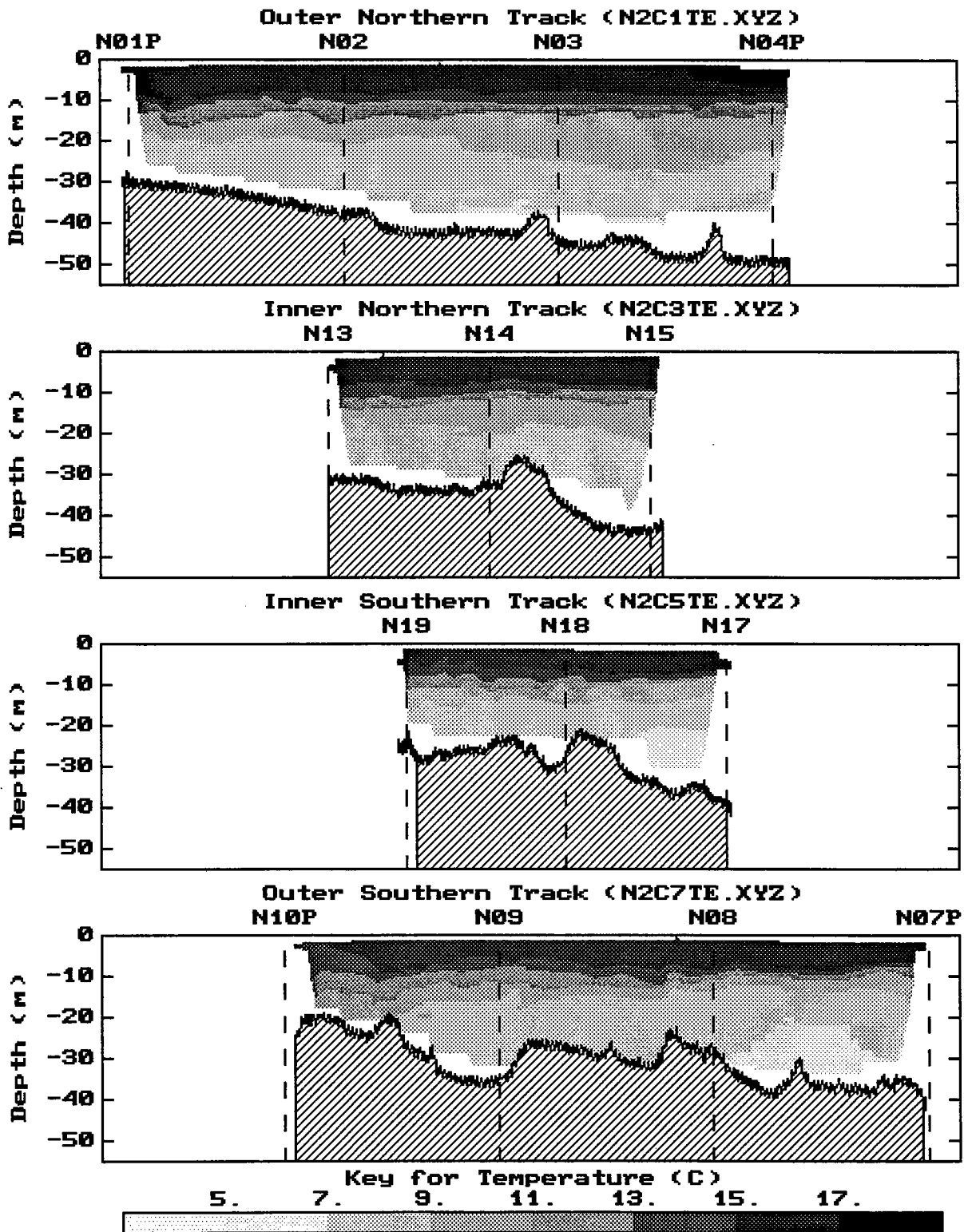


Figure 5-4a. Vertical section contours of temperature generated for tow-yo profiling in early September 1993. The view is towards the North.

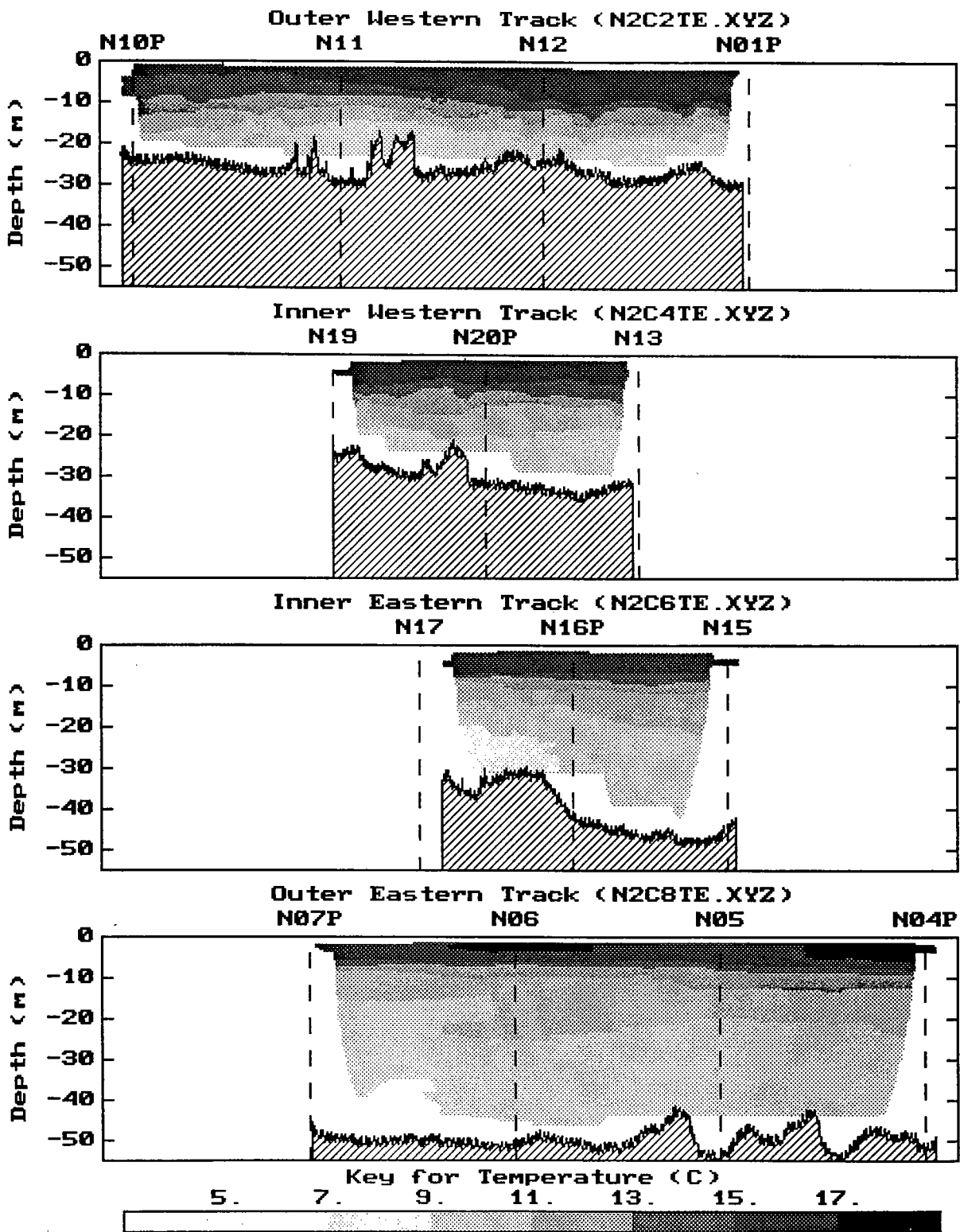


Figure 5-4b. Vertical section contours of temperature generated for tow-yo profiling in early September 1993. The view is towards Boston Harbor.

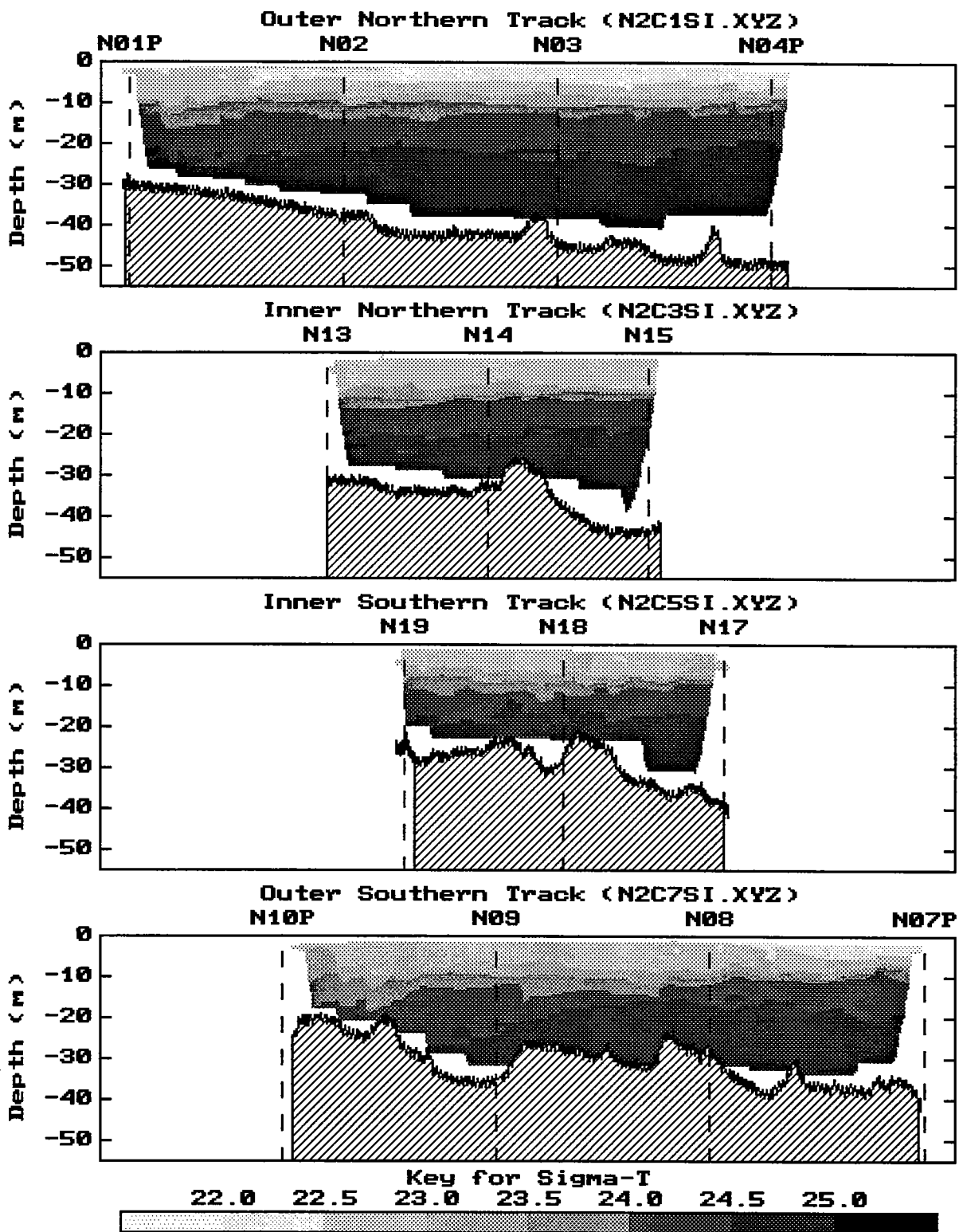


Figure 5-5a. Vertical section contours of σ_T generated for tow-yo profiling in early September 1993. The view is towards the North.

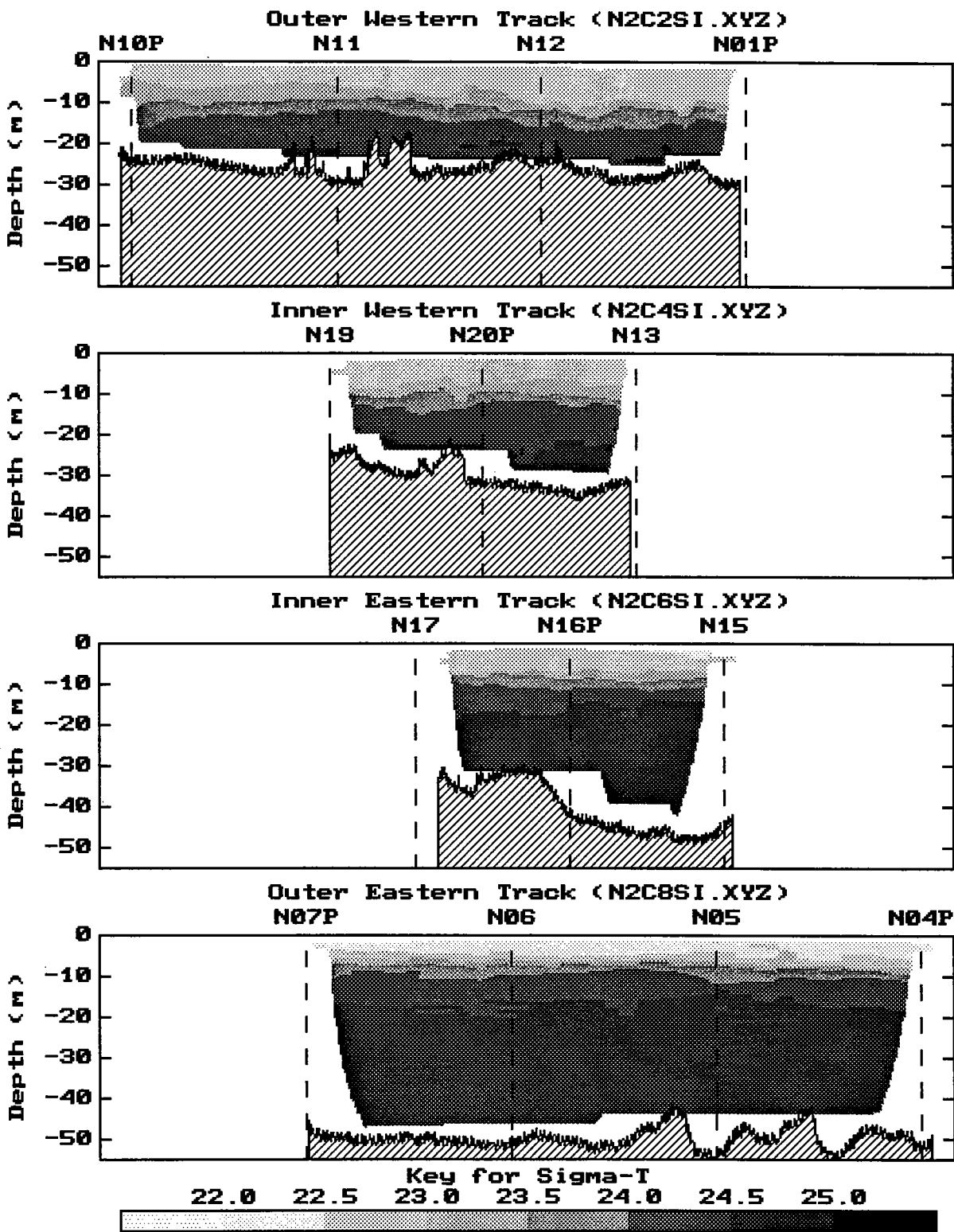


Figure 5-5b. Vertical section contours of σ_T generated for tow-yo profiling in early September 1993. The view is towards Boston Harbor.

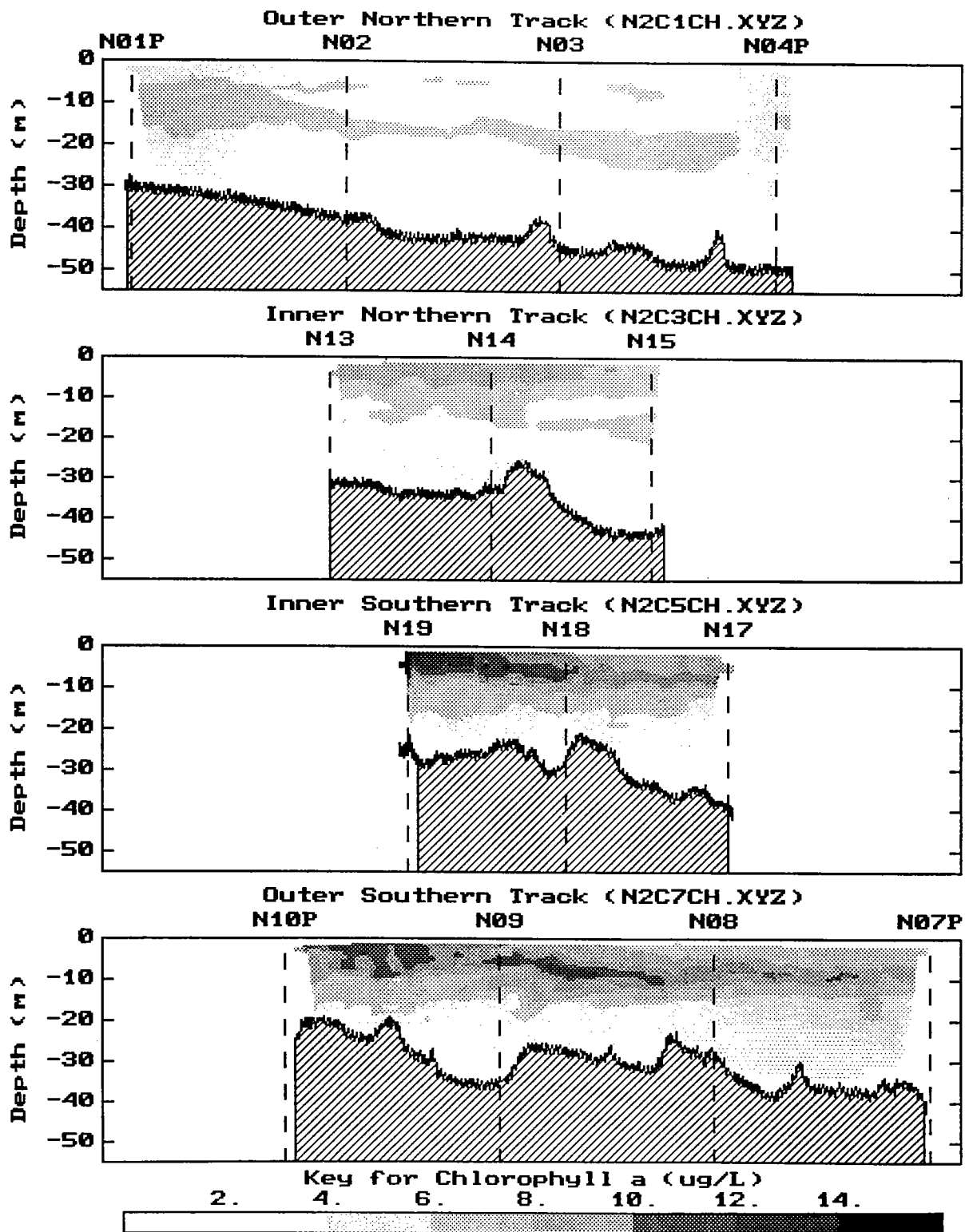


Figure 5-6a. Vertical section contours of fluorescence (as $\mu\text{g Chl L}^{-1}$) generated for tow-yo profiling in early September 1993. The view is towards the North.

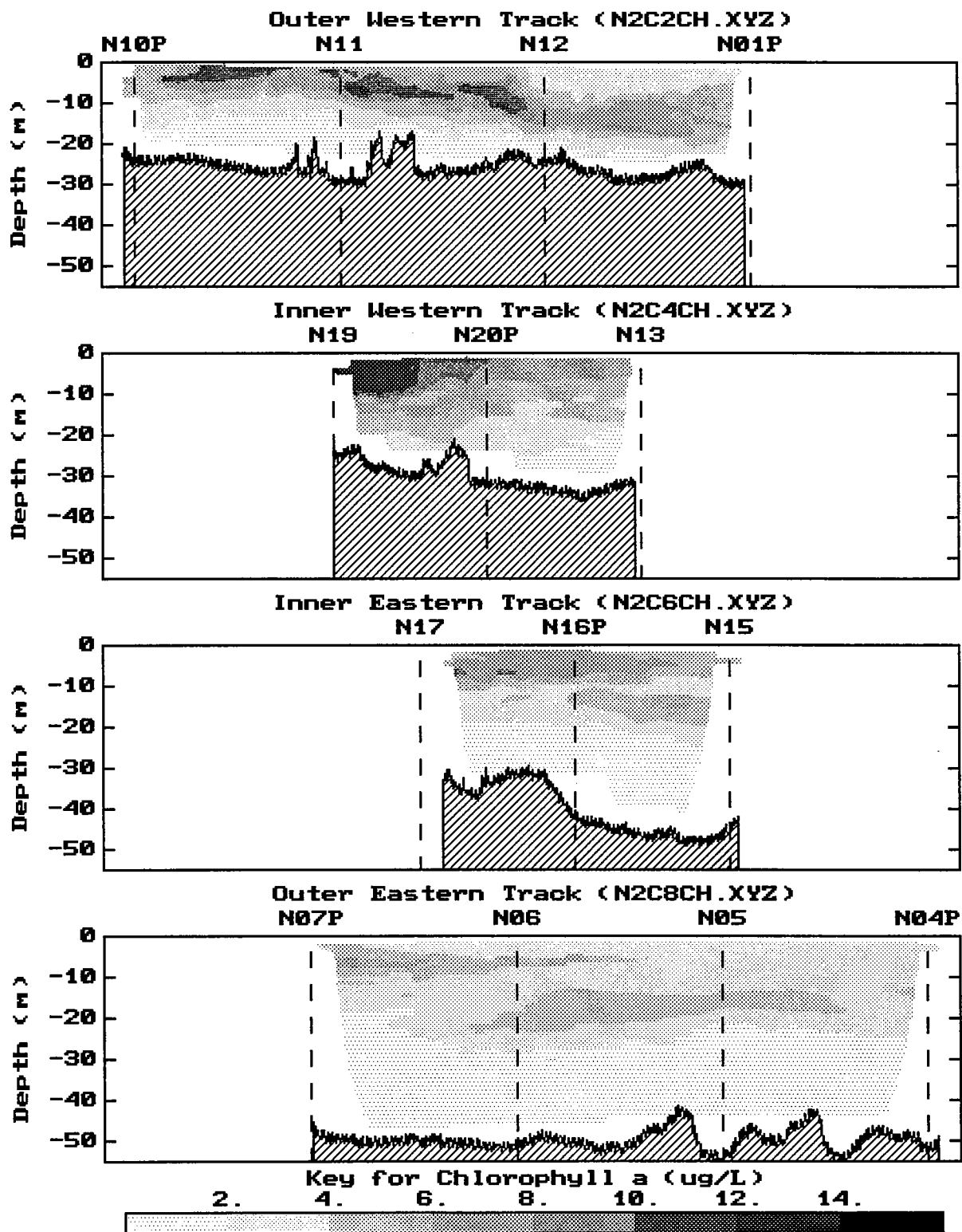


Figure 5-6b. Vertical section contours of fluorescence (as $\mu\text{g Chl L}^{-1}$) generated for tow-yo profiling in early September 1993. The view is towards Boston Harbor.

6.0 RESULTS OF LATE SEPTEMBER 1993 NEARFIELD SURVEY (W9313)

6.1 Distribution of Water Properties from Vertical Profiling

The T-S pattern detected during the late September survey was strikingly similar across all 21 nearfield stations (Figure 6-1a). Vertical stratification was noted virtually everywhere (Appendix B). However, the difference in temperature, from top-to-bottom, was smaller than noted several weeks earlier during survey W9312. Surface temperatures were, at maximum, $\sim 14^{\circ}\text{C}$ and temperatures of almost 8°C were recorded near the bottom. Relative to early September, the salinity range increased; surface salinities were ~ 31.4 PSU compared with ~ 31.05 - 31.15 PSU in early September. Bottom salinities recorded in late September were > 32 PSU compared with 31.7 PSU in late August and 31.9 PSU in early September.

Surface layer beam attenuation increased from the early September survey to values $> 2 \text{ m}^{-1}$; highest values were associated with low salinity and high chlorophyll (Figure 6-1a). Very high concentrations of chlorophyll ($> 18 \mu\text{g L}^{-1}$) were recorded in the surface layer and a subsurface maximum at 10 m was noted at some stations (Figure 6-1b). As typically noted for summer/early fall 1993, lower surface chlorophyll concentrations and a more distinct maximum at mid-depth were observed at the offshore stations. Highest surface chlorophyll concentrations were centered near stations N12, N13, N14, and N15. Below 10 m, chlorophyll concentrations declined sharply. The surface most chlorophyll concentrations varied widely; similar variability was noted in surface DO, which was usually supersaturated (100-120%). As noted for chlorophyll, percent DO saturation also fell sharply with depth. DO reached 81-83% saturation at virtually all stations within the nearfield (see Appendix A).

Dissolved nutrients generally increased as a function of depth (Figure 6-2). Compared with early September, concentrations of DIN, NH_4 , and NO_3 in the surface layer were frequently higher and well above detection limits (Figures 6-2a,b). Concentrations of bottom water DIN and NO_3 also increased about $1 \mu\text{M}$ from early September. Concentrations of PO_4 in the surface layer varied widely; in some

locations, surface-water PO_4 concentrations were more depleted than in early September (Figure 6-2c). In contrast to DIN, SiO_4 concentrations remained generally depleted in the surface but high ($\sim 7 \mu\text{M}$) at depth. The high ($> 8 \mu\text{M}$) SiO_4 concentrations at intermediate depths (near-bottom at most inshore shallower stations) that had been measured in early September were not observed during the late September survey. In contrast to the early September observations, the nearfield in late September appeared to be characterized uniformly by a strong silicate-depth trend.

Dissolved nutrient concentrations did not all co-vary during the late September survey. The increase in DIN within the surface layer is illustrated in Figure 6-3a. The concentration range at low salinity was large enough to encompass the higher values generally detected at high salinity and greater depth. A decrease in NH_4 concentrations with increasing salinity (Figure 6-3b) was suggested, and the increase in surface DIN was due to NH_4 concentrations more than to increases in NO_3 (Figure 6-3b). The silicate pattern was similar to the NO_3 pattern, but with a more uniformly constrained increase with increasing salinity (Figure 6-3c) and the PO_4 pattern generally resembled the DIN pattern, but with some high values at low salinities (Figure 6-3c).

6.2 Distribution of Water Properties from Towing

The tow-yo profiling images of the thermal and density data on tracks around and within the nearfield reinforce and illustrate several observations made from the vertical profile data. Patterns showed a small range in physical parameters, and smooth transitional regions between surface and bottom layers. For much of the region, the thermocline and pycnocline had deepened between the early September and the late September surveys; in most locations, the thermocline/pycnocline impinged upon the bottom (Figures 6-4 and 6-5). The water column was virtually unstratified near station N10P (Figure 6-5a).

Along the outer western track (Figure 6-5b), a plume of warmer, lower-density water was centered around station N12. Water masses characterized by higher surface densities were observed north (station N01P) and south (station N11) of station N12. The surface layer density and vertical layering

structure at station N12 was more similar to the rest of the field than the water immediately north or south of it (stations N01P, N11, and N10P). Interestingly, chlorophyll mapped distinctly upon this physical distribution, with lower concentrations recorded at stations N01P, N11, and N10P, and higher concentrations at all other locations (Figure 6-6a). Aside from those three specified stations, within the surface 10 m, the entire field was very rich in chlorophyll. Moving offshore, the chlorophyll maximum tended to be subsurface and a broad inshore-offshore concentration gradient was noted. Concentrations of chlorophyll in the subsurface maximum layer offshore still exceeded $6 \mu\text{g L}^{-1}$. Inshore concentrations were regularly $>8\text{-}10 \mu\text{g L}^{-1}$ through the entire surface layer (10-12 m). The peak concentrations and the center of this extensive chlorophyll patch was near the center and west/northwest of the center of the nearfield (stations N12, N13, N14, N20P, and N15). From Figure 6-6, it is possible to estimate that the areas having a 5-m to 10-m-thick layer of chlorophyll, with minimum concentrations of 6, 8, and $10 \mu\text{g L}^{-1}$, respectively, were roughly 100, 75, and 60 km^2 .

6.3 Water Types and Analysis of Small-Scale Variability

The high chlorophyll concentrations and their areal extent throughout the field were the central defining features for this survey, and marked the strongest nearfield bloom event recorded to date as part of the 1992 and 1993 MWRA baseline monitoring. A similar geographic distribution was noted from both vertical profiling and tow-yo profiling — the repeated observations suggest field-wide persistence of the feature over a period of days.

More minor was the indication that nutrient concentrations in nearshore shallow waters were beginning a seasonal increase. NH_4 and PO_4 were enriched at station N10P, an interesting observation because chlorophyll concentrations were generally lowest at that location (although concentrations were still $\sim 6 \mu\text{g L}^{-1}$). Nutrient forms that were elevated at station N10P were also occasionally elevated at several other stations, primarily along the inshore track. These samples were generally distinguished by lower salinities. For NH_4 and PO_4 concentrations (Figures 6-3b and 6-3c), the distribution with salinity marked the re-emergence of a V-shaped pattern which was not observed for NO_3 or SiO_4 . The V-

shaped pattern occurred at the initiation of stratification in the spring and reappeared as stratification weakened in the fall. The rising left arm of the "V" has been associated with the Boston Harbor-Bay gradient, a dilution of fresher water enriched in nutrients, and was generally characteristic of the unstratified period. In contrast, the rising right arm of the "V" is characteristic of increasing nutrients with depth and was found throughout the summer of 1993.

In summary, the late September survey may offer geochemical data that serve as a harbinger of the normal seasonal transition from stratified to mixed conditions in the nearfield. In this context, it seems noteworthy that the extensive concentrations of chlorophyll occurred within a surface layer underlain by a weakened thermocline/pycnocline (compared to several weeks earlier), but the nearfield water column, with minor local anomalies (e.g., station N10P), was nevertheless stratified.

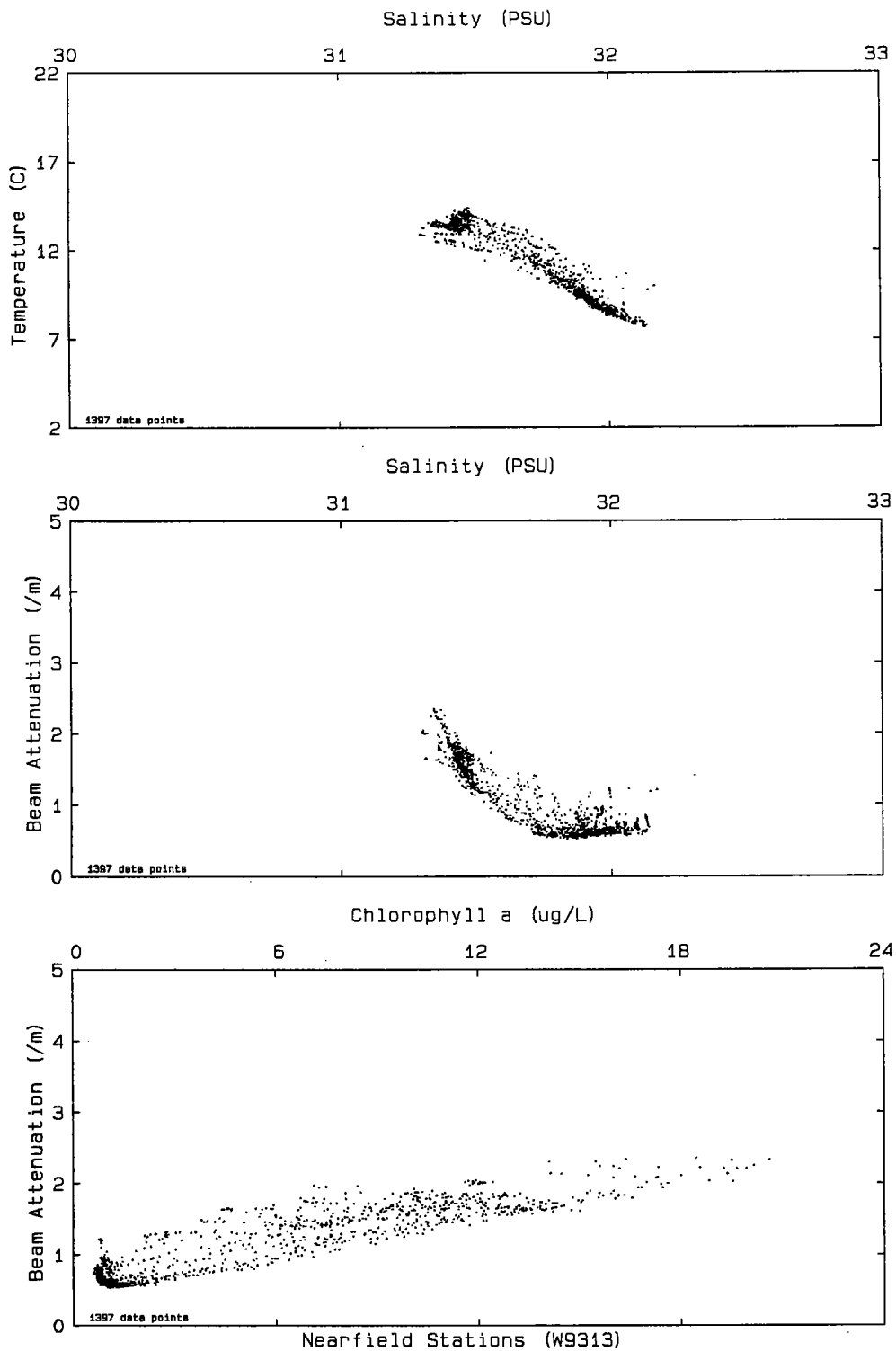


Figure 6-1a. Scatter plots of data acquired by *in situ* sensor package during vertical downcasts at all nearfield stations occupied in late September 1993. Individual station casts that were used to produce this composite are in Appendix B. Chlorophyll is estimated from *in situ* fluorescence.

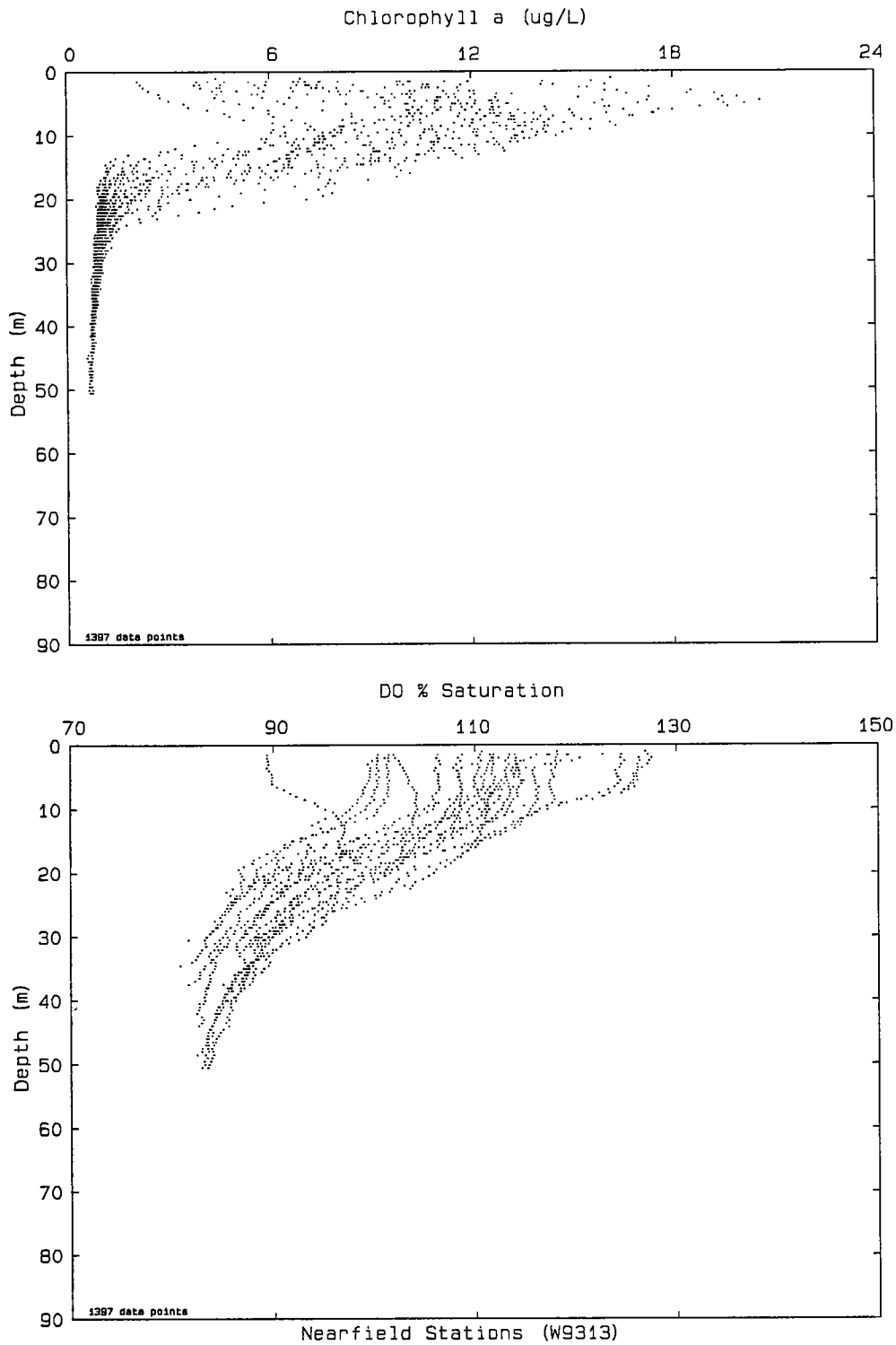


Figure 6-1b. Scatter plots of data acquired by *in situ* sensor package during vertical downcasts at all nearfield stations occupied in late September 1993. Individual station casts that were used to produce this composite are in Appendix B. Chlorophyll is estimated from *in situ* fluorescence.

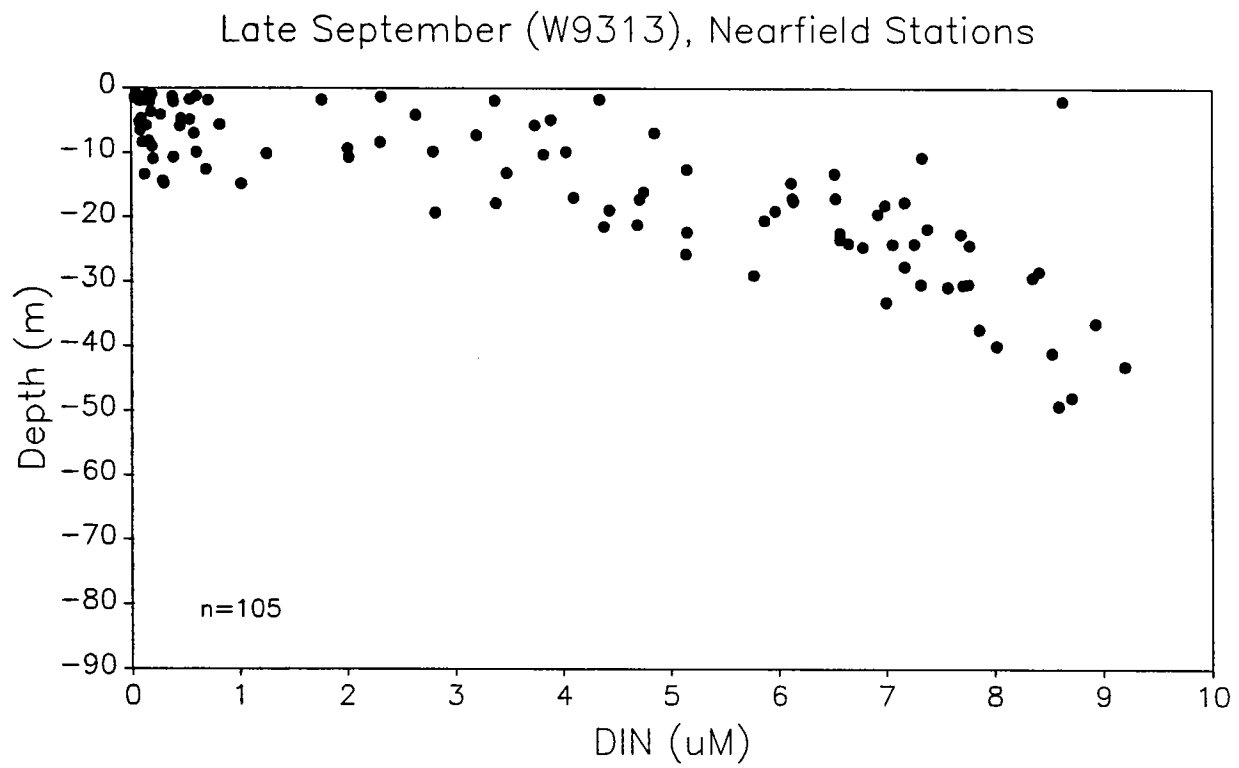
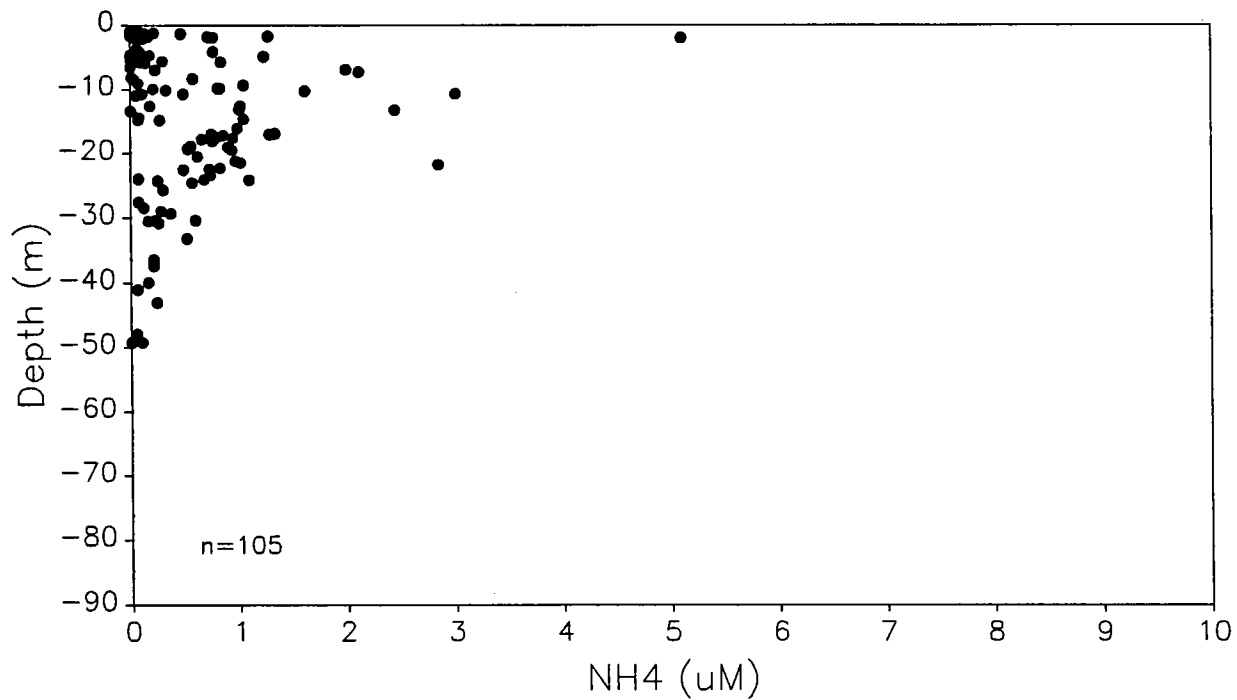


Figure 6-2a. DIN vs. depth in late September 1993.

Late September (W9313), Nearfield Stations



Late September (W9313), Nearfield Stations

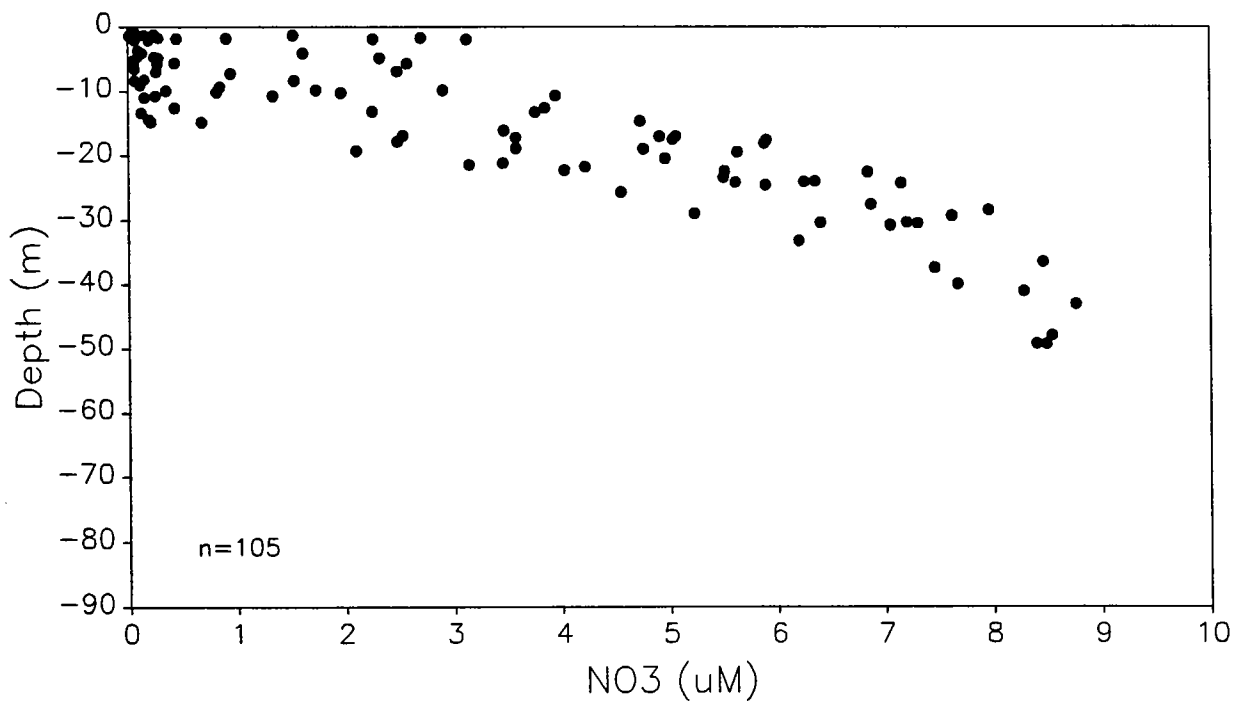
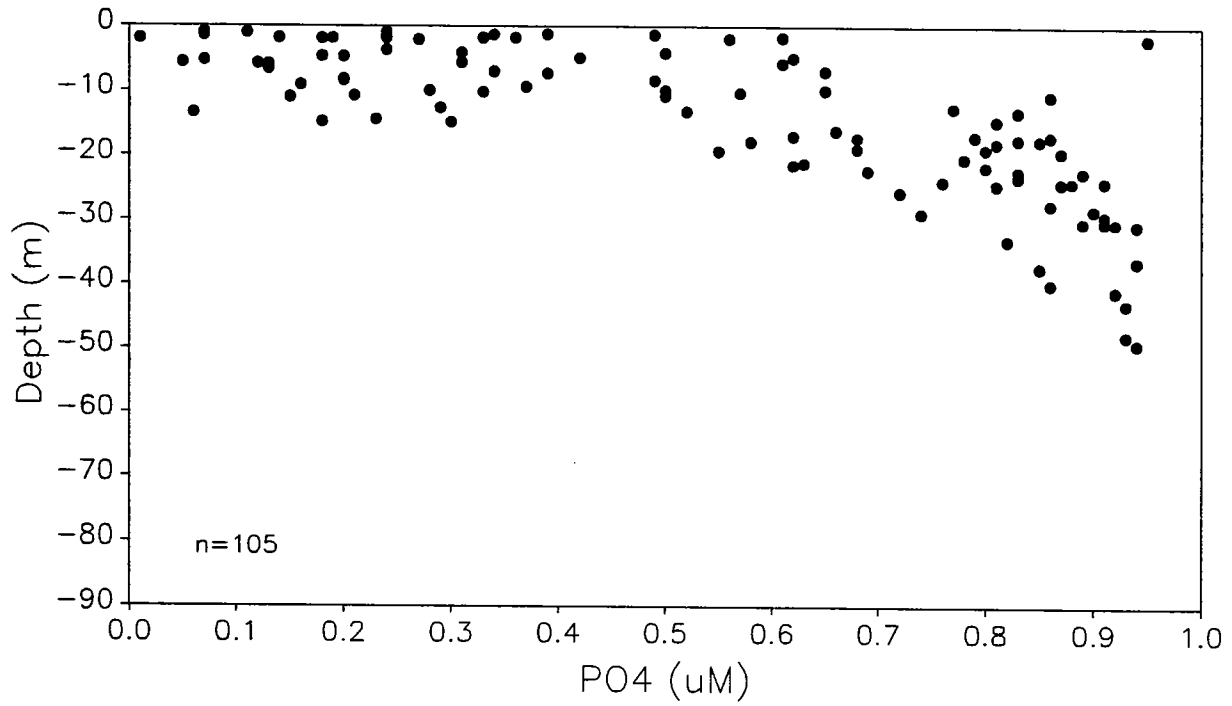


Figure 6-2b. NH_4 and NO_3 vs. depth in late September 1993.

Late September (W9313), Nearfield Stations



Late September (W9313), Nearfield Stations

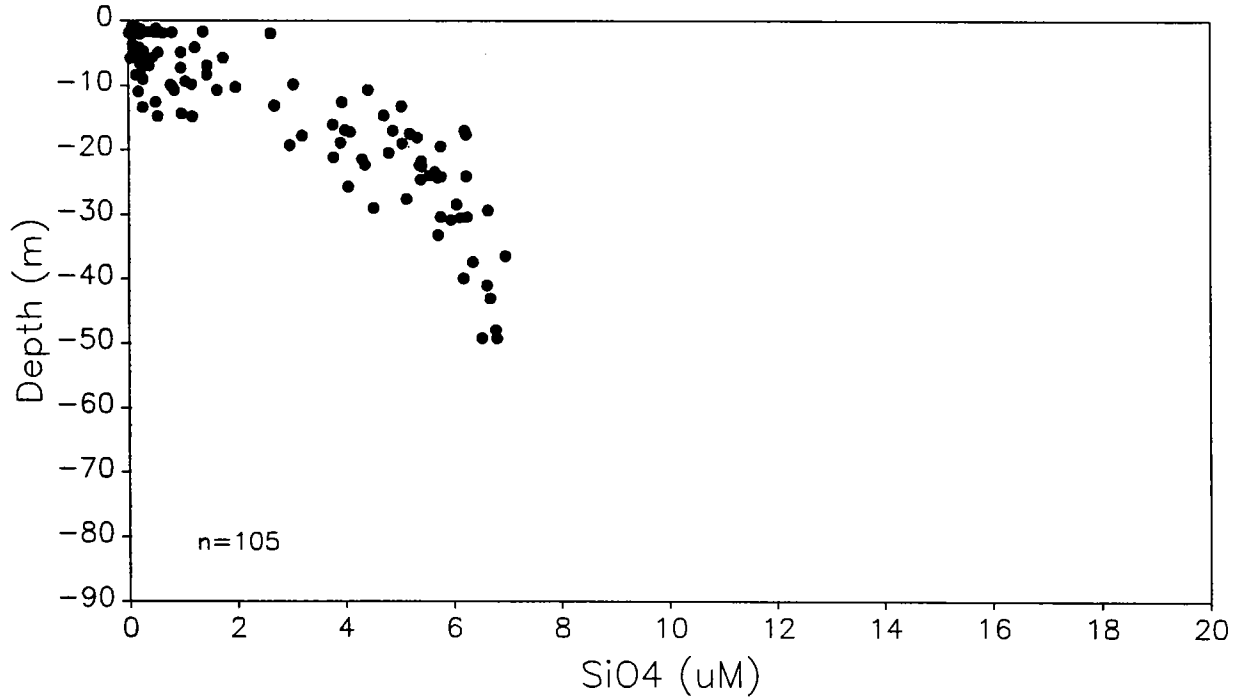


Figure 6-2c. PO_4 and SiO_4 vs. depth in late September 1993.

Late September (W9313), Nearfield Stations

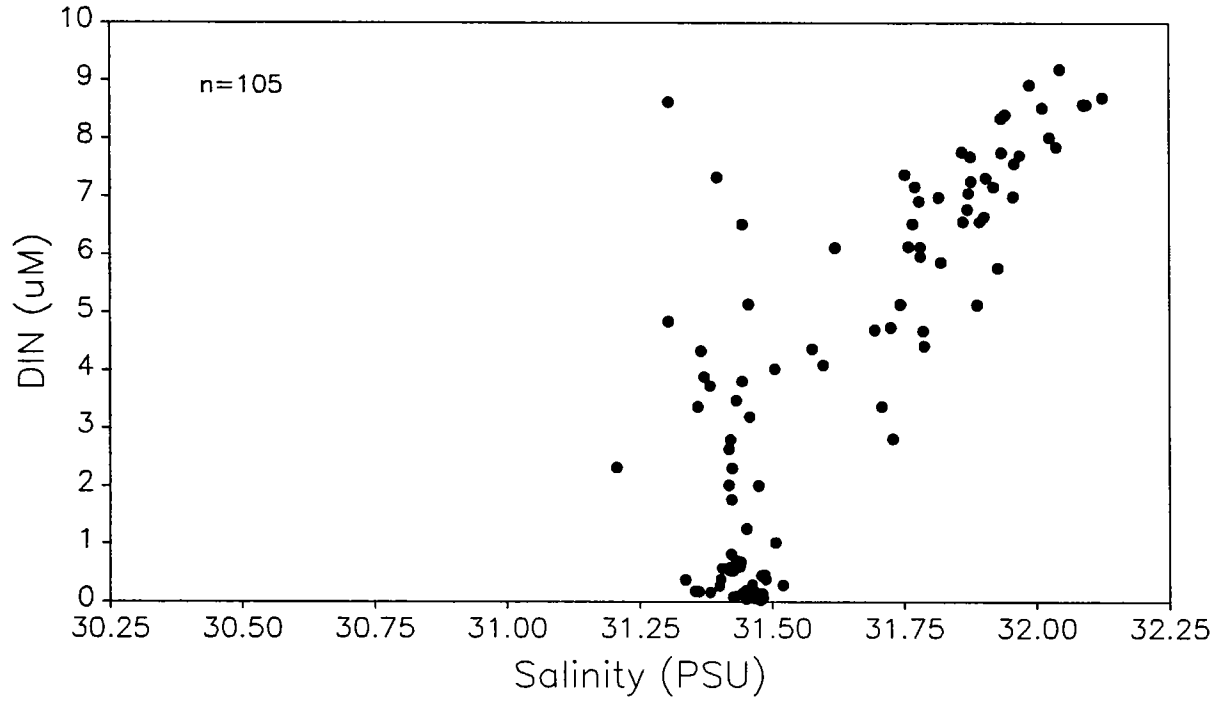
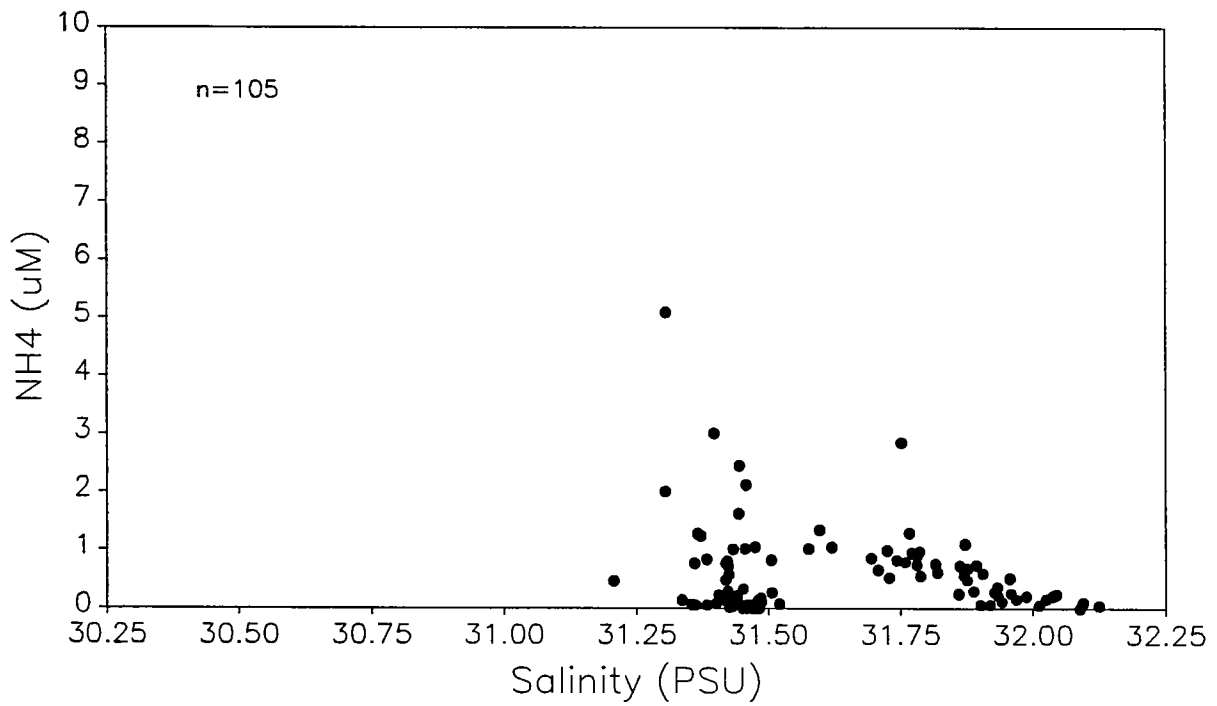


Figure 6-3a. DIN vs. salinity in late September 1993.

Late September (W9313), Nearfield Stations



Late September (W9313), Nearfield Stations

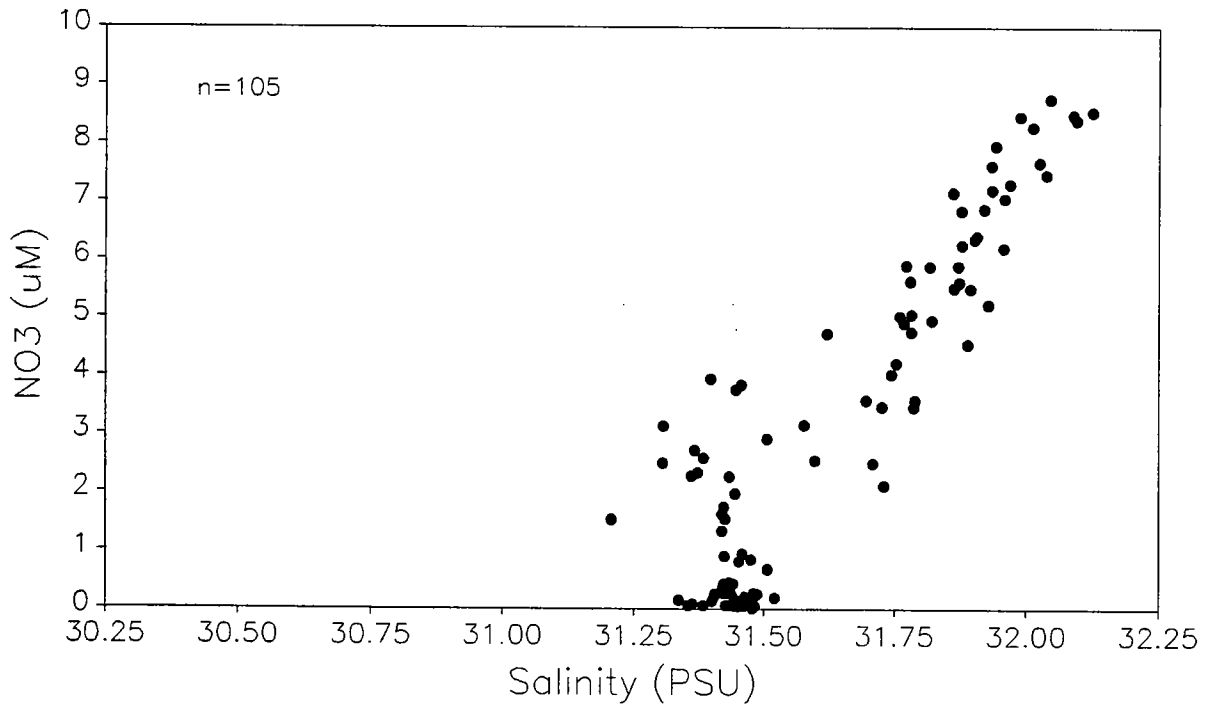
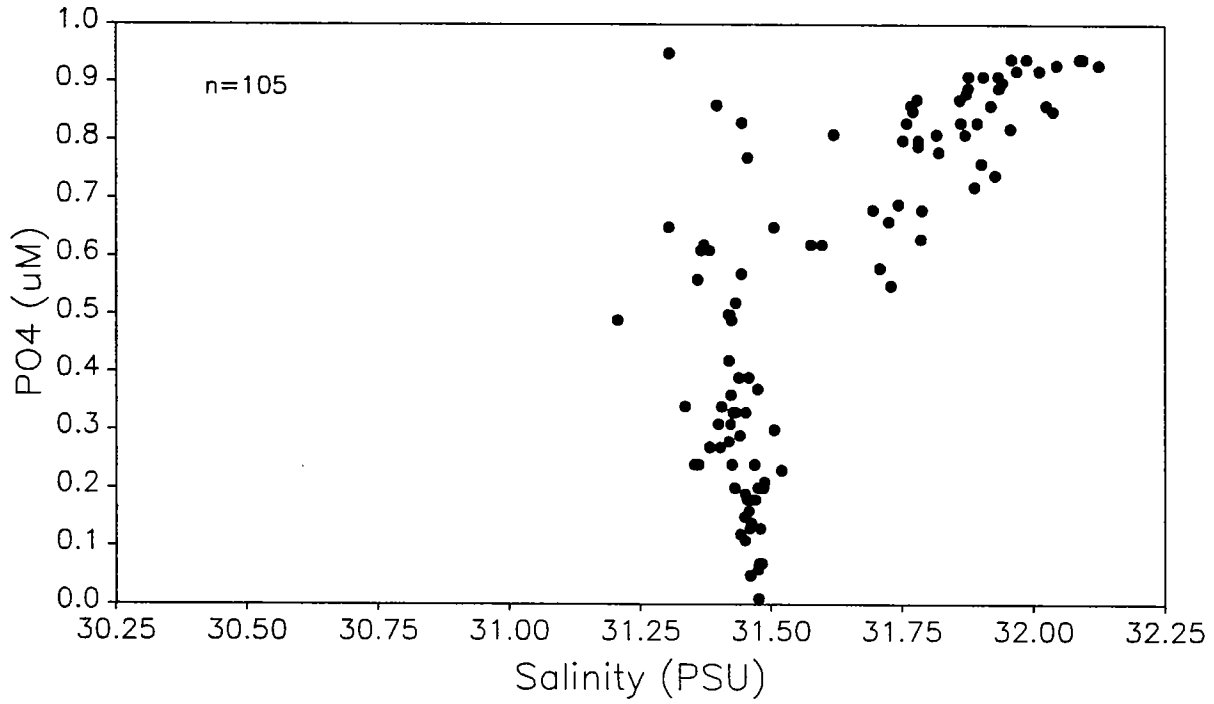


Figure 6-3b. NH₄ and NO₃ vs. salinity in late September 1993.

Late September (W9313), Nearfield Stations



Late September (W9313), Nearfield Stations

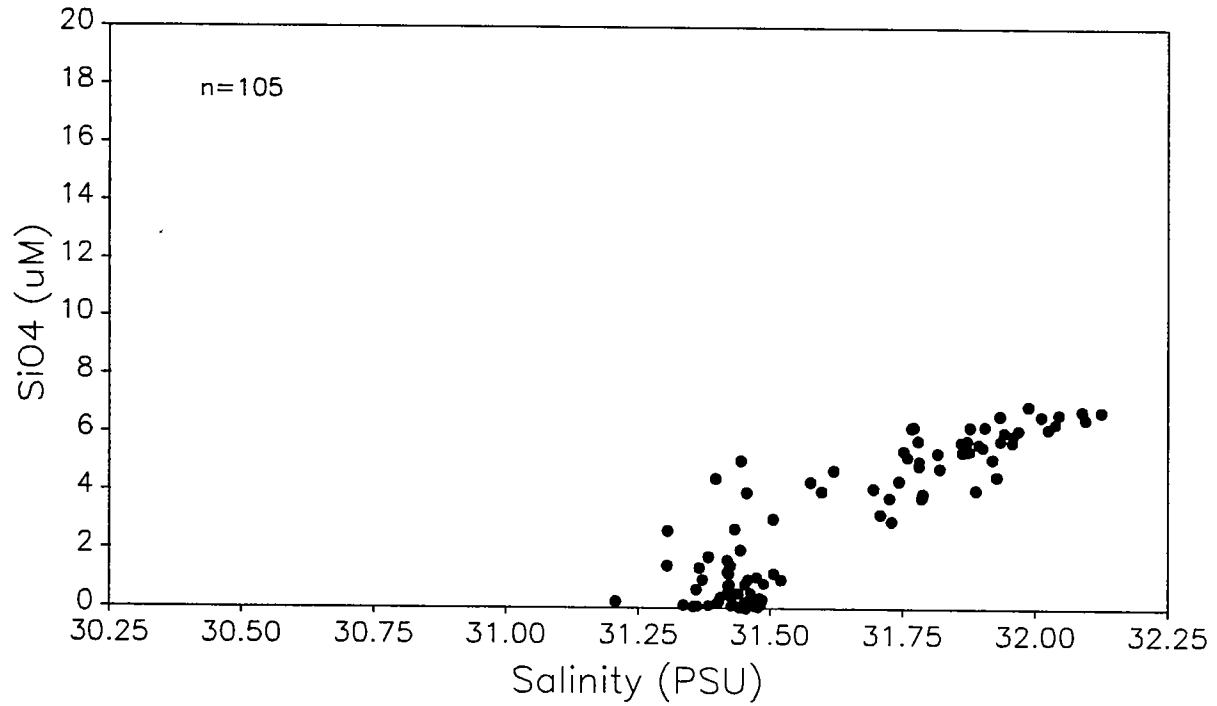


Figure 6-3c. PO₄ and SiO₄ vs. salinity in late September 1993.

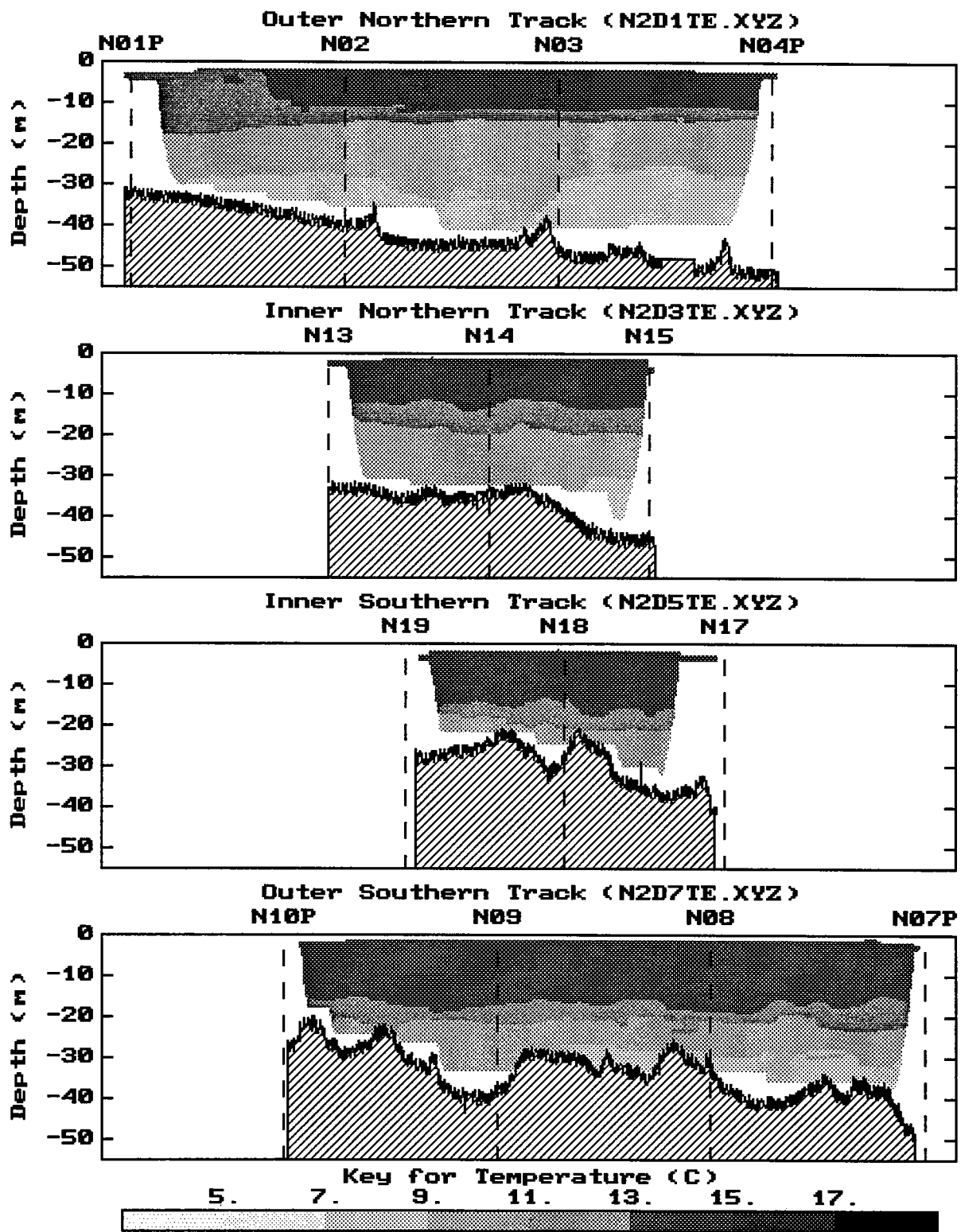


Figure 6-4a. Vertical section contours of temperature generated for tow-yo profiling in late September 1993. The view is towards the North.

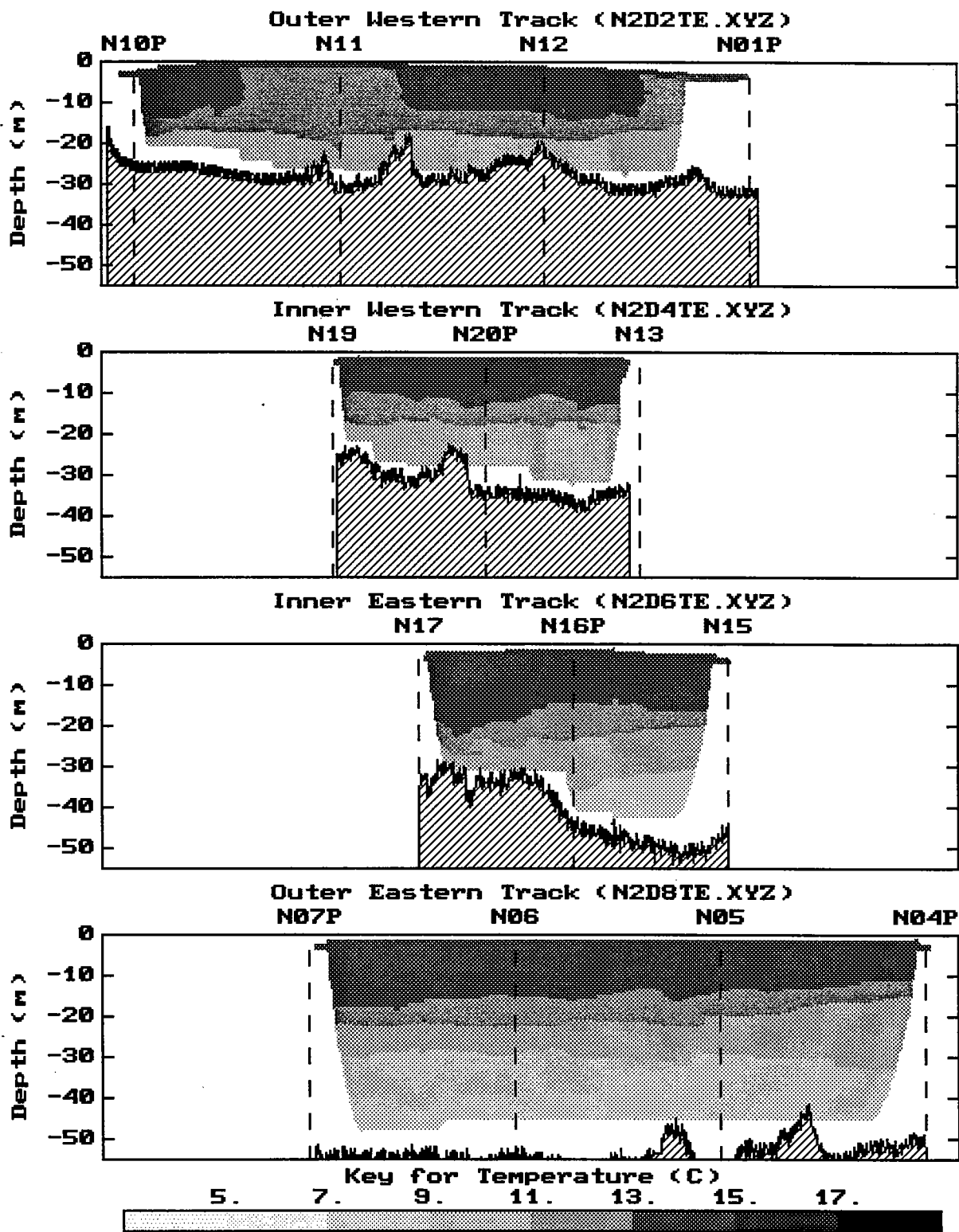


Figure 6-4b. Vertical section contours of temperature generated for tow-yo profiling in late September 1993. The view is towards Boston Harbor.

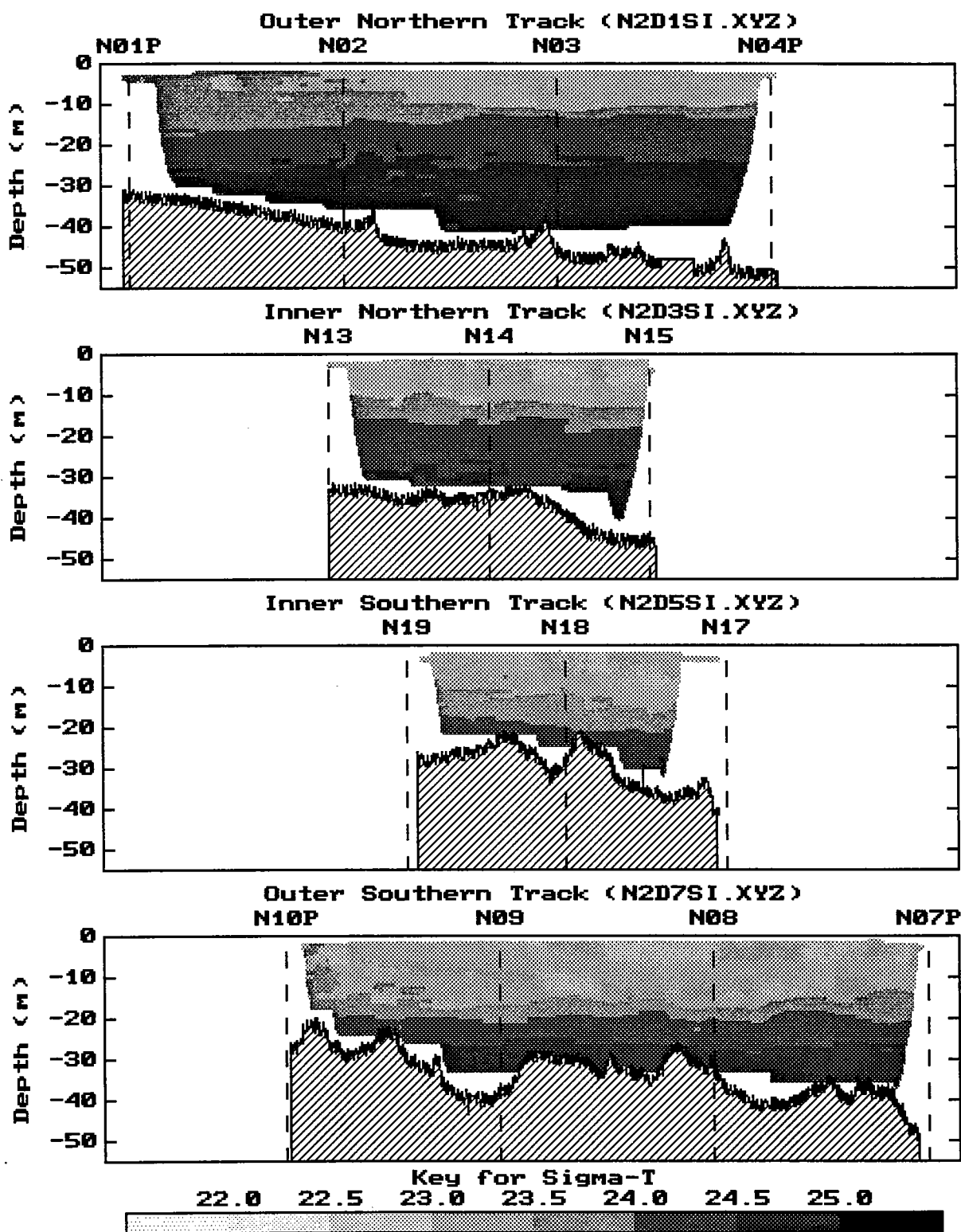


Figure 6-5a. Vertical section contours of σ_T generated for tow-yo profiling in late September 1993. The view is towards the North.

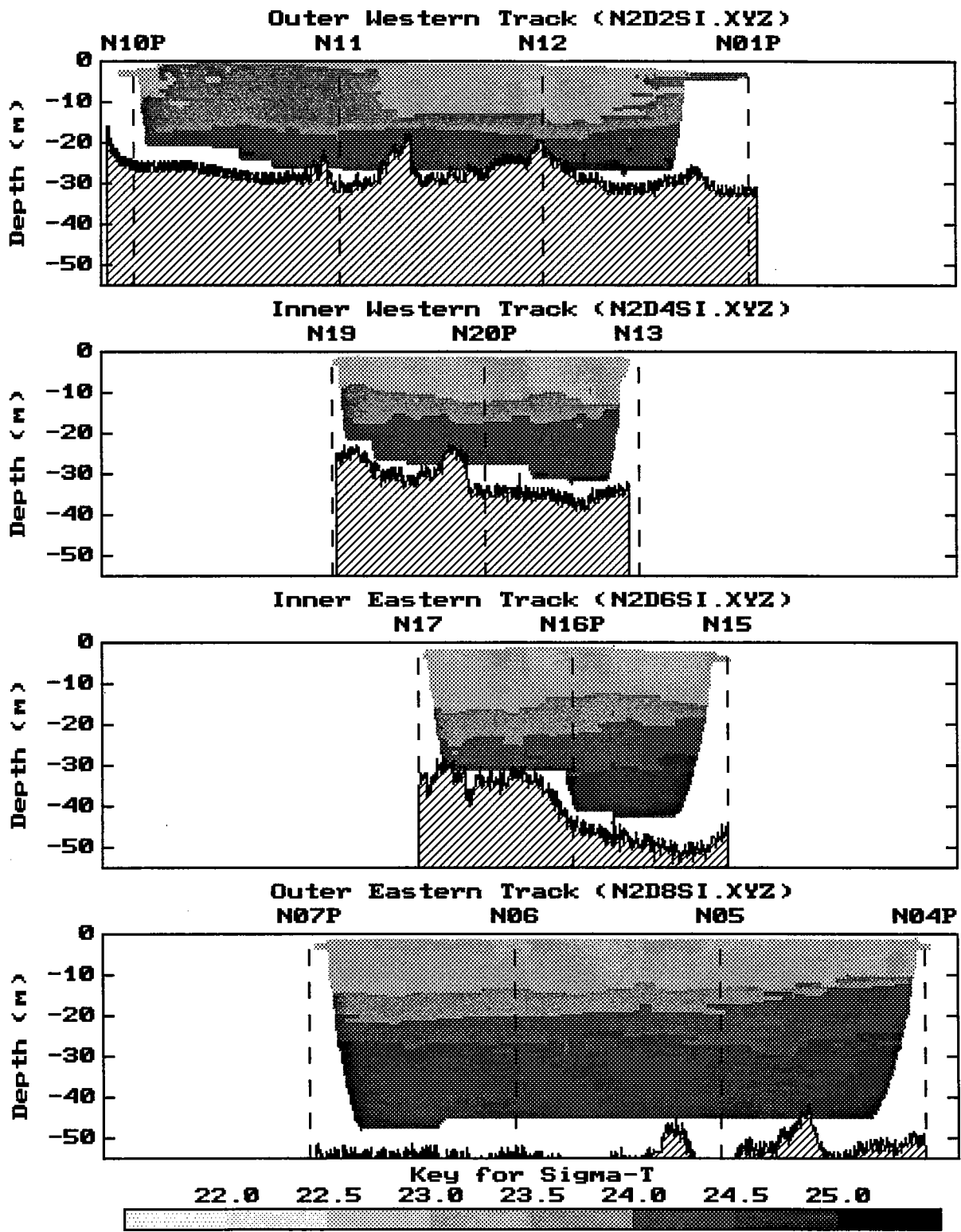


Figure 6-5b. Vertical section contours of σ_T generated for tow-yo profiling in late September 1993. The view is towards Boston Harbor.

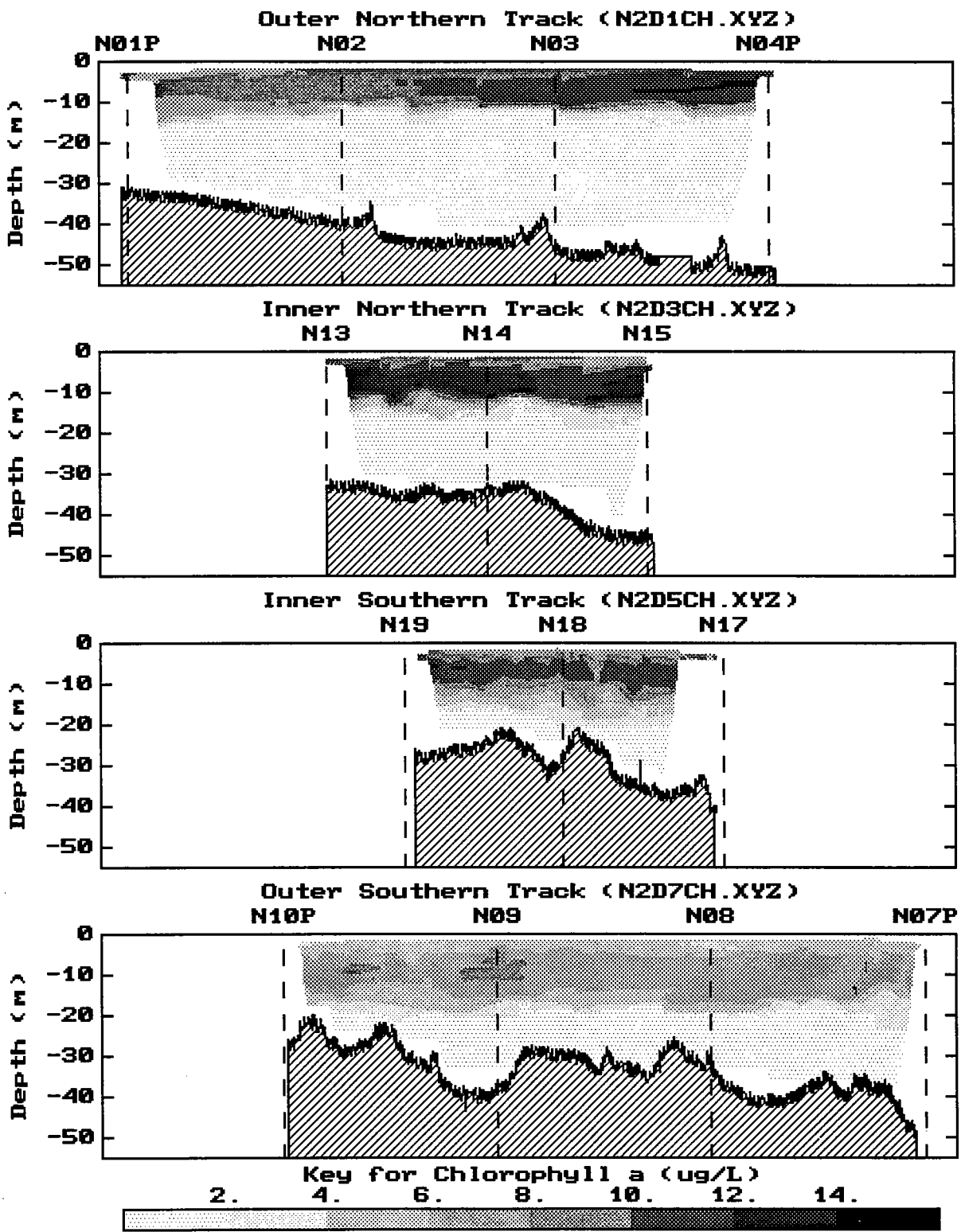


Figure 6-6a. Vertical section contours of fluorescence (as $\mu\text{g Chl L}^{-1}$) generated for tow-yo profiling in late September 1993. The view is towards the North.

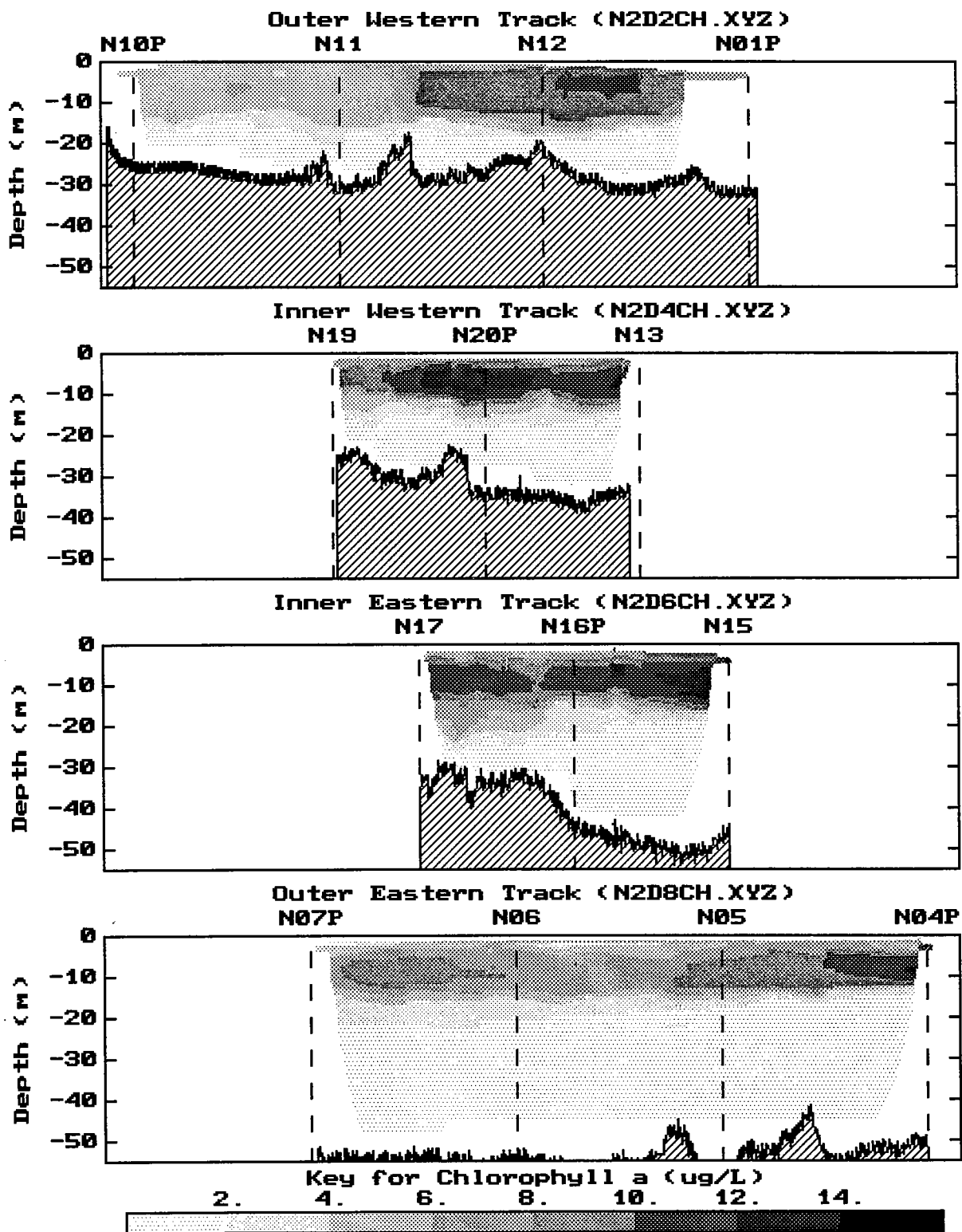


Figure 6-6b. Vertical section contours of fluorescence (as $\mu\text{g Chl L}^{-1}$) generated for tow-yo profiling in late September 1993. The view is towards Boston Harbor.

7.0 DISCUSSION OF THE LATE SUMMER/ EARLY FALL PERIOD OF SURVEYS

7.1 Water Properties

7.1.1 Variability at the Regional Scale

In August, when the entire Bay was surveyed, most of the variability in physical properties was due to strong stratification. Minor regional features were noted but, in general, the geographic variability in surface salinity and temperature was small. For example, striking differences between Cape Cod Bay and Massachusetts Bay were absent, and virtually no salinity gradient was observed out from Boston Harbor.

Regional observations included cooler surface temperatures (and perhaps greater mixing) near the coast along the South Shore, and gradual deepening of the thermocline/pycnocline with distance offshore and increasing water depth. Finally, some axial trends were noted in the deep waters of Stellwagen Basin; these trends may suggest some directional flow of the Basin's deep water during the summer of 1993.

7.1.2 Variability in the Nearfield

During the survey periods, a gradual physical transition was observed in the nearfield. It appeared that this transition occurred as an aggregate unit rather than as a mosaic of disconnected local changes. In general, the field was spatially uniform; a gradual inshore-offshore deepening of the pycnocline was the only consistent notable feature. In August, surface temperatures approached the annual maximum, and the differences between surface and bottom water temperatures were greatest. During September, bottom water continued to warm as the surface cooled. Water stratification was beginning to weaken but was still persistent in the field, except at the inshore, southwest corner near Nantasket Roads

(station N10P). Because of the persistent stratification and because bottom water temperatures were warm, DO gradually decreased in bottom waters, to 81-84% saturation by the end of September. Bottom water salinity increased between early August and late September; some advection of bottom water may have occurred during this period.

7.1.3 Coherence of Nearfield and Farfield Station Properties

The principal feature of most water column properties was a relationship to depth that corresponded to physical layering. The relationship was sufficiently ubiquitous in most of the nearfield and farfield that, at a given water depth within the Bays, similar physical and geochemical properties were found and only subtle anomalies were noted in space and time. This observation suggests that effective "communication" of water masses could occur horizontally across density surfaces.

7.1.4 Special Features: Comparison of 1993 with 1992

Figure 7-1 shows the progression of temperature in the nearfield surface waters that was described above. Maximum temperatures in August 1993 were higher and had progressively increased in a more regular fashion between July and August 1993 than during the same period in 1992. Bottom water DO in the nearfield decreased continuously throughout August and September 1993, as it had in 1992 (Figure 7-2). Percent DO saturation in early September was higher in 1993 than in 1992.

Unfortunately, no late September survey was performed in 1992; however, DO concentrations in late September 1993 were in the same range as measured in early October 1992, the time of the annual DO minimum for bottom waters in 1992.

7.2 Water Column Nutrient Dynamics

7.2.1 Vertical Structure and Initiation of Seasonal Mixing

Stratification determined nutrient patterns and, in general, depleted surface waters of dissolved inorganic nitrogen. As often noted previously, phosphate concentrations in surface waters were consistently above detection limits when DIN concentrations were essentially undetectable. This condition is usually indicative of nitrogen limitation, rather than phosphorus limitation.

In late August, surface silicate concentrations were slightly higher in Cape Cod Bay than at other locations; surface salinity in Cape Cod Bay was also slightly higher during this period. However, relative to the salinities, samples from Cape Cod Bay were enriched in silicate throughout the water column. It is unclear if this geographic difference was associated with stratification. It had previously been noted that the water column at stations in western Cape Cod Bay was more vertically mixed than at stations in eastern Cape Cod Bay. Mixing of the water column, perhaps induced by winds, may have influenced the physical characteristics of Cape Cod Bay and, therefore, the nutrient distributions throughout the water column in this Basin. However, differences in silicate concentrations between Cape Cod Bay and much of Massachusetts Bay were also influenced by differences in the development and growth of the phytoplankton community between the Basins (see below).

Nutrients in bottom waters were either stable or rose gradually over the period, while DO decreased slowly. Nutrient concentrations, particularly NH_4 and SiO_4 , were elevated in bottom waters on the western edge of the nearfield in early September. Although speculative, this enrichment may have been a local phenomenon related to the presence of major sediment depositional sites and locally high rates of benthic remineralization.

During the survey periods, stratification gradually weakened throughout the nearfield. Complete mixing of the water column, however, progressed from shallow areas outward, as evidenced by

isopycnals impinging upon the bottom sediments. Mixing of the water column was more intense in areas influenced by tidal stirring and interaction with Harbor ebb-flood waters (e.g., station N10P).

7.2.2 Inshore-offshore Gradients

Although minor differences in the concentrations of dissolved nutrients were noted between inshore waters near Boston Harbor and deeper offshore surface waters, no broad geographic gradients were detected during the August-September period. TN concentrations were lower in Cape Cod Bay than in other locations and an indication of a weak TN gradient from the Harbor to western Massachusetts Bay was noted. By the end of September, there were indications that vertical stratification was deteriorating and that, near Boston Harbor, the horizontal gradients of dissolved nutrients, typical of most of the unstratified period in Massachusetts Bay, were re-developing.

7.2.3 Special Features: Comparison of 1993 with 1992

The temporal trends for surface DIN concentrations were similar during the August-September periods in 1992 and 1993 (Figure 7-3). In the fall when water-column mixing is generally initiated, the concentration range broadens. This phenomenon may occur as productivity in the Harbor decreases and export of dissolved nutrient forms (particularly NH_4) gains prominence. Both physical and chemical distributions during this time portend a seasonal restructuring from vertical layering to horizontal banding, expressed as gradients where strong sources are prominent. For DIN, the fall expansion of the concentration range is simply the reverse of the chronology that occurs in the spring (late March to May) when stratification is initiated.

7.3 Biology in Relation to Water Properties and Nutrient Dynamics

7.3.1 Phytoplankton-Zooplankton Relationships and Plankton-Water Property Trends

Zooplankton and phytoplankton, as cell counts or biomass, were not closely correlated (Figure 7-4). Generally, zooplankton counts were higher in August than in June (cf. Kelly *et al.*, 1994c).

Regional taxonomic groupings that indicate distinct coupled phytoplankton-zooplankton communities were not immediately obvious; such associations may be revealed by multivariate analyses. Taxon-level distributions (Section 4) suggested that Harbor water may have contributed minor components to the western Massachusetts Bay plankton community. The Bays were fairly well mixed taxonomically and there was no indication of distinct water masses, other than the Harbor, that could serve to import species. Therefore, taxonomic variations that were observed across the Bays may have been due primarily to differential expression of species from within the indigenous community. The speculation is that biological variability was, to a large extent, forced by spatial and temporal responses to small-scale physical variability. Notably, the biological variability was relatively small; if characterized as a temporal-spatial patchwork of colors, it would have mostly graded tones, not different hues.

The weak relationship between total zooplankton and phytoplankton abundance during the summer could suggest that zooplankton numbers poorly reflect zooplankton biomass and energetics. At an energetics level there should be a relationship between phytoplankton and zooplankton; but the underlying taxonomic structure of the community may vary without altering fundamental energy flows and nutrient dynamics. Recently funded studies by the EPA Laboratory in Narragansett, intended to provide supplemental data for the monitoring program, may aid in developing some understanding of the energetic coupling of phytoplankton and zooplankton (J. Garber, personal communication).

The biological composition trends that can be assessed across surveys during the sampling period are limited to observations on surface-water phytoplankton at station N10P (Tables 7-1 and 7-2). This station receives Harbor outflow at the surface and, although the water quality varies with the tidal

cycle, this station has water-quality characteristics of the Harbor as well as western Massachusetts Bay. From early August through late September, microflagellates were a dominant and stable component of the phytoplankton community. The other major components were the diatoms. Dinoflagellates were present, but in low numbers (Table 7-2).

There was a chronological sequence of several diatom species, from *Rhizosolenia delicatula* in early August, to *Leptocylindrus danicus* in late August/early September, to *Asterionellopsis glacialis* (at 2 million cells L⁻¹) in late September. *Asterionellopsis* was present in significant numbers in early September even though it was not yet dominant (Appendix G). *Skeletonema costatum* also occurred in high numbers in both early and late September samples. A minor increase in some dinoflagellates was noted in early September. The total number of cells increased over the period (as did chlorophyll); in both September samples the total exceeded 3.7 x 10⁶ cells L⁻¹. Review of the temporal trends for nutrients in the surface water at station N10P revealed that higher DIN, NH₄, and PO₄ concentrations occurred in both September surveys. Data on phytoplankton taxa, cell counts, and nutrient trends offer some evidence to propose a hypothesis that the diatom bloom developing in the nearfield in September was related to nutrient increases and that these were, in part, a consequence of Harbor outflow of nutrient-rich water.

7.3.2 Chlorophyll Biomass and Nutrients

Significant spatial and temporal trends in water quality throughout the Bays were most often observed as variations in chlorophyll concentrations. Spatially, an inshore-offshore grading from high concentrations of chlorophyll in the inshore surface waters to a constrained subsurface layer in deeper water was regularly noted. During the farfield survey in August, enrichment of western Massachusetts Bay and a large portion of the nearfield was obvious. Chlorophyll generally remained high and even increased substantially in September, resulting in the most extensive distribution and acutely high concentration of chlorophyll in the Bays documented to date as part of the MWRA monitoring program.

A strong relationship between chlorophyll and total nitrogen (TN) was maintained during August, when organic nutrient chemistry data were available (Figure 7-5). With rapid assimilation of dissolved nutrients at high temperature, in August most available nutrients are found in particles and as organic forms, rather than dissolved in the water column. The pattern shown in Figure 7-5 suggests a relationship of slightly more than $1 \mu\text{g L}^{-1}$ increase in chlorophyll for each $1 \mu\text{M}$ increase in TN. This familiar pattern confirms results obtained from the June 1993 survey, as well as data summaries for seasonal and annual means (e.g., Kelly *et al.*, 1994c; Kelly, 1994). However, in contrast to many observations made at station F23P (at the edge of the Harbor in President Roads), chlorophyll did not fall off at the highest TN concentrations. Instead, TN concentrations and chlorophyll concentrations at station F23P were among the highest observed.

It has been speculated that the characteristic fall off of chlorophyll concentrations at the Harbor edge is due, in part, to high turbidity and light limitation. In this context, the contrast between the June and August chlorophyll patterns is of special interest; therefore, some of the differences in water quality and environmental conditions at station F23P were examined for these two months. The difference between the June chlorophyll pattern (with fall off) and the August pattern (without fall off) was apparently not related to differences in irradiance; mid-day irradiance measured during the June survey was $2679 \mu\text{E m}^{-2} \text{sec}^{-1}$ compared to $2759 \mu\text{E m}^{-2} \text{sec}^{-1}$ during the August survey. Moreover, light extinction, TSS, and beam attenuation were all slightly higher in August than in June — observations that would, in principle, suggest greater potential light limitation in August. Thus, the chlorophyll-nitrogen trends that were observed appear to contradict a simple notion of light limitation.

Review of other data from station F23P in June and August indicates that the phytoplankton and zooplankton communities were similar. The dominant organisms (e.g., 2-3 diatoms, microflagellates, and 2-3 copepods) were similar in both months and occurred in approximately the same numbers. Aside from the fact that it was cooler in June (12°C) than in August ($16\text{-}17^\circ\text{C}$), a main observed difference between the two sampling periods was a higher concentration of TN in June ($\sim 20 \mu\text{M}$) than in August ($15 \mu\text{M}$). The difference in TN concentration was due primarily to DIN and less to dissolved organic nitrogen (DON). In June, TN concentrations ranged between 1 and $6 \mu\text{M}$ throughout the entire water column, suggesting less nutrient limitation than in August, when DIN was near zero. The range

for P_{\max} was higher in June (about 10-12 $\mu\text{gC } \mu\text{gChl}^{-1} \text{ h}^{-1}$) than in August (6-10 $\mu\text{gC } \mu\text{gChl}^{-1} \text{ h}^{-1}$) — also suggesting less nutrient limitation in June.

Although average chlorophyll concentrations were lower in June, productivity calculations were similar for June and August (3.1 and 3.2 $\text{g C m}^{-2} \text{ d}^{-1}$, respectively). These data imply that the turnover of biomass was slower in August when nutrient concentrations were lower. With similar rates of productivity in June and August, the lower chlorophyll concentrations observed in June could represent increased grazing of phytoplankton by shellfish. However, concentrations of chlorophyll are influenced by various other factors, including variations in flushing, chemical or photoinhibition, effluent delivery rates, or the time effluent is discharged relative to the sample collection.

In summary, the comparison suggests that light limitation may be more severe when DIN is more abundant (June); but lacking DIN (i.e., having more severe nutrient limitation), the effect of light is not evident in chlorophyll (August). Moreover, productivity may be equivalent in spite of differences in limiting factors. Perhaps more importantly, the discussion above merely emphasizes the complexity of the chlorophyll-productivity-nutrient-light relationship. In spite of the striking patterns observed and a wealth of data relevant to understanding the ecological conditions, the data do not fully identify the relative influences of nutrients and light between the summer 1993 surveys.

7.3.3 Metabolism and Environment

High production was found in locations where biomass was high (chlorophyll and TN). This was true on a volumetric basis, where the production rate consistently paralleled the vertical profile of chlorophyll at virtually all stations. It was also true on an areal basis, where the integrated chlorophyll biomass within the photic zone (defined by $Z_{0.5\%I_0}$) and production rates were related across stations (cf. Section 4).

High levels of production and high concentrations of chlorophyll were found, in all cases, only to the irradiance level of the P-I curves where P is less than P_{\max} and becomes linearly dependent on I (about

150-300 $\mu\text{E m}^{-2} \text{sec}^{-1}$). When chlorophyll concentrations were high throughout the surface layer, production fell off exponentially below this layer, following the exponential decrease in irradiance with depth. When a subsurface chlorophyll maximum occurred, it was characteristically found at a depth where midday irradiance was above 150 $\mu\text{E m}^{-2} \text{sec}^{-1}$, a level which is well above the $Z_{0.5\%I_0}$ or $Z_{1.0\%I_0}$ light levels. If chlorophyll was found as a peak well below this level, no corresponding peak in production was suggested by modeling. In summary, the observations indicate that low rates of production can occur at light levels significantly below P_{max} , but in the Bay the highly productive layers of peak chlorophyll concentrations were confined to shallower depths where light levels were high enough to induce near-maximal chlorophyll-normalized production rates.

Kelly (1993) previously discussed the relationships between chlorophyll, production, and light that characterized conditions observed in all 1993 surveys prior to the August survey. A simplified approach to calculating production was explored using a composite variable, $BZ_p I_0$ — the multiplication product of average chlorophyll biomass (B), $Z_{0.5\%I_0}$ (Z_p), and incident irradiance (I_0). As shown in Figure 7-6, comparison of the August 1993 ^{14}C production data to the composite variable ($BZ_p I_0$) indicates a strong correlation ($R^2=0.828$). These new results support the overall correspondence between the composite parameter calculation and 1993 incubation data and, therefore, strengthen the conclusion of Kelly (1993): the composite parameter is a means to obtain integrated production estimates that is simple, valid, and an economical alternative to bottle incubations.

DO in surface and mid waters reflected much of the spatial variability observed in chlorophyll and production in surface waters, as did respiration rates measured in bottle incubations. But, in contrast, bottom water DO was not highly variable across the nearfield throughout the entire August-September period (Figure 7-2), and bottom water respiration rates were generally low or insignificant.

The coupling of metabolic processes between surface and bottom waters is not well described for the Bay or for the nearfield, in particular. But the data from August and September 1993 provide some insight into the nature of the coupling. For example, as of the end of September, there was no indication that the unprecedented phytoplankton bloom had altered the rate of DO decline in bottom water. Also, the uniformity in the percent DO saturation in bottom waters clearly contrasts with the

high variability in DO saturation in surface waters and the evidence suggests that, to this stage of the fall bloom, the majority of the metabolism occurred in the upper water column and was not transferred to subpycnocline layers. The homogeneous bottom-water DO also could suggest that (1) sedimentation is not as patchy as surface chlorophyll or that (2) rates of bottom-water metabolism occur on timescales slower than bottom water movements. Assuming the latter, the effects of localized increases in metabolism on DO in the water could be uniformly mixed in the bottom-layer by tide-driven currents. The interaction of such physical processes with metabolic effects on bottom water properties are of interest in predicting future events in the nearfield.

7.3.4 Special Features: Comparison of 1993 with 1992

The central water quality feature observed in early fall 1993 was the progressive increase in chlorophyll concentrations which resulted in extensive areal coverage of chlorophyll-rich waters throughout the nearfield by the end of September. Although there was much variability across the nearfield, the trend is apparent in Figure 7-7. Because there were no measurements outside the nearfield after the end of August, it is not clear whether the bloom was initiated and spread from inshore; however, the spatial chlorophyll patterns in late August and the nutrient data from the western edge of the nearfield in September could support such a hypothesis. Moreover, the nearfield bloom culminating in October was caused by the diatom species *Asterionellopsis* (Libby *et al.*, 1994); by September, this species increased to become the single dominant taxa at the Harbor outflow sentinel station (N10P).

Average chlorophyll concentrations and variabilities during the late summer/early fall were similar in 1993 and 1992 (Figure 7-7). Peak concentrations were higher in 1993, but this may be a consequence of having data for 1992 that are limited to one survey in *early* September.

7.4 Summary and Recommendations

Stratification and early signs of seasonal destratification were the dominant features in the Bays during the August and September period. For many of the biological, chemical, and physical variables, the main temporal patterns observed in the nearfield in 1993 were similar to patterns observed during the same months in 1992. Although major spatial and temporal variations in chlorophyll concentrations were noted, the chemical or physical parameters did not parallel the chlorophyll trends. Underlying the variations in chlorophyll biomass was minor variability in phytoplankton species composition; the overall variability in taxa was basically due to spatial and temporal changes in just a few diatom species.

In late August, high rates of primary production were measured, indicating a very productive autotrophic surface layer. An empirical model, proposed and explored with previous MWRA data, was successful in explaining most of the variance in production estimates that were made using ^{14}C bottle incubations at 10 stations across the Bay. Bottom water changes accompanying high rates of surface-layer production were slow and showed gradual decline in DO saturation.

Table 7-1. Abundance of the top five dominant phytoplankton taxa in near-surface whole-water samples at station N10P collected in August and September 1993.

TAXA	DATE	AUG 11	AUG 24	AUG 27	SEP 9	SEP 29
CERATAULINA PELAGICA			.387 (3)	0.046 (5)		
CRYPTOMONADS		0.052 (3)	.074 (5)	0.072 (4)		0.076 (5)
SKELETONEMA COSTATUM					0.739 (3)	0.477 (3)
LEPTOCYLINDRUS DANICUS			.128 (4)	0.482 (2)	1.139 (1)	0.153 (4)
MICROFLAGELLATES		0.661 (1)	.766 (1)	0.945 (1)	0.85 (2)	0.778 (2)
RHIZOLENIA DELICATULA		0.078 (2)	.642 (2)	0.099 (3)		
CHAETOCEROS SP. (10-20 μ M)		0.043 (4)				.009 (5)
EUTREPTIA/EUTREPTIELLA SPP.		0.037 (5)				
ASTERIONELLOPSIS GLACIALIS						2.005 (1)
CHAETOCEROS DIDYMUS					0.252 (4)	
NITZSCHIA SPP.					0.191 (5)	

Units are 10^6 cells L^{-1}

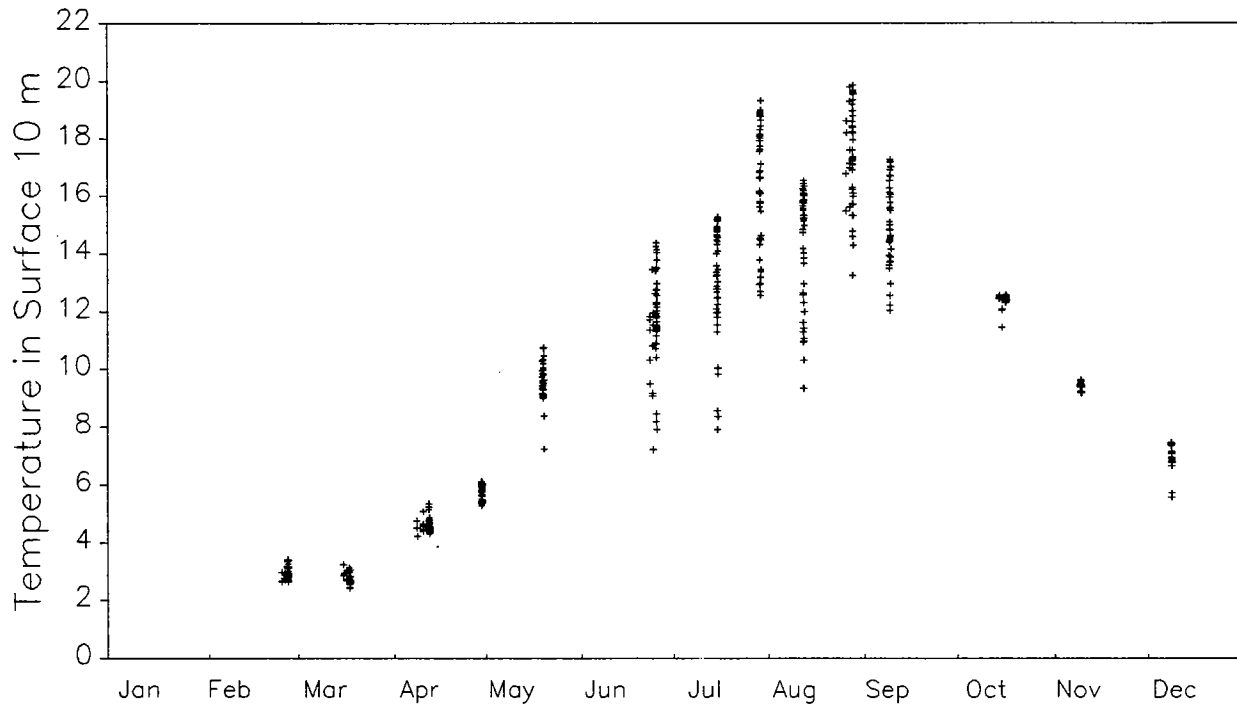
Values in parentheses give rank order of abundance

Table 7-2. Abundance of all identified phytoplankton taxa in near-surface screened samples from N10P only.

SPECIES	STATION	N10P	N10P	N10P	N10P	N10P
	SAMPLE ID	W93100012	W93110091	W93110542	W93120200	W93130198
	DATE	Aug 11	Aug 24	Aug 27	Sep 09	Sep 29
ALEXANDRIUM TAMARENSE		0	0	0	19	3
ALORICATE CILIATES		0	3	25	96	0
CERATIUM FUSUS		55	243	243	193	110
CERATIUM LONGIPES		60	70	15	183	23
CERATIUM MACROCEROS		0	0	5	0	0
CERATIUM TRIPOS		5	45	78	29	20
DICTYOCHA FIBULA		0	0	0	0	0
DICTYOCHA SPECULUM		3	3	3	48	3
DINOPHYSIS ACUMINATA		5	10	0	19	0
DINOPHYSIS NORVEGICA		23	20	0	10	13
DIPLOPSALIS SPP.		0	0	0	4562	8
EBRIA TRIPARTITA		0	0	0	19	3
EUTREPTIA/EUTREPTIELLA SPP.		0	0	0	0	0
GLENODINIUM ROTUNDUM		0	0	3	29	0
GONYAULAX SPINIFERA		0	0	0	424	3
GONYAULAX SPP.		0	0	0	10	0
GYMNODINIUM SPP.		0	0	0	29	0
GYRODINIUM SPIRALE		0	0	0	10	0
GYRODINIUM SPP.		0	0	3	0	0
HETEROCAPSA TRIQUETRA		0	0	0	19	5
MESODINIUM RUBRUM		0	0	0	0	0
PROROCENTRUM MICANS		0	0	35	48	3
PROROCENTRUM MINIMUM		0	0	0	10	0
PROTOPERIDINIUM BIPES		0	0	3	19	0
PROTOPERIDINIUM BREVE		0	0	0	67	0
PROTOPERIDINIUM DEPRESSUM		13	10	0	67	5
PROTOPERIDINIUM PELLUCIDUM		0	0	0	58	0
PROTOPERIDINIUM PENTAGONUM		0	0	0	0	0
PROTOPERIDINIUM SPP.		5	30	68	1781	15
SCRIPPSIELLA TROCHOIDEA		0	70	8	809	33
TINTINNIDS		18	38	185	39	198
UNID. ATHECATE DINOFLAGELLATE		0	3	8	58	8
UNID. THECATE DINOFLAGELLATES		3	10	5	154	33

Values are Cells/L

1992, Nearfield Stations



1993, Nearfield Stations

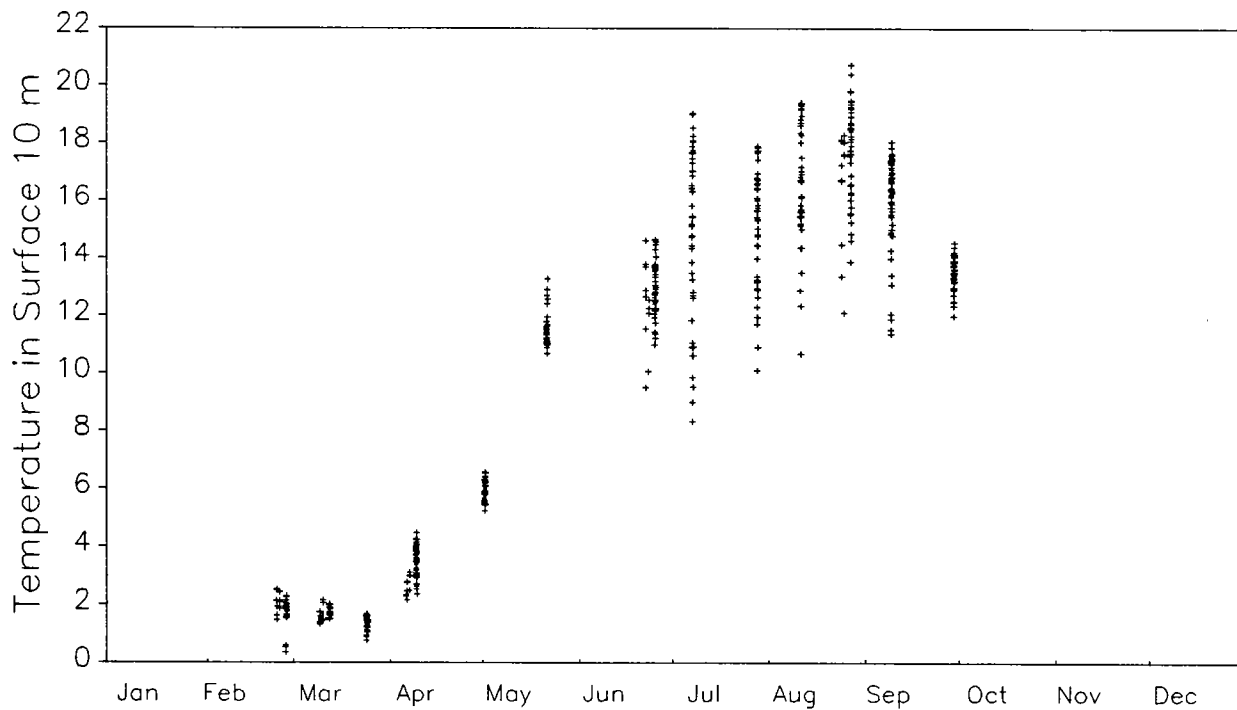
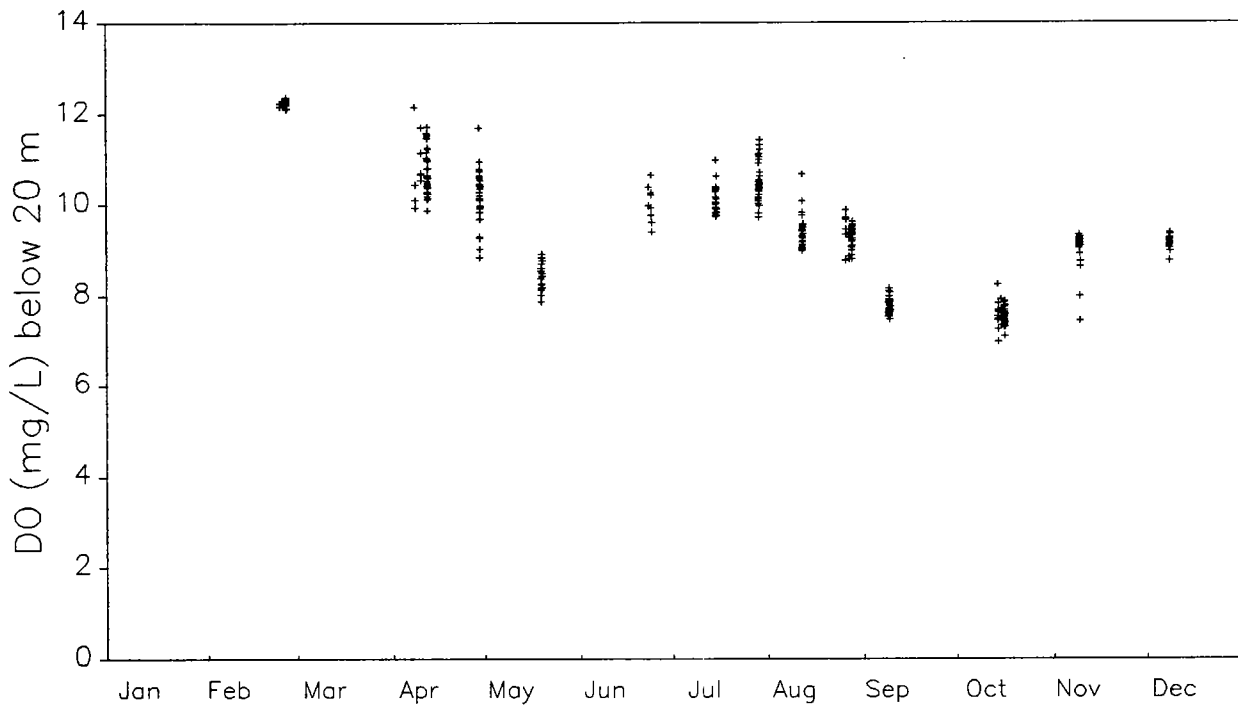


Figure 7-1. Comparison of the nearfield region in 1993 to the annual cycle of 1992: temperature (°C).

1992, Nearfield Stations



1993, Nearfield Stations

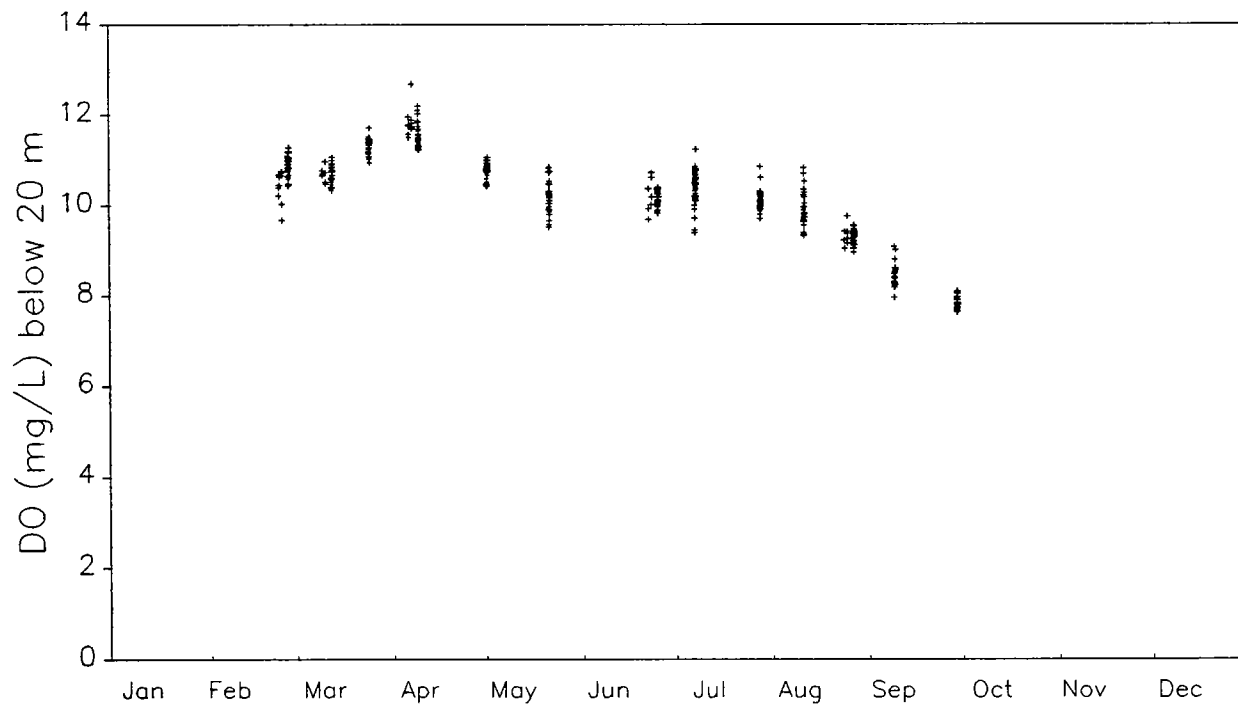
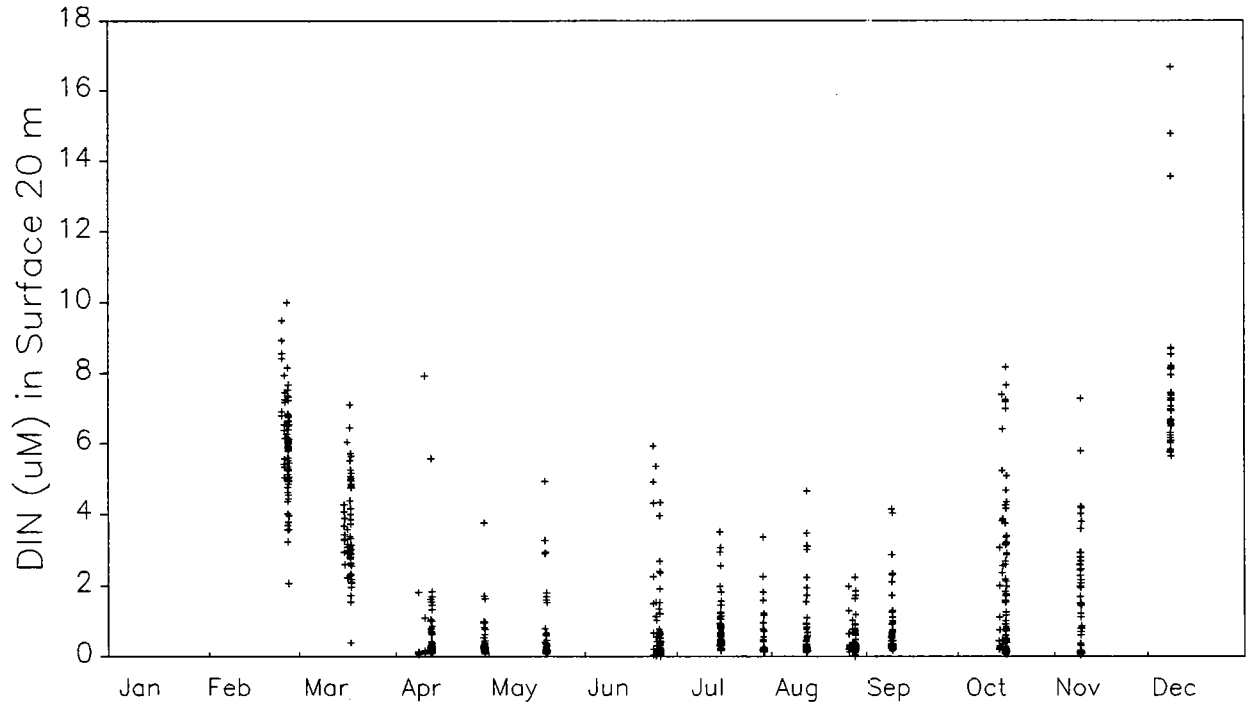


Figure 7-2. Comparison of the nearfield region in 1993 to the annual cycle of 1992: dissolved oxygen (mg/L).

1992, Nearfield Stations



1993, Nearfield Stations

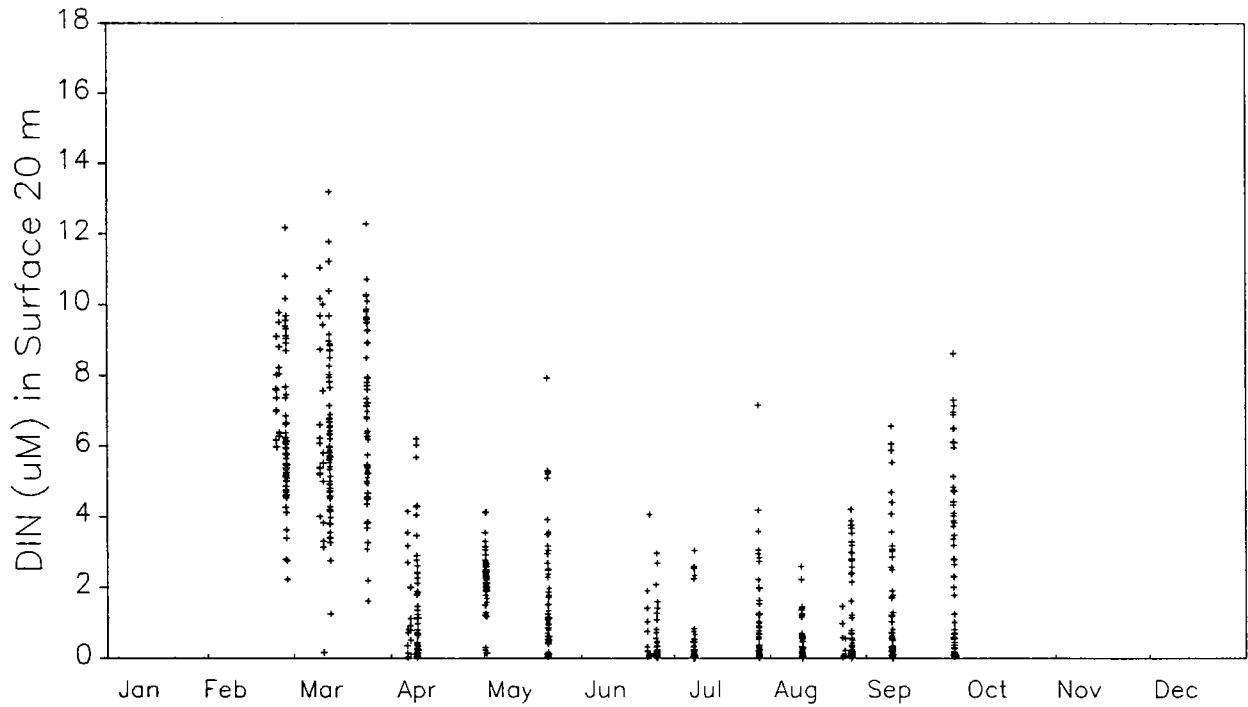


Figure 7-3. Comparison of the nearfield region in 1993 to the annual cycle of 1992: dissolved inorganic nitrogen (μM).

Late August (W9311)

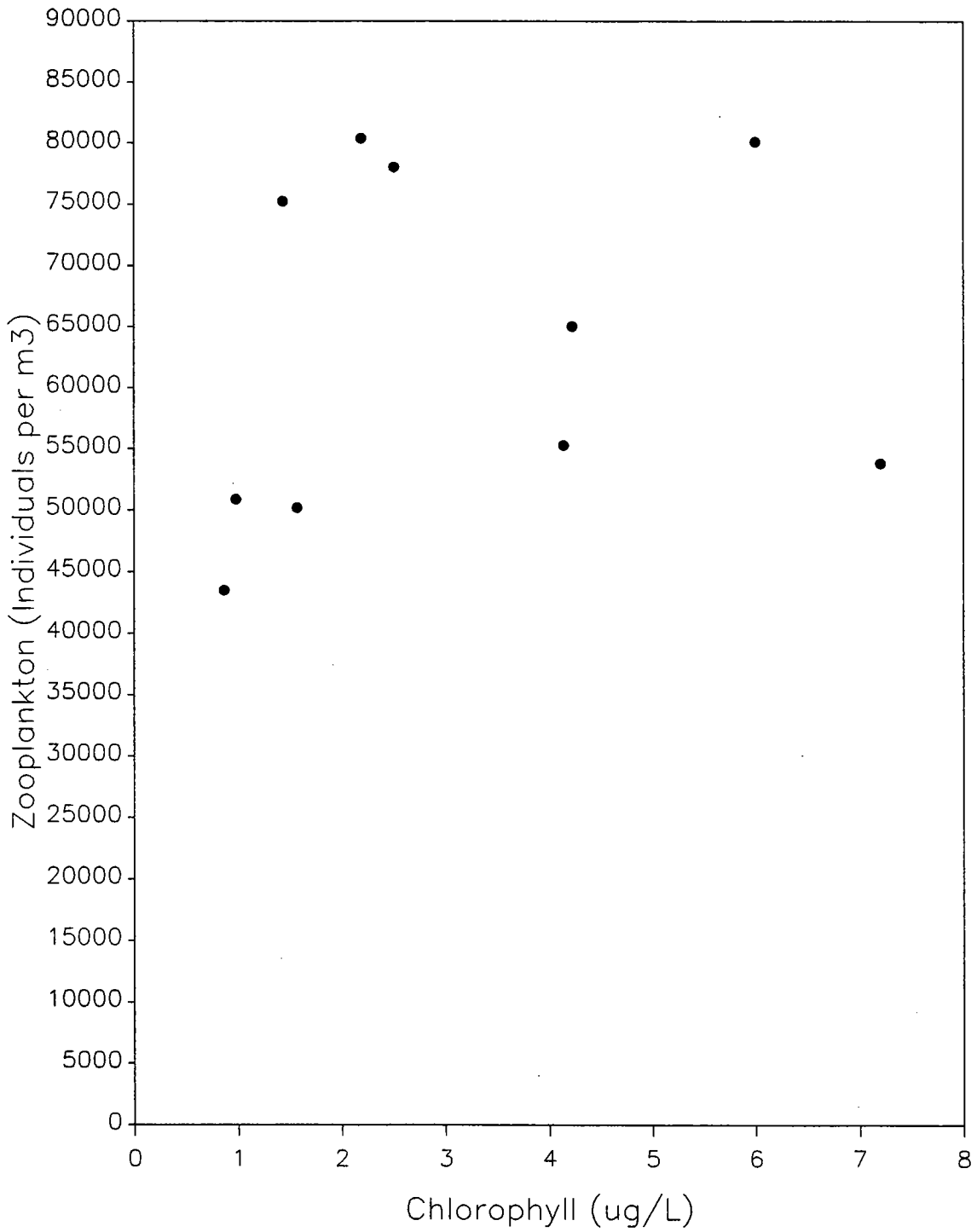


Figure 7-4. Zooplankton abundance compared to the average chlorophyll concentration (n=2 depths) in the water column in late August 1993.

Late August (W9311)

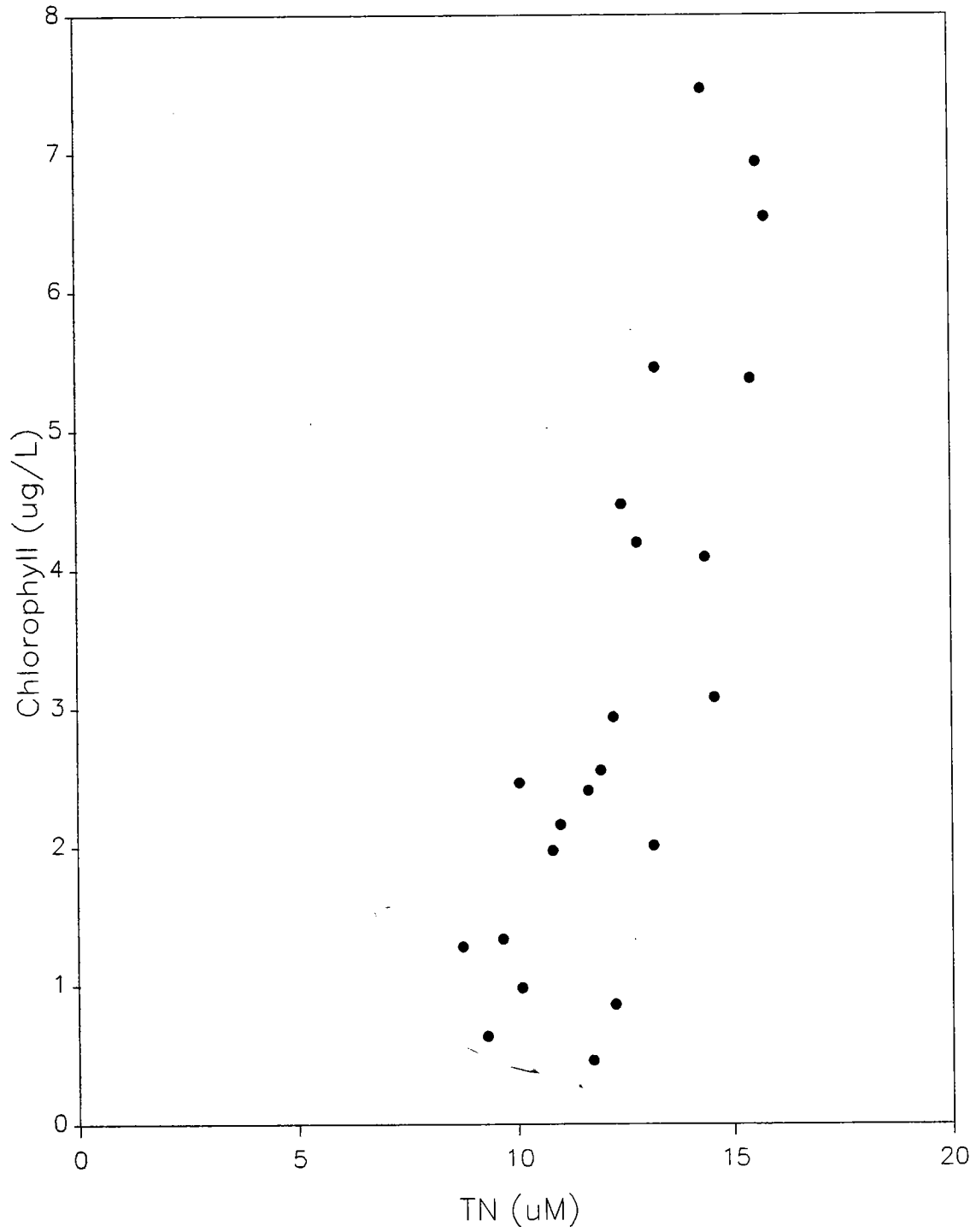


Figure 7-5. Chlorophyll and total nitrogen in samples from late August 1993.

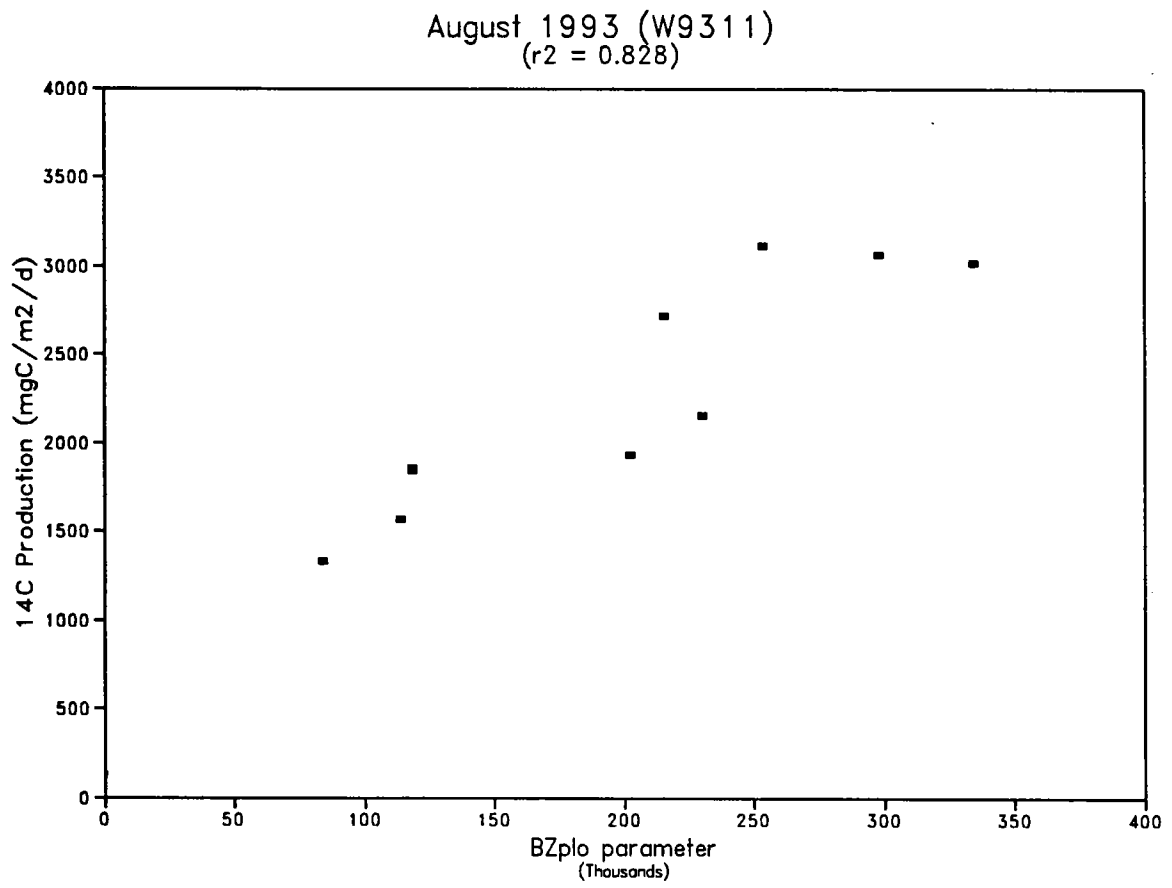
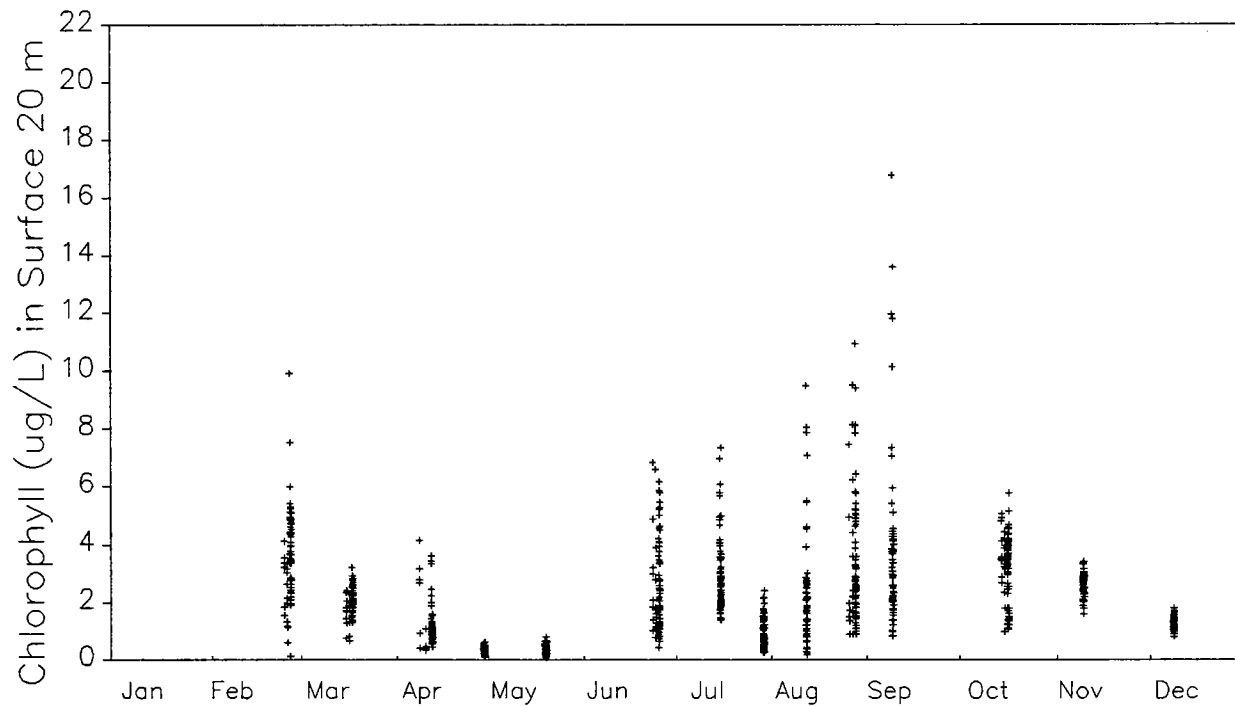


Figure 7-6. ^{14}C production compared to the composite parameter BZ_pI_0 for late August 1993.

1992, Nearfield Stations



1993, Nearfield Stations

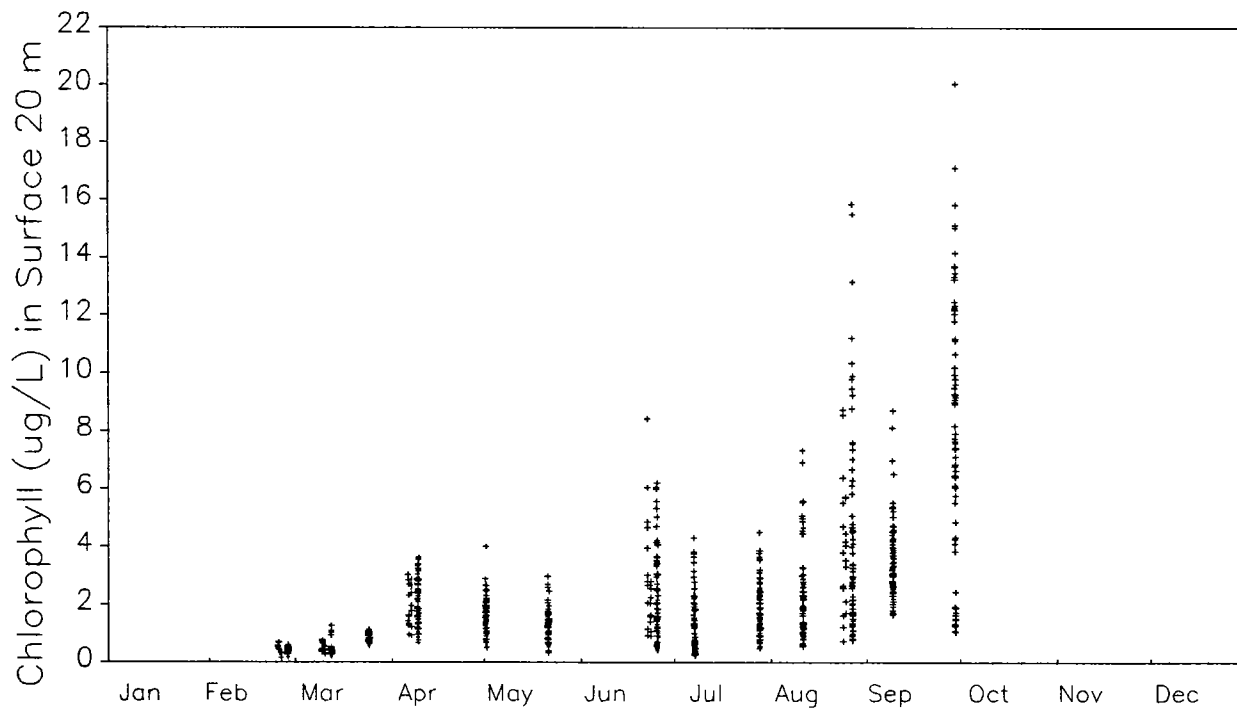


Figure 7-7. Comparison of the nearfield region in 1993 to the annual cycle of 1992: chlorophyll ($\mu\text{g/L}$). Chlorophyll is estimated from *in situ* fluorescence.

8.0 REFERENCES

- Albro, C.S., J.R. Kelly, J. Hennessy, P. Doering, and J. Turner. 1993. Combined work/quality assurance project plan for baseline water quality monitoring: 1993-1994. Massachusetts Water Resources Authority, Boston, MA. Miscellaneous Report 14. 73pp.
- Bechtold, J.H. 1993. Water column survey W9312 report for baseline water quality monitoring. Prepared for the Massachusetts Water Resources Authority, Boston, MA, September 1993.
- Dragos, P. 1993a. Water column survey W9310 report for baseline water quality monitoring. Prepared for the Massachusetts Water Resources Authority, Boston, MA, September 1993.
- Dragos, P. 1993b. Water column survey W9311 report for baseline water quality monitoring. Prepared for the Massachusetts Water Resources Authority, Boston, MA, September 1993.
- Frenette, J-J., S. Demers, L. Legendre, and J. Dodson. 1993. Lack of agreement among models for estimating the photosynthetic parameters. *Limnol. Oceanogr.* 38(3):679-686.
- Giblin, A.G., C. Hopkinson, J. Tucker, B. Nowicki, and J.R. Kelly. 1994. Metabolism, nutrient cycling and denitrification in Boston Harbor and Massachusetts Bay sediments in 1993. MWRA Environ. Qual. Dept. Tech. Rpt. Ser. No. 94-5. Massachusetts Water Resources Authority, Boston MA. 55 pp.
- I.O. Corp. 1984. Model 200 total carbon analyzer, operating procedures and service manual. 315 pp.
- Kelly, J.R. 1993. Letter report on primary production modeling comparison. To Massachusetts Water Resources Authority, Boston, MA. December 6, 1993. 14 pp.
- Kelly, J.R. 1994. Nutrients and Massachusetts Bay: An update of eutrophication issues. MWRA Environ. Qual. Dept. Tech. Rpt. Ser. No. 93-17. Massachusetts Water Resources Authority, Boston, MA. Final report. June 1994.
- Kelly, J.R. and C.S. Albro. 1994. June 1993 Harbor-Bay Mapping. Final letter report to Massachusetts Water Resources Authority, Boston, MA. 25 pp + 35 pp. Appendix.
- Kelly, J.R., C.S. Albro, J.T. Hennessy, and D. Shea. 1992. Water quality monitoring in Massachusetts and Cape Cod Bays: February-March 1992. MWRA Environ. Qual. Dept. Tech. Rpt. Ser. No. 92-8. Massachusetts Water Resources Authority, Boston, MA. 171 pp.
- Kelly, J.R., C.S. Albro, and J.T. Hennessy. 1993a. Water quality monitoring in Massachusetts and Cape Cod Bays: April-August 1992. MWRA Environ. Qual. Dept. Tech. Rpt. Ser. No. 93-1. Massachusetts Water Resources Authority, Boston, MA. 270 pp.

- Kelly, J.R., C.S. Albro, and J.T. Hennessy. 1993b. Water quality monitoring in Massachusetts and Cape Cod Bays: August-November 1992. MWRA Environ. Qual. Dept. Tech. Rpt. Ser. No. 93-15. Massachusetts Water Resources Authority, Boston, MA. 213 pp.
- Kelly, J.R., C.S. Albro, P. Doering, K. Foster, J.T. Hennessy, L. Reed, and E. Requentina. 1993c. Water column monitoring in Massachusetts and Cape Cod Bays: Annual Report for 1992. MWRA Environ. Qual. Dept. Tech. Rpt. Ser. No. 93-16. Massachusetts Water Resources Authority, Boston, MA. Draft Report, May 1993.
- Kelly, J.R., C.S. Albro, J.T. Hennessy, J. Turner, D. Borkman, and P. Doering. 1994a. Water quality monitoring in Massachusetts and Cape Cod Bays: December 1992, February and March 1993. MWRA Environ. Qual. Dept. Tech. Rpt. Ser. No. 94-2. Massachusetts Water Resources Authority, Boston, MA. 197 pp.
- Kelly, J.R., C.S. Albro, J.T. Hennessy, J. Turner, D. Borkman, and P. Doering. 1994b. Water quality monitoring in Massachusetts and Cape Cod Bays: April and May 1993. MWRA Environ. Qual. Dept. Tech. Rpt. Ser. No. 94-3. Massachusetts Water Resources Authority, Boston, MA. 143 pp.
- Kelly, J.R., C.S. Albro, J.T. Hennessy, J. Turner, and P. Doering. 1994c. Water quality monitoring in Massachusetts and Cape Cod Bays: June and July 1993. MWRA Environ. Qual. Dept. Tech. Rpt. Ser. No. 94-11. Massachusetts Water Resources Authority, Boston, MA. 146 pp.
- Libby, S., J.R. Kelly, C.S. Albro, J.T. Hennessy, J. Turner, and P. Doering. 1994. Water quality monitoring in Massachusetts and Cape Cod Bays: October-December 1993. MWRA Environ. Qual. Dept. Tech. Rpt. Ser. No. 94-13. Massachusetts Water Resources Authority, Boston, MA. Draft Report, July 1994.
- MWRA. 1991. Massachusetts Water Resources Authority effluent outfall monitoring plan phase I: baseline studies. MWRA Environ. Qual. Dept., Massachusetts Water Resources Authority, Boston, MA. November 1991. 95 pp.
- Natrella, M.G. 1963. Experimental statistics National Bureau of Standards handbook 91. U.S. Government Printing Office, Washington, DC.
- Platt, T., C.L. Gallegos, and W.G. Harrison. 1980. Photoinhibition of photosynthesis in natural assemblages of marine phytoplankton. *J. Mar. Res.* 38:687-701.
- Platt, T. and A.D. Jassby. 1976. The relationship between photosynthesis and light for natural assemblages of coastal marine phytoplankton. *J. Phycol.* 12:421-430.
- SAS. 1985. SAS User's Guide: Statistics, Version 5 Edition: SAS Institute Incorporated, Cary, NC. 956 pp.

- Vollenweider, R.P. 1966. Calculation models of photosynthesis depth curves and some implications regarding day rate estimates in primary production measurements. Pages 427-457 In: Goldman, C.R. (ed.) Primary Production in Aquatic Environments. University of California, Berkeley, CA.
- Webb, W.L., M. Newton, and D. Starr. 1974. Carbon dioxide exchange of *Alnus ubra*: a mathematical model. *Oecologia* 17:281-291.
- West, D. 1993. Water column survey W9313 report for baseline water quality monitoring. Prepared for the Massachusetts Water Resources Authority, Boston, MA, October 1993.



The Massachusetts Water Resources Authority
Charlestown Navy Yard
100 First Avenue
Charlestown, MA 02129
(617) 242-6000